INDUS RIVER SYSTEM AUTHORITY

IMPROVEMENT OF WATER RESOURCES MANAGEMENT OF INDUS BASIN TO ENHANCE THE CAPACITY OF INDUS RIVER SYSTEM AUTHORITY

WATER SECTOR CAPACITY BUILDING AND ADVISORY SERVICES PROJECT

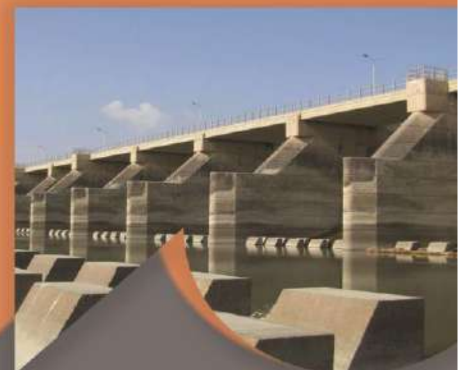

VOLUME I
FINAL REPORT

December 2015

MESPAK In Association With AHT GROUP AG Management & Engineering Deltares Enabling Delta Life

IMPROVEMENT OF WATER RESOURCES MANAGEMENT OF INDUS BASIN TO ENHANCE THE CAPACITY OF INDUS RIVER SYSTEM AUTHORITY

FINAL REPORT

VOLUME I	**FINAL REPORT**
VOLUME II	**ANNEXURES TO FINAL REPORT**
VOLUME III	**FLOW MEASUREMENT REPORT**

This page intentionally left blank.

IMPROVEMENT OF WATER RESOURCES MANAGEMENT OF INDUS BASIN TO ENHANCE THE CAPACITY OF INDUS RIVER SYSTEM AUTHORITY

FINAL REPORT

TABLE OF CONTENTS

Page No.

VOLUME I: FINAL REPORT

ANNEXURES (VOLUME-II)

DVD 1: DATA BOOK

DVD 2: DISCHARGE MEASUREMENT SHEETS

This page intentionally left blank.

LIST OF TABLES

Page No.

This page intentionally left blank.

LIST OF FIGURES

Page No.

LIST OF ABBREVIATIONS / ACRONYMS

ADB	Asian Development Bank
ADCP	Acoustic Doppler Current Profiler
asl	Above see level
AWC	Available Water Holding Capacity
BS	Balloki Sidhnai
CCCma	Canadian Centre for Climate Modelling and Analysis
CCSM	Community Climate System Model (NCARs' atmosphere ocean coupled Global Circulation Model)
CDC	Conventional Depletion Curves
Cds	Coefficients of Discharge
CGCM	Canadian General Circulation Model
CIAT	Centre for Tropical Agriculture
CJLC	Chashma Jhelum Link Canal
CMIP5	Coupled Model Inter comparison Project Phase 5
CRBC	Chashma Right Bank Canal
CREST	Coupled Routing and Excess Storage model
CRUTEM	Climate Research Unit Temperature
CSIRO	Commonwealth Scientific and Industrial Research Organisation (Australia)
D/S	Down Stream
DAU	Data Acquisition Unit
DCP	Data Collection Platform
DDF	Degree Day Factor
DEM	Digital Elevation Model
DGKC	Dera Ghazi Khan Canal
DRS	Digital Radio System
DSS	Decision Support System
DVD	Digital Video Disc
DWD	Deutscher Wetterdienst (German Weather Service)
ELA	Equilibrium Line Altitude
FAO	Food and Agriculture Organization
FEWS	Famine Early Warning Systems
FMS	Flow Measurements System
FORTRAN	derived from Formula Translating System
FTP	File Transfer Protocol
GCISC	Global Change Impact Studies Centre
GCM	General Circulation Model
TIFF	Tagged Image File Format
GIS	Geographic Information System
GLCF	Global Land Cover Facility (Univ. of Maryland)
GLIMS	Global Land Ice Measurements from Space

GMTED2010	Global Multi-resolution Terrain Elevation Data 2010
GPCC	Global Precipitation Climate Centre
GPRS	General Packet Radio Service
GRACE	Gravity Recovery And Climate Experiment
GSM	Global System for Mobile communications
GSOD	Global Summary of the Day (climate data)
GUI	Graphical User Interface
H&RD	Hydrology and Research Directorate of WAPDA
HADGEM	Hadley Centre Global Environment Model
HDF	Hierarchical Data Format
HEC-HMS	Hydrological Engineering Centre - Hydrologic Modeling System
HEC-RAS	Hydrological Engineering Centre - River Analysis System
HMI	Human Machine Interface
IBIS	Indus Basin Irrigation System
ICESat	NASA's Ice, Cloud and land Elevation Satellite
ICIMOD	International Centre for Integrated Mountain Development
IDRC	International Development Research Centre
IPCC	Intergovernmental Panel on Climate Change
IRSA	Indus River System Authority
ISO	International Organization for Standardization
ISRIP	International Sedimentation Research Institute Pakistan
K2	Karakoram 2
KPK	Khyber Pakhtunkhwa
LANDSAT	Land Remote-Sensing Satellite
LCLU	Land Cover / Land Use
LEGOS	Laboratoire d'Etudes en Géophysique et Océanographie Spatiales
LUIB	Lower UIB
MAE	Mean Absolute Error
MAF	Million Acre Ft
MDC	Modified Depletion Curve
MIS	Management Information System
MODIS	Moderate Resolution Imaging Spectroradiometer
MRLC	Marala Ravi Link Canal
MRT	MODIS Re-projection Tool
NASA	National Aeronautics and Space Administration
NCAR	National Centre for Climatic Research (USA)
NCDC	National Climate Data Centre
NDII	Normalized Difference Ice Index
NDVI	Normalized Difference Vegetation Index
NESPAK	National Engineering Services Pakistan (Pvt) Ltd
netCDF	network Common Data Form
NOAA	National Oceanographic and Atmospheric Administration
NVR	Network Video Recorders
O&M	Operation and Maintenance

PCRWR	Pakistan Council of Research in Water Resources
PET	Potential Evapotranspiration
PID	Provincial Irrigation Department
PLCs	Programmable Logic Controller
PMD	Pakistan Meteorological Department
PSHIP	Pakistan Snow and Ice Hydrology Project
R	Statistical LanGauge
RD	Reduced Distance
RegCM	Regional Climate Model
RFE	Rainfall Estimates
SCA	Snow Cover Area
SCADA	Supervisory Control And Data Acquisition
SID	Sindh Irrigation Department
SLUPR	Semi-distributed Land Use-based Runoff Processes
SMS	Short Message Service
SRES	Special Report on Emissions Scenarios
SRM	Snowmelt Runoff Model
SRM+G	Snowmelt Runoff + Glacier Melt Model
SRTM	Shuttle Radar Topographic Mission
SUPARCO	Pakistan Space and Upper Atmosphere Research Commission
SWHP	Surface Water Hydrology Project of WAPDA
TOA	Top of Atmosphere (radiation)
TOPKAPI	Topographic Kinematic Approximation and Integration
ToR	Term of Reference
TPLC	Taunsa Panjnad Link Canal
TRMM	Tropical Rainfall Mapping Mission
U/S	Up Stream
UAT	User Acceptance Test
UBCWM	University of British Columbia Watershed Model
UCC	Upper Chenab Canal
UIB	Upper Indus Basin
UUIB	Upper UIB
UTM	Universal Transverse Mercator coordinate system
VSAT	Very Small Aperture Terminal
WAA	Water Apportionment Accord
WAPDA	Water and Power Development Authority
WCAP	Water Sector Capacity Building and Advisory Services Project
WDLS	Withdrawals
WLS	Water Level Sensors
WMO	World Meteorological Organization
WRMD	Water Resources Management Directorate
XEN	Executive Engineer

This page intentionally left blank.

EXECUTIVE SUMMARY

The Indus River System Authority (IRSA) was established on December 10, 1992 with the purpose of regulating and monitoring the distribution of waters of the Indus River System in accordance with the WAA of 1991. IRSA's prime responsibility includes reservoir, river and canal operations in accordance with the WAA of 1991, and irrigation and hydropower requirements. Accurate and reliable flow measurement system is a pre-requisite to ensure fair and equitable distribution of river supplies among the provinces.

The overall aim of the study was to develop an effective, reliable and transparent flow measurement system at five (5) pilot sites amongst the twenty three (23) key water regulation/distribution sites to ensure the effective water resources management of the IBIS in context of substantial economic, social and environmental changes. The five (5) pilot water regulation/distribution sites are mentioned below

- Chashma Barrage
- Taunsa Barrage
- Guddu Barrage
- Garang Regulator - Kirther Canal
- Marala Barrage

Further the study also required to develop a river flow forecasting system to study the change in Indus River flows due to climate change impacts on the Upper Indus Basin. The study was executed under Water Sector Capacity Building and Advisory Services Project (WCAP) funded by the World Bank. The funding was a part of the World Bank assistance to strengthen the water resources management and strategic planning capability of IRSA.

The Consultants were also awarded additional services during course of the study which included additional flow measurements at Garang, Saifullah Magsi, Pat Feeder Canal and Chashma Right Bank Canal (CRBC).

Stakeholders Participation

Focal persons were nominated by the provincial irrigation departments and WAPDA well before the start of study. All the stakeholders or their representatives witnessed thirteen (13) flow measurement missions at 5 pilot sites. A total of seven (07) workshops/meetings were also held at Islamabad and Lahore on submission of various Consultants reports. Further, stakeholders' consultation/incorporation of comments were made mandatory in approval of all the Consultants' reports.

Review and Analysis of Flow Measurement Information

The review was made to understand the present procedures being followed for flow measurements at the 23 key sites of IBIS. To determine the correctness of water accounting by means of discharge calculation procedures being practised at the 23 key sites, field visits were conducted and the field formations interviewed.

At barrages, discharge calculations were carried out using formulas and coefficients generally mentioned in their Operation and Maintenance manuals by designer. It was observed that using PID documented formulas and data from gauge registers, Consultants estimated flow magnitudes do not compare with PID reported flow magnitudes. Analysis indicate a difference between PID reported values with estimates from formula being used by PID itself which indicates that PID is not implementing its own formula correctly and random adjustments are being applied over PID estimates for subsequent reporting.

In the absence of a reference flow value (like magnitudes obtained from physical flow measurements for 5 pilot sites) ISO formula was used to compare with PID estimated flow magnitudes and PID reported flow magnitudes. It has been noted that due to inherent application limitation of ISO formula comparison of result may not develop basis for declaring a formula or its coefficients to be non-representative.

As regards canals, the Provincial Irrigation Departments (PIDs) regulate diversions by the stage-discharge relations developed at certain canal section in the vicinity of head-regulator. These relations should ideally be developed through a series of direct flow measurements to represent the dominant flow ranges being encountered by the canal, and are required to be revised at least twice in a year. However in practice it was noticed that the canal ratings have been based in most of the cases one or maximum two measurements, and the periodic revisions are also not followed at the recommended interval, rendering the ratings non-representative. The Chashma-Jhelum Link Canal (CJLC) and the Chashma Right Bank Canal (CRBC) - both operated by WAPDA - are the exceptions in terms that the diversions were made by the application of hydraulic formulae. It is to mention, however, that WAPDA also does not undertake the direct flow-measurements as a routine task.

Flow Measurements at Pilot Sites

Thirteen (13) flow measurement missions were conducted to cover the pre-dominant flow ranges at 28 locations of the five pilot sites. A total of 139 number of flow measurement observations were made during the course of present study. The locations comprised all the head-regulators of the canals off-taking from the four barrages and also the additional locations deemed necessary to enunciate the recommendations for development of a reliable water distribution system.Two new Price type-AA current meters were procured for the flow measurement activity and the manufacturer’s revolution-velocity rating equations were used during measurements. The discharges in the rivers and canals were measured by the current meter method, which was accepted by all stakeholders.

Uncertainties in Flow Measurement

A comprehensive analysis was carried out using ISO-748(2007) for estimation of errors in the discharge computed by the area velocity method using the mid-section approach.

The uncertainties (95%) computed for the pilot sites were within the following ranges:

- Chashma barrage and off-takings: 3-5%
- Taunsa barrage and off-takings: 3-8%
- Guddu barrage and off-takings: 3-7%
- Marala barrage and off-takings: 3-8%
- Kirther Canal at Garang Regulator: 3-5%

Calibration of Discharge Coefficients (Cds)

Flow measurements carried out downstream of Chasma barrage, Taunsa barrage, Guddu barrage and Marala barrage were used to calculate the applicable coefficient of discharges under the actual hydraulic and geometric conditions observed on site at the measurement day. Regression analysis of the corrected discharge coefficients was carried out to obtain a best fit line.

The results of regression analysis carried out for corrected discharge coefficients at Chashma, Taunsa, Guddu and Marala barrages are shown in Figures E-1 to E-4, respectively.

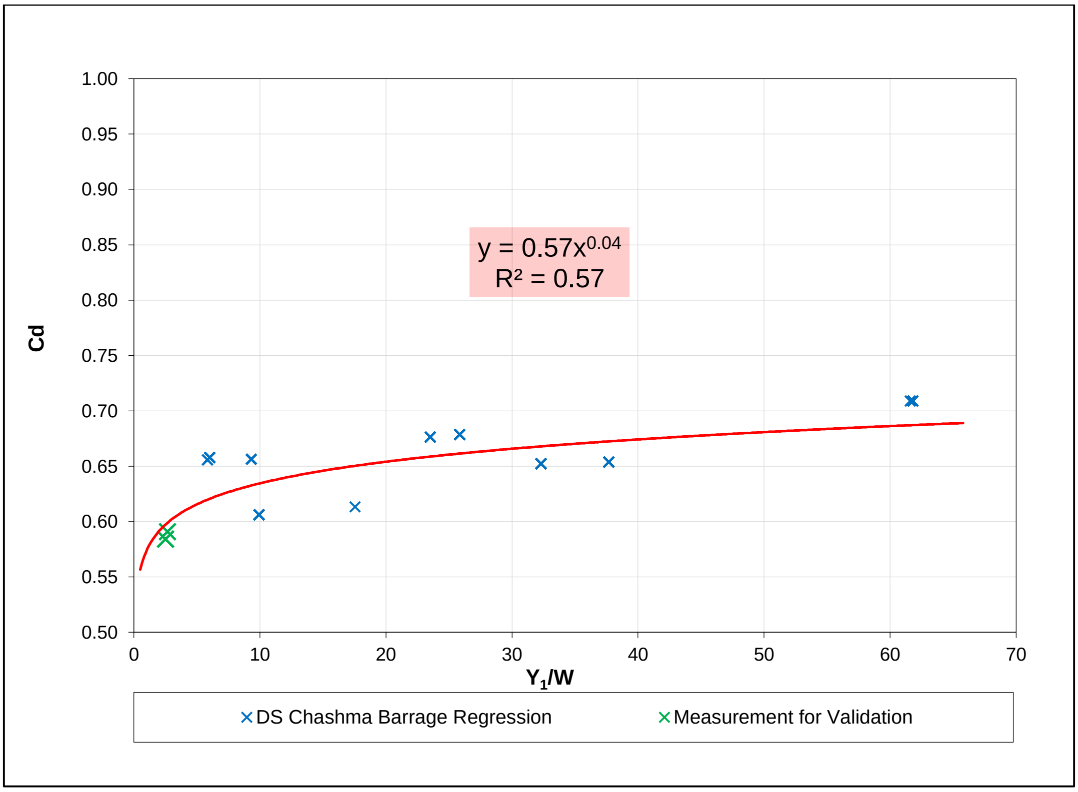

Figure E-1: Regression Analysis of Corrected Discharge Coefficients for Chashma Barrage

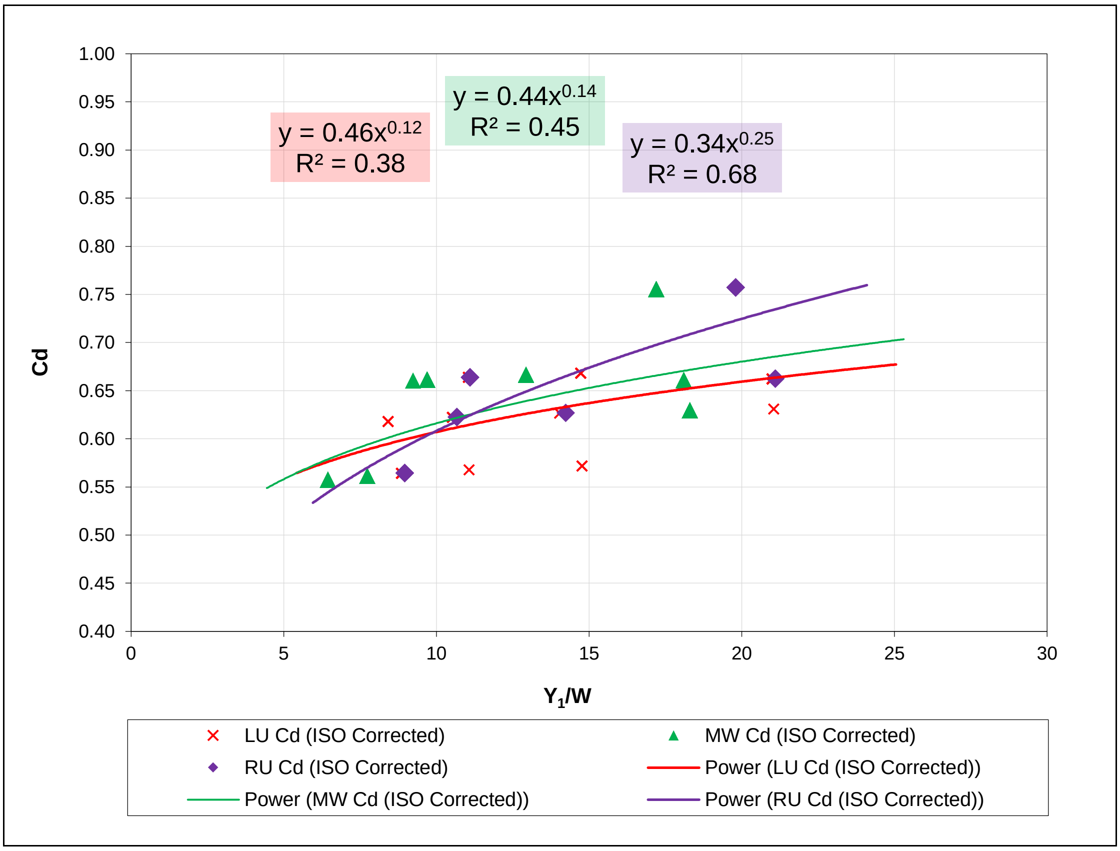

Figure E-2: Regression Analyses of Corrected Discharge Coefficients for Taunsa Barrage

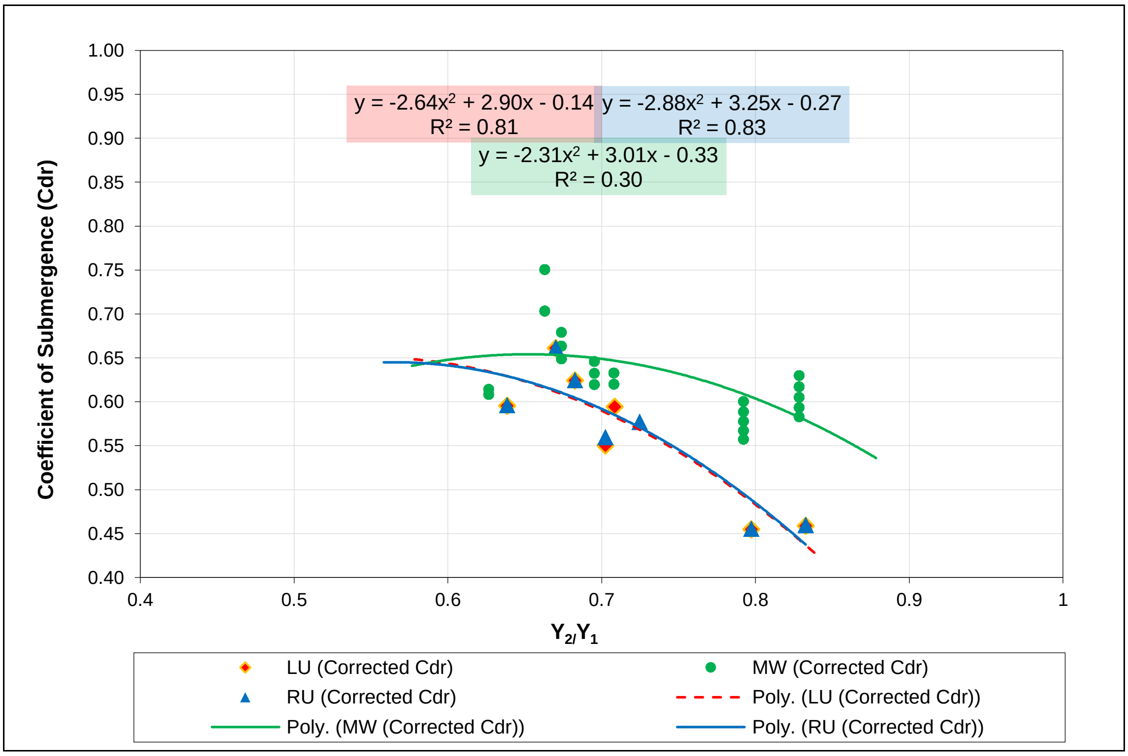

Figure E-3: Regression Analysis of Corrected Discharge Coefficients for Guddu Barrage

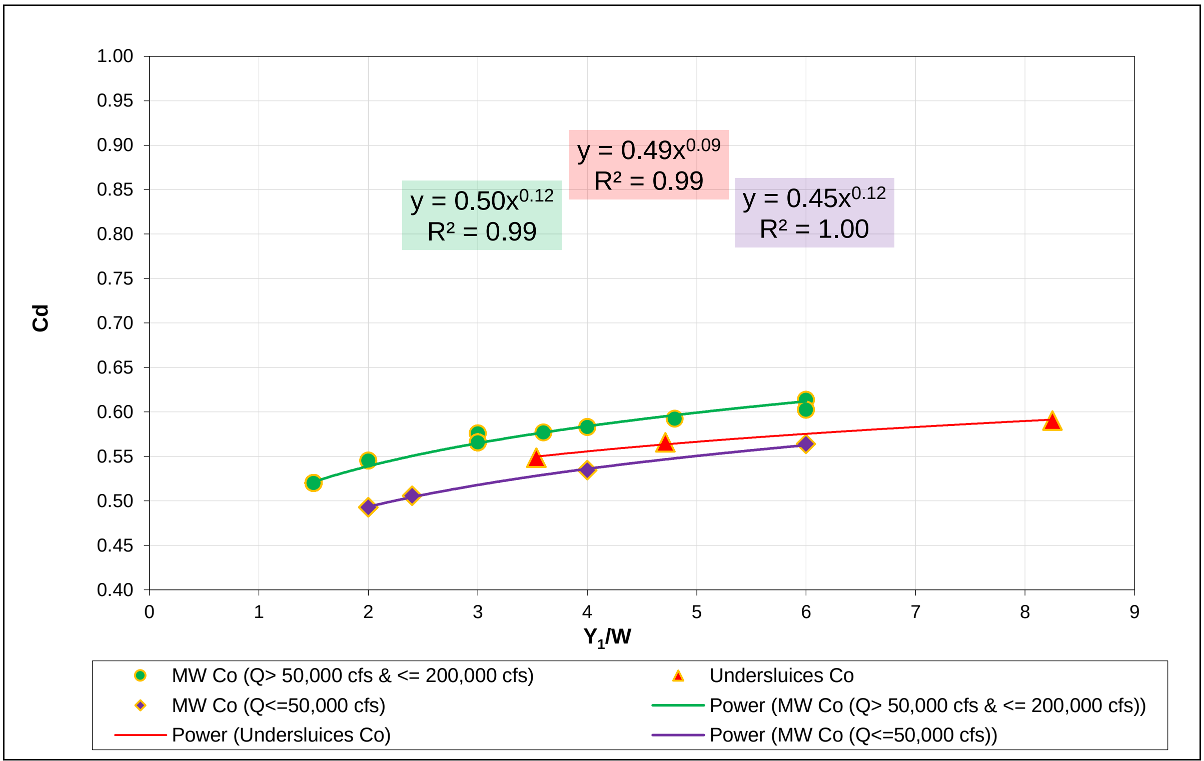

Figure E-4: Regression Analysis of Corrected Discharge Coefficients for Marala Barrage

Following are the specific conclusions on calibration of discharge coefficients.

- The comparison with the flow measurements yielded the difference within ±6% of measured discharges which in turn confirm the applicability of the newly developed equation at Chashma Barrage.
- For Taunsa and Guddu Barrages, the best results were obtained by applying the regression equation developed in the present study for Main Weir to whole Barrage.
- The best results for Marala Barrage were obtained by applying the three distinct regression equations developed for main weir. It is however important to mention that in real time operation, it is hard to fix the gate settings at a uniform opening during flood days.

Establishment of Stage-Discharge Relationships

Stage-Discharge relationships were established with 95% confidence intervals using the discharge measurements carried out for the current study.

Stage-discharge relations were established on thirteen (13) locations downstream head-regulators of the canals off taking from the four barrages. All stage-discharge relations are of the shifted power type;

$Q = K\,(h+a)^{n}$

Where,
Q = Discharge (cusecs)
K = Coefficient
h = Gauge height (ft)
a = Correction to reflect the stage of zero discharge
n = Exponent

Table E-1 gives the details of stage-discharge relationships for all the canals.

Table E-1: Stage -Discharge Relationships for the Canals

Sr. No.	Canal	Location	Stage-Discharge Relationship
1	Chashma Right Bank Canal (CRBC)*	Downstream Head Regulator	$Q = 2.44(h-0.181)^{3.003}$
2	Chashm Jhelum (CJ) Link Canal	Downstream Thal Canal X-Regulator RD-36+000	$Q = 993.01(h-1.807)^{1.27}$
3	Muzaffargarh Canal	Downstream Head Regulator	$Q = 400.63(h-6.133)^{1.5}$
4	Muzaffargarh Canal	RD 5+500	$Q = 9.9535(h)^{3.0674}$
5	Dera Ghazi (DG) Khan Canal	Downstream Head Regulator	$Q = 217.58(h-3.426)^{1.491}$
6	Dera Ghazi (DG) Khan Canal	RD 21+500	$Q = 36.641(h)^{2.0958}$
7	Taunsa Panjnad (TP) Link Canal	Downstream Head Regulator	$Q = 1273.7(h-1.579)^{1.1}$
8	Ghotki Feeder Canal	Downstream Head Regulator	$Q = 199.3(h-0.643)^{1.722}$
9	Begari Sindh Feeder Canal	Downstream Head Regulator	$Q = 325.87(h-1.448)^{1.72}$
10	Desert Pat Feeder Canal	Downstream Head Regulator	$Q = 89.02(h+1.995)^{1.966}$
11	Pat Feeder Canal	Downstream Cross Regulator RD 109+000	$Q = 44.961(h)^{2.0309}$
12	Kirther Canal	Downstream Garang Cross Regulator RD-102+000 (Kharif)	$Q = 60.73(h)^{1.6463}$
		Downstream Garang Cross Regulator RD-102+000 (Rabi)	$Q = 9.97(h)^{2.4141}$
13	Marala Ravi (MR) Link Canal	Downstream Head Regulator	$Q = 71.94(h-0.456)^{1.987}$

***** The stage-discharge relationship was not recommended for reasons elaborated in Flow Measurement Report (Volume-III)

Development of Standardised Flow Measurement System at Five Pilot Sites

The salient features of the standardised system comprise:

(i) calibrated discharge coefficients at barrages and canal heads
(ii) standard procedure for revision of stage-discharge relationships at canals

The steps involved in devising a standardised flow measurement system includes;

1. *Use of standard formulas at each site for respective flow conditions (Free Orifice, Submerged Orifice, Free Weir or Submerged Weir):* For different flow conditions, the formulas defined by ISO along with recommended methodology and definition of parameters should be implemented at 5 pilot sites to keep uniformity in computational methodologies.
2. *Use of standard coefficients, as available in literature, in formulas corresponding to respective flow conditions:* As a first step, use of calibrated discharge coefficients as estimated under current studies are advised to be implemented for the flow ranges corresponding to which they were calibrated for each of 5 pilot sites. The flow ranges covered in the study were the dominant flow range covering flows of more than 95% of the time.
3. *Shifting of canal measurements form rating curve method to structure formula method:* The rating curves need continuous adjustment/ correction due to morphological changes in the channel and annual desilting activity at each canal.
4. *Observation and transmission of real-time gauge and gate opening data:* It is recommended that existing telemetry system should be replaced/updated with latest technology available for transparent and efficient data communication. The new/improved system may be installed at the 5 pilot sites, initially, to monitor the performance for at least two seasons before implementing the same to whole system of 23 sites.

Review and Give Recommendations for Upgrading/Development of Water Distribution Monitoring System

The Consultants conducted a comprehensive condition survey of the existing telemetry network by the electronics engineers of Consultants and the staff of WAPDA telemetry directorate on all the 23 sites of IBIS. This survey provided basis for giving recommendations to upgrade/develop a comprehensive system of monitoring of water distribution.

Two solutions were proposed i.e. alternatives for fixing the existing system (updating) and secondly replacing with a totally new system altogether. Further it was concluded that updating the existing telemetry system is not a long term solution as the refurbished system would have an active life span of 3-5 years. Further, it is recommended that for a reliable and obsolescence proof long term solution which enjoys the full confidence of all the stakeholders, a completely new system shall need to be designed, procured and commissioned from scratch. Nevertheless for either of the options to be practicable it has been recommended that the system be maintained and operated by none other than the owner of the system i.e., IRSA.

Keeping in view the lessons learnt and the technological advancements, the Consultants have proposed three options with rudimentary cost estimates for developing a totally new telemetry system for IBIS. The various options concluded rudimentary cost estimates of Rs. 866 million, Rs 1,251 million and Rs 902 million for Options A, B and C, respectively. The options included installation of absolute gate positioning sensors, water level observation sensors, improved power backups, Micro power PLCs, video surveillance (optional) and state of art data communication options.

Review and Development of Water Accounting and Auditing Mechanism

The existing water accounting and auditing mechanism of IRSA were reviewed. Based on the available data and procedures adopted for estimation of water share amongst the provinces, details updated mechanism for water accounting and auditing were provided. The audit and accounting included water availability, provincial utilization and system loss and gain in Indus Basin Irrigation System (IBIS). MIS and webGIS components of the MIS/GIS and DSS application were accordingly updated.

Proposal for Implementation of Findings of Study

To implement findings of the study, through provincial irrigation departments (PIDs), following key tasks were proposed.

Standardization of flow measurements for 5 pilot sites: Estimate discharges at 5 pilot sites using developed formulas, improved coefficients and procedures recommended under current studies. The flow measurements be made frequently at least fortnightly basis, to verify the validity of ratings at canals. PIDs to follow the flow measurement methodology (mid-section with at least 25 verticals) for carrying out discharge measurements at canals. Future measurements should be carried out through ADCP to minimize the physical efforts and increase the measurement accuracy.

Standardization of flow measurements for 18 remaining sites: Based on the consensus developed among the stakeholders for flow measurement procedure, methodologies used in development of stage-discharge rating and calibration of discharge coefficients, as agreed in the consultative meetings, the same approaches be initiated for remaining 18 IBIS flow monitoring sites. Stage-discharge ratings at canals and calibration of discharge coefficients at barrages be developed using the procedures developed in the present study. In parallel, model studies be initiated at barrages and canal head regulators for better estimation of discharge coefficients under various flow ranges. Validate results of sectional model formulas through physical flow measurements covering flow ranges up to high flood level at barrage locations.

Water distribution monitoring system: Various alternatives have been proposed to make the existing telemetry system operational. However, the updated telemetry system would have an active life span of 3-5 years. Therefore, for a reliable and obsolescence proof long term solution which enjoys the full confidence of all the stakeholders, a completely new telemetry system shall need to be designed procured and commissioned from scratch. For the best techno economical solution, it is imperative that an independent yet comprehensive design exercise be conducted. Herein all present day, state of art available technologies and equipment should be studied culminating in the proposal of a new system.

Hydrologic Modelling for Flow Forecasting of Indus River Basin

The models like UBCWM setup the Hydrology and Research Directorate of WAPDA, Statistical model by IRSA and Hydromet Model 1 by Pakistan Meteorological Department were reviewed in order to avoid the repetition of the work already done.

Different off-the-shelf available models like CREST, TOPKAPI, SRM and SRM+G were tested and applied in the different sub-catchments of the UIB. The input data preparation for the CREST model was so lengthy that was not possible to use this model in the operational forecast. TOPKAPI was a good model with GIS compatible GUI but it works fine only for the areas having the elevation of less than 4,000 m asl. Finally, Snowmelt runoff model (SRM) was tested as it was successfully developed and applied by the Consultants for the Mangla watershed. The problem in using the SRM was that it only considers the snow, while in the case of UIB there is quite a large area covered with the glaciers which emphasis to incorporate the glacier component in the model. A customize model named SRM+G, where “G” stands for glaciers was developed and successfully applied in this study.

The input data for SRM+G is the snow cover area obtained from the MODIS satellite, with a resolution of approximately 500m, precipitation data downloaded from NOAA RFE rainfall estimates for central Asia, with a resolution of 10km, glacier exposed area, obtained from the LANDSAT satellite and temperatures downloaded from the Global summary of the day data source. While daily discharge data is needed to compare the simulated and observed flows in order to check the model accuracy.

The SRM+G was calibrated and validated for the UIB using 2003-2012 satellite data. For the forecasting of flows the scenario based approach was used. In this approach, the initial condition was taken from the 2014 observed data while the seasonal input data came from the historic observed data. It was very difficult to get the daily quantitative forecast for six months, therefore, the scenario approach was used which gave very promising results.

Finally, UIB was divided into two sub-catchments i.e., (i) upstream of Khurmong and (ii) between Khurmong and Tarbela. SRM+G calibrated and validated for both the Upper and Lower catchments. The hind-cast results after combining the flows generated from both catchments are given in Table E-2 to Table E-4.

Table E-2: Indus @ Tarbela Kharif Results Comparison for three Models

Total Kharif [SRM+G]					Total Kharif [IRSA]			Total Kharif [UBCWM]		
Years	**Observed**	**Most Likely**	**Error**	**|Error| [ABS]**	**Most Likely**	**Error**	**|Error| [ABS]**	**Most Likely**	**Error**	**|Error| [ABS]**
2003	55.1	51.3	-7%	7%	52.0	-6%	6%	51.6	-6%	6%
2004	42.1	49.4	17%	17%	49.2	17%	17%	51.7	23%	23%
2005	56.0	49.5	-12%	12%	56.1	0%	0%	59.6	6%	6%
2006	55.1	50.1	-9%	9%	55.6	1%	1%	59.6	8%	8%
2007	49.2	49.6	1%	1%	60.9	24%	24%	57.0	16%	16%
2008	46.9	43.8	-7%	7%	55.7	19%	19%	48.1	3%	3%
2009	46.8	50.7	8%	8%	51.8	11%	11%	54.6	17%	17%
2010	62.3	49.9	-20%	20%	51.5	-17%	17%	55.6	-11%	11%
2011	48.8	48.7	0%	0%	54.6	12%	12%	57.6	18%	18%
2012	45.0	49.1	9%	9%	49.8	11%	11%	50.2	12%	12%

Total Kharif [SRM+G]					Total Kharif [IRSA]			Total Kharif [UBCWM]		
Years	**Observed**	**Most Likely**	**Error**	**|Error| [ABS]**	**Most Likely**	**Error**	**|Error| [ABS]**	**Most Likely**	**Error**	**|Error| [ABS]**
2013	53.3	48.6	-9%	9%	52.8	-1%	1%	47.8	-10%	10%
2014	43.0	49.9	16%	16%	52.5	22%	22%	52.2	21%	21%
Bias/Absolute Average Error			**-0.9%**	**9.6%**		**7.7%**	**11.7%**		**8.0%**	**12.6%**
Average Error (Excluding Flood year-2010)				**8.7%**			**11.2%**			**12.8%**

Table E-3: Indus @ Tarbela Early Kharif Results Comparison

Early Kharif [SRM+G]					Early Kharif [IRSA]		
Years	**Observed**	**Most Likely**	**Error**	**|Error| [ABS]**	**Most Likely**	**Error**	**|Error| [ABS]**
2003	12.0	10.4	-13%	13%	8.1	-32%	32%
2004	9.1	9.0	0%	0%	8.1	-11%	11%
2005	9.1	9.8	7%	7%	9.5	4%	4%
2006	12.1	9.5	-22%	22%	9.5	-21%	21%
2007	10.6	9.5	-10%	10%	10.5	-2%	2%
2008	9.1	7.9	-14%	14%	9.2	1%	1%
2009	9.7	10.0	3%	3%	8.4	-13%	13%
2010	8.6	9.8	15%	15%	9.2	7%	7%
2011	10.8	9.7	-10%	10%	9.9	-8%	8%
2012	6.6	9.3	41%	41%	8.9	34%	34%
2013	8.6	9.2	7%	7%	9.5	11%	11%
2014	6.6	9.8	50%	50%	9.5	44%	44%
Bias/Absolute Average Error			**4.5%**	**16.0%**		**1.3%**	**15.8%**

Table E-4: Indus @ Tarbela Late Kharif Results Comparison

Late Kharif [SRM+G]					Late Kharif [IRSA]		
Years	**Observed**	**Most Likely**	**Error**	**|Error| [ABS]**	**Most Likely**	**Error**	**|Error| [ABS]**
2003	43.1	40.9	-5%	5%	43.9	2%	2%
2004	33.0	40.4	22%	22%	41.1	25%	25%
2005	46.9	39.7	-15%	15%	46.5	-1%	1%
2006	43.0	40.6	-5%	5%	46.1	7%	7%
2007	38.5	40.0	4%	4%	50.5	31%	31%
2008	37.8	35.9	-5%	5%	46.5	23%	23%
2009	37.1	40.7	10%	10%	43.4	17%	17%
2010	53.7	40.1	-25%	25%	42.3	-21%	21%
2011	38.0	39.0	3%	3%	44.7	18%	18%
2012	38.4	39.8	4%	4%	40.9	7%	7%
2013	44.7	39.5	-12%	12%	43.3	-3%	3%
2014	36.4	40.2	10%	10%	43.1	18%	18%
Bias/Absolute Average Error			**-1.3%**	**10.1%**		**10.2%**	**14.4%**
Average Error (Excluding Flood year-2010)				**8.7%**			**13.7%**

Climate Change Impacts in the Upper Indus Basin

The study was intended to give orientation in the future development of water resources in the Upper Indus Basin under the assumption of different climate change scenarios. Particular interest was on the impact of climate change on downstream water availability e.g., needed for irrigation and how the situation of glaciers might change over the next 100 years. For reasons their still remain uncertainties in the reliable description of both future climate situation(s) and in the quantification of its possible impacts on water resources in the UIB. Nevertheless, presented results describe realistic, general developments of the future situation of climate, water and glaciers in UIB.

The study used data from General Circulation Models (GCM) to describe future climate change and used this information as an input to hydrological models to describe the situation of current, hydro-meteorological parameters as well as the changes they undergo under a B1, an A1b and an A2 climate change scenarios.

Though GCM data from state of the art climate change models was used. It is important to mention that modelled parameters may not perfectly describe neither the current nor the future climate situation in all details. While there is great confidence into the general, global trends given by these data, local characteristics may be described with less accuracy with regard to their timing and their magnitude. For the region of the UIB the role of the El Nino and its effects on the Indian monsoon that make long term forecasts difficult and causes climate models to produce controversial results, are uncertain. As climate models as well as hydrological models are continuously improving, it is advisable to update climate and hydrological studies in future to narrow the spread in predicted climate and hydrological variables, thus increasing our confidence in modelled scenarios. The decadal change in annual discharge volume and Glacierized area due to various climate change scenarios are given in Table E-5 and Table E-6, respectively.

Table E-5: Approximates of Projected Average Decadal Glacier Losses under Different Climate Change Scenarios

Decade	Glacierized Area (2013) [km^2]	B1		A1b		A2	
		Glacierized Area [%]	Glacierized Area [km^2]	Glacierized Area[2] [%]	Glacierized Area [km^2]	Glacierized Area [%]	Glacierized Area [km^2]
2000-2009	16,746	100	16,746	100	16,746	100	16,746
2010-2019		87	14,550	90	15,050	93	15,546
2020-2029		80	13,413	77	12,931	75	12,580
2030-2039		77	12,871	73	12,305	72	12,042
2040-2049		73	12,213	61	10,258	62	10,318
2050-2059		64	10,646	50	8,381	63	10,466
2060-2069		62	10,434	42	7,068	32	5,428
2070-2079		53	8,827	35	5,918	22	3,753
2080-2089		55	9,202	34	5,735	16	2,723
2090-2099		49	8,142	25	4,152	7	1,152

Table E-6: Approximates of Change in Indus River Discharge for Different Climate Change Scenarios

Decade	Average annual total discharge (1969-2006) [km^3]	B1		A1b		A2	
		Change in discharge [%]	Change in discharge [km^3]	Change in discharge [%]	Change in discharge [km^3]	Change in discharge [%]	Change in discharge [km^3]
	77						
2000-2009		0	77	0	77	0	77
2010-2019		-7	72	-10	69	-2	75
2020-2029		-4	74	-4	74	-2	75
2030-2039		0	77	4	80	2	79
2040-2049		4	80	9	84	4	80
2050-2059		6	82	8	83	11	85
2060-2069		6	81	7	83	5	81
2070-2079		8	83	11	85	10	85
2080-2089		8	83	14	88	13	87
2090-2099		10	84	11	85	5	81

The negative signs are because of the removal of the glacier tongues from the analysis. Which amounts to reduction of about 1/3rd to the actual glacier coverage.

The overall observation from the climate change results showed that there is a decreasing trend in the glacier covered area and by the end of this century the glacier covered area will reduce to 6.88% as per A2 emission scenario. On the other hand, the average annual flow volume is showing the increasing trend and there will be approximately 14% to 21% increment in the flow volumes by the end of the century, depending on scenario. Evaporative losses will increase to about 25% by 2099. Peak flows will be reached at around mid-century (A2) and 2080 (A1b). Peak flows for a B1 scenario fall beyond this century. This is also worth noting that there will be seasonal shift in the flow patterns and according to these shifted patterns there will be change in irrigated agriculture priorities.

1 INTRODUCTION

1.1 BACKGROUND

On March 21, 1991, the four provinces of Pakistan signed to an agreement to apportion the waters of the Indus system of rivers. As per the agreement, a distribution framework was established for sharing the waters of the Indus River System. This agreement is known as the Water Apportionment Accord (WAA) of 1991.

The Indus River System Authority (IRSA) was established on December 10, 1992 with the purpose of regulating and monitoring the distribution of waters of the Indus River System in accordance with the WAA of 1991. Powers and duties of IRSA are detailed in Government of Pakistan's Act No. XXII of 1992 (Pakistan, IRSA Act No. XXII of 1992). IRSA's powers and duties include reservoir, river and canal operations in accordance with the WAA of 1991, and irrigation and hydropower requirements.

Accurate and reliable flow measurement system is a pre-requisite to ensure fair and equitable distribution of river supplies among the provinces, which is the prime responsibility of IRSA. Although the telemetry system at 23 locations was installed in 2004, as per IRSA's understanding, the procedure for computation of discharges incorporated in the software was based on un-calibrated formulae/discharge relationships provided by the provincial irrigation departments/barrage offices.

In addition, the mismatch between manually measured and electronic data allegedly created controversies that resulted in mistrust on the computed discharges among the provinces/ stakeholders. These discharge formulae therefore need refinements and/or improvements in order to accurately compute the flows through the gate openings and stage data. In this regard it is necessary to review, and if required validate/improve the discharge formulae and a methodology should be adopted to diagnose and rectify/calibrate/up-grade the system for satisfaction of stakeholders and ensuring the accurate distribution of irrigation flows, to the extent possible.

In this study, beside reviewing and rectifying the existing flow measurement system at control structures in the system, a river flow forecasting system for upper Indus basin i.e. upstream of Tarbela dam was required to be developed as flows from Upper Indus Basin (UIB) are stored in Tarbela dam which along with Mangla Dam plays a vital role in regulating water supplies to the Indus irrigated areas. Around 90% of the Upper Indus Basin lies in the rain shadow of the Himalayas and is not directly affected by the summer monsoons. The snowmelt and glacier runoff in the higher altitudes of the UIB and intense rainfall runoff in the lower altitudes of UIB contributes mainly towards the inflow to Tarbela reservoir. Base-flow generated from snowmelt is of prime importance and a major source of water-supplies to irrigate the Indus Basin downstream of Tarbela reservoir both in Rabi and Kharif seasons.

It is postulated that the climate change is causing glaciers to retreat and deterioration of watersheds thus posing potential threats to the sustainability of the Indus Basin Irrigation System (IBIS) and increasing the severity of floods and droughts. It was therefore contemplated to develop an improved river flow forecasting system to assess the variability in river flows due to climate-change impacts on the upper catchments and their corresponding impacts on the water availability for agriculture as well as other usage in IBIS.

The report in hand is the outcome of the study which intended to develop a reliable and transparent water flow measurement system and also to develop a river flow forecasting system to study the change in Indus River flows due to climate change impacts on the Upper Indus Basin under Water Sector Capacity Building and Advisory Services Project (WCAP) funded by the World Bank. The funding was a part of the World Bank assistance to strengthen the water resources management and strategic planning capability of IRSA.

1.2 OBJECTIVES OF THE STUDY

The overall aim of the study was to develop an effective, reliable and transparent flow measurement system at five (5) pilot sites amongst the twenty three (23) key water regulation/distribution sites as given in Table 1-1 below, to ensure the effective water resources management of the IBIS in context of substantial economic, social and environmental changes. Figure 1-1 shows schematic diagram of IBIS along with location of 05 pilot sites.

Table 1-1: Key Water Regulation/Distribution Sites of IBIS

Sr. No.	Locations		Sr. No.	Locations
1	Tarbela Dam/Ghazi Barrage		13	Khanki Head-works
2	Noshera		14	Qadirabad Barrage
3	Jinnah Barrage		15	Trimmu Head-works
4	Chashma Barrage	***(pilot site 1)***	16	Panjnad Head-works
5	Taunsa Barrage	***(pilot site 2)***	17	Balloki Head-works
6	Guddu Barrage	***(pilot site 3)***	18	Sidhnai Barrage
7	Sukkur Barrage		19	Sulemanki Barrage
8	Garang Regulator-Kirther Canal	***(pilot site 4)***	20	Islam Head-works
9	Kotri Barrage		21	Pat Feeder Canal (RD 109)
10	Mangla Dam		22	Uch Canal
11	Rasul Barrage		23	Manuthy Canal
12	Marala Barrage	***(pilot site 5)***	-	-

The main objectives of the study were:

(i) Development of stage-discharge relationships and calibration of discharge coefficients ‘Cd’ after discharge measurements at the five pilot sites for different flow conditions (ranging from low to high flows).

(ii) Development of water monitoring, accounting and auditing system for proper water distribution and sharing among the stakeholders at the five pilot sites.

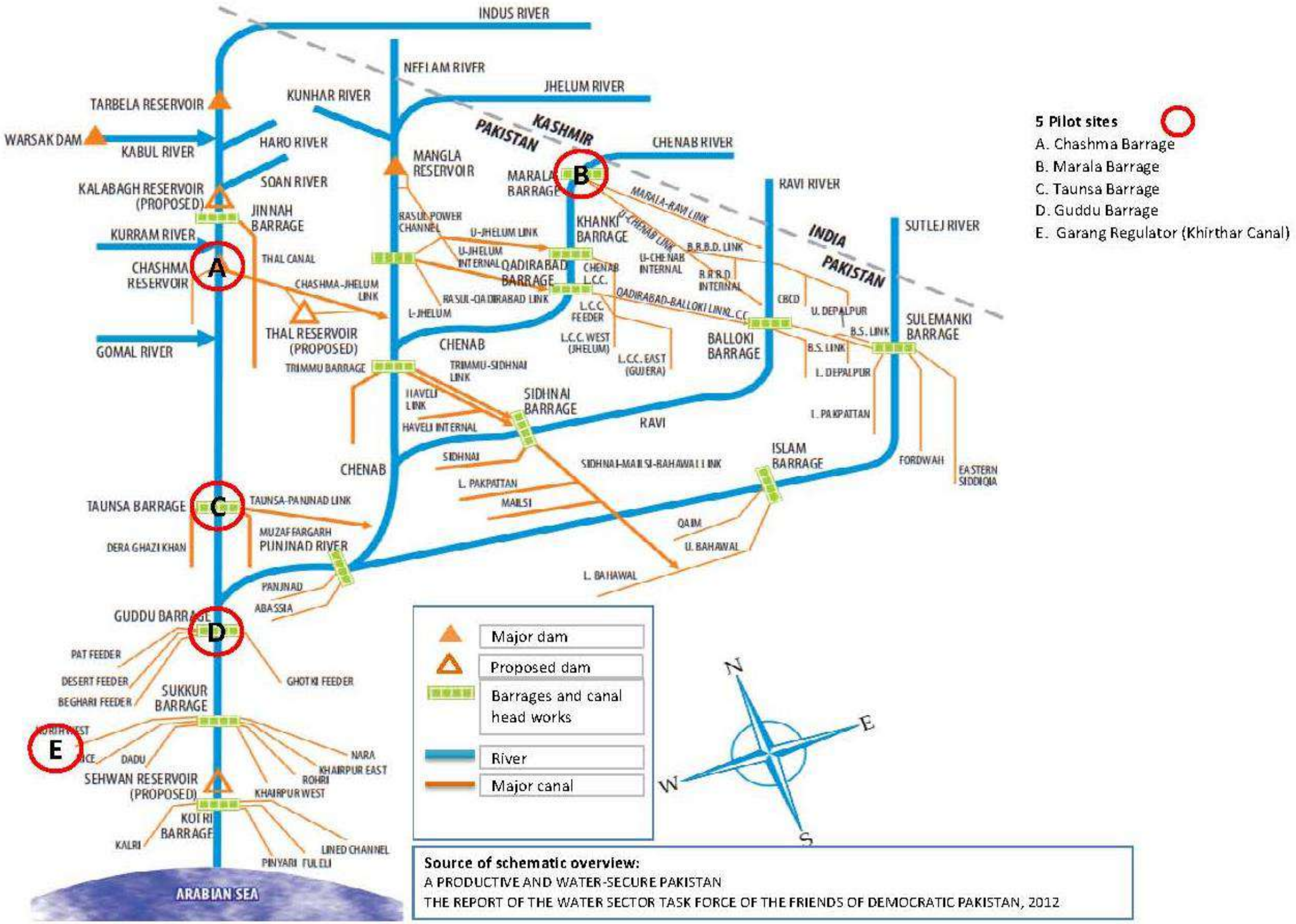

Figure 1-1: Schematic Diagram of IBIS Showing Location of 05 Pilot Sites

(iii) Give recommendations for development of water monitoring, accounting and auditing system for proper water distribution and sharing among the stakeholders at remaining (other than five pilot) sites of IBIS.

(iv) Development of an improved river flow forecasting system to assess the vulnerability of the river inflows due to climate change impacts in the upper Indus catchment for adopting and practicing the integrated approach of water resources management to assure the sustainable availability of water resource.

1.3 SCOPE OF SERVICES

The Consultants scope of services comprised two main tasks viz. (i) river flow measurements, and (ii) flow forecasting of Upper Indus basin; details are as follows:

1.3.1 Task-I: River Flow Measurements at 5 Pilot Sites to Monitor the Storage and Flow of Major Components of the Indus Basin Irrigation System

(i) Review and analyse all available information on flow measurement at all 23 sites in IBIS (Table 1-1) with reference to their formulae, discharge coefficients, stage discharge relationships and receiving and transmitting of data for operation of IBIS.

(ii) Development of stage-discharge relationships and calibration of discharge coefficients after discharge measurements for different flow conditions (ranging from low to high flow conditions) at five (5) pilot water regulation/distribution sites mentioned below:

- Chashma Barrage
- Taunsa Barrage
- Guddu Barrage
- Garang Regulator - Kirther Canal
- Marala Barrage

(iii) Design and development of a standardized water flow measurement system at five (5) pilot sites and give comprehensive recommendations for a reliable flow measurement system at remaining eighteen (18) sites of the IBIS to enhance transparency and efficiency in the water distribution system and efficient and transparent retrieval and transmittal of data for management and operation of IBIS.

(iv) Review and recommend for upgrading/developing a comprehensive monitoring system for transparent water distribution amongst the provinces.

(v) Review and develop a mechanism of proper water accounting and auditing on the water distribution and sharing of the stakeholders.

(vi) Hold consultative meetings with all IRSA's stakeholders (four provinces and WAPDA) to assess the full implications of flow measurements and to ensure the consensus on procedures/methodology and finding/outcomes. Also ensure that those stakeholders which could not be consulted in this process should have the opportunity to provide their opinion/feedback.

(vii) Formulate a proposal for implementation of recommendations and findings of the study (standardized water flow measurement, water distribution monitoring system and mechanism of proper water accounting and auditing) with full participation/consensus of IRSA and its stakeholders (four provinces and WAPDA).

(viii) Develop procedures to link these developments to Indus Basin Decision Support System (DSS) in consultation with IRSA.

1.3.2 Task-II: Hydrological Modelling for Flow Forecasting of Upper Indus Basin (Upstream of Tarbela)

(i) Review all existing information and previous studies carried out by various departments, organizations, agencies, and research institutions in areas of Upper Indus Basin for flow forecasting and climate change impacts evaluation (but not limited to Snow and Ice Hydrology Project as of WAPDA) and identify key gaps and uncertainties associated with the forecast of inflows of Upper Indus Basin.

(ii) Select appropriate snow/glacier melt model that can be used in conjunction with Remote Sensing Data for flow forecasting of upper Indus Basin above Tarbela.

(iii) Develop procedures for main hydrological activities of melt of seasonal snow and glacier forecast for information on early Kharif snow melt and 10-day flow forecasts for Indus River at Tarbela as per IRSA's requirements.

(iv) Calibrate and validate all developed procedures using previous available records in consultation with IRSA.

(v) Assess change in Indus River inflows at Tarbela due to global warming or climate change impacts in the Upper Indus Basin.

(vi) Design and develop procedures to link all developed model/procedures to Indus Basin Decision Support System (DSS).

(vii) Conduct training programs for relevant staff of IRSA on the River Flow Forecasting System and prepare training modules.

1.3.3 Additional Services

As per requirement of the Client and stakeholders additional services were agreed with the Consultants vide Amendment No. 3. Scope of the “Additional Services” was included.

(i) Carryout additional flow measurements at Garang and Saifullah Magsi for Kharif 2015 to include/improve the stage-discharge relationship for Kirther Canal.

(ii) Flow measurements at Pat Feeder Canal at RD 109+000 and installation of Gauges.

(iii) Flow measurements at Chashma Right Bank Canal's cross regulators at Stage-II and III including Ramak at RD 513+000.

1.4 DELIVERABLES

The deliverables of the study were as follows:

(i) Inception Report
(ii) Interim Report
(iii) Mid Term Report
(iv) Technical Report on Calibration of Cds and Development of Ratings for the Five Pilot Sites
(v) Draft Final Study Report
(vi) Final Study Report

Briefs of the reports submitted under the project, are given hereunder.

1.4.1 Inception Report

The report presented the data collection and review methodologies at 23 key water distribution sites which was also shared with the executive engineers of all barrages in IBIS. Methodology of discharge measurements downstream of the barrage was also made part of the report. At the Inception stage of the project, the Consultants invited the stakeholders to witness the calibration of the current meters to be used in flow measurement activity at five pilot sites. During this calibration activity, eight current meters of ISRIP were individually calibrated and the distinct equations for conversion of rotor revolutions in a given time to the flow velocity, were developed and shared with the stakeholders for review and comment.

Pursuant to the calibration activity, nominated focal person of Sindh Irrigation Department (SID) raised several differences in the calibration process and suggested of procuring the new current meters; all the other stakeholders were satisfied with the overall activity undertaken to calibrate the current meters. The Consultants submitted a technical reply (made part of the report) and resolved the differences which did not technically hold. Nevertheless, given the fact that confidence of all the stakeholders in all the activities of the project was of paramount importance, procurement of two brand-new current meters had been effected which were used in flow measurement activity, subsequent to submission of the report.

As regards to Task-II, the report presented the methodology for modelling hydrological process of Upper Indus River Basin (UIB). Details of available satellite data of temperature, precipitation, glaciers and snow were also discussed in the report.

The Inception Report was also presented to all stakeholders of the project in a workshop held on March 24, 2014 wherein the report was approved without any comments except on the overall progress of the study.

1.4.2 Interim Report

The report presented the progress achieved till the time of its submission, on the activities pertaining to Tasks I & II of the contract i.e., (I) physical flow measurements at the five pilot sites and the development of reliable water distribution system, and (II) development of snow and glacial melt modelling for UIB upstream of Tarbela for having reliable forecast of the runoff available for distribution.

The report provided the description of the accomplished activities and the discussion on the interim outcomes of the ongoing activities. Besides, the report also provided the future course to be adopted to achieve the successful accomplishment of the given scope of services.

An appraisal of the challenges and way forward relevant to the successful completion of the study was also presented along with the revised schedule of activities. Though ‘First Flow Measurement Report’ was to be included as part of the ‘Mid-Term Report’, however, keeping in view the progress achieved for flow measurement activity, the ‘First Flow Measurement Report’ was appended in the ‘Interim Report’.

As mentioned above, the report was supported with the Annexes and Appendices to provide the field data of flow measurements at the five pilot sites and the discharge calculation procedure for the selective periods representing different flow conditions, followed by PIDs and WAPDA at various key water regulation/distribution sites. The field data of the flow measurement accomplished was provided in the form of appendices, whereas the selective record of discharge calculations and the other relevant details at various water regulation sites were included in the report as annexes. A detailed modelling report concerning the outcomes from the trial runs of the selected glacial and snowmelt model was also provided in the report.

The Interim Report was presented to all stakeholders of the project in a workshop held on October 14, 2014 wherein the report was approved without any comments except on the overall progress of the study.

1.4.3 Mid-Term Report

The report presented the updated progress on various activities being carried out in accordance with the Terms of Reference of the study subsequent to submission of Interim Report of the project. Through review of literature was made while arriving at technical reference for Hydraulic Formulae for the various flow condition and the same was presented in the report as an annexure.

Initial working of stage-discharge relationships for Kharif and Rabi seasons at Garang regulator and calibration of discharge coefficient at Taunsa barrage were presented in the report. Water accounting and auditing mechanism implemented at IRSA, was reviewed and calculations based on two seasons and for two zones were presented in the report for the last 11-years (2003-04 to 2013-14). The water audit and accounts included water availability, provincial utilization and system loss/gain.

Evaluation of various candidate models was made and Snow Runoff Model (SRM) and SRM+G was selected as snow runoff and glacier runoff simulations. Snow/glacier modelling procedures were presented in the report.

The Mid-Term Report was presented to all stakeholders of the project in a workshop held on December 23, 2014 wherein the report was approved without any comments except few comments on presentation of flow measurement data at Garang regulator. The comments were incorporated and made part of the Final Mid Term Report.

1.4.4 Technical Report on Calibration of Cds and Development of Ratings for the Five Pilot Sites

The report presented the outcome of flow measurement activity at the five pilot sites. The report highlighted the uncertainty analysis of all the flow measurements carried out at the five pilot sites. The analysis showed that 95% confidence interval for the measured discharge was between 3-5% for 93% of the measurements in the flow measurement missions.

The procedure of calibration of discharge coefficients (Cds) at the five pilot sites were discussed in detail. Calibrated Cds at the Chashma, Taunsa, Guddu and Marala were presented in the report.

Stage-discharge relationship at canals off-taking from the above mentioned barrage locations, Garang regulator and Pat Feeder were prepared using the flow measurements and presented in tabular form in the report.

The Technical Report was presented to all stakeholders of the project in a workshop held on June 06, 2015 wherein the calibrated Cds at barrages and stage-discharge relations at canals, developed by the consultants as an outcome of the flow measurement activity were discussed at length and approved.

1.4.5 Draft Final Study Report

The Draft Final Report highlighted the various outcome of the tasks carried out during the course of the study. The report presented the methodology adopted in carrying out flow measurement, calibration of the equipment and various flow measurements carried out at the 5 pilot sites. The report also presented various analyses carried out to arrive at calibration of discharge coefficients at the barrage locations and stage-discharge relationships at the canal sites. The important analysis reported was the uncertainty analysis which concluded that 95% of the flow measurements are within uncertainty range of 3-5% while the remaining 5% are within 5-8%. This showed that the flow measurements are reliable with error margin of only 3-5% and can be used with confidence for further analysis. Based on the reliable outcome of the flow measurement, further analyses were carried out for calibration of Cds and stage-discharge relationships.

The report discussed various regressed equations for estimation of flows at barrages and canals. The comparisons of measured discharges at the f5 pilot sites with regressed equations, literature (ISO/M.G. Bos) and PID estimates showed that the recommended regressed equations resulted in better estimate of discharges.

The review and analysed of discharge measurements at the remaining 18 key sites were also presented in the report. It was concluded that the physical model studies and actual discharge measurements, as carried out at the pilot sites may be initiated to ascertain the accuracy of discharge estimates.

Mechanism for water audit and accounts were prepared and presented in the report. The mechanism was incorporated in the MIS/GIS and DSS application, developed under a separate study funded by WCAP.

The report presented the snow runoff modelling results using the observed weather data of stations operated by Pakistan Meteorological Department (PMD) and Snow and Ice Hydrology, WAPDA. The report showed that the forecasting results obtained were within acceptable limits, however, the comparison of Early Kharif and Late Kharif demanded further refinement of the forecasting model. Revised methodology split the catchment into two basins and the results showed improvements not only in total Kharif but also in early and late Kharif as compared to statistical approach as well as over UBC by WAPDA.

The review of telemetry system was also presented in the report which concluded that the system has outlived its useful capacity and should be replaced with new using available technological advancements in data communication systems.

The report was finalized after detailed discussions on the in the Workshop held on September 09, 2015 and comments received from various stakeholders.

1.4.6 Final Study Report

The report in hand is the Final Report of the study which incorporated all the comments raised by the stakeholders in the various workshops/meetings in particular workshop of September 09, 2015 where the draft final report was presented to various stakeholders including focal persons from provincial irrigation departments, system regulation staff from barrages and canals and WAPDA.

The Final Study Report has been prepared and presented separately in the following three (03) volumes:

Volume I Final Report
Volume II Annexures to Final Report
Volume III Flow Measurement Report

Volume I (Final Report) contains an executive summary giving a brief synopsis of the final study report.

Chapter 1 gives the background of the project, describes its objectives, scope of services and details of the various submissions made during the study duration, Minutes/proceedings of the various stakeholders' workshops/meetings have also been presented in Chapter 1.

Chapter 2 describes the various outcomes of the Task-I related to river flow measurements at 5 pilot sites to monitor the storage and flow of major components of the Indus Basin Irrigation System.

Chapter 3 provides details of hydrological modelling for flow forecasting of Upper Indus Basin, upstream of Tarbela.

1.5 CONSULTATIVE MEETINGS/WORKSHOPS

The study was designed to involve all the stakeholders which included provincial irrigation departments and WAPDA to involve and witness all the field activities. Similarly the terms of reference of the Consultants demanded to involve the stakeholders in each phase of development of the project components. Further, stakeholders' consultation/incorporation of comments were made compulsory in approval of all the Consultants' reports.

The project started with the consultative meeting held at IRSA headquarters, Islamabad on September 16, 2013 within first week of mobilization of consultants. The agenda of the consultative meeting was to get the opinion of IRSA and its stakeholders relating to the implications of flow measurements, and to discuss and arrive at consensus on schedules and procedures/methodology of flow measurement. A working paper, prepared for the consultative meeting, is attached as Annexure-A.

All the stakeholders or their representatives witnessed all the flow measurement missions at 5 pilot sites; thirteen (13) in total. The subsequent sections highlight the various flow measurement missions. Attendance sheets of the various missions are attached as Annexure-B.

A number of workshops/meetings were held on submission of various Consultants reports. The chronology of submitted reports and meetings/workshops is given in Table 1-2 hereunder.

Table 1-2: The Chronology of Submitted Reports and Meetings/Workshops

Sr. No.	Description	Date of Submission	Date of Meeting/ Workshop	Remarks
1	Calibration of Current Meter / Demonstration of flow measurement procedure at Chashma Barrage	-	October 02, 2013 / October 06, 2013	Proceedings of the workshop are enclosed as Annexure-C
2	Inception Report	January 01, 2014	March 24, 2014	Proceedings of the workshop are enclosed as Annexure-D
3	Interim Report	September 10, 2014	October 14, 2014	Proceedings of the workshop are enclosed as Annexure-E
4	Mid-Term Report	December 04, 2014	December 23, 2014	Proceedings of the workshop are enclosed as Annexure-F
5	Workshop on Flow Measurement Missions	-	January 23, 2015	Proceedings of the workshop are enclosed as Annexure-G
6	Technical Report on Calibration of Cds and Development of Ratings for the Five Pilot Sites	May 22, 2015	June 06, 2015	Proceedings of the workshop are enclosed as Annexure-H
7	Draft Final Report	August 03, 2015	September 09, 2015	Proceedings of the workshop are enclosed as Annexure-I

2 TASK-I: RIVER FLOW MEASUREMENTS AT 5 PILOT SITES TO MONITOR THE STORAGE AND FLOW OF MAJOR COMPONENTS OF THE INDUS BASIN IRRIGATION SYSTEM

2.1 REVIEW AND ANALYSIS OF FLOW MEASUREMENT INFORMATION AT 23 KEY WATER REGULATION/DISTRIBUTION SITES

The first sub-task under the Task-I pertained to review and analysis of the available information on flow measurement at all 23 sites in IBIS (Table 1-1) with reference to their formulae, discharge coefficients, stage discharge relationships, and receipt and transmission of data for operation of IBIS.

The review was made to understand the present procedures being followed for flow measurement at the 23 key sites of IBIS. In this regard a generalised methodology was formulated with following components viz.

i. Site visits and data collection;
ii. Review of sites' layouts;
iii. Review of flow measurement and discharge calculation setup; and
iv. Review of data communication protocols.

The first component was for developing a first-hand understanding of the system by visiting at each individual site, interviewing the establishment in-charge, and collecting the relevant data.

The second component related to understanding the perspective of overall layout of each site with reference to water use and accounting. This understanding was considered important to differentiate between the consumptive diversions to provinces (to account for their share as per the WAA 1991) and the non-consumptive diversions for other uses, for instance power generation, cooling, silt management etc. The non-consumptive uses may only be accounted as non-consumptive if the diverted surface water for non-consumptive use is returned to the river.

The third component was included to review the flow measurement and discharge calculation setup being required for ensuring proper water accounting.

The fourth component was included to understand the communication protocols used to transmit discharge information from sites to the stakeholders. This component was incorporated to ensure that current communication protocols at all sites were reviewed and understood.

2.1.1 Site Visits & Data Collection

To determine the correctness of water accounting by means of discharge calculation procedures being practised at the 23 key sites, field visits were conducted and the field formations interviewed. The relevant data required for discharge calculation at the 23 key sites were categorised into three forms, viz. the data required for:

(i) barrages and canal head-regulators
(ii) open profile river gauging station, and
(iii) the dams

The relevant data/parameters collected on the basis of above categorisation are listed below.

(i) <u>Barrages and canal head-regulators</u>

a. Layout plans
b. Upstream and downstream water levels
c. Gate openings
d. Discharge formulae being applied for different flow conditions
e. Configuration of control structure including weir type, shape and crest level
f. Discharge coefficients
g. Upstream and downstream floor levels
h. Number of bays
i. Bay widths
j. Width between abutments
k. The latest stage-discharge rating tables and the canal cross section at the gauge site (for canals only)

(ii) <u>Open profile river gauging station (Noshera)</u>

a. Site layout
b. River cross section
c. The latest stage-discharge rating curve
d. Flow measurement setup i.e. current meter measurements from bridge, boat or cable way
e. Information concerning frequency of flow measurements during flood and normal flows

(iii) <u>Dams (Tarbela, Mangla and Chashma)</u>

a. Layout plans
b. Reservoir levels at dams
c. Spillway type and configurations including crest shape, sill level, overt level (for Mangla's spillway only), bay widths
d. Other outlets' configurations which are used for normal releases
e. Procedure for estimation of inflows and outflows by using the reservoir's latest storage capacity at various levels and the spillways/outlets discharge ratings

The above mentioned data were collected for all 23 sites. Details of site visits are provided in Table 2-1.

Table 2-1: Details of Site Visits for Data Collection Activity

Sr. No.	Site	Visit Dates	Personnel
1.	Tarbela Dam/ Ghazi Barrage	4 Apr, 2014	Muhammad Haseeb
2.	Jinnah Barrage	4-5 Apr, 2014	
3.	Chashma Barrage	2 May, 2014	
4.	Taunsa Barrage	1-2 Jan, 2014	
5.	Guddu Barrage	25-31 Jan, 2014	
6.	Sukkur Barrage		
7.	Kotri Barrage	20-23 May, 2014	Muhammad Umar Farooq
8.	Mangla Dam	17-18 Jan, 2014	Muhammad Haseeb
9.	Rasul Barrage		
10.	Marala Barrage	1-2 Jan, 2014	Dr. Taimoor Akhtar
11.	Khanki Headwork	2-4 Jan, 2014	
12.	Qadirabad Barrage	15-16 Jan, 2014	Muhammad Haseeb
13.	Trimmu Headwork	4 Jan, 2014	
14.	Panjnad Headwork	1-2 May, 2014	
15.	Balloki Headwork	1-2 Nov, 2013	
16.	Sidhnai Barrage	3 Jan, 2014	
17.	Sulemanki Headwork	8-9 Apr, 2014	
18.	Islam Headwork	10-11 Apr, 2014	
19.	Noshera	3 & 7 Apr, 2014	
20.	Garang Regulator – Kirther Canal	16-17 Mar, 2014	
21.	Pat Feeder Canal (RD 109+000)		
22.	Uch Canal		
23.	Manuthy Canal		

2.1.2 Review of Site's Layouts

The data review process envisioned by the Consultants initiates with a general understanding of the layout of each site. In this regard, the sites were divided into four categories, viz. i. Diversion sites, ii. Rights exchange sites, iii. Storage sites, and iv. Stream gauging sites. The primary purpose of this categorisation was to differentiate the 23 key sites with the perspective of water use, required for proper water accounting.

The breakdown of 23 sites into the above mentioned four categories is given below.

2.1.3 Diversion Sites

There are 16 out of 23 key sites in IBIS which can be placed under this category thereby making it the dominant amongst others. List of key sites falling under this category are given in Table 2-2.

Table 2-2: Key Sites under 'Diversion Sites' Category

Sr. No.	Locations	Sr. No.	Locations
1	Jinnah Barrage	9	Khanki Headwork
2	Chashma Barrage	10	Qadirabad Barrage
3	Taunsa Barrage	11	Trimmu Headwork
4	Guddu Barrage	12	Panjnad Headwork
5	Sukkur Barrage	13	Balloki Headwork
6	Kotri Barrage	14	Sidhnai Barrage
7	Rasul Headwork	15	Sulemanki Headwork
8	Marala Barrage	16	Islam Headwork

Diversion sites listed in Table 2-2 can further be categorised into 'consumptive and non-consumptive use' sites with reference to the underlying perspective of water accounting.

The consumptive use sites are those which draw water for irrigation and the water is consumed by the crops. At the non-consumptive sites, water is withdrawn for non-consumptive uses like for cooling of thermal and nuclear power plants facilities at Guddu and Chashma respectively, silt escapes, etc. Besides, the non-consumptive sites also include the diversion of river flows into the inter-river link canals for augmenting the river flows at the receiving end. For example, BS Feeder off-takings from Guddu Barrage; in its initial reach it supplies water for cooling of Guddu thermal plant and returns the water into Indus River during Rabi season, however during Kharif the water drawn for cooling is routed to the BS Feeder again, below the plant. Therefore, the cooling water withdrawal from BS Feeder in Rabi becomes the non-consumptive use and in Kharif the same withdrawal lie under the consumptive use category. These factors are important to consider for proper water accounting and distribution of provincial shares.

2.1.4 Rights Exchange Sites

The 'rights exchange sites' category covers the specific locations where the water rights are transferred from upstream province to the downstream. In the given 23 sites of IBIS, the rights exchange site category includes 4 sites within the IBIS. It is, however, pertinent to note that RD 513+000 of Chashma Right Bank Canal (CRBC) is one of those sites where the water rights exchanged from one province (KP) to the other (Punjab). Since this site was not included in the 23 key sites therefore not counted under this category, however, it is believed that this site should also be made part of the key water regulation/diversion sites in the IBIS for undertaking the proper water accounting of provincial shares as per the WAA of 1991. Taunsa Barrage is another distinct type which at the same time can be categorised as 'Diversion' as well as 'Rights Exchange' site; the water released below Taunsa is for Sindh and Baluchistan. The 4 (+ 2) 'Rights Exchange sites' are listed in Table 2-3.

Table 2-3: Key Sites under 'Rights Exchange' Category

Sr. No.	Locations	Exchange of Water Rights	
		From	To
1	Garang Regulator (Kirther Canal)	Sindh Province	Baluchistan Province
2	Pat Feeder Canal (RD 109)	Sindh Province	Baluchistan Province
3	Uch Canal	Sindh Province	Baluchistan Province
4	Manuthy Canal	Sindh Province	Baluchistan Province
5	CRBC at RD 513+000	KP Province	Punjab Province
6	Taunsa Barrage	Punjab Province	Sindh Province

2.1.5 Storage Sites

The water storage reservoirs at Tarbela, Mangla and Chashma are the three sites which fall under this category. The discharges released, past these dams, are through the power and/or irrigation tunnels and the water exceeding the discharging capacity of the tunnels/outlets is released by opening the spillway gates. Operation of spillways are generally made to release the floods.

2.1.6 Stream Gauging Site

Noshera gauging station is the only site in the 23 key sites which can be placed under this category. This site has been included to account for the river supplies of Kabul and Swat rivers into the Indus. The site is located at some distance upstream of confluence of Kabul River with the Indus. There is no channel off-taking at this site. Water accounting is done by application of stage-discharge relation on the river stages observed at a predetermined interval viz. hourly during the flood season and six hourly during normal (non-flood) season.

The validity/correctness of stage-discharge relation is frequently checked by comparing the rated discharges with the direct measurements at any given river stage. For this purpose the direct measurements of river discharges are undertaken by using a current meter mounted on a trolley-crane which runs at the road bridge across the Kabul River. During normal flows frequency of conducting discharge measurements is at least twice per month, however during flood season the frequency is increased to four per month. At the end of water year i.e. end September, the directly measured discharges along with the corresponding river stages are analysed to ascertain the validity of the last year discharge rating. In case of variation exceeding $\pm$10% between the rated and the direct measured discharges persisted throughout the year of measurement, the rating curve is revised as per the trend analysed from the last year's direct measurements.

2.1.7 Review of Flow Measurement and Discharge Calculation Setup

It was learnt through the interaction with various offices of provincial irrigation departments that as per the official standards flow measurement in rivers and canals is an essential task to be undertaken at frequent intervals by the establishment in-charge at the respective head-works and barrages. However, in actual practice the *direct flow measurements*[1] are not

[1] by making use of current meter or more advanced equipment like Acoustic Doppler Current Profiler (ADCP)

undertaken per se. The water released below the barrage is calculated by application of hydraulic formulae which makes use of gate openings, the upstream and downstream water-levels and the appropriate coefficients subject to various hydraulic and geometric conditions.

The hydraulic conditions can be universally categorised into two main types, and each main type can be further categorised into two sub-types:

I. Orifice condition (partial gate opening)
   a. Free orifice (the orifice is not influenced by the tail-water)
   b. Submerged orifice (the orifice is drowned due to high tail-water)

II. Overflow or weir condition (full gate opening)
   a. Free weir (the discharge flowing above the weir crest is not influenced by the tail-water)
   b. Submerged weir (the discharge flowing above the weir crest is under the influence of tail-water)

Limits of Modularity

In case of weir flow condition i.e. gates fully lifted, as a general guideline, for quick application in field, the weir will be considered drowned when the downstream water level rises to a level greater than two-thirds of the upstream head. Strictly, the tailwater or downstream water level has a small effect even when it is at the level of the weir crest, but this two-thirds criterion is a useful rule of thumb to determine the drowning state of a weir.

In case of orifices or gated flow condition, the limit defined in ISO-13550 is:

$$\frac{y_2}{w} = \frac{C_c}{2} . \left[\sqrt{1 + 16\left(\frac{H_1}{wC_c} - 1 \right)} - 1 \right]$$

where:
y_2 = downstream water level with reference to the weir crest
w = gate opening
C_c = coefficient of contraction which is function of shape of the gate lip
H_1 = upstream energy head

Mathematical forms of hydraulic formulae for various conditions are given below.

<u>Condition I (a): Free Orifice</u>

a. Gates partially opened,
b. standing wave formed, and
c. downstream water level below the weir crest

$$Q = C.B.d.\sqrt{2.g.H} \qquad \text{I (a)}$$

Where: Q = discharge in cusecs
C = discharge coefficient *(varies w.r.t. weir and gate geometry, and head)*

B = bay width in ft.
d = gate opening in ft.
H = working head in ft.; equivalent to (upstream water level minus crest level minus half of gate opening)
g = acceleration due to gravity in ft/s^2

Condition I (b): Submerged Orifice

a. Gates partially opened,
b. No standing wave, and
c. downstream water level above the weir crest

$$Q = C.B.d.\sqrt{2.g.H} \qquad \text{I (b)}$$

Where: Q = discharge in cusecs
C = discharge coefficient *(varies w.r.t. weir and gate geometry, head and drowning ratio)*
B = bay width in ft.
d = gate opening in ft.
H = working head in ft.; equivalent to (upstream water level minus downstream water level)
g = acceleration due to gravity in ft/s^2

Condition II (a): Free Overflow

a. Gates fully opened,
b. standing wave formed, and
c. downstream water level below the weir crest

$$Q = C.B.H^{1.5} \qquad \text{II (a)}$$

Where: Q = discharge in cusecs
C = discharge coefficient *(varies w.r.t. weir geometry and head)*
B = bay width in ft.
H = working head in ft.; equivalent to (upstream water level minus crest level)
g = acceleration due to gravity in ft/s^2

Condition II (b): Submerged Overflow

a. Gates fully opened,
b. No standing wave, and
c. downstream water level above the weir crest

$$Q = C.B.H^{1.5} \qquad \text{II (b)}$$

Where: Q = discharge in cusecs
C = discharge coefficient *(varies w.r.t. weir geometry, head and drowning ratio)*
B = bay width in ft.
H = working head in ft.; equivalent to (upstream water level minus downstream water level w.r.t. weir crest)
g = acceleration due to gravity in ft/s^2

The details concerning the variation in discharge coefficients and the modular limits can be consulted in Publication No. 20 of International Institute for Land Reclamation and Improvement (ILRI) Delft Hydraulics Laboratory, University of Agriculture, Department of Hydraulics and Irrigation, The Netherlands. Technical details concerning the above formulae are also provided in Flow Measurement Report on Calibration of Discharge Coefficients (Cd) & Development of Ratings for the Five Pilot Sites, submitted as Volume III.

At barrages, discharge calculations were carried out using formulas and coefficients generally mentioned in their Operation and Maintenance manuals by designer. Certain parameters were estimated using experience and predefined flow ranges. A summary of flow calculation formulas and coefficients for various flow conditions being used at 23 sites, is provided in Tables 2-4 to 2-19. Whereas, description of said flow calculation formulas along with salient features is provided as Annexure-J. The data collected and subsequently digitized for analysis of discharge computations at 23 sites is provided in soft copy; attached as DVD-1 in this report.

Calculations were made using PID formulas and the data obtained from gauge register to reproduce PID flow estimates. It was observed that using PID documented formulas and data from gauge registers, Consultants estimated flow magnitudes do not compare with PID reported flow magnitudes. Analysis indicate a difference between PID reported values with estimates from formula being used by PID itself which indicates that PID is not implementing its own formula correctly and random corrections (high step ranges in approach velocity estimation by PID and consideration of discharge coefficient beyond limits defined in documents by PID & adjustments based on discharge values reported at upstream structure) are being applied over PID estimates for subsequent reporting. Results are provided in Annexure-J for each barrage site other than Chashma, Taunsa, Marala and Gudd barrage.

In the absence of a reference flow value (like magnitudes obtained from physical flow measurements for 5 pilot sites) ISO formula was used to compare with PID estimated flow magnitudes and PID reported flow magnitudes. Results of comparisons with PID reported flow magnitudes are presented in Annexure-J. It is to be noted that due to inherent application limitation of ISO formula (i.e., use of uniform approach flow conditions and uniform water levels without super elevation impact across abutment) comparison of result may not develop basis for declaring a formula or its coefficients to be non-representative. The only standard which evaluates the formula application and validity of coefficients is the physical flow measurement.

As regards canals, the Provincial Irrigation Departments (PIDs) regulate diversions by the stage-discharge relations (or rating curves or ratings) developed at certain canal section in the vicinity of head-regulator. These relations should ideally be developed through a series of direct flow measurements to represent the dominant flow ranges being encountered by the canal, and are required to be revised at least twice in a year. However in practice it was noticed that the canal ratings have been based in most of the cases one or maximum two measurements, and the periodic revisions are also not followed at the recommended interval, rendering the ratings non-representative.

The Chashma-Jhelum Link Canal (CJLC) and the Chashma Right Bank Canal (CRBC) - both operated by WAPDA - are the exceptions in terms that the diversions were made by the application of hydraulic formulae. It is to mention here that WAPDA also does not undertake the direct flow-measurements as a routine task.

Table 2-4: Summary of Collected Formulas, Discharge Coefficients, Velocity Head Measurement and Location of Canal Gauging Stations at 23 Sites

Sites	Conditions			
	Free Overflow	Submerged Overflow	Free Orifice	Submerged Orifice
Tarbela Dam/ Ghazi Barrage	Standard inflow estimation techniques for reservoirs are being used at Tarbela which make use of outflows (irrigation releases, power releases, spillway releases) and prevailing storage corresponding to reservoir level.			
Jinnah Barrage	NA		$Q = C\,B\,[(H+H_a)^{3/2} - (H+H_a-w)^{3/2}]$	$Q = C\,B\,w\sqrt{H+H_a}$
Chashma Barrage	NA		Q = q x N	NA
Taunsa Barrage	$Q = C\,B\,(H+H_a)^{3/2}$		$Q = C_d\,B\,w\sqrt{2g(H+H_a-0.5\,w)}$	$Q = C\,B\,w\sqrt{H+H_a}$
Guddu Barrage	Table 2-7		NA	$Q = C_d\,B\,w\sqrt{2g(H+H_a)}$
Sukkur Barrage	$Q = C\,B\,(H+H_a)^{3/2}$		NA	$Q = C_d\,B\,w\sqrt{2g(H+H_a)}$
Kotri Barrage	$Q = C\,B\,(H+H_a)^{3/2}$		$Q = C\,B\,[(H+H_a)^{3/2} - (H+H_a-w)^{3/2}]$	$Q = C_d\,B\,w\sqrt{2g(H+H_a)}$
Mangla Dam	Standard inflow estimation techniques for reservoirs are being used which make use of outflows (irrigation releases, power releases, spillway releases) and prevailing storage corresponding to reservoir level.			
Rasul Barrage	$Q = C\,B\,(H+H_a)^{3/2}$		$Q = C\,B\,[(H+H_a)^{3/2} - (H+H_a-w)^{3/2}]$	
Marala Barrage	$Q = \frac{2}{3} C_d \sqrt{2g}\,B\,(H+H_a)^{3/2}$	NA	$Q = \frac{2}{3} C_d \sqrt{2g}\,B\,[(H+H_a)^{3/2} - (H+H_a-w)^{3/2}]$	$Q = C_d\,B\,w\sqrt{2g(H+H_a)}$
Khanki Headwork	System is under construction.			
Qadirabad Barrage	$Q = C\,B\,(H+H_a)^{3/2}$		$Q = C\,B\,[(H+H_a)^{3/2} - (H+H_a-w)^{3/2}]$	$Q = C_d\,B\,w\sqrt{2g(H+H_a)}$
Trimmu Headwork	$Q = C\,B\,(H+H_a)^{3/2}$		$Q = C\,B\,[(H+H_a)^{3/2} - (H+H_a-w)^{3/2}]$ (Un-submerged gates and submerged weir at downstream) $Q = C\,B\,w\sqrt{H+H_a}$ (Un-submerged gates and un-submerged weir at downstream)	$Q = C\,B\,w\sqrt{H+H_a}$
Panjnad Headwork	$Q = C\,B\,(H+H_a)^{3/2}$		$Q = C\,B\,w\sqrt{H+H_a-{}^{2}/_{3}\,w}$	$Q = C\,B\,w\sqrt{H+H_a}$
Balloki Headwork	$Q = C\,B\,(H+H_a)^{3/2}$		$Q = C\,B\,[(H+H_a)^{3/2} - (H+H_a-w)^{3/2}]$	$Q = C\,B\,w\sqrt{H+H_a}$
Sidhnai Barrage	$Q = C\,B\,(H+H_a)^{3/2}$		$Q = C\,B\,[(H+H_a)^{3/2} - (H+H_a-w)^{3/2}]$	$Q = C\,B\,w\sqrt{H+H_a}$
Sulemanki Headwork	$Q = C\,(B-0.20)\,(H+H_a)^{3/2}$	$Q = C\,B\,(H+H_a)^{3/2}$	$Q = C\,B\,[(H+H_a)^{3/2} - (H+H_a-w)^{3/2}]$	$Q = C\,B\,w\sqrt{H+H_a}$
Islam Headwork	$Q = C\,B\,(H+H_a)^{3/2}$		$Q = C\,B\,[(H+H_a)^{3/2} - (H+H_a-w)^{3/2}]$	$Q = C\,B\,w\sqrt{H+H_a}$

Sites	Coefficients				Velocity Head Estimation	Off-Taking Canals (Main Gauging Site)
	Free Overflow	Submerged Overflow	Free Orifice	Submerged Orifice		
Tarbela Dam/ Ghazi Barrage	Standard inflow estimation techniques for reservoirs are being used at Tarbela which make use of outflows (irrigation releases, power releases, spillway releases) and prevailing storage corresponding to reservoir level.					1. Pehur High Level Canal (Head)
Jinnah Barrage	$C = Cd \times {}^{2}/_{3} \times \sqrt{2g}$			$C = Cd \times \sqrt{2g}$	No standard criterion	1. Thal Canal (RD 10+800)
	-	-	3.20	6.50		
Chashma Barrage	-	-	-	-	Iteration method is used.	1. Chashma Jhelum Link Canal (Head) 2. Chashma Right Bank Canal (Head)
Taunsa Barrage	$C = Cd \times {}^{2}/_{3} \times \sqrt{2g}$		0.60	$C = Cd \times \sqrt{2g}$	Criterion exists (Table 2-6)	1. Taunsa Panjnad Link Canal (Head) 2. Muzaffargarh Canal (RD 5+500) 3. Dera Ghazi Khan Canal (RD 21+500)
	3.30[2]	Table 2-5		6.50		
Guddu Barrage	-	-	-	Table 2-8	No standard criterion	1. Ghotki Feeder Canal (Head) 2. Desert Pat Feeder Canal (Head) 3. Pat Feeder Canal (RD 109+000) 4. Begari Sindh Feeder Canal (Head)
Sukkur Barrage	$C = Cd \times {}^{2}/_{3} \times \sqrt{2g}$		-	Table 2-10	Not considered	1. Nara Canal (Head) 2. Khairpur East Canal (Head) 3. Khairpur West Canal (Head) 4. Rohri Canal (Head) 5. North West Canal (Head) 6. Rice Canal (Head) 7. Dadu Canal (Head)
	3.30	Table 2-9				
Kotri Barrage	$C = Cd \times {}^{2}/_{3} \times \sqrt{2g}$			Table 2-11	No standard criterion[3]	1. Old Fuleli Canal (Sub-regulator) 2. New Fuleli Canal (Sub-regulator) 3. Akram Wah Canal (Sub-regulator) 4. Kalri Baghar Feeder Canal (Head)
	3.30	Table 2-5	3.20			

[2] Value of C = 3.30 has been obtained from Taunsa barrage documentation. However according to the Barrage Personnel C = 3.20 is used in free overflow condition.

[3] Velocity head is not considered on regular basis. Sometimes floating tube is used to calculate velocity head.

Sites	Coefficients				Velocity Head Estimation	Off-Taking Canals (Main Gauging Site)
	Free Overflow	Submerged Overflow	Free Orifice	Submerged Orifice		
Mangla Dam	Standard inflow estimation techniques for reservoirs are being used which make use of outflows (irrigation releases, power releases, spillway releases) and prevailing storage corresponding to reservoir level.					1. Upper Jhelum Canal (Head)
Rasul Barrage	$C = Cd \times {}^{2}/_{3} \times \sqrt{2g}$				No standard criterion	1. Rasul Qadirabad Link Canal (Head) 2. Lower Jhelum Canal (Head)
	3.80	Table 2-12	3.80	Table 2-12		
Marala Barrage	0.62	-	0.62	$[0.615 + (0.007 \times 2^{(5-H)})]$	Experience based criterion	1. Marala Ravi Link Canal (Head) 2. Upper Chenab Canal (Head)
Khanki Headwork	System is under construction.					1. Lower Chenab Canal (RD 2+000)
Qadirabad Barrage	$C = Cd \times {}^{2}/_{3} \times \sqrt{2g}$			0.65	No standard criterion	1. Qadirabad Balloki Canal (Head)
	3.80	Table 2-12	Table 2-12			
Trimmu Headwork	$C = Cd \times {}^{2}/_{3} \times \sqrt{2g}$			$C = Cd \times \sqrt{2g}$	Criterion exists (Table 2-13)	1. Trimmu Sidhnai Link Canal (Head and RD 10+000) 2. Haveli Main Line Canal (Head) 3. Rangpur Canal (Head)
	3.30	Table 2-5	3.30			
			$C = Cd \times \sqrt{2g}$	6.50		
			4.80			
Panjnad Headwork	$C = Cd \times {}^{2}/_{3} \times \sqrt{2g}$		$C = Cd \times {}^{2}/_{3} \times \sqrt{2g}$		Criterion exists (Table 2-14)	1. Panjnad Main Line Canal (RD 1+000) 2. Abbasia Canal (RD 2+000) 3. Abbasia Link Canal (RD 4+000)
	3.30	Table 2-5	4.80	6.40		
Balloki Headwork	$C = Cd \times {}^{2}/_{3} \times \sqrt{2g}$			$C = Cd \times \sqrt{2g}$	Criterion exists[4]	1. Balloki Sulemanki Link Canal (Head) 2. Lower Bari Doab Canal (RD 27+100)
	3.30	3.05	3.30	6.50		
Sidhnai Barrage	$C = Cd \times {}^{2}/_{3} \times \sqrt{2g}$			$C = Cd \times \sqrt{2g}$	Criterion exists[5]	1. Sidhnai Canal (RD 0+500) 2. Sidhnai Mailsi Bahawal Link Canal (RD 0+500)
	3.30	3.10	3.10	6.50		
Sulemanki Headwork	$C = Cd \times {}^{2}/_{3} \times \sqrt{2g}$			$C = Cd \times \sqrt{2g}$	Criterion exists[6]	1. Fordwah Canal (Head) 2. Eastern Sadquia Canal (RD 3+000) 3. Upper Pakpattan Canal (RD 2+000)
	3.10-3.33[7]	3.00-3.10[8]	3.10	6.5		

[4] Velocity head of 0.50 ft is considered only in free orifice condition.

[5] Velocity head of 0.14 ft is considered only in free orifice condition.

[6] No velocity head is considered below 45,000 ft^3/s. However when the discharge is above 45,000 ft^3/s then in overflow condition velocity head is taken as 10% of water depth above weir crest, whereas, in orifice condition it is taken as 10% of gate opening.

[7] 3.33 is used when the downstream water level is up to 550 ft. The value gradually decreases to 3.10 with the rise in water level

[8] 3.00 is used when the downstream water level is at weir crest. Whereas, 3.10 is used for water level just below weir crest

<table>
<tr><th rowspan="2">Sites</th><th colspan="4">Coefficients</th><th rowspan="2">Velocity Head Estimation</th><th rowspan="2">Off-Taking Canals (Main Gauging Site)</th></tr>
<tr><th>Free Overflow</th><th>Submerged Overflow</th><th>Free Orifice</th><th>Submerged Orifice</th></tr>
<tr><td rowspan="2">Islam Headwork</td><td colspan="3">$C = Cd \times {}^{2}/_{3} \times \sqrt{2g}$</td><td>$C = Cd \times \sqrt{2g}$</td><td rowspan="2">No standard criterion</td><td rowspan="2">1. Qaim Canal (Head)
2. Upper Bahawal Canal (RD 1+000)</td></tr>
<tr><td>3.30</td><td>3.10</td><td>3.10</td><td>6.50</td></tr>
<tr><td>Noshera</td><td colspan="6">A discharge versus gauge curve is developed at gauging site. Discharge measurement is carried out ar bridge. Generally, observation is carried out once in a week which becomes twice in case of flood season. Subjected to quality check, observation are used for development of said curve. Consistency check is applied by marking the observed points on the existing rating curve. If the observations show change in trend then rating curved is revised otherwise the same remain in use. In general, rating curve is revised every year. However, keeping in view the observations’ trend it may be revised twice a year if find necessary.

Discharge Rating Curve Equation

$Q = a \times (Gauge\ Height + b)^{c}$

Where,
Q = discharge in cusecs
Gauge Height = reading of gauge in ft (fixed at bridge)
a, b, c = coefficients
Rating curve for year 2013: $406.1 \times (GH + 0.06890)^{1.508}$</td></tr>
<tr><td>Garang Regulator – Kirther Canal</td><td colspan="6">Discharge rating tables are used as shown in Table 2-15 and Table 2-16.</td></tr>
<tr><td>Pat Feeder Canal (RD 109+000)</td><td colspan="6">Discharge rating tables is used as shown in Table 2-17.</td></tr>
<tr><td>Uch Canal</td><td colspan="6">Discharge rating tables is used as shown in Table 2-18.</td></tr>
<tr><td>Manuthy Canal</td><td colspan="6">Discharge rating tables is used as shown in Table 2-19.</td></tr>
</table>

General

Q = discharge in cusecs
C = coefficient (C is replaced with C' for taking into account the effect of submergence.)
B = bay width in ft
H = u/s water depth above crest in ft
= u/s water level-downstream water level (only in case of submerged orifice flow.)
H_a = head due to velocity in ft
w = gate opening in ft
C_d = coefficient of discharge
g = gravitational acceleration (32.2 ft/s^2)
NA = not applicable; barrage is operated in such a way that flow condition does not occur.

Only for Chashma Barrage

$$Q = q \times N$$

Where,
Q = discharge in cusecs
q = discharge per gate
N = no. of gates
w = gate opening (notation 'T' has been used in the official documents of Chashma Barrage for gate opening)
H = upstream water depth over crest

Discharge is calculated by computing discharge per gate (q) using the Fortran LanGauge based rating tables with the help of head above crest (H) and gate opening (w).

Table 2-5: Submergence Correction for Discharge Calculation

Ratio of H_2 / H_1		C
From	To	
0.95	0.96	3.00
0.93	0.94	3.05
0.90	0.92	3.10
0.80	0.90	3.15
0.70	0.80	3.20

H_1 = Upstream water depth above weir crest in ft
H_2 = Downstream water depth above weir crest in ft

Table 2-6: Calculation of Velocity Head at Taunsa Barrage

Discharge (ft^3/s)		Velocity Head
from	to	(ft)
0	30,000	0.30
30,000	80,000	0.50
80,000	100,000	0.80
100,000	150,000	1.00
150,000	300,000	1.50
300,000 & above		1.80

Procedure:

- Calculate the discharge without considering the velocity head.
- Select the value of velocity head from the table below, in accordance with the flow range in which calculated discharge prevails.
- Again calculated the discharge after addition of the velocity head into effective head.

Table 2-7: Outflow Rating Table at Guddu Barrage for Overflow Condition

Downstream Gauge (ft)	Discharge (ft^3/s)	Downstream Gauge (ft)	Discharge (ft^3/s)
240	4,000	251	110,000
241	8,000	252	140,000
242	12,000	253	200,000
243	16,000	254	260,000
244	20,000	255	320,000
245	30,000	256	420,000
246	40,000	257	550,000
247	50,000	258	700,000
248	60,000	259	900,000
249	70,000	260	1,100,000
250	90,000	261	1,300,000

Table 2-8: Values of Discharge Coefficients for Submerged Orifice Flow at Guddu Barrage

Discharge (ft^3/s)		Value of Cd
From	To	
0	50,000	0.60
50,000	100,000	0.65
100,000	200,000	0.70
200,000	250,000	0.75
250,000	300,000	0.80
Above 300,000		0.90

Table 2-9: Submergence Correction for Discharge Calculation at Sukkur Barrage

Ratio of H_2 / H_1		C
From	To	
0.95	0.96	3.00
0.93	0.94	3.05
0.90	0.92	3.10
0.80	0.90	3.15
0.70	0.80	3.20
0.60	0.70	3.25

H_1 = Upstream water depth above weir crest in ft
H_2 = Downstream water depth above weir crest in ft

Table 2-10: Values of Discharge Coefficients for Submerged Orifice Flow at Sukkur Barrage

Discharge (ft^3/s)		Value of Cd
From	To	
0	25,000	0.61
25,000	30,000	0.62
30,000	35,000	0.63
35,000	40,000	0.64
Above 40,000		0.65

Table 2-11: Values of Discharge Coefficients for Submerged Orifice Flow at Kotri Barrage

Cd	Discharge Range (ft^3/s)	Cd	Discharge Range (ft^3/s)
0.62	500-12,500	0.81	200,000-210,000
0.63	12,500-25,000	0.82	210,000-220,000
0.64	25,000-37,500	0.83	220,000-230,000
0.65	37,500-50,000	0.84	230,000-240,000
0.66	50,000-60,000	0.85	240,000-250,000
0.67	60,000-70,000	0.86	250,000-260,000
0.68	70,000-80,000	0.87	260,000-270,000
0.69	80,000-90,000	0.88	270,000-280,000
0.70	90,000-100,000	0.89	280,000-290,000
0.71	100,000-110,000	0.90	290,000-300,000
0.72	110,000-120,000	0.91	300,000-310,000
0.73	120,000-130,000	0.92	310,000-320,000
0.74	130,000-140,000	0.93	320,000-330,000
0.75	140,000-150,000	0.94	330,000-340,000
0.76	150,000-160,000	0.95	340,000-355,000
0.77	160,000-170,000	0.96	355,000-370,000
0.78	170,000-180,000	0.97	370,000-385,000
0.79	180,000-190,000	0.98	385,000 & above
0.80	190,000-200,000		

Table 2-12: Gibson Curve for Submergence Correction

H_2/H_1	C'/C	C'	H_2/H_1	C'/C	C'	H_2/H_1	C'/C	C'	H_2/H_1	C'/C	C'
0.01	0.9988	3.80	0.26	0.9685	3.68	0.51	0.9370	3.56	0.76	0.8150	3.10
0.02	0.9975	3.79	0.27	0.9670	3.67	0.52	0.9350	3.55	0.77	0.8050	3.06
0.03	0.9963	3.79	0.28	0.9655	3.67	0.53	0.9320	3.54	0.78	0.7975	3.03
0.04	0.9951	3.78	0.29	0.9640	3.66	0.54	0.9300	3.53	0.79	0.7890	3.00
0.05	0.9938	3.78	0.30	0.9625	3.66	0.55	0.9275	3.52	0.80	0.7800	2.96
0.06	0.9926	3.77	0.31	0.9615	3.65	0.56	0.9250	3.52	0.81	0.7675	2.92
0.07	0.9913	3.77	0.32	0.9605	3.65	0.57	0.9225	3.51	0.82	0.7550	2.87
0.08	0.9901	3.76	0.33	0.9595	3.65	0.58	0.9175	3.49	0.83	0.7425	2.82
0.09	0.9888	3.76	0.34	0.9585	3.64	0.59	0.9150	3.48	0.84	0.7300	2.77
0.10	0.9875	3.75	0.35	0.9575	3.64	0.60	0.9100	3.46	0.85	0.7125	2.71
0.11	0.9865	3.75	0.36	0.9565	3.63	0.61	0.9075	3.45	0.86	0.7000	2.66
0.12	0.9855	3.74	0.37	0.9555	3.63	0.62	0.9025	3.43	0.87	0.6800	2.58
0.13	0.9845	3.74	0.38	0.9545	3.63	0.63	0.8990	3.42	0.88	0.6625	2.52
0.14	0.9835	3.74	0.39	0.9535	3.62	0.64	0.8925	3.39	0.89	0.6400	2.43
0.15	0.9825	3.73	0.40	0.9525	3.62	0.65	0.8880	3.37	0.90	0.6225	2.37
0.16	0.9815	3.73	0.41	0.9513	3.61	0.66	0.8840	3.36	0.91	0.6000	2.28
0.17	0.9805	3.73	0.42	0.9500	3.61	0.67	0.8775	3.33	0.92	0.5750	2.19
0.18	0.9795	3.72	0.43	0.9488	3.61	0.68	0.8725	3.32	0.93	0.5450	2.07
0.19	0.9785	3.72	0.44	0.9475	3.60	0.69	0.8670	3.29	0.94	0.5125	1.95
0.20	0.9775	3.71	0.45	0.9463	3.60	0.70	0.8600	3.27	0.95	0.4750	1.81
0.21	0.9760	3.71	0.46	0.9450	3.59	0.71	0.8525	3.24	0.96	0.4450	1.69
0.22	0.9745	3.70	0.47	0.9438	3.59	0.72	0.8450	3.21	0.97	0.4050	1.54
0.23	0.9730	3.70	0.48	0.9425	3.58	0.73	0.8380	3.18	0.98	0.3500	1.33
0.24	0.9715	3.69	0.49	0.9413	3.58	0.74	0.8300	3.15	0.99	0.2850	1.08
0.25	0.9700	3.69	0.50	0.9400	3.57	0.75	0.8225	3.13	1.00	0.0000	0.00

H_1 = Upstream water depth above weir crest in ft H_2 = Downstream water depth above weir crest in ft

Table 2-13: Calculation of Velocity Head at Trimmu Barrage

Discharge (ft^3/s)		Velocity Head
from	To	(ft)
0	50,000	0.10
50,000	75,000	0.20
75,000	100,000	0.40
100,000	125,000	0.60
125,000	150,000	0.80
150,000	175,000	1.00
175,000	200,000	1.30
200,000	225,000	1.50
225,000	250,000	1.70
250,000	300,000	2.00
300,000	350,000	2.20
350,000 & above		2.50

Procedure:

- Calculate the discharge without considering the velocity head.
- Select the value of velocity head from the table below, in accordance with the flow range in which calculated discharge prevails.
- Again calculated the discharge after addition of the velocity head into effective head.

Table 2-14: Calculation of Velocity Head at Panjnad Barrage

Discharge (ft^3/s)		Velocity Head
from	to	(ft)
0	5,000	0.03
5,000	10,000	0.04
10,000	25,000	0.07
25,000	40,000	0.11
40,000	50,000	0.12
50,000	75,000	0.16
75,000	100,000	0.20
100,000	150,000	0.26
150,000	200,000	0.31
200,000	250,000	0.36
250,000	300,000	0.41
300,000	350,000	0.45
350,000	400,000	0.49
400,000	450,000	0.53
450,000	500,000	0.57
500,000	550,000	0.61
550,000	600,000	0.65
600,000	650,000	0.68
650,000 & above		0.72

Table 2-15: Discharge Rating Table of Kirther Canal at Garang Regulator for Kharif Season

Upstream Gauge (ft)	Discharge (ft^3/s)	Upstream Gauge (ft)	Discharge (ft^3/s)
2.0	198	8.6	1,907
3.0	373	8.7	1,940
4.0	582	8.8	1,974
5.0	820	8.9	2,007
5.5	910	9.0	2,041
6.0	1,038	9.1	2,075
6.5	1,224	9.2	2,110
7.0	1,370	9.3	2,144
7.5	1,522	9.4	2,179
8.0	1,711	9.5	2,214
8.1	1,733	9.6	2,249
8.2	1,763	9.7	2,284
8.3	1,796	9.8	2,319
8.4	1,833	9.9	2,355
8.5	1,873	10.0	2,391

Table 2-16: Discharge Rating Table of Kirther Canal at Garang Regulator for Rabi Season

Upstream Gauge (ft)	Discharge (ft^3/s)	Upstream Gauge (ft)	Discharge (ft^3/s)
5.00	330	6.70	663
5.10	340	6.80	692
5.20	350	6.90	721
5.30	360	7.00	750
5.40	370	7.10	779
5.50	380	7.20	808
5.60	390	7.30	837
5.70	400	7.40	866
5.80	420	7.50	901
5.90	440	7.60	936
6.00	450	7.70	971
6.10	490	7.80	1,006
6.20	518	7.90	1,041
6.30	547	8.00	1,080
6.40	576	8.10	1,120
6.50	605	8.20	1,160
6.60	634		

Table 2-17: Discharge Rating Table of Pat Feeder Canal at RD 109+000

Gauge (ft)	Discharge (ft^3/s)	Gauge (ft)	Discharge (ft^3/s)
0.0	0	6.0	2,900
0.5	50	6.5	3,400
1.0	100	7.0	3,700
2.0	400	7.5	4,000
2.5	600	8.0	4,800
3.0	800	8.5	5,400
3.5	1,000	9.0	6,000
4.0	1,400	9.5	6,500
4.5	1,700	9.7	6,700
5.0	2,000	10.0	7,000
5.5	2,600		

Table 2-18: Discharge Rating Table of Uch Canal

Gauge (ft)	Discharge (ft^3/s)	Gauge (ft)	Discharge (ft^3/s)	Gauge (ft)	Discharge (ft^3/s)
4.0	100	6.1	310	8.2	520
4.1	115	6.2	320	8.3	530
4.2	120	6.3	330	8.4	540
4.3	130	6.4	340	8.5	550
4.4	140	6.5	350	8.6	560
4.5	150	6.6	360	8.7	570
4.6	160	6.7	370	8.8	580
4.7	170	6.8	380	8.9	590
4.8	180	6.9	390	9.0	600
4.9	190	7.0	400	9.1	610
5.0	200	7.1	410	9.2	620
5.1	210	7.2	420	9.3	630
5.2	220	7.3	430	9.4	640
5.3	230	7.4	440	9.5	650
5.4	240	7.5	450	9.6	660
5.5	250	7.6	460	9.7	670
5.6	260	7.7	470	9.8	680
5.7	270	7.8	480	9.9	690
5.8	280	7.9	490	10.0	700
5.9	290	8.0	500		
6.0	300	8.1	510		

Table 2-19: Discharge Rating Table of Manuthi Canal

Gauge (ft)	Discharge (ft^3/s)	Gauge (ft)	Discharge (ft^3/s)	Gauge (ft)	Discharge (ft^3/s)
4.0	10	6.1	210	8.2	425
4.1	20	6.2	220	8.3	435
4.2	30	6.3	230	8.4	440
4.3	40	6.4	240	8.5	455
4.4	50	6.5	250	8.6	475
4.5	60	6.6	260	8.7	485
4.6	65	6.7	270	8.8	490
4.7	70	6.8	280	8.9	495
4.8	80	6.9	290	9.0	505
4.9	90	7.0	300	9.1	513
5.0	100	7.1	310	9.2	524
5.1	110	7.2	320	9.3	535
5.2	120	7.3	330	9.4	545
5.3	130	7.4	340	9.5	555
5.4	140	7.5	350	9.6	565
5.5	150	7.6	360	9.7	575
5.6	160	7.7	370	9.8	585
5.7	170	7.8	380	9.9	595
5.8	180	7.9	390	10.0	605
5.9	190	8.0	405		
6.0	200	8.1	410		

2.1.8 Review of Data Communication Protocols

The basic data of water levels and gate openings, and the discharges are being observed and calculated at the 23 key sites, in accordance with the earlier discussions and communicated to the respective provincial headquarters of irrigation departments through telephone and/or facsimile. The observed data and calculated discharges are logged in the registers maintained at each barrage site. On the canal sites, usual practice is to maintain the gauge register. The observed gauges are sent to the XEN offices being in-charge of regulation where corresponding discharges are read from the respective canal's rating tables.

In parallel, a SCADA[9] based remote gauging and telemetry system was installed at all the barrages and the heads of canals i.e. 23 key sites of IBIS in 2004 with the core objective to automate conventional manual system and make a historical log of data at dams, barrages and head-regulators. This system utilises water level sensors (installed at specific locations to observe upstream and downstream water levels) and gate position sensors (installed at each gate to observe gate opening) to estimate parameters used in discharge calculations. The real time data of sensors is transmitted to control rooms where it is processed to calculate discharges in real-time. The quantities so measured are transmitted to all the stakeholders using VSAT as communication infrastructure for data transmission. During course of the project, field survey to assess existing performance and health of telemetry system, installed at specific sites, were carried out. Details of survey results are provided in Section 2.5.

2.2 FLOW MEASUREMENTS AT PILOT SITES

The second sub-task under Task-I of the ToR was to establish stage discharge relationships and calibrate discharge coefficients after discharge measurements for different flow conditions (ranging from low to high flow condition) at five (5) pilot sites mentioned earlier with the coordination of Provincial Irrigation Departments (PIDs) and Pakistan Water & Power Development Authority (WAPDA).

To establish the stage-discharge relations and calibrate the discharge coefficients, flow measurements were conducted at the five pilot sites with the coordination and active participation of the nominated focal persons of all the stakeholders from PIDs and WAPDA. Total thirteen (13) flow measurement missions were conducted to cover the pre-dominant flow ranges at 28 locations of the five pilot sites. The locations comprised all the head-regulators of the canals off-taking from the four barrages and also the additional locations deemed necessary to enunciate the recommendations for development of a reliable water distribution system. A summary of all the completed flow measurements along with their locations is given in Table 2-20. The flow measurement and cross-section sheets (for 389 number of observations) observed by the stakeholders are provided in the soft copy; DVD-2 attached with this report. A total number of 139 discharge measurements were carried out at the pilot locations including 15 discharge measurements under additional scope of services.

Table 2-20: Completed Flow Measurements at Five (5) Pilot Sites

[9] Supervisory Control and Data Acquisition

Sr.#	Pilot Site	River/Canal	Location (RD)	Flow Measurements (Nos.)
1.	Chashma Barrage	Indus	Downstream Barrage*	4+1*
		Chashma Right Bank Canal (CRBC)*	6+280	8+3*
			259+350	3*
			380+100	3*
			515+000	1+2*
		Chashm Jhelum (CJ) Link Canal	36+000 downstream Thal Regulator	4
		Tailrace of Chashma Hydropower Plant	2+000	4
		Tailrace of Chashma Nuclear Power Plant Channel	220 ft. upstream of 1 MW Hydel Power Station at Tail	4
2.	Taunsa Barrage	Indus	Downstream Barrage	6
		Muzaffargarh Canal	1+930/2+060	5
			5+500/5+850	2
		Silt Ejector of Muzaffargarh Canal	1+586/3+000	5
		Dera Ghazi (DG) Khan Canal	1+500	7
			23+000	2
		Silt Ejector of Dera Ghazi (DG) Khan Canal	4+000	7
		Taunsa Panjnad (TP) Link Canal	4+500/5+000	6
3.	Guddu Barrage	Indus	Downstream Barrage	7
		Ghotki Feeder Canal	1+500	6
		Begari Sindh Feeder Canal	1+500	4
		Escape Channel	Downstream of Guddu Power Plant	4
		Desert Pat Feeder Canal	1+500	6
		Pat Feeder Canal*	110+600	5+1*
		Rainee Canal	0+470	1
4.	Garang Regulator -Kirther Canal	Kirther Canal*	98+000/100+000 (upstream Garang Regulator)	2
			103+400 (downstream Garang Regulator)	10+2*
		Saifullah Magsi Branch	0+800/1+430	2
		Gokalpur Minor	0+408	1
5.	Marala Barrage	Chenab	Downstream Barrage	5
		Marala Ravi (MR)Link Canal	19+500	3
		Upper Chenab Canal (UCC)	8+850	3
Total Measurements				**124+15*=139**

* Measurements carried out under additional scope of services

The discharges in the rivers and canals were measured by the current meter method. Concurrent with the flow measurement, the water levels and gate settings at the barrages and regulator were also monitored.

In this section, the flow measurement approach, equipment calibration, discharge computations and measurement uncertainties have been discussed in brief. Details are provided in Flow Measurement Report, submitted as Volume III.

2.2.1 Flow Measurement Approach

The discharges in the rivers and canals were measured by the current meter method, which were duly witnessed and accepted by all the stakeholders. The current meter method involves the measurement of the flow velocity in a number of verticals in a cross-section at one or two points per vertical dependent on the depth of flow. By measuring the depth and the distance between successive verticals, the discharge through a segment in between each vertical (mid-section method) can be obtained and the total discharge through the cross-section is computed through summation of the segment flows.

The cross-sections were carefully selected to measure the entire flow in the cross-section; at a few occasions (at Marala and Guddu downstream of the barrages), where the flow was concentrated in a few creeks, measurements were carried out in the creeks separately. The creek discharges, for the day, were subsequently combined to arrive at the total cross-sectional flow. In the selection of a discharge measurement cross-section, the following criteria were considered:

- straight streamlines at right-angles to the cross-section,
- regular velocity distribution, vertically and horizontally,
- velocities greater than 0.3-0.5 ft/s
- regular and stable channel bed
- no flooding at the measurement site, and
- no aquatic weed growth.

It appeared that not in all instances all the criteria was fulfilled, particularly with respect to the first bulleted point; for a few measurements corrections were made for oblique flow. During the measurements, water levels and gate settings at the barrages were monitored. Temporary staff gauges were established and levelled where the existing network was insufficient to accurately determine the energy head.

2.2.2 Equipment Calibration

Two new Price AA type current meters were procured for the flow measurement activity and the manufacturer’s revolution-velocity rating equations were used during measurements.

2.2.3 Discharge Computation

The discharge was computed by the *mid-section method*. In this method of computation, it is assumed that the velocity sampled at each vertical ($\bar{v}_i$) represents the mean velocity in a segment. Similarly, it is assumed that the depth of the vertical (d_i) is the mean depth in the segment. The segment area extends laterally from half the distance from the preceding vertical to half the distance to the next as shown as the hatched area in Figure 2-1.

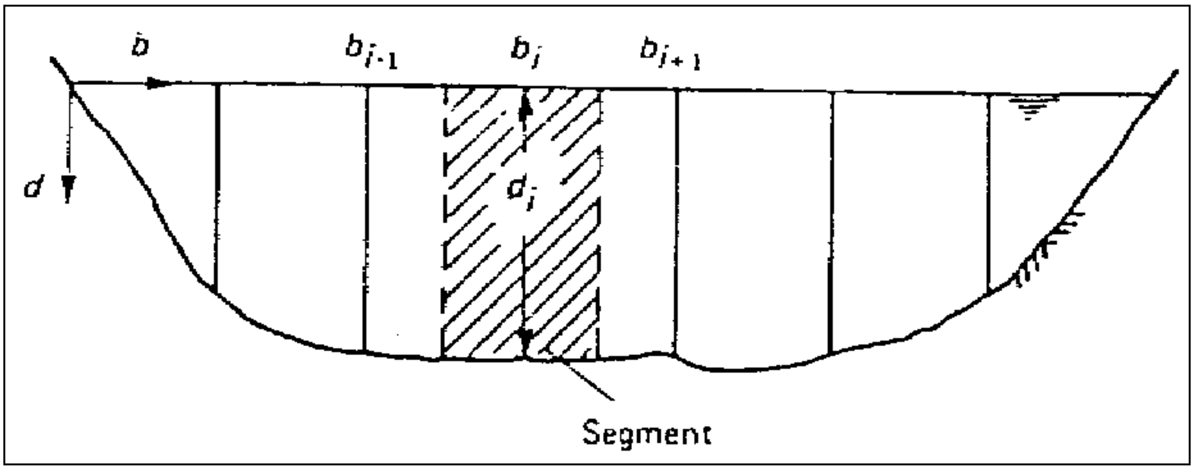

Figure 2-1: Sketch of Discharge Computation by Using the Mid-Section Method

The segment discharge (q_i) is then computed for each segment and these are summed to obtain the total discharge as follows:

$$Q = \sum_{i=1}^{n} q_i = \sum_{i=1}^{n} \bar{v}_i \,.\, A_{s_i} = \sum_{i=1}^{n} \bar{v}_i \,.\, d_i. \frac{(b_{i+1} - b_{i-1})}{2} \qquad (2.1)$$

$$with: b_0 = b_1 \; and \; b_{n+1} = b_n$$

Where b_i is the distance of the measuring point (*i*) from a bank datum and *n* is the number of measured verticals and sub-areas.

2.2.4 Uncertainties in Flow Measurements and Discharge

Errors in the discharge computed by the area velocity method using the mid-section method are due to uncertainties in the width, depth, mean flow velocity in the vertical and the number of verticals. The overall uncertainty in the discharge is given by:

$$X_Q = \pm\left(X_n^2 + X_s^2 + \frac{\sum_{i=1}^{n}(b_i d_i \bar{v}_i)^2 (X_b^2 + X_d^2 + X_{\bar{v}}^2)_i}{(\sum_{i=1}^{n} b_i d_i \bar{v}_i)^2} \right)^{1/2} \qquad (2.2)$$

Where:

X_Q = overall uncertainty in discharge

X_n = uncertainty due to limited number of verticals

X_s = uncertainty due to variable responsiveness
X_v = uncertainty in the segment mean velocity
X_b = uncertainty in width measurement
X_d = uncertainty in depth measurement

Technical Report on Calibration of Discharge Coefficients (Cd) & Development of Ratings for the Five Pilot Sites provides details on each type of measurement uncertainty along with calculation procedure.

2.2.5 Applied Procedures

The following tests on the discharge measurements using the mid-section method were carried out:

- Validation of entries in discharge measurement notes
- Graphical validation of depth versus mean velocity in cross-section
- Graphical validation of depth versus segment discharge in cross-section
- Graphical validation of vertical velocity distribution
- Graphical validation of Manning hydraulic roughness in sections
- Graphical validation of current meter rating
- Computation of hydraulic parameters for inter-comparison
- Inter-comparison of cross-sectional profiles and velocity distributions

Typical graphical validations are shown in Figures 2-2 to 2-9. Details on validations of discharge measurements are provided in Flow Measurement Report, submitted as Volume III.

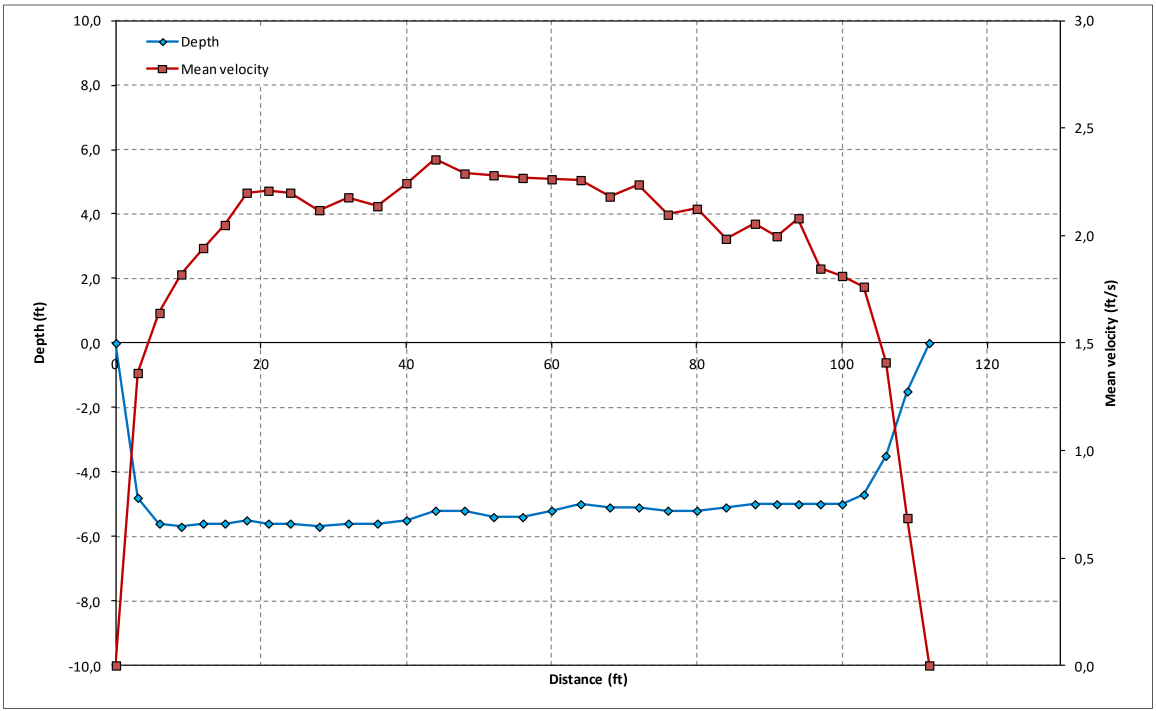

Figure 2-2: Graphical Validation of Depth versus Mean Velocity in Cross-Section

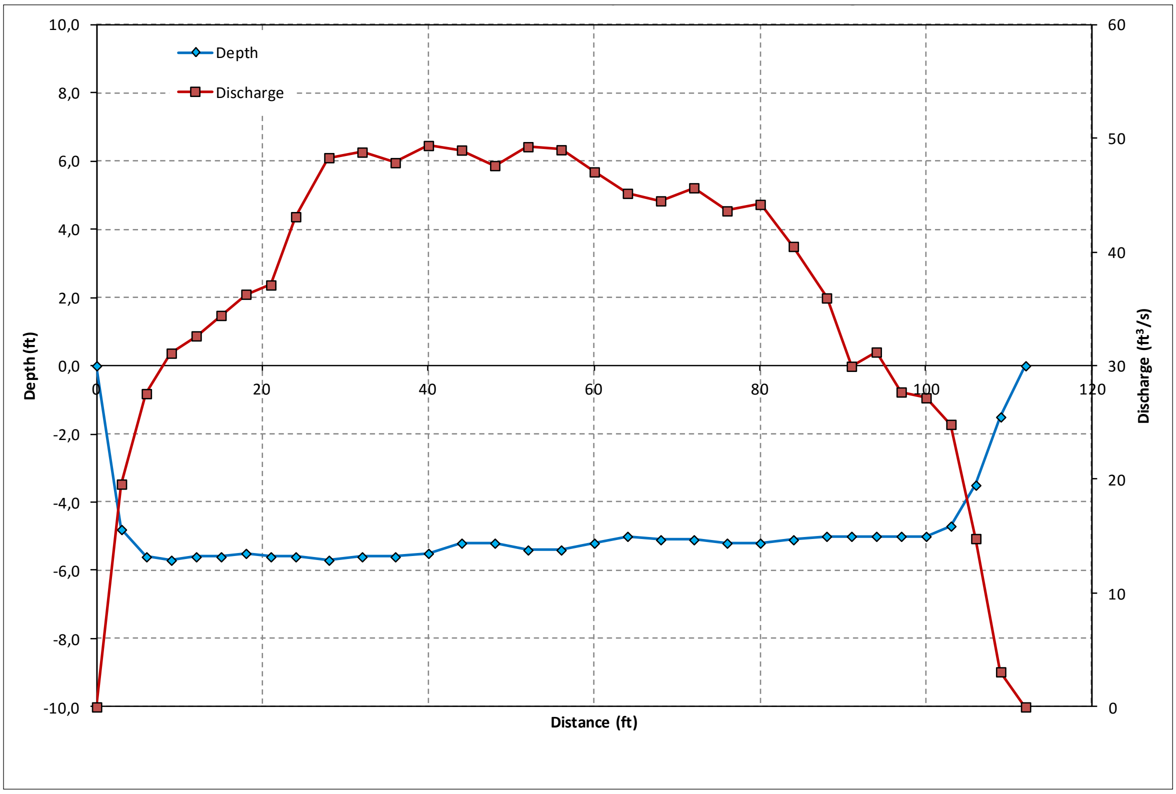

Figure 2-3: Graphical Validation of Depth versus Section Discharge in Cross-Section

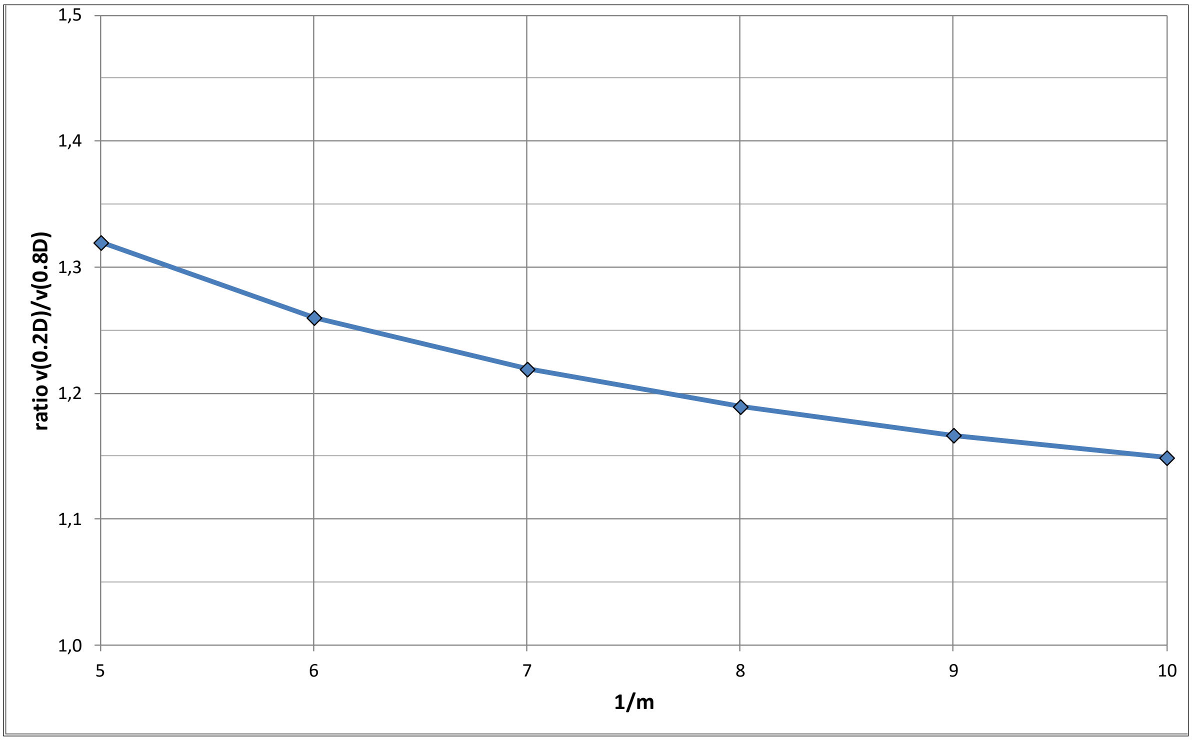

Figure 2-4: Ratio of v (0.2D)/ v (0.8D) in a Regular Turbulent Velocity Profile for Different Roughness Conditions

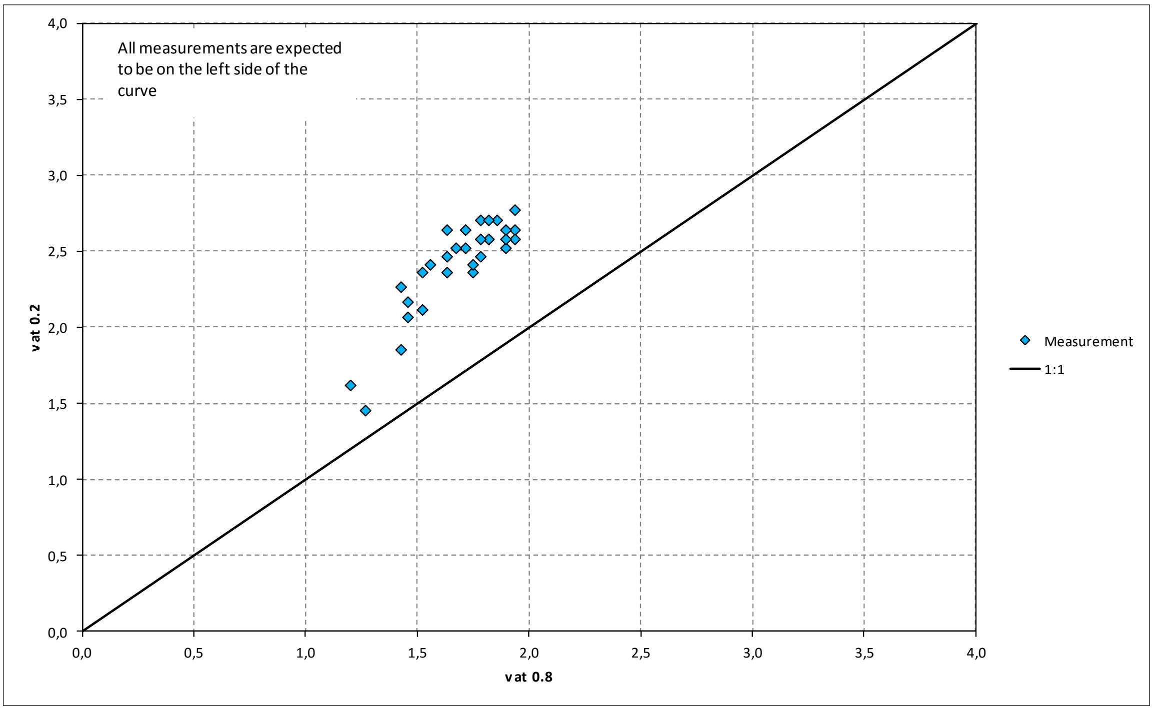

Figure 2-5: Graphical Validation of Vertical Velocity Distribution

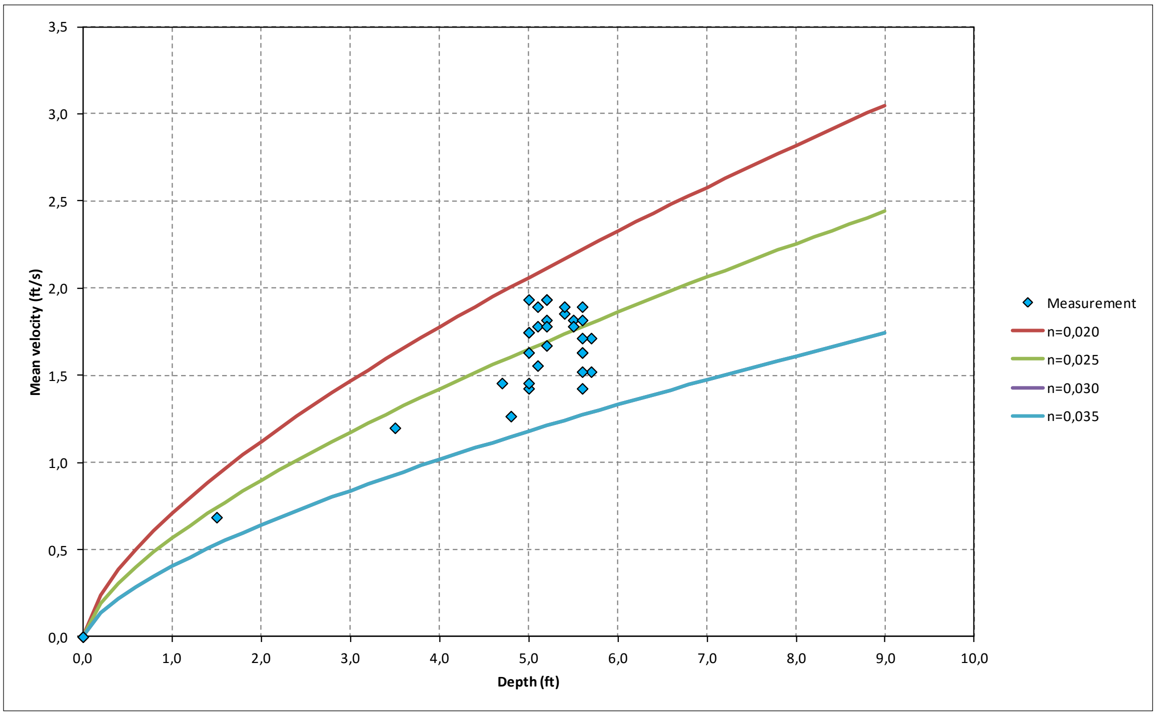

Figure 2-6: Graphical Validation of Manning Hydraulic Roughness in Sections

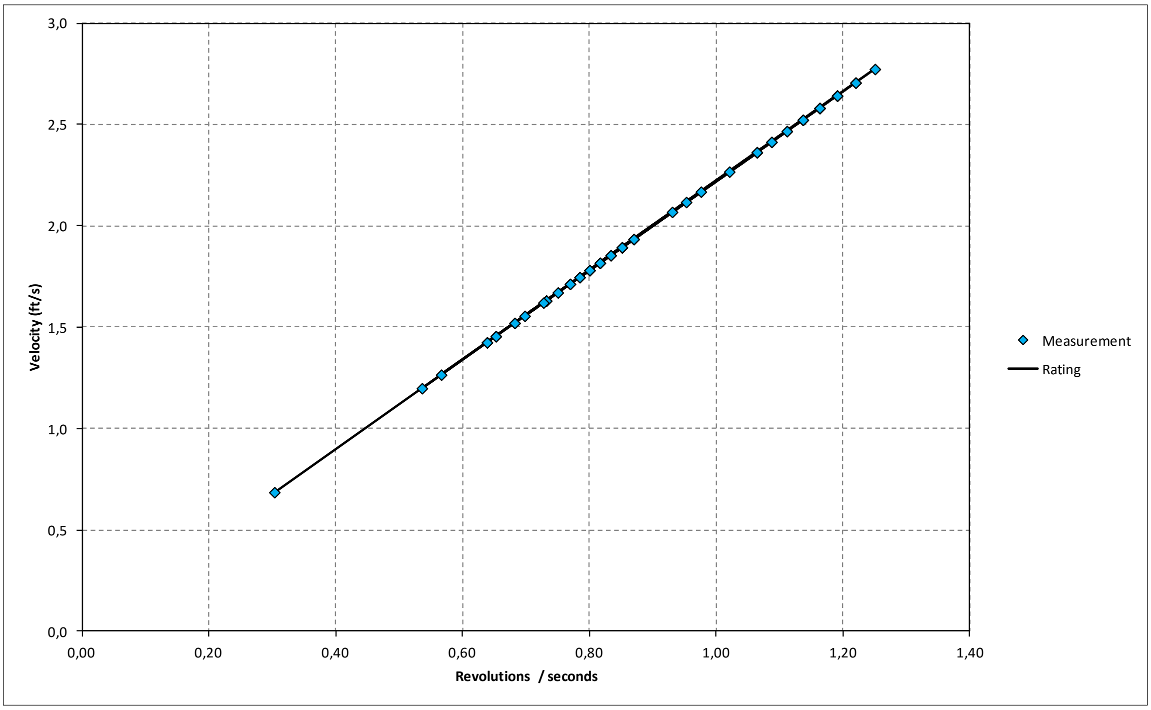

Figure 2-7: Graphical Validation of Current Meter Rating

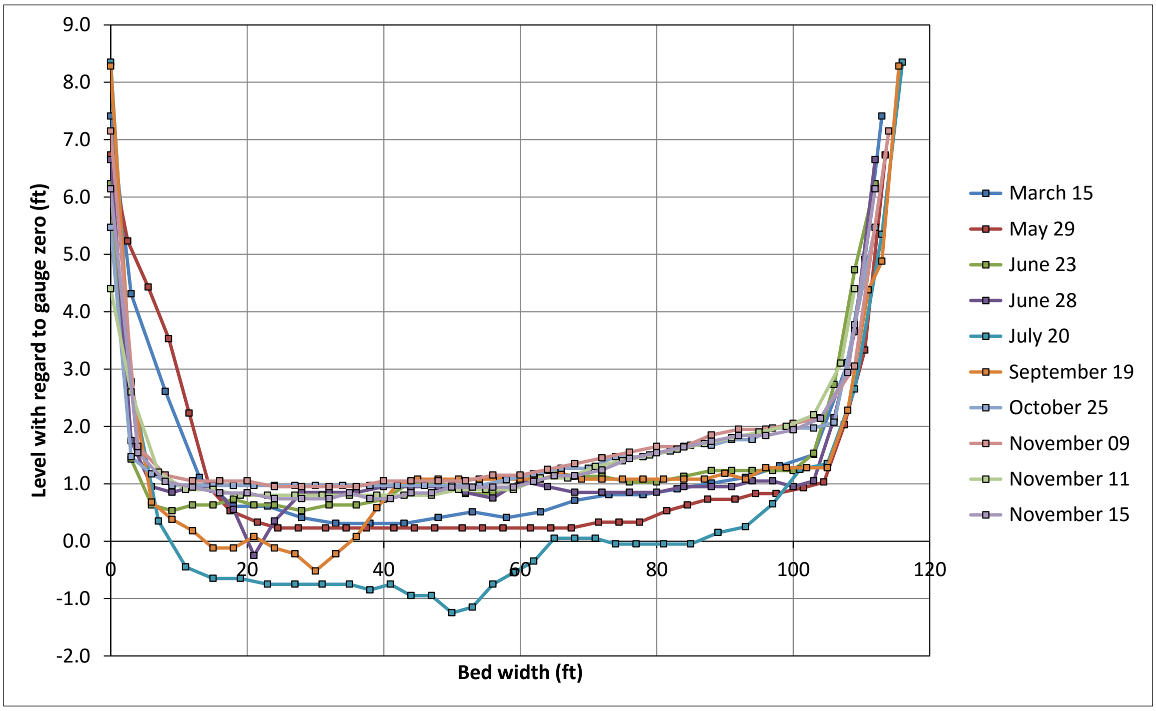

Figure 2-8: Graphical Validation of Measured Bed Profiles

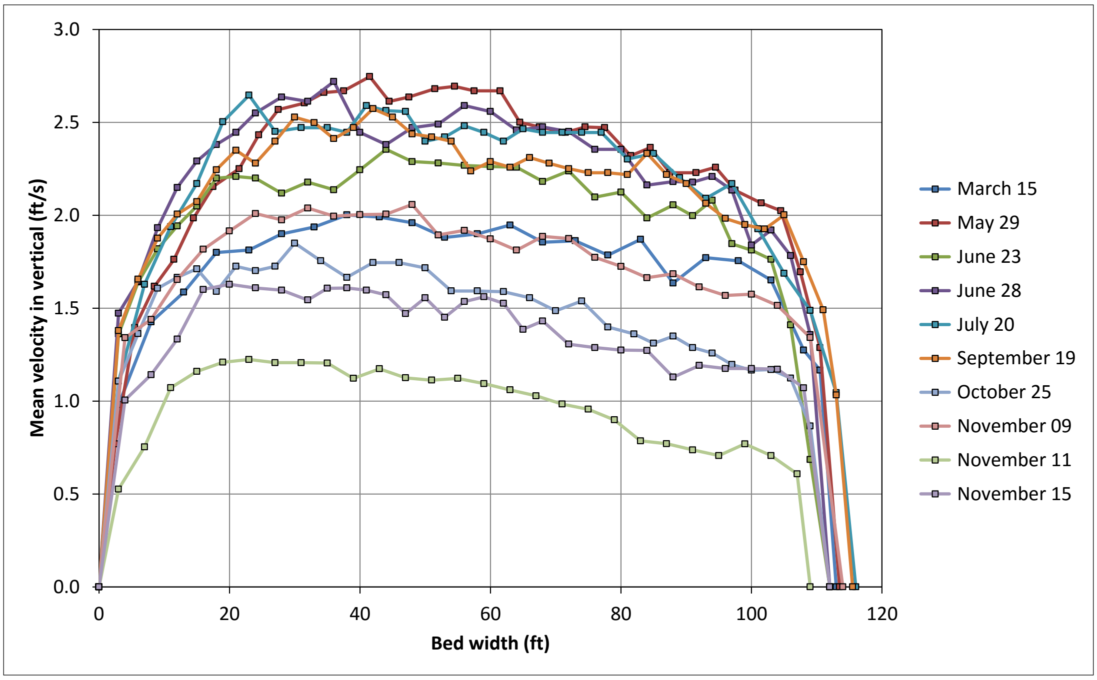

Figure 2-9: Graphical Validation of Measured Mean Velocity Distributions

2.2.6 Measurements at Chashma Barrage

2.2.6.1 Measurement Approach

A total number of 25 discharge measurements were made downstream of Chashma Barrage and in the off-taking canals under the study in 2014. The measurements are summarised in Table 2-21. Details on data analysis are provided in Flow Measurement Report submitted as Volume III.

Table 2-21: Summary of Discharge Measurements Carried out Downstream of Chashma Barrage and in the Off-taking Canals

Sr. No.	Date	Location (RD)	Gauge height (ft)	Q-measured (cfs)	Q-Authorities (cfs)	Percentage Difference (%)
I	Chashma Barrage – downstream					
1	19-05-2014	1+600	611.44	36,145	45,186	25
2	19-06-2014	1+600	614.84	130,013	145,262	12
3	12-07-2014	1+600	617.10	217,474	217,015	0
4	31-08-2014	1+600	613.15	84,981	86,677	2
5	31-07-2015	1+600*	617.56	446,941	452,808	2
II	Chashma Right Bank Canal (CRBC)					
1	10-03-2014	515+000	10.60	1,394	1,490	6
2	11-03-2014	6+280	634.82	1,963	2,000	2
3	25-04-2014	6+280	635.80	2,854	2,900	2
4	19-05-2014	6+280	637.60	4,331	4,200	-3
5	20-06-2014	6+280	637.38	4,762	4,400	-8
6	13-07-2014	6+280	637.45	4,781	4,400	-8
7	30-08-2014	6+280	637.60	4,407	4,400	-0
8	17-10-2014	6+280	636.55	3,878	3,717	-4
9	17-10-2014	6+280	636.55	3,779	3,730	-1
10	18-12-2014	6+280*	636.25	3,640	3,500	-4
11	24-03-2014	6+280*	634.70	1,629	1,700	4
12	02-06-2015	6+280*	636.92	4,318	4,200	-3
13	19-12-2014	259+350*	12.80	2,729	2,950	8

Sr. No.	Date	Location (RD)	Gauge height (ft)	Q-measured (cfs)	Q-Authorities (cfs)	Percentage Difference (%)
14	24-03-2015	259+350*	608.93	1,091	1,299	19
15	02-06-2015	259+350*	612.63	3,185	3,400	7
16	19-12-2014	380+100*	14.90	2,067	2,069	0
17	25-03-2015	380+100*	11.20	763	1,025	34
18	03-06-2015	380+100*	14.75	2,232	2,325	4
19	25-03-2015	515+000*	09.20	426	454	7
20	03-06-2015	515+000*	10.85	1,378	1,428	4
III	Chashma Jhelum (CJ) Link Canal – downstream Thal Regulator					
1	26-04-2014	36+000	3.50	1,768	2,000	13
2	29-08-2014	36+000	9.40	12,421	13,530	9
3	01-09-2014	36+000	5.40	5,360	6,000	12
4	16-10-2014	36+000	10.40	15,600	15,000	-4
IV	Tailrace of Chashma Nuclear Power Plant Channel					
1	26-04-2014	220 ft u/s of 1MW Hydel Power Station at Tail	89.50	564	560	-1
2	29-08-2014		637.83	1,534	1,720	12
3	01-09-2014		638.03	1,600	1,720	8
4	16-10-2014		638.25	1,084	1,220	13
V	Tailrace of Chashma Hydropower Plant					
1	10-03-2014	2+000	607.28	48,750	48,357	-1
2	20-06-2014	2+000	615.19	36,241	64,908	79
3	12-07-2014	0+900	616.47	32,436	32,160	-1
4	18-10-2014	2+000	607.71	64,492	58,952	-9
Total number of measurements = 4+1*+9+3*+3*+3*+2*+4+4+4=25+12*=37						

* Measurements carried out under additional scope of services

2.2.6.2 Uncertainty Analysis

The uncertainty of each of the measurements was determined according to the procedures outlined in Flow Measurement Report. Results of uncertainty in measurements are shown in Figure 2-10. It was observed that generally the relative uncertainty was less than 5%.

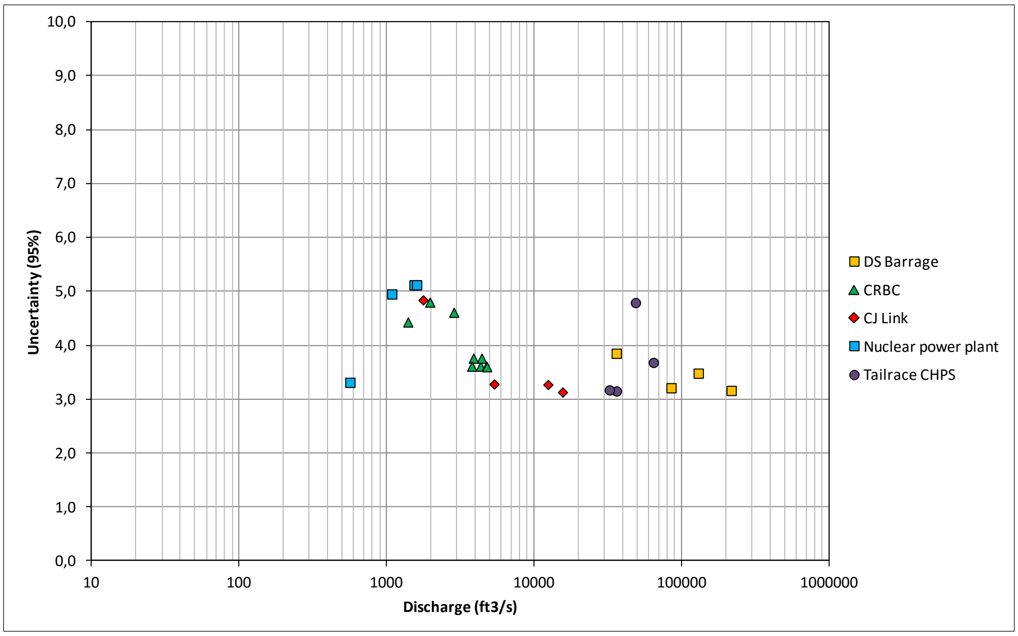

Figure 2-10: Flow Measurement Uncertainty: Chashma Barrage and Off-taking Canals

2.2.7 Measurements at Taunsa Barrage

2.2.7.1 Measurement Approach

A total number of 40 discharge measurements were made downstream Taunsa Barrage and in the off-taking canals under the Project. The measurements are summarised in Table 2-22. Details on data analysis are provided in Flow Measurement Report submitted as Volume III.

Table 2-22: Summary of Discharge Measurements Carried out Downstream of Taunsa Barrage and in the Off-taking Canals

Sr. No.	Date	Location (RD)	Gauge height (ft)	Q-measured (cfs)	Q-Authorities (cfs)	Percentage Difference (%)
I	Taunsa Barrage – downstream					
1	12-02-2014	1+105	425.00	38,523	32,355	-19
2	13-02-2014	1+105	423.10	38,007	29,960	-11
3	29-04-2014	1+230	426.65	57,225	51,532	2
4	23-05-2014	1+230	428.50	100,129	96,883	4
5	22-06-2014	1+230	446.74	169,354	154,393	-6
6	18-07-2014	1+230	430.60	211,788	222,215	5
II	Muzaffargarh Canal					
1	13-02-2014	5+850	440.50	5,181	4,494	-7
2	14-02-2014	5+850	440.82	5,792	5,000	-17
3	30-04-2014	2+060	12.80	7,088	6,700	-4
4	17-07-2014	1+930	442.55	8,476	7,700	-10
5	13-09-2014	2+060	442.25	7,173	7,200	1
6	19-10-2014	2+060	7.95	1,026	2,191	166
7	12-11-2014	2+060	9.50	2,434	3,400	69
III	Silt Ejector of Muzaffargarh Canal – off-taking at RD 4+140					
1	30-04-2014	1+586	424.88	321	200	-38
2	17-07-2014	3+000	428.24	234	300	28
3	13-09-2014	1+586	426.97	203	200	-2
4	19-10-2014	1+586	424.26	193	300	55
5	12-11-2014	1+586	423.39	76	200	163
IV	Dera Ghazi (DG) Khan Canal					
1	14-02-2014	23+000	10.85	5,539	5,500	-1
2	21-02-2014	23+000	10.95	5,634	5,500	-2
3	21-02-2014	1+500	13.00	6,760	6,100	-10
4	28-04-2014	1+500	8.10	2,062	2,200	1
5	25-05-2014	1+500	14.28	8,156	7,600	-9
6	16-07-2014	1+500	15.90	9,714	8,903	-6
7	12-09-2014	1+500	15.63	8,613	8,025	-7
8	20-10-2014	1+500	10.40	3,862	3,700	-4
9	11-11-2014	1+500	7.12	1,402	1,742	26
V	Silt Ejector of DG Khan Canal – off-taking at RD 7+500					
1	14-02-2014	4+000	425.49	792	600	-24
2	28-04-2014	4+000	426.04	506	200	-61
3	25-05-2014	4+000	427.68	645	600	-7
4	16-07-2014	4+000	430.22	512	600	17
5	12-09-2014	4+000	429.47	504	300	-41
6	20-10-2014	4+000	427.97	429	200	-53
7	11-11-2014	4+000	429.65	387	200	-48
VI	Taunsa Panjnad (TP) Link Canal					
1	01-05-2014	4+500	2.21	768	1,000	30
2	23-05-2014	4+500	8.09	10,935	8,628	-21
3	24-05-2014	4+500	6.43	8,156	5,947	-27
4	15-07-2014	4+500	8.70	11,642	11,390	-2
5	21-10-2014	4+500	2.40	1,016	3,575	252
6	13-11-2014	4+500	4.25	3,602	5,500	53
Total number of measurements = 6+7+5+9+7+6=40						

2.2.7.2 Uncertainty Analysis

The uncertainty of each of the measurements were determined according to the procedures outlined in Flow Measurement Report. Results of uncertainty in measurements are shown in Figure 2-11. It was observed that generally the relative uncertainty was less than 5%, with a few exceptions for some measurements in the silt excluders due to limited number of verticals or use of 0.6D measurement method.

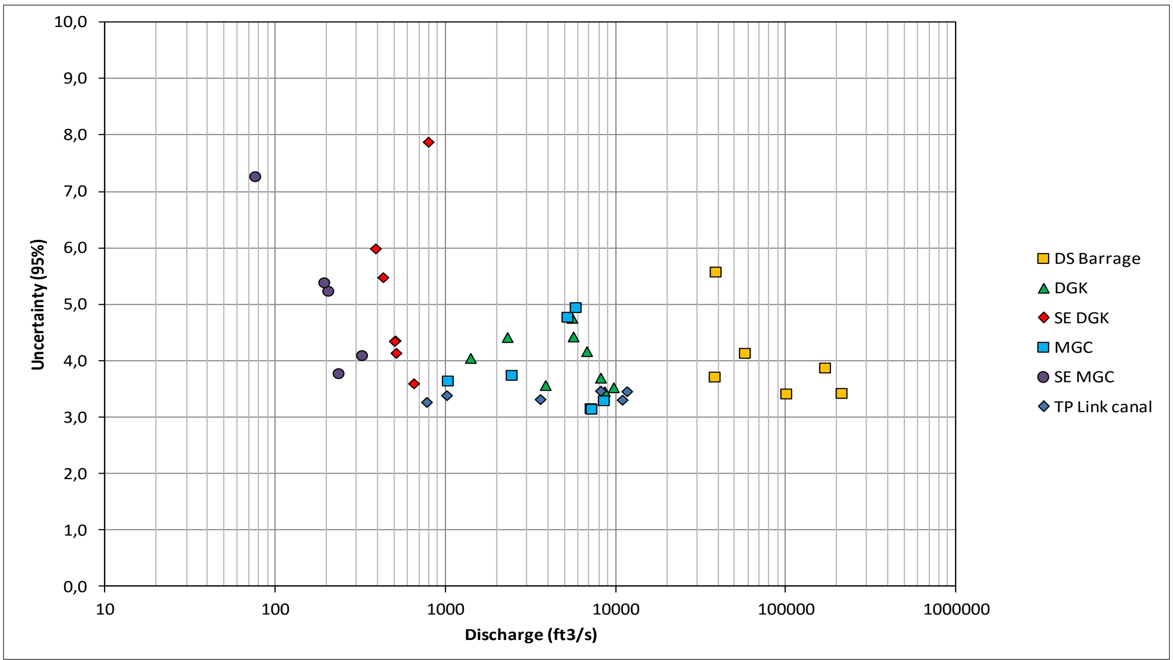

Figure 2-11: Flow Measurement Uncertainty: Taunsa Barrage and Off-taking Canals

2.2.8 Measurements at Guddu barrage

2.2.8.1 Measurement Approach

A total number of 34 discharge measurements were made downstream of Guddu Barrage and in the off-taking canals under the Project. The measurements are summarised in Table 2-23.

Table 2-23: Summary of Discharge Measurements Carried out Downstream of Guddu Barrage and in the Off-taking Canals

Sr. No.	Date	Location (RD)	Gauge height (ft)	Q-measured (cfs)	Q-Authorities (cfs)	Percentage Difference (%)
I	Guddu Barrage – downstream					
1	16-02-2014	0+450	245.68	41,789	37,408	-10
2	26-05-2014	2+550	248.50	79,133	70,529	-12
3	25-06-2014	2+550	250.75	122,045	121,293	-11
4	21-07-2014	2+550	251.50	162,055	161,987	0
5	15-09-2014	2+550	252.34	226,800	238,880	5
6	18-09-2014	2+550	253.22	298,587	307,455	3
7a	22-10-2014	2+550 C1	247.84	47,339		
7b	22-10-2014	2+550 C2	247.84	24,881		
				Σ 72,220	63,294	-12

Sr. No.	Date	Location (RD)	Gauge height (ft)	Q-measured (cfs)	Q-Authorities (cfs)	Percentage Difference (%)
II	Ghotki Feeder Canal					
1	19-02-2014	1+500	249.40	1,147	1,467	28
2	28-05-2014	1+500	225.25	6,769	7,000	3.0
3	25-06-2014	1+500	256.85	11,161	9,050	-19
4	20-07-2014	1+500	258.60	14,051	11,610	-17
5	20-09-2014	1+500	255.99	10,102	7,850	-22
6	23-10-2014	1+500	251.60	3,285	3,831	17
III	Begari Sindh Feeder Canal					
1	18-02-2014	1+500	250.20	1,049	Nil	-
2	24-06-2014	1+500	257.30	17,966	13,508	-25
3	23-07-2014	1+500	258.10	17,782	15,210	-14
4	16-09-2014	1+500	254.75	10,421	7,998	-23
IV	Escape Channel – downstream of Guddu Power Plant					
1	18-02-2014	N.A	N.A	539	N.A	-
2	24-06-2014	N.A	N.A	683	N.A	-
3	23-07-2014	N.A	N.A	1,155	N.A	-
4	16-09-2014	N.A	N.A	486	N.A	-
V	Desert Pat Feeder Canal					
1	18-02-2014	1+500	249.00	2,142	2,095	-2
2	27-05-2014	1+500	251.67	5,064	5,000	-8
3	26-06-2014	1+500	256.59	13,863	2,202	-10
4	22-07-2014	1+500	256.35	12,115	11,450	-5
5	17-09-2014	1+500	254.80	8,607	9,068	7
6	17-11-2014	2+000	248.18	2,001	1,419	-25
VI	Pat Feeder Canal					
1	17-02-2014	110+106	6.35	2,059	3,400	65
2	27-05-2014	110+106	8.30	3,542	5,000	45
3	26-06-2014	110+106	9.30	5,115	6,300	37
4	22-07-2014	110+106	11.00	5,856	7,000	22
5	17-11-2014	110+106	5.78	1,656	1,415	-14
6	29-07-2015	110+106*	8.90	4,109	3,864**	-6
VII	Rainee Canal					
1	21-07-2014	0+470	249.98	443	N.A	-
Total number of measurements =7+6+4+4+6+5+1*+1=33+1*=34						

C1= Creek 1 C2 = Creek 2

* Measurements carried out under additional scope of services

** Discharge reported based on newly developed rating table by the Consultants

2.2.8.2 Uncertainty Analysis

The uncertainty of each of the measurements were determined. The results are presented in Figure 2-12. It was observed that generally the relative uncertainty was less than 5%. The outliers were caused by a limited number of vertical taken during the measurement.

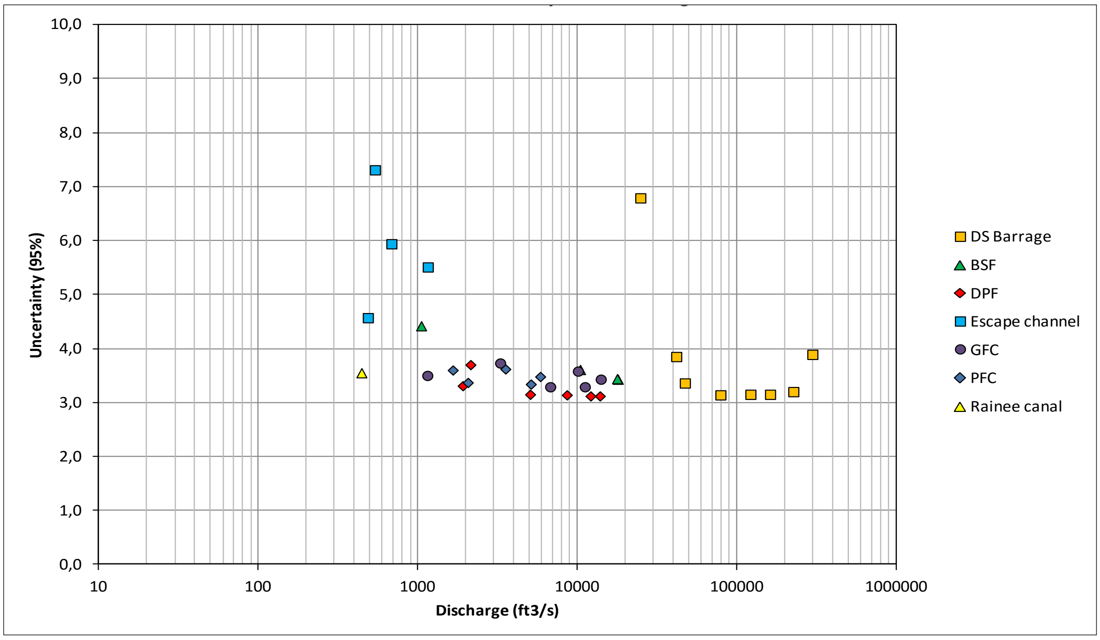

Figure 2-12: Flow Measurement Uncertainty: Guddu Barrage and Off-taking Canals

2.2.9 Measurements at Marala Barrage

2.2.9.1 Measurement Approach

A total number of 15 discharge measurements were made downstream of Marala Barrage and in the off-taking canals. The measurements are summarised in Table 2-24.

Table 2-24: Summary of Discharge Measurements Carried out Downstream of Marala Barrage and in the Off-taking Canals

Sr. No.	Date	Location (RD)	Gauge height (ft)	Q-measured (cfs)	Q-Authorities (cfs)	Percentage Difference (%)
I	Marala Barrage – downstream					
1a	22-04-2014	1+380 LC	799.00	10,608		
1b	22-04-2014	0+941 RC	798.70	4,956		
				Σ 15,563	16,428	6
2a	17-06-2014	1+510 LC	801.25	24,846		
2b	17-06-2014	2+160 MC	801.80	6,098		
2c	17-06-2014	1+000 RC	801.80	18,563		
				Σ 49,507	43,888	-11
3a	10-07-2014	0+941 LC	801.30	18,435		
3b	10-07-2014	1+710 RC	800.05	10,930		
				Σ 29,365	29,317	0
4	07-09-2014	0+550	805.88	258,135	254,470	-1
5	08-09-2014	0+550	804.30	147,645	124,488	-16
II	Marala Ravi (MR) Link Canal					
1	12-03-2014	8+550 UCC	795.60	6,868	7,450	8
2	23-04-2014	8+550 UCC	795.48	6,691	7,000	5
3	21-05-2014	19+500	12.90	10,677	12,310	16
4	17-06-2014	19+500	17.45	19,943	20,000	0
5	08-08-2014	19+500	17.18	19,429	19,422	0
III	Upper Chenab Canal (UCC					
1	13-10-2014	8+550	19.10	11,790	12,796	9
Total number of measurements =5+5+1=11						

LC = Left Creek MC = Middle Creek RC = Right Creek

2.2.9.2 Uncertainty Analysis

The uncertainty of each of the measurements was determined. The results are presented in Figure 2-13. It was observed that generally the relative uncertainty was less than 5%. The uncertainty in measurements for Marala Ravi Link Canal was seen to be generally in the order of 3-4%. The accuracy of the high flow measurements downstream of Marala Barrage was less due to application of 0.6D method and/or limited number of verticals to speed up the measurements and horizontal angle corrections in some cases. The measurements carried out in separate channels were seen to lead to total discharges with uncertainties also in the order of 3-4% as for the canal.

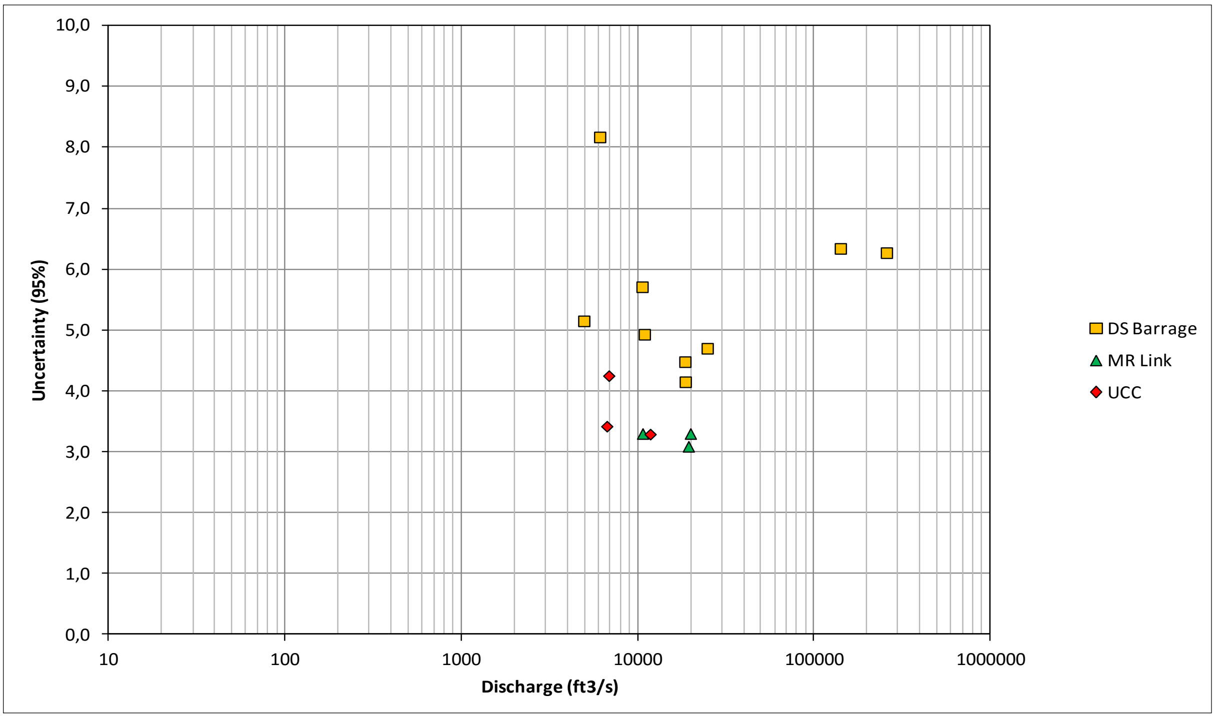

Figure 2-13: Flow Measurement Uncertainty: Marala Barrage and Off-taking Canals

2.2.10 Measurements at Garang Regulator (Kirther Canal)

2.2.10.1 Measurement Approach

A total number of 15 discharge measurements were made upstream and downstream of the Garang Regulator in Kirther Canal and in the off-taking canals. The measurements are summarised in Table 2-25.

Table 2-25: Summary of Discharge Measurements Carried out in Kirther Canal and in the Off-taking Canals

Sr. No.	Date	Location (RD)	Gauge height (ft)	Q-measured (cfs)	Q-Authorities (cfs)	Percentage Difference (%)
I	Kirther Canal – upstream of Garang Regulator					
1	15-03-2014	98+000	7.26	1,743	N.A.	-
2	15-11-2014	100+000	6.20	1,671	N.A.	-

Sr. No.	Date	Location (RD)	Gauge height (ft)	Q-measured (cfs)	Q-Authorities (cfs)	Percentage Difference (%)
II	Kirther Canal – downstream of Garang Regulator					
1	15-03-2014	103+400	7.338	1,245	780	-37
2	29-05-2014	103+400	6.795	1,518	1,254	-17
3	23-06-2014	103+400	6.230	1,156	1,149	0
4	28-06-2014	103+400	6.660	1,420	1,254	-12
5	20-07-2014	103+400	8.325	2,105	1,833	-13
6	19-09-2014	103+400	8.250	1,799	1,833	2
7	25-10-2014	103+400	5.520	686	380	-45
8	09-11-2014	103+400	7.120	1,119	500	-55
9	11-11-2014	103+400	4.355	337	380	13
10	15-11-2014	103+400	6.120	736	400	-45.65
11	26-07-2015*	103+400*	8.315	2,002	1,985**	-1
12	27-07-2015*	103+400*	9.345	2,357	2,406**	2
III	Saifullah Magsi Branch Canal					
1	15-03-2014	1+430	2.07	525	N.A.	-
2	15-11-2014	0+800	5.25	924	N.A.	-
IV	Gokalpur Minor					
1	16-03-2014	0+408	5.74	18	N.A.	-
Total number of measurements =2+10+2+1=15						

Zero of gauges = 165.80 ft

* Measurements carried out under additional scope of services

** Discharge reported based on newly developed rating table by the Consultants

2.2.10.2 Uncertainty Analysis

The uncertainty in each of the measurements was determined. The results are presented in Figure 2-14. It was observed that generally the relative uncertainty was less than 5% except for one measurement in Gokalpur Minor, due to the small number of verticals applied.

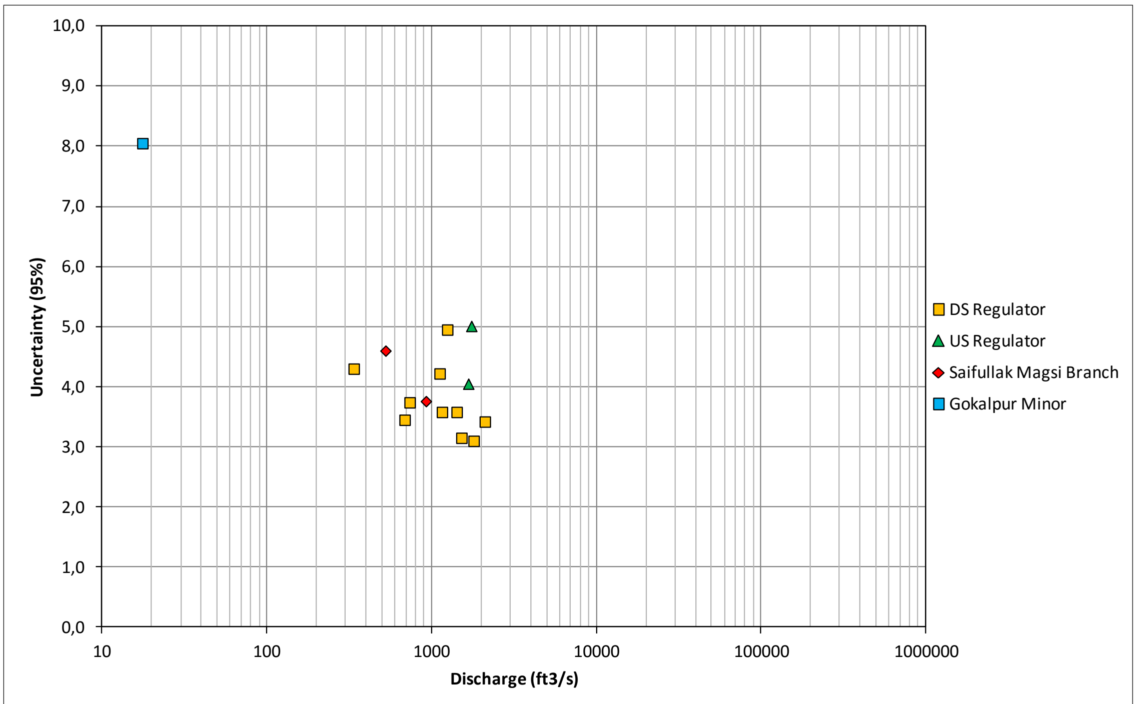

Figure 2-14: Flow Measurement Uncertainty: Kirther Canal at Garang Regulator and Off-taking Canals

2.2.11 Conclusions on Discharge Measurements

1. The discharge measurements used to calibrate/upgrade the discharge coefficients or to establish a stage-discharge relation at the five (5) pilot sites covered the most dominant range of discharges in the river as well as in the canals.

2. The discharges in the rivers and canals were measured by the current meter method; agreed by all the stakeholders. However, for future flow measurements, it was agreed that conventional current meter methods may be used for the narrow and shallow channels while the Acoustic Doppler Current Profiler (ADCP) may be used for the wider canals and rivers.

3. All the flow measurements carried out under the project in rivers and canals, passed the validation test.

4. The uncertainties (95%) computed for the 5 pilot sites were within the following acceptable ranges:

   - Chashma barrage and off-takings: 3-5%
   - Taunsa barrage and off-takings: 3-8%
   - Guddu barrage and off-takings: 3-7%
   - Marala barrage and off-takings: 3-8%
   - Kirther Canal at Garang Regulator: 3-5%

5. At present, there is no proper arrangement for monitoring the discharges of Silt Ejectors which is compulsory for estimating the overall water balance at the structures.

2.3 CALIBRATION OF DISCHARGE COEFFICIENTS AND ESTABLISHMENT OF STAGE DISCHARGE RELATIONSHIPS

Flow measurements carried out downstream of Chasma barrage, Taunsa barrage, Guddu barrage and Marala barrage were used to calculate the applicable coefficient of discharges under the actual hydraulic and geometric conditions observed on site at the measurement day.

The results of regression analysis carried out for corrected discharge coefficients at Chashma, Taunsa, Guddua and Marala barrages are shown in Figures 2-15 to 2-18, respectively.

Details on stepwise procedure followed for calibration of discharge coefficients, evaluation of discharge relations, comparison with discharge measurements, morphological aspects and establishment of stage-discharge relations at respective locations is provided in Flow Measurement Report submitted as Volume III.

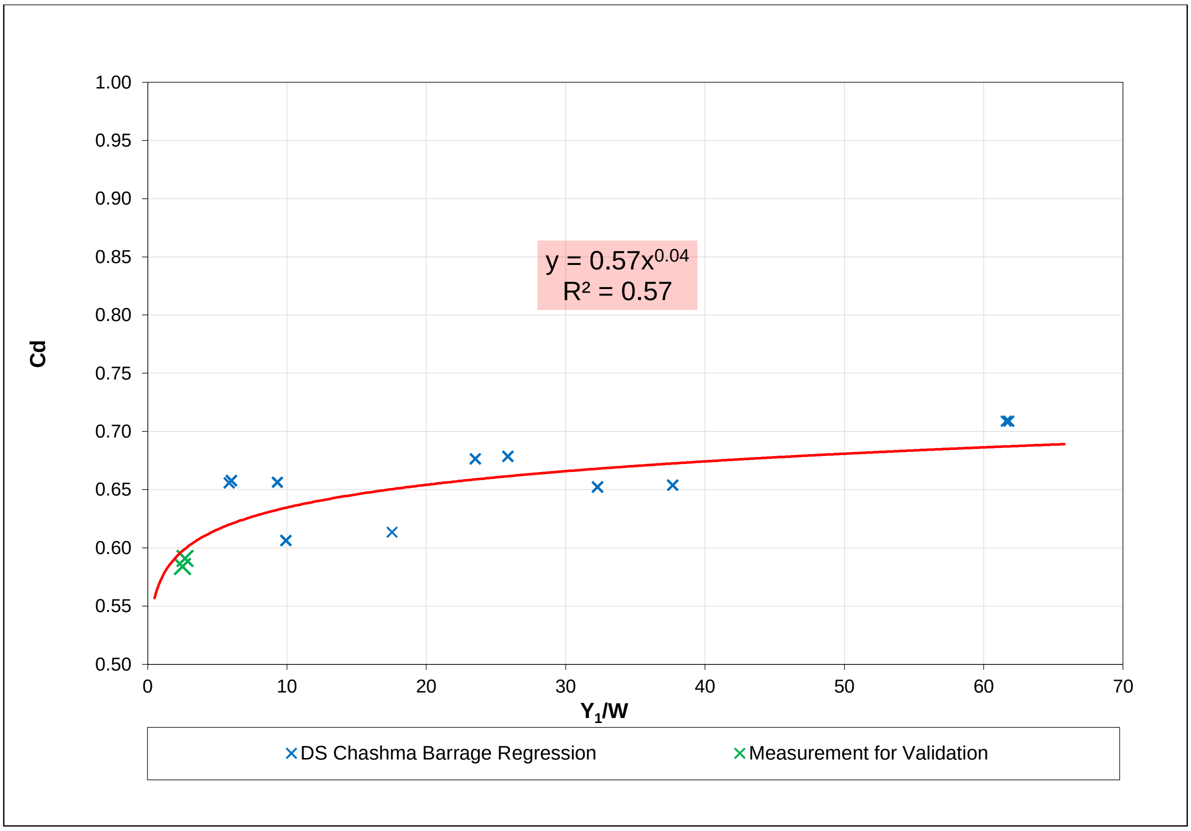

Figure 2-15: Regression Analysis of Corrected Discharge Coefficients for Chashma Barrage

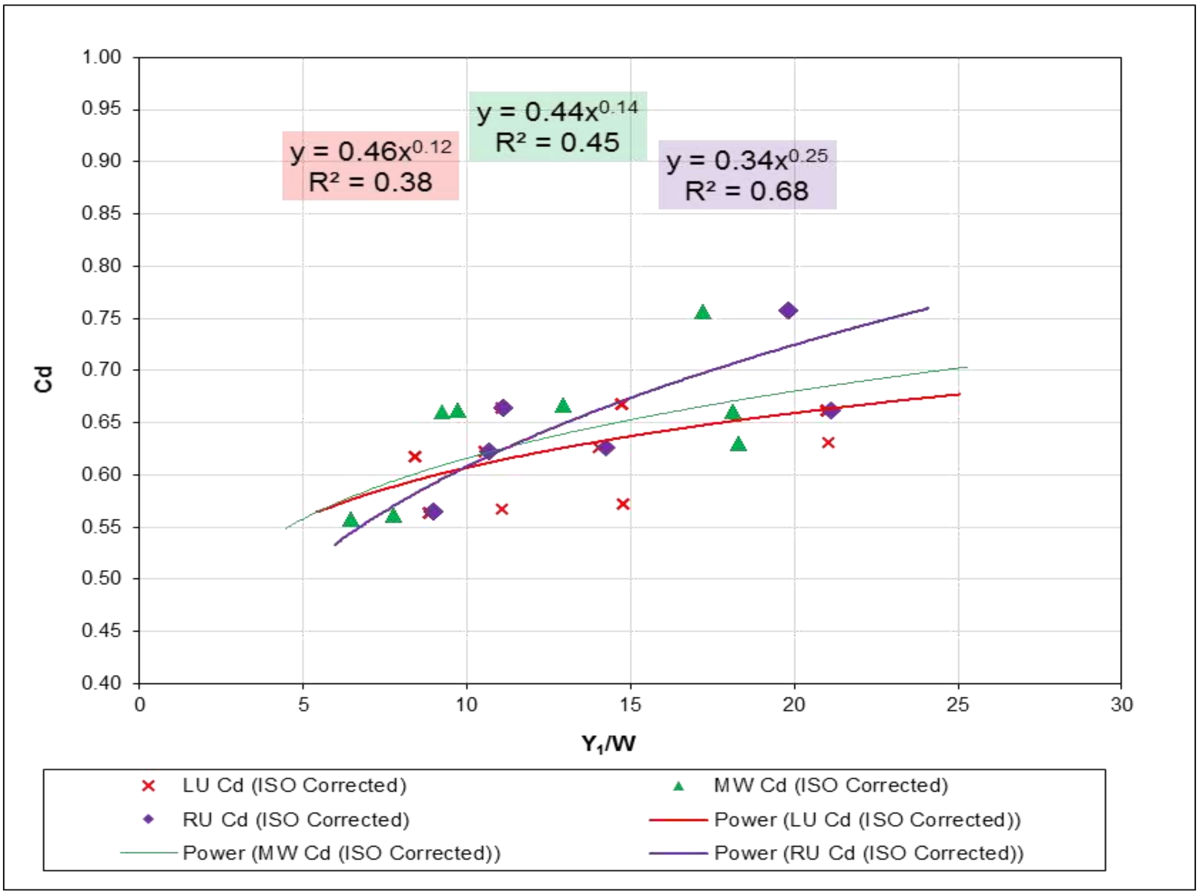

Figure 2-16: Regression Analyses of Corrected Discharge Coefficients for Taunsa Barrage

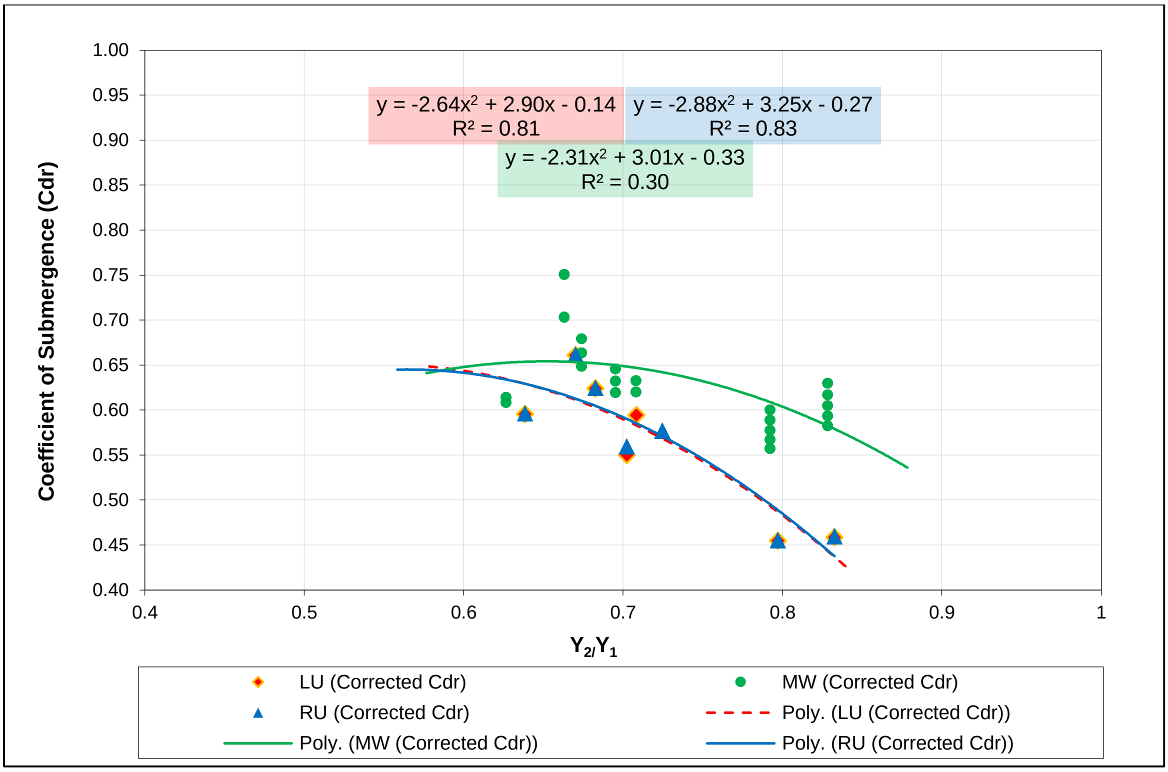

Figure 2-17: Regression Analysis of Corrected Discharge Coefficients for Guddu Barrage

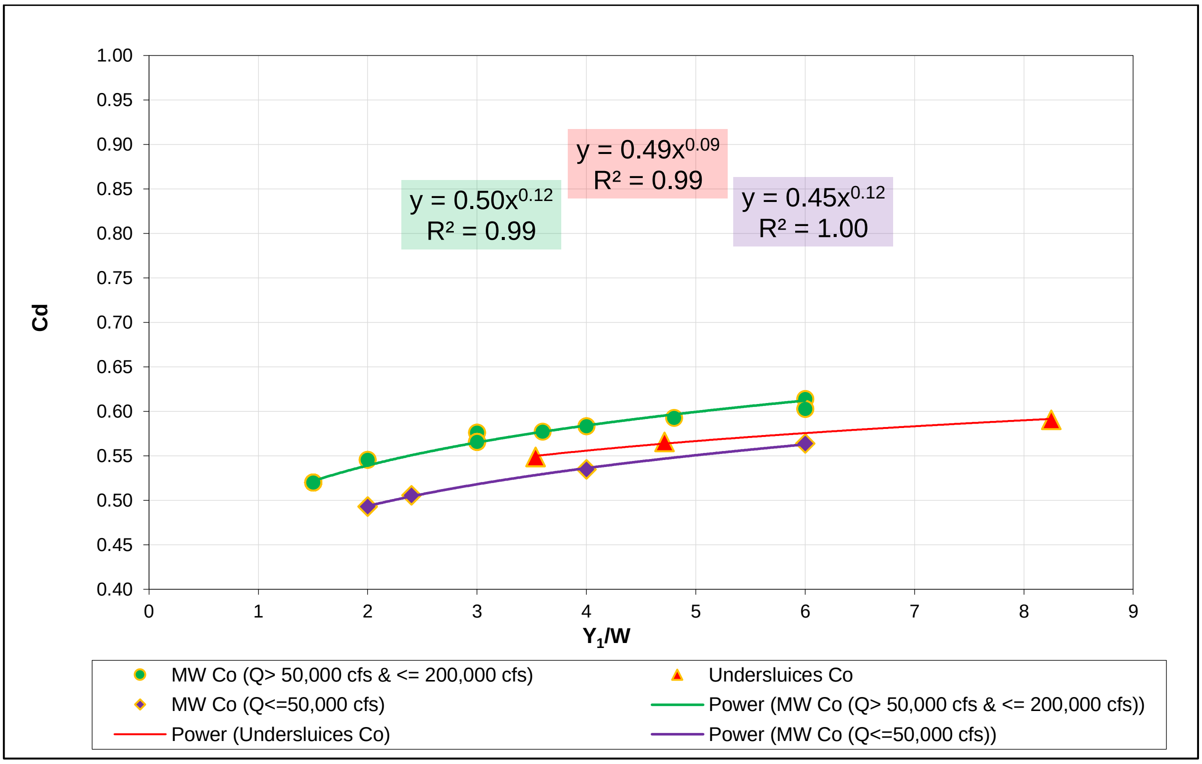

Figure 2-18: Regression Analysis of Corrected Discharge Coefficients for Marala Barrage

Recommended stage-discharge relationships for various canals are shown in Figures 2-19 to 2-31 while gauge-discharge rating tables are given in Tables 2-26 to 2-39.

Please note, the rating tables, developed under the study are applicable for both Rabi 2015-16 and Kharif 2016 seasons and needs to be revised after Kharif 2016. The rating tables incorporated the 2014-15 morphological changes in the canals.

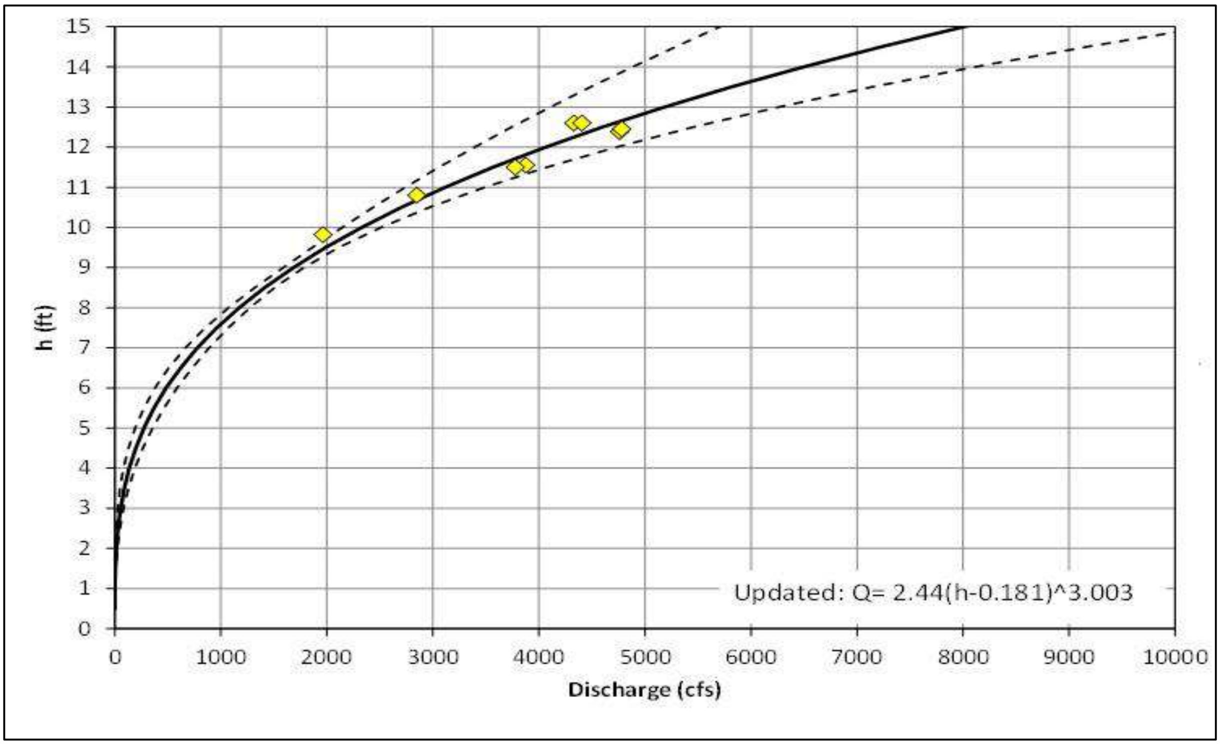

Figure 2-19: Stage- Discharge Relationship for CRBC D/S Head Regulator

Table 2-26: Gauge- Discharge Rating Table for CRBC D/S Head Regulator

Gauge / Fraction (Ft)	0.0	0.1	0.2	0.3	0.4	0.5	0.6	0.7	0.8	0.9
	Discharge in Cusecs									
625 (0)	-	-	-	-	-	-	-	-	1	1
626 (1)	1	2	3	3	4	6	7	9	10	12
627 (2)	15	17	20	23	27	31	35	39	44	49
628 (3)	55	61	67	74	82	90	98	107	116	126
629 (4)	136	147	159	171	184	197	211	226	242	258
630 (5)	274	292	310	329	349	369	390	412	435	459
631 (6)	483	509	535	562	590	619	649	680	712	744
632 (7)	778	813	849	886	923	962	1,002	1,044	1,086	1,129
633 (8)	1,174	1,219	1,266	1,314	1,363	1,414	1,465	1,518	1,572	1,628
634 (9)	1,685	1,743	1,802	1,863	1,925	1,988	2,053	2,119	2,186	2,255
635 (10)	2,326	2,398	2,471	2,546	2,622	2,700	2,779	2,860	2,943	3,027
636 (11)	3,112	3,199	3,288	3,379	3,471	3,564	3,660	3,757	3,856	3,956
637 (12)	4,058	4,162	4,268	4,376	4,485	4,596	4,709	4,824	4,940	5,059
638 (13)	5,179	5,302	5,426	5,552	5,680	5,810	5,942	6,076	6,212	6,350

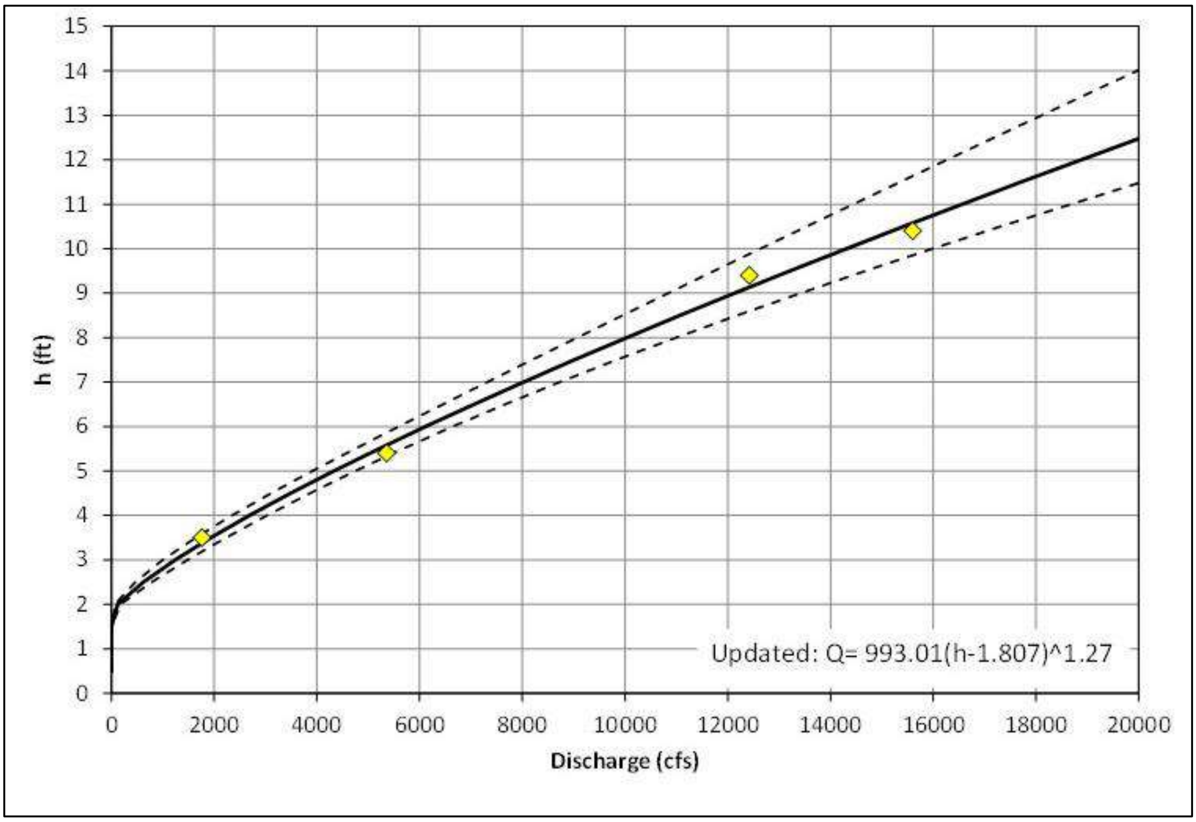

Figure 2-20: Stage- Discharge Relationship D/S Thal Regulator of CJLC at RD 36+000

Table 2-27: Gauge- Discharge Rating Table for CJLC D/S Thal X-Regulator at RD 36+000

Gauge / Fraction (Ft)	0.0	0.1	0.2	0.3	0.4	0.5	0.6	0.7	0.8	0.9
	Discharge in Cusecs									
0	-	-	-	-	-	-	-	-	-	-
1	-	-	-	-	-	-	-	-	-	49
2	123	209	303	404	511	623	740	860	984	1,112
3	1,242	1,376	1,513	1,652	1,794	1,938	2,084	2,233	2,384	2,537
4	2,692	2,849	3,008	3,168	3,330	3,494	3,660	3,827	3,996	4,166
5	4,338	4,511	4,686	4,862	5,039	5,218	5,398	5,580	5,762	5,946
6	6,131	6,318	6,505	6,694	6,884	7,075	7,266	7,460	7,654	7,849
7	8,045	8,242	8,441	8,640	8,840	9,041	9,244	9,447	9,651	9,856
8	10,062	10,268	10,476	10,685	10,894	11,104	11,315	11,527	11,740	11,954
9	12,168	12,384	12,600	12,816	13,034	13,252	13,472	13,692	13,912	14,134
10	14,356	14,579	14,802	15,027	15,252	15,477	15,704	15,931	16,159	16,387
11	16,617	16,847	17,077	17,308	17,540	17,773	18,006	18,240	18,474	18,709
12	18,945	19,181	19,418	19,656	19,894	20,133	20,372	20,613	20,853	21,094
13	21,336	21,579	21,821	22,065	22,309	22,554	22,799	23,045	23,291	23,538

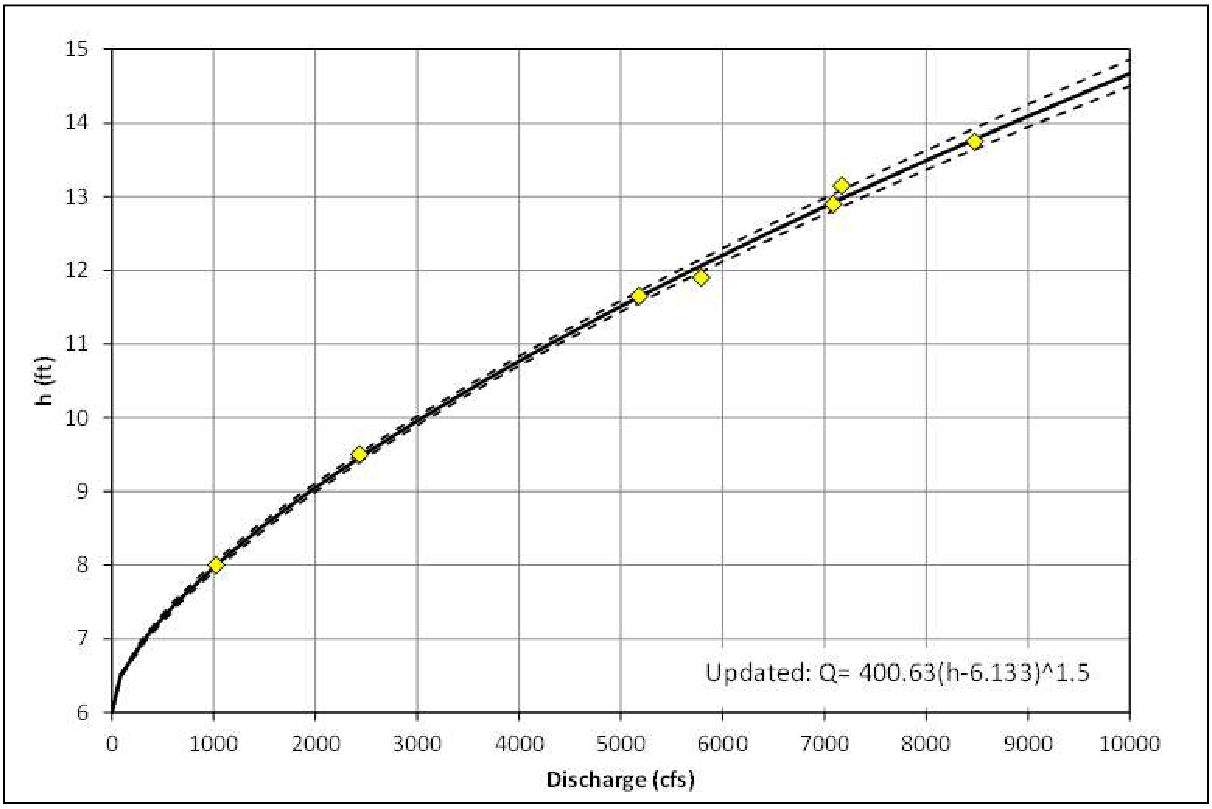

Figure 2-21: Stage- Discharge relationship for Muzaffargarh Canal D/S Head Regulator

Table 2-28: Gauge- Discharge Rating Table for Muzaffargarh Canal D/S Head Regulator

Gauge / Fraction (Ft)	0.0	0.1	0.2	0.3	0.4	0.5	0.6	0.7	0.8	0.9
	Discharge in Cusecs									
0	-	-	-	-	-	-	-	-	-	-
1	-	-	-	-	-	-	-	-	-	-
2	-	-	-	-	-	-	-	-	-	-
3	-	-	-	-	-	-	-	-	-	-
4	-	-	-	-	-	-	-	-	-	-
5	-	-	-	-	-	-	-	-	-	-
6	-	-	7	27	55	89	128	171	218	269
7	323	381	442	505	571	640	712	786	862	941
8	1,022	1,105	1,191	1,278	1,367	1,459	1,552	1,648	1,745	1,844
9	1,945	2,047	2,152	2,258	2,366	2,475	2,586	2,699	2,813	2,929
10	3,047	3,165	3,286	3,408	3,531	3,656	3,782	3,910	4,039	4,170
11	4,302	4,435	4,570	4,705	4,843	4,981	5,121	5,262	5,405	5,548
12	5,693	5,840	5,987	6,136	6,285	6,436	6,589	6,742	6,897	7,052
13	7,209	7,367	7,527	7,687	7,848	8,011	8,175	8,339	8,505	8,672

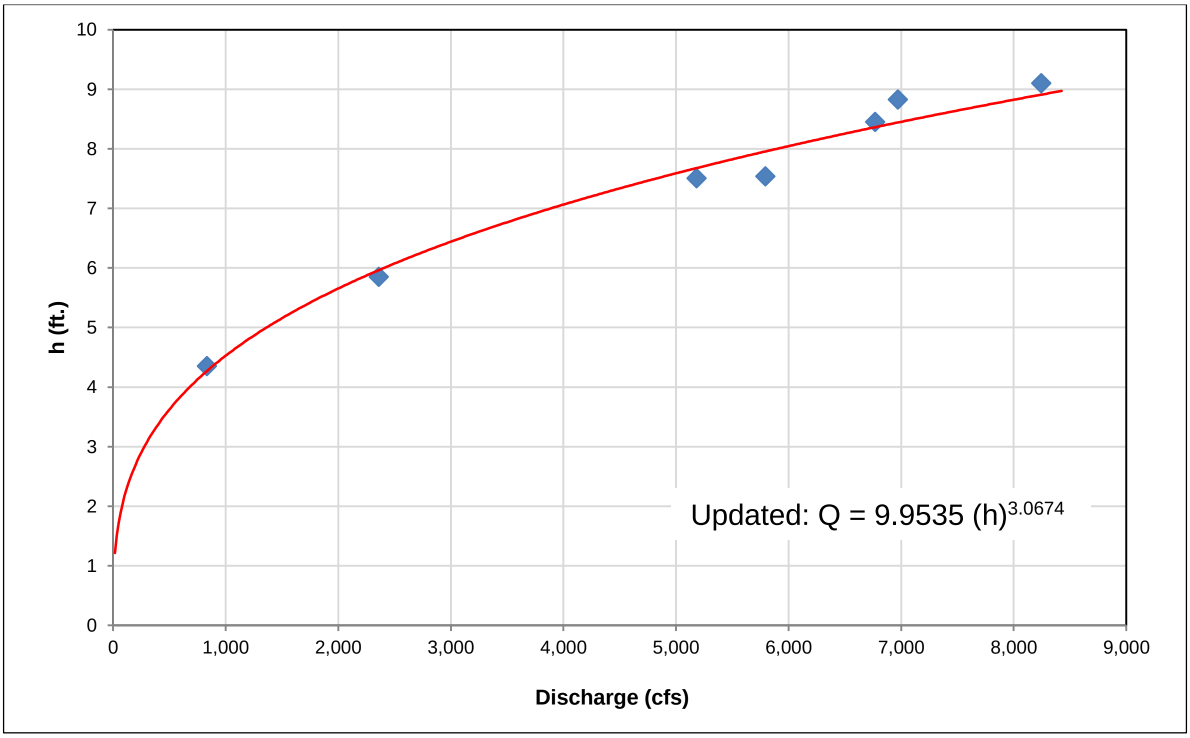

Figure 2-22: Stage- Discharge relationship for Muzaffargarh Canal at RD 5+500

Table 2-29: Gauge- Discharge Rating Table for Muzaffargarh Canal at RD 5+500

Gauge / Fraction (Ft)	0.0	0.1	0.2	0.3	0.4	0.5	0.6	0.7	0.8	0.9
	Discharge in Cusecs									
433 (0)	-	-	-	-	-	0	0	0	0	1
434 (1)	2	3	4	6	9	12	15	20	25	31
435 (2)	38	46	55	66	77	90	104	120	137	155
436 (3)	176	198	222	247	275	304	336	370	406	444
437 (4)	485	528	574	622	673	727	783	842	905	970
438 (5)	1,038	1,110	1,185	1,263	1,345	1,430	1,518	1,611	1,707	1,806
439 (6)	1,910	2,017	2,129	2,245	2,364	2,488	2,617	2,750	2,887	3,028
440 (7)	3,175	3,326	3,482	3,642	3,808	3,978	4,154	4,335	4,521	4,712
441 (8)	4,909	5,111	5,319	5,532	5,751	5,976	6,207	6,443	6,686	6,935
442 (9)	7,189	7,450	7,718	7,992	8,272	8,559	8,852	9,152	9,459	9,773

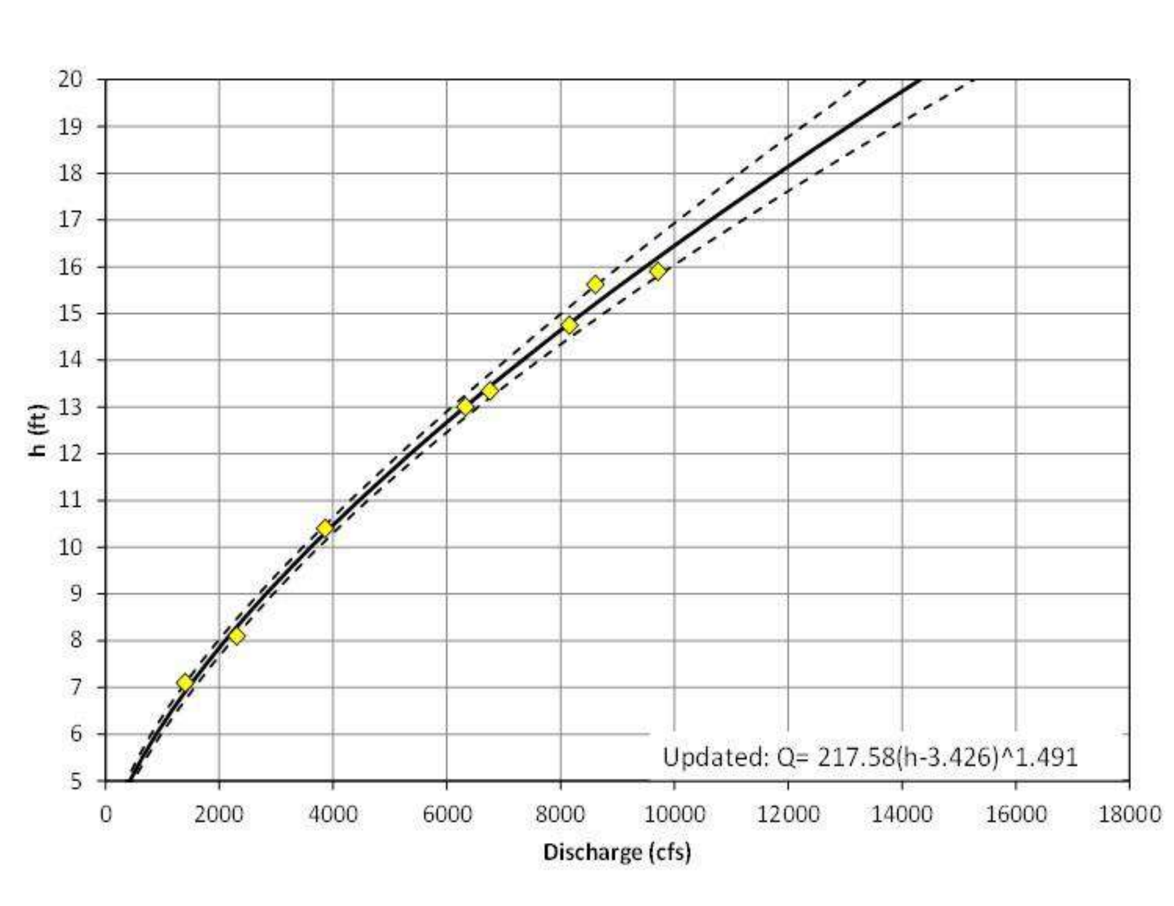

Figure 2-23: Stage- Discharge Relationship for Dera Ghazi Khan Canal D/S Head Regulator

Table 2-30: Gauge- Discharge Rating Table for DG Khan Canal D/S Head Regulator

Gauge / Fraction (Ft)	0.0	0.1	0.2	0.3	0.4	0.5	0.6	0.7	0.8	0.9
	Discharge in Cusecs									
0	-	-	-	-	-	-	-	-	-	-
1	-	-	-	-	-	-	-	-	-	-
2	-	-	-	-	-	-	-	-	-	-
3	-	-	-	-	-	4	16	32	50	71
4	95	121	149	178	209	242	276	312	349	388
5	428	469	511	555	600	646	693	741	790	840
6	891	943	996	1,050	1,105	1,161	1,218	1,275	1,334	1,393
7	1,453	1,514	1,576	1,639	1,702	1,767	1,832	1,898	1,964	2,031
8	2,100	2,168	2,238	2,308	2,379	2,451	2,523	2,596	2,670	2,744
9	2,819	2,895	2,972	3,049	3,126	3,205	3,284	3,363	3,443	3,524
10	3,606	3,688	3,771	3,854	3,938	4,022	4,107	4,193	4,279	4,366
11	4,453	4,541	4,630	4,719	4,809	4,899	4,990	5,081	5,173	5,265
12	5,358	5,451	5,545	5,640	5,735	5,830	5,926	6,023	6,120	6,218
13	6,316	6,414	6,514	6,613	6,713	6,814	6,915	7,017	7,119	7,221
14	7,324	7,428	7,532	7,636	7,741	7,847	7,952	8,059	8,166	8,273
15	8,381	8,489	8,597	8,706	8,816	8,926	9,036	9,147	9,259	9,371
16	9,483	9,595	9,709	9,822	9,936	10,050	10,165	10,281	10,396	10,512

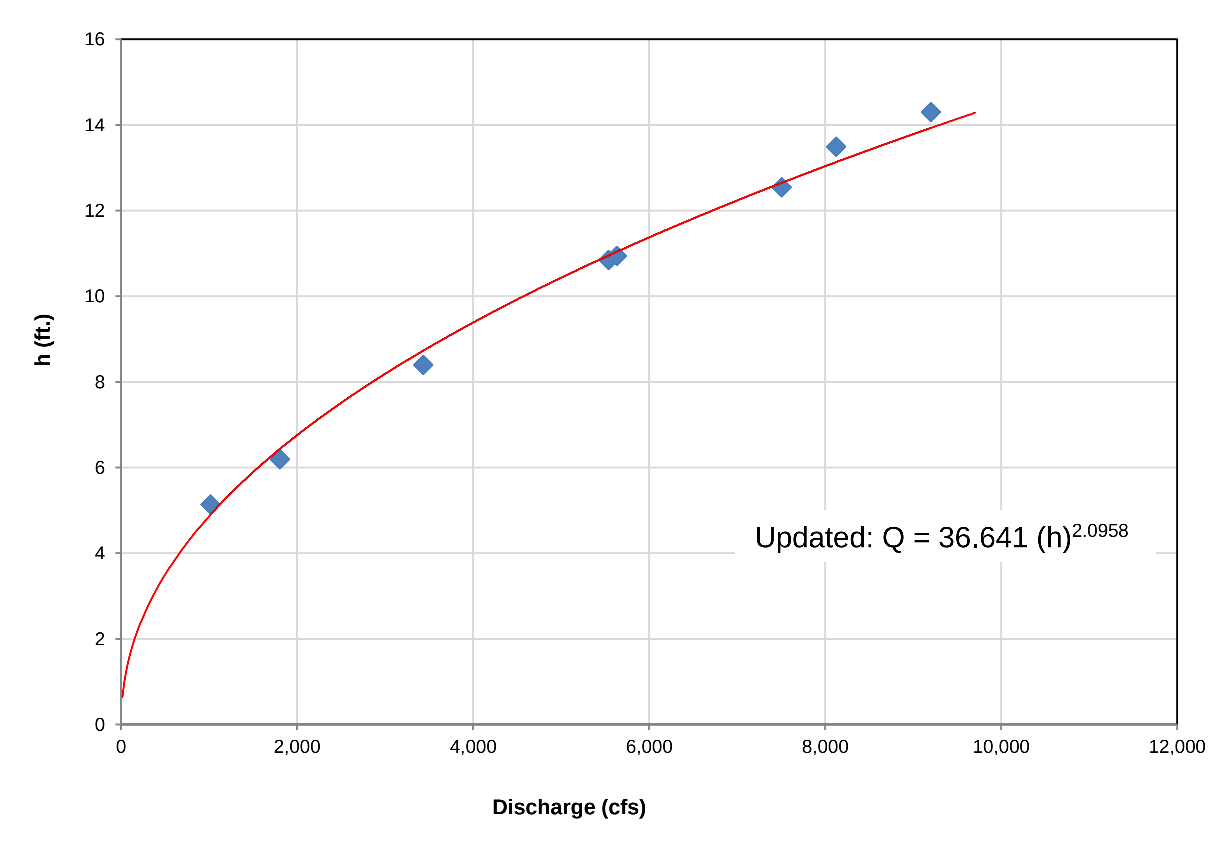

Figure 2-24: Stage- Discharge Relationship for Dear Ghazi Khan Canal at RD 21+500

Table 2-31: Gauge- Discharge Rating Table for DG Khan Canal at RD 21+500

Gauge / Fraction (Ft)	0.0	0.1	0.2	0.3	0.4	0.5	0.6	0.7	0.8	0.9
	Discharge in Cusecs									
0	-	0	1	3	5	9	13	17	23	29
1	37	45	54	63	74	86	98	111	126	141
2	157	173	191	210	230	250	271	294	317	341
3	366	392	419	447	476	506	537	569	601	635
4	670	705	742	779	818	857	897	939	981	1,024
5	1,069	1,114	1,160	1,208	1,256	1,305	1,355	1,406	1,459	1,512
6	1,566	1,621	1,677	1,735	1,793	1,852	1,912	1,974	2,036	2,099
7	2,163	2,229	2,295	2,362	2,431	2,500	2,570	2,642	2,714	2,787
8	2,862	2,937	3,014	3,092	3,170	3,250	3,330	3,412	3,495	3,578
9	3,663	3,749	3,836	3,924	4,013	4,103	4,194	4,286	4,379	4,473
10	4,568	4,665	4,762	4,860	4,960	5,060	5,162	5,264	5,368	5,473
11	5,579	5,685	5,793	5,902	6,012	6,123	6,235	6,349	6,463	6,578
12	6,694	6,812	6,930	7,050	7,171	7,292	7,415	7,539	7,664	7,790
13	7,917	8,045	8,175	8,305	8,436	8,569	8,702	8,837	8,973	9,110
14	9,247	9,386	9,526	9,668	9,810	9,953	10,098	10,243	10,390	10,537
15	10,686	10,836	10,987	11,139	11,292	11,446	11,602	11,758	11,916	12,074

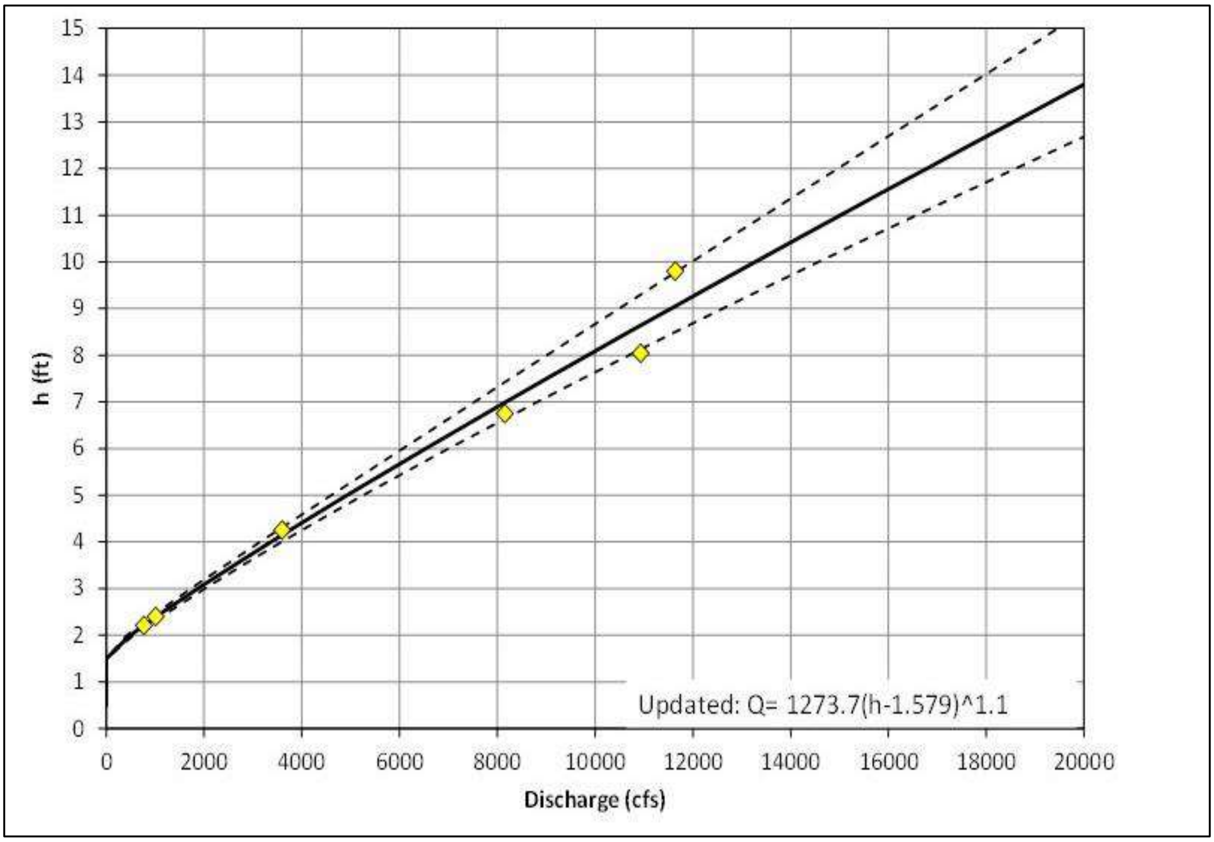

Figure 2-25: Stage- Discharge Relationship D/S Head Regulator of TP Link Canal

Table 2-32: Gauge- Discharge Rating Table for TP Link Canal D/S Head Regulator

Gauge / Fraction (Ft)	0.0	0.1	0.2	0.3	0.4	0.5	0.6	0.7	0.8	0.9
	Discharge in Cusecs									
0	-	-	-	-	-	-	-	-	-	-
1	-	-	-	-	-	-	18	125	242	365
2	492	622	754	889	1,025	1,163	1,303	1,444	1,587	1,730
3	1,875	2,020	2,167	2,314	2,463	2,612	2,762	2,912	3,064	3,216
4	3,369	3,522	3,676	3,831	3,986	4,141	4,298	4,454	4,612	4,769
5	4,928	5,086	5,245	5,405	5,565	5,725	5,886	6,047	6,209	6,371
6	6,533	6,696	6,859	7,023	7,187	7,351	7,515	7,680	7,845	8,011
7	8,176	8,342	8,509	8,675	8,842	9,010	9,177	9,345	9,513	9,681
8	9,850	10,019	10,188	10,357	10,527	10,697	10,867	11,037	11,208	11,379
9	11,550	11,721	11,893	12,064	12,236	12,409	12,581	12,754	12,927	13,100

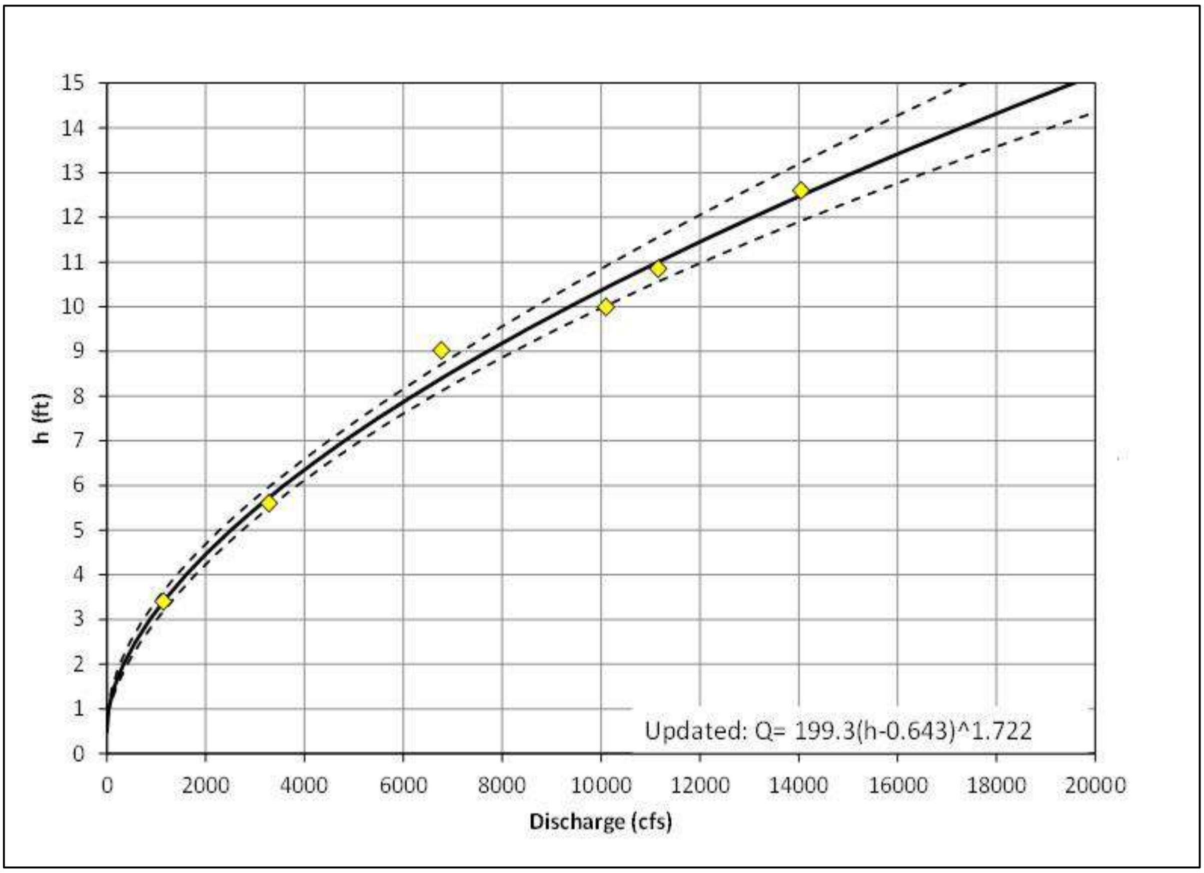

Figure 2-26: Stage- Discharge Relationship Relation D/S Head Regulator of Ghotki Feeder

Table 2-33: Gauge- Discharge Rating Table for Ghotki Feeder D/S Head Regulator

Gauge / Fraction (Ft)	0.0	0.1	0.2	0.3	0.4	0.5	0.6	0.7	0.8	0.9
	Discharge in Cusecs									
246 (0)	-	-	-	-	-	-	-	1	8	19
247 (1)	34	52	73	97	123	153	185	219	256	296
248 (2)	337	381	427	476	526	579	633	690	749	810
249 (3)	872	937	1,004	1,072	1,143	1,215	1,289	1,365	1,443	1,523
250 (4)	1,604	1,687	1,772	1,859	1,947	2,037	2,129	2,222	2,318	2,414
251 (5)	2,513	2,613	2,715	2,818	2,923	3,030	3,138	3,248	3,359	3,472
252 (6)	3,587	3,703	3,821	3,940	4,060	4,183	4,306	4,432	4,558	4,687
253 (7)	4,816	4,947	5,080	5,214	5,350	5,487	5,625	5,765	5,907	6,050
254 (8)	6,194	6,340	6,487	6,635	6,785	6,936	7,089	7,243	7,399	7,556
255 (9)	7,714	7,874	8,035	8,197	8,361	8,526	8,692	8,860	9,029	9,200
256 (10)	9,371	9,545	9,719	9,895	10,072	10,250	10,430	10,611	10,793	10,977
257 (11)	11,162	11,348	11,536	11,725	11,915	12,106	12,299	12,493	12,688	12,884
258 (12)	13,082	13,281	13,481	13,683	13,885	14,089	14,295	14,501	14,709	14,918
259 (13)	15,128	15,339	15,552	15,766	15,981	16,197	16,415	16,634	16,854	17,075

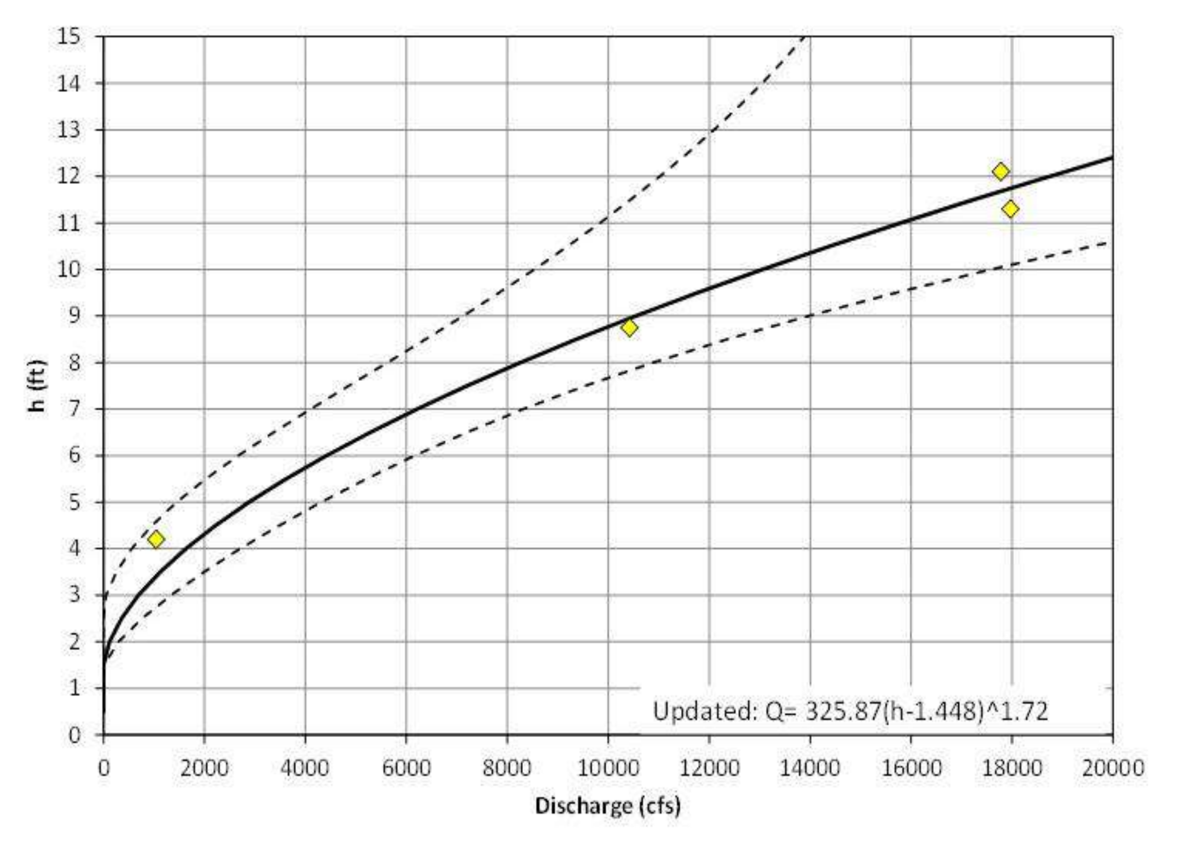

Figure 2-27: Stage- Discharge Relationship D/S Head Regulator of BS Feeder Canal

Table 2-34: Gauge- Discharge Rating Table for BS Feeder Canal D/S Head Regulator

Gauge / Fraction (Ft)	0.0	0.1	0.2	0.3	0.4	0.5	0.6	0.7	0.8	0.9
	Discharge in Cusecs									
247 (0)	-	-	-	-	-	-	-	-	-	-
248 (1)	-	-	-	-	-	2	13	30	54	83
249 (2)	117	156	200	247	299	356	416	480	547	619
250 (3)	694	773	855	941	1,030	1,122	1,218	1,317	1,419	1,524
251 (4)	1,633	1,744	1,859	1,977	2,097	2,221	2,348	2,477	2,610	2,745
252 (5)	2,883	3,024	3,168	3,315	3,464	3,616	3,771	3,928	4,089	4,252
253 (6)	4,417	4,585	4,756	4,930	5,106	5,284	5,466	5,649	5,836	6,024
254 (7)	6,216	6,410	6,606	6,805	7,006	7,210	7,416	7,624	7,835	8,049
255 (8)	8,264	8,482	8,703	8,926	9,151	9,379	9,609	9,841	10,075	10,312
256 (9)	10,551	10,793	11,037	11,283	11,531	11,781	12,034	12,289	12,547	12,806
257 (10)	13,068	13,332	13,598	13,866	14,137	14,409	14,684	14,961	15,241	15,522
258 (11)	15,805	16,091	16,379	16,669	16,961	17,255	17,551	17,850	18,150	18,453
259 (12)	18,758	19,065	19,373	19,684	19,997	20,312	20,630	20,949	21,270	21,593

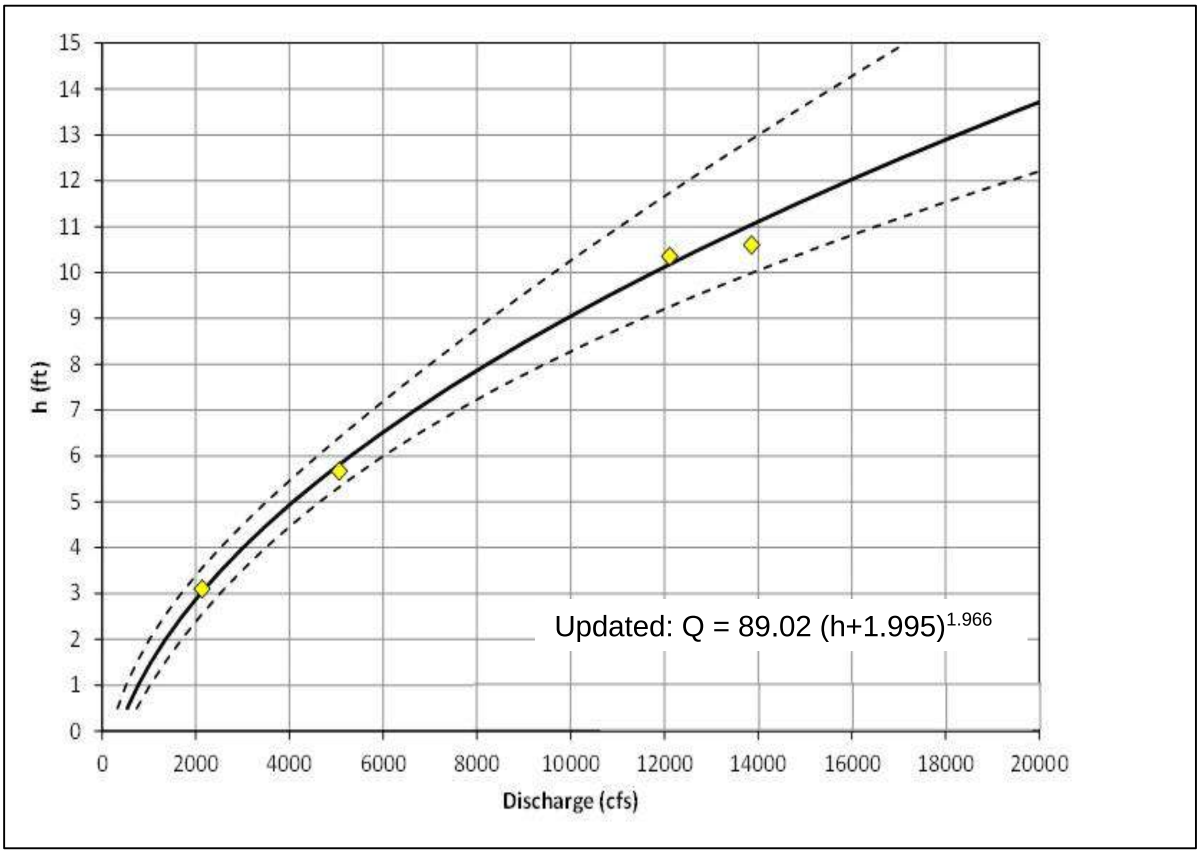

Figure 2-28: Stage- Discharge Relationship D/S Head Regulator of Desert Pat Feeder Canal

Table 2-35: Gauge- Discharge Rating Table for Desert Pat Feeder D/S Head Regulator

Gauge / Fraction (Ft)	0.0	0.1	0.2	0.3	0.4	0.5	0.6	0.7	0.8	0.9
	Discharge in Cusecs									
244 (0)	-	1	4	8	14	22	32	44	57	72
245 (1)	88	106	126	148	171	196	223	251	281	313
246 (2)	346	381	418	456	496	537	580	625	672	720
247 (3)	769	821	874	928	984	1,042	1,102	1,163	1,225	1,290
248 (4)	1,355	1,423	1,492	1,563	1,635	1,709	1,785	1,862	1,941	2,021
249 (5)	2,103	2,186	2,272	2,358	2,447	2,537	2,628	2,721	2,816	2,912
250 (6)	3,010	3,110	3,211	3,314	3,418	3,524	3,631	3,740	3,851	3,963
251 (7)	4,077	4,192	4,309	4,428	4,548	4,670	4,793	4,918	5,044	5,172
252 (8)	5,302	5,433	5,566	5,700	5,836	5,973	6,112	6,253	6,395	6,539
253 (9)	6,684	6,831	6,980	7,130	7,281	7,434	7,589	7,745	7,903	8,063
254 (10)	8,224	8,386	8,550	8,716	8,883	9,052	9,222	9,394	9,568	9,743
255 (11)	9,919	10,097	10,277	10,458	10,641	10,826	11,011	11,199	11,388	11,579
256 (12)	11,771	11,964	12,160	12,356	12,555	12,755	12,956	13,159	13,364	13,570
257 (13)	13,778	13,987	14,198	14,410	14,624	14,839	15,056	15,275	15,495	15,716
258 (14)	15,939	16,164	16,390	16,618	16,847	17,078	17,311	17,545	17,780	18,017

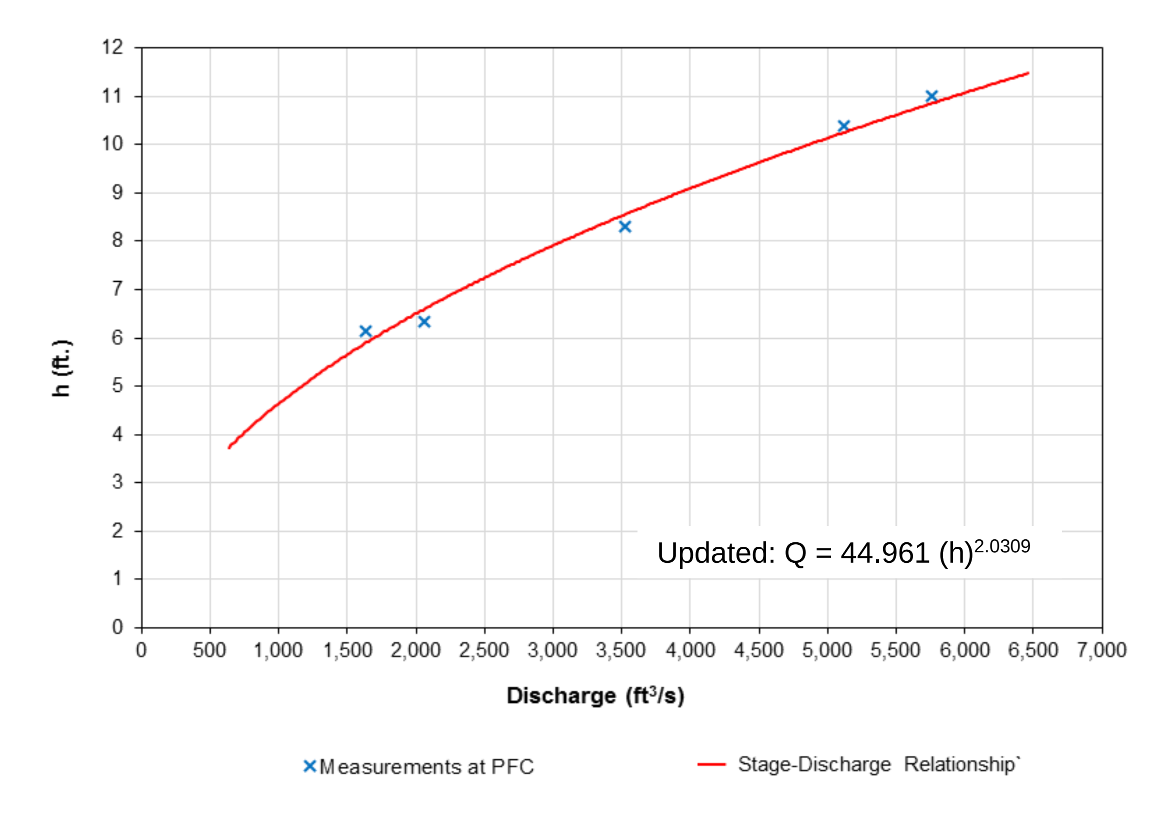

Figure 2-29: Stage- Discharge Relationship for Pat Feeder Canal at RD 109+000

Table 2-36: Gauge- Discharge Rating Table for Pat Feeder Canal D/S RD-109+000

Gauge / Fraction (Ft)	0.0	0.1	0.2	0.3	0.4	0.5	0.6	0.7	0.8	0.9
	Discharge in Cusecs									
0	-	0	2	4	7	11	16	22	29	36
1	45	55	65	77	89	102	117	132	148	166
2	184	203	223	244	266	289	313	338	364	391
3	419	447	477	508	540	573	606	641	677	713
4	751	789	829	870	911	954	997	1,042	1,087	1,134
5	1,181	1,230	1,279	1,330	1,381	1,434	1,487	1,541	1,597	1,653
6	1,711	1,769	1,829	1,889	1,950	2,013	2,076	2,140	2,206	2,272
7	2,340	2,408	2,477	2,548	2,619	2,692	2,765	2,839	2,915	2,991
8	3,068	3,147	3,226	3,307	3,388	3,471	3,554	3,638	3,724	3,810
9	3,898	3,986	4,076	4,166	4,258	4,350	4,444	4,538	4,634	4,730
10	4,828	4,926	5,026	5,126	5,228	5,331	5,434	5,539	5,644	5,751
11	5,859	5,967	6,077	6,188	6,299	6,412	6,526	6,641	6,756	6,873

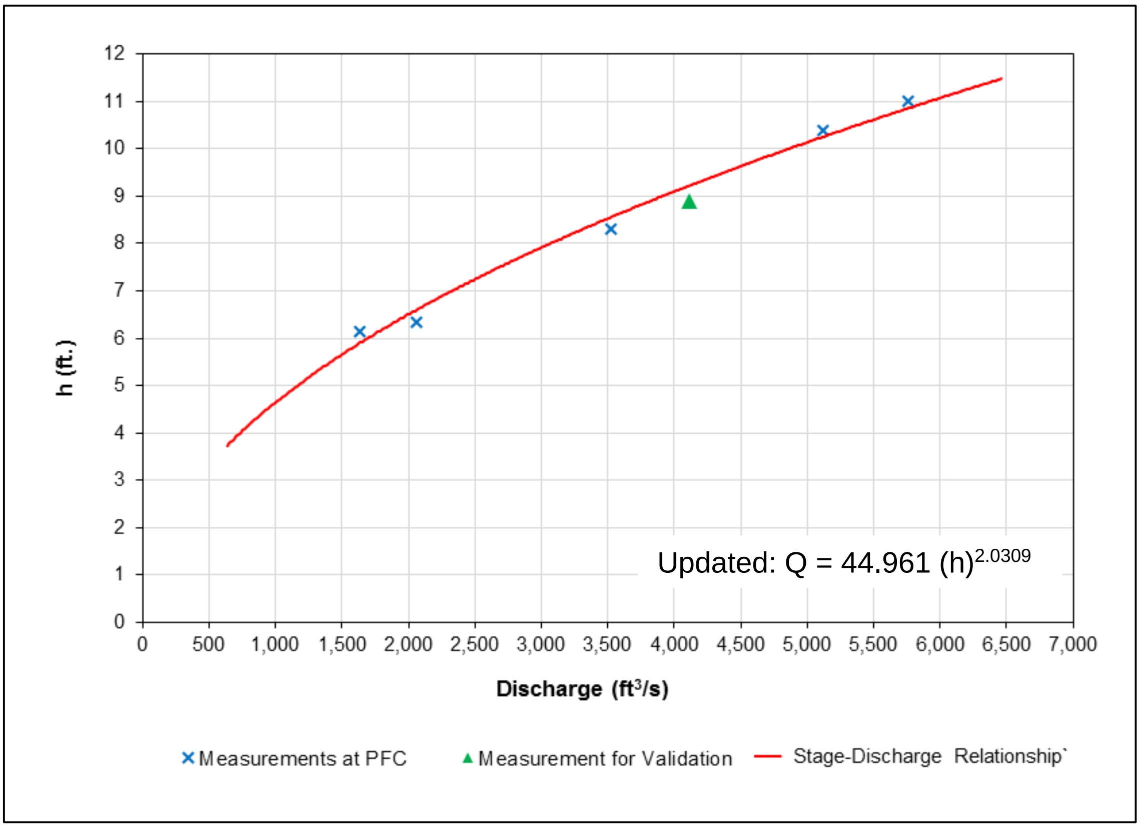

Figure 2-29 (a): Validation of Rating Curve of Pat Feeder Canal at RD 109+000

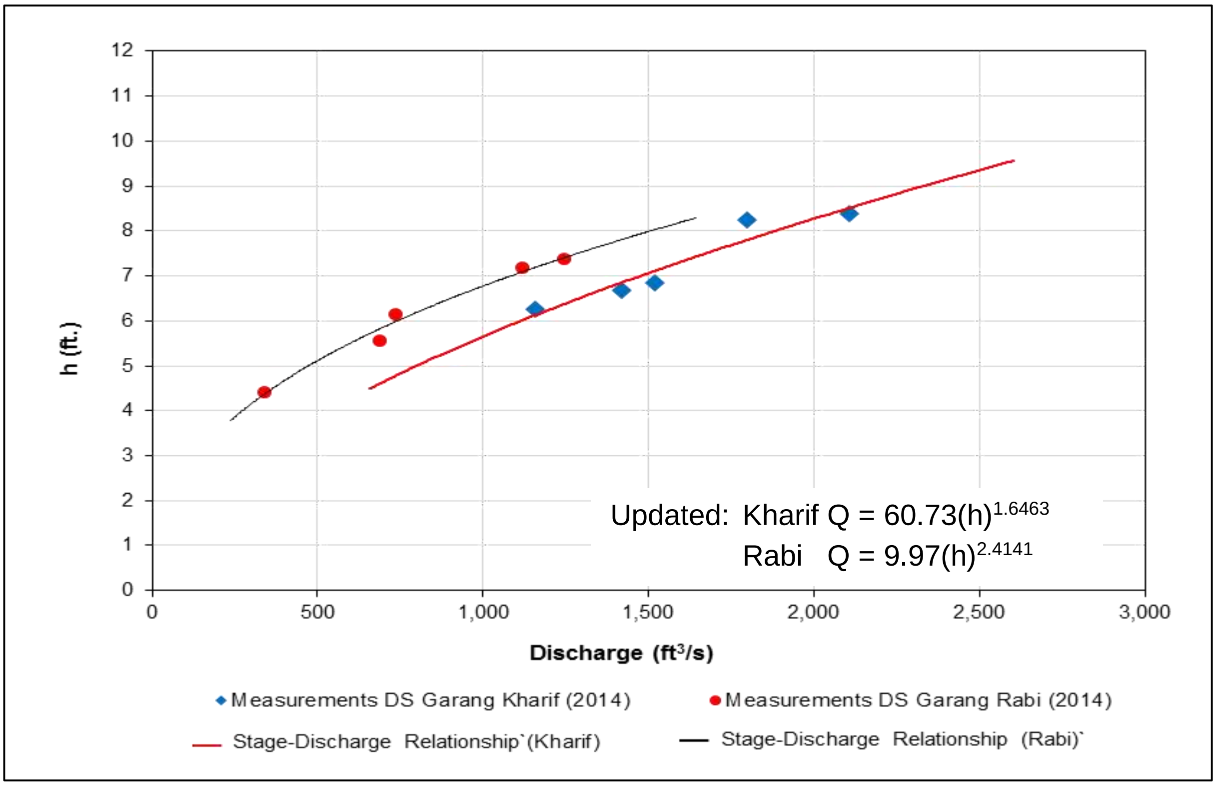

Figure 2-30: Head-discharge Relations of Kirther Canal D/S Garang X-Regulator

Table 2-37: Gauge- Discharge Rating Table of Kirther Canal D/S Garang for Rabi Season

Gauge / Fraction (Ft)	0.0	0.1	0.2	0.3	0.4	0.5	0.6	0.7	0.8	0.9
	Discharge in Cusecs									
0	0	0	0	1	1	2	3	4	6	8
1	10	13	15	19	22	27	31	36	41	47
2	53	60	67	74	83	91	100	110	120	130
3	141	153	165	178	191	205	220	235	250	266
4	283	301	319	337	356	376	397	418	440	462
5	485	509	534	559	584	611	638	666	695	724
6	754	784	816	848	881	914	949	984	1,020	1,056
7	1094	1,132	1,171	1,210	1,251	1,292	1,334	1,376	1,420	1,464
8	1510	1,555	1,602	1,650	1,698	1,747	1,797	1,848	1,900	1,953

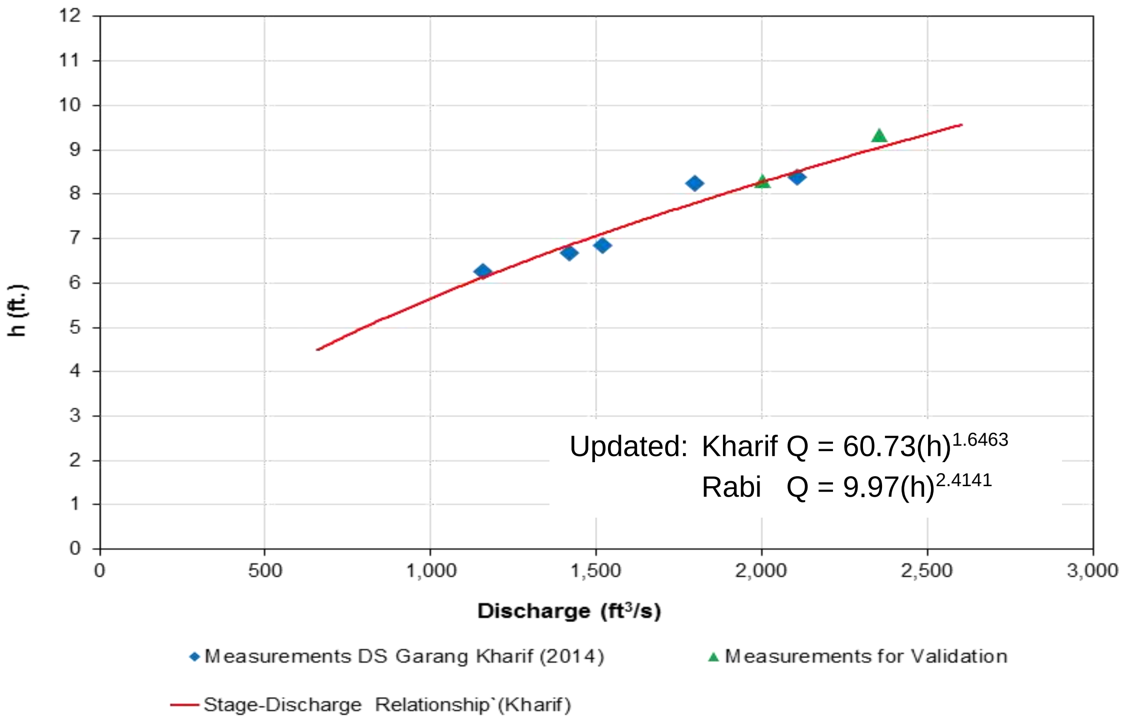

Figure 2-30 (a): Validation of Rating Curve of Kirther Canal at Garang Regulator

Table 2-38: Gauge- Discharge Rating Table of Kirther Canal D/S Garang for Kharif Season

Gauge / Fraction (Ft)	0.0	0.1	0.2	0.3	0.4	0.5	0.6	0.7	0.8	0.9
	Discharge in Cusecs									
0	0	1	4	8	13	19	26	34	42	51
1	61	71	82	94	106	118	132	145	160	175
2	190	206	222	239	257	274	293	312	331	350
3	371	391	412	434	455	478	500	523	547	571
4	595	620	645	670	696	722	749	776	803	831
5	859	888	917	946	975	1,005	1,035	1,066	1,097	1,128
6	1160	1,192	1,224	1,257	1,290	1,323	1,357	1,391	1,425	1,460
7	1495	1,530	1,566	1,602	1,638	1,675	1,712	1,749	1,787	1,825
8	1863	1,901	1,940	1,979	2,019	2,058	2,098	2,139	2,179	2,220
9	2261	2,303	2,345	2,387	2,429	2,472	2,515	2,558	2,602	2,646

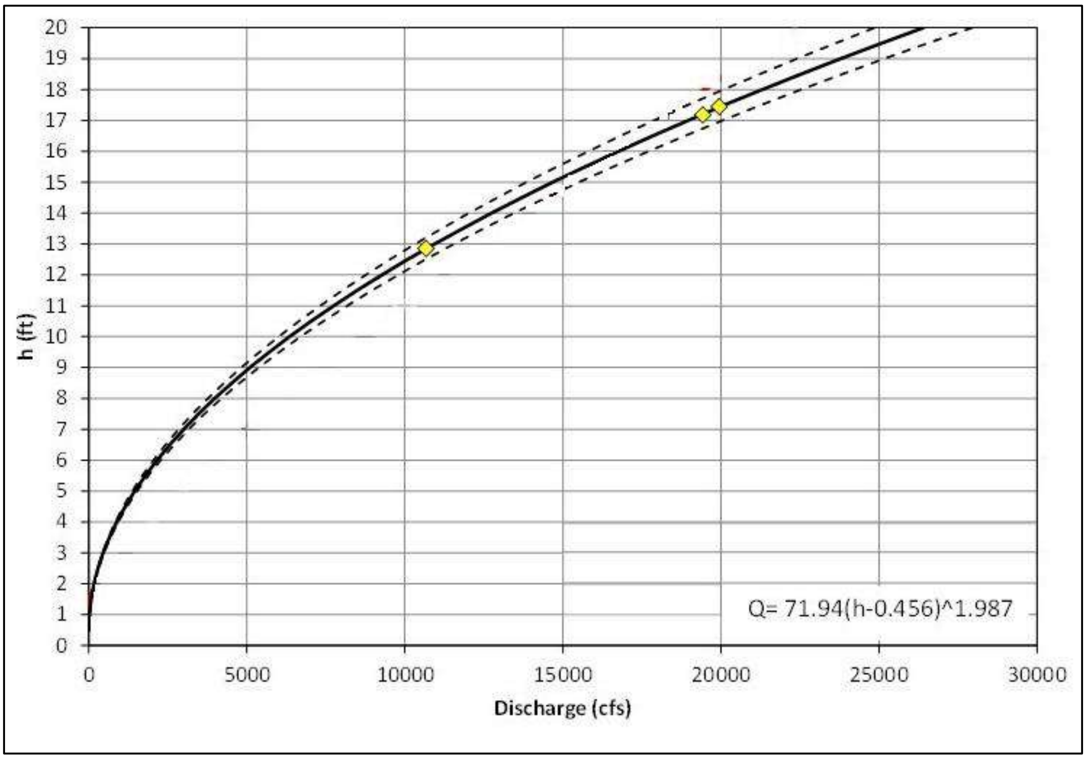

Figure 2-31: Stage- Discharge Relationship D/S Head Regulator of MR Link Canal

Table 2-39: Gauge- Discharge Rating Table for MR Link Canal D/S Head Regulator

Gauge / Fraction (Ft)	0.0	0.1	0.2	0.3	0.4	0.5	0.6	0.7	0.8	0.9
	Discharge in Cusecs									
0	0	0	0	0	0	0	2	4	9	14
1	21	30	40	51	64	78	94	111	129	149
2	171	193	217	243	270	298	327	358	391	425
3	460	497	535	574	615	657	701	746	792	840
4	889	939	991	1,045	1,099	1,155	1,213	1,272	1,332	1,393
5	1,456	1,521	1,587	1,654	1,722	1,792	1,863	1,936	2,010	2,086
6	2,162	2,241	2,320	2,401	2,484	2,567	2,652	2,739	2,827	2,916
7	3,006	3,098	3,192	3,286	3,383	3,480	3,579	3,679	3,781	3,884
8	3,988	4,094	4,201	4,309	4,419	4,530	4,643	4,757	4,872	4,989
9	5,107	5,227	5,347	5,470	5,593	5,718	5,845	5,972	6,101	6,232
10	6,363	6,497	6,631	6,767	6,904	7,043	7,183	7,324	7,467	7,611
11	7,757	7,904	8,052	8,201	8,352	8,505	8,658	8,814	8,970	9,128
12	9,287	9,447	9,609	9,773	9,937	10,103	10,271	10,439	10,609	10,781
13	10,954	11,128	11,304	11,480	11,659	11,838	12,019	12,202	12,386	12,571
14	12,757	12,945	13,134	13,325	13,517	13,710	13,905	14,101	14,298	14,497
15	14,697	14,898	15,101	15,305	15,511	15,718	15,926	16,136	16,347	16,559
16	16,773	16,988	17,204	17,422	17,641	17,862	18,084	18,307	18,532	18,758
17	18,985	19,214	19,444	19,675	19,908	20,142	20,378	20,614	20,853	21,092
18	21,333	21,575	21,819	22,064	22,310	22,558	22,807	23,058	23,310	23,563

2.3.1 Conclusions for Stage-Discharge Relationship and Calibration of Discharge Coefficients

General conclusions regarding stage discharge relationships were as follows;

1. Morphological conditions showed that regular, at least annual, updating of stage – discharge would be required for reliable discharge computation in the canals. At least four to five data sets of gauge and flow measurements should be used for the establishment of reliable stage-discharge relations.

2. To facilitate the field staff of WAPDA/PID, the Gauge- Discharge rating table for each of 5 pilot sites was prepared to cover the full range of water stages at a gauge increment of 0.1 ft.

Site specific conclusions were as follows;

Chashma Barrage

1. Initially the regression analysis was carried out using 4 flow measurements downstream Chashma Barrage. As per the additional scope of services one high flow measurement was carried out in July, 2015 for the validation of equation developed using regression analyses. It was found that the additional flow measurement in high flows when added to data set of regression analysis, it improved R^2 value from 0.17 to 0.57.

   It was therefore proposed to use equation for Chashma having improved R^2 value. The improved relationship for estimation of discharge coefficient using y_1/w is shown in figure 2-15. The comparison with the flow measurements yielded the difference within ±6% of measured discharges which in turn confirmed the applicability of the newly developed equation at Chashma Barrage. It was therefore proposed to carry out additional measurements for combinations of gate settings and water levels. The measurements are to be carried out for selected uniform gate openings to be able to properly check the WAPDA table values. The sedimentation depth on the upstream glacis has to be monitored as well. It is however important to mention that in real time operation it is hard to fix the gate settings at a uniform opening therefore the prototype measurements may be verified at the scale model.

   The analyses given in the tables above show that the differences in measured and calculated discharges for the four measurements ranging from 50,000 cusecs to 450,000 cusecs were in the acceptable range of $\pm$6%.

2. Given the significant transitions starting just downstream of the CRBC head regulator, it was established that it is not appropriate to consider the downstream gauge of CRBC for development of a stage-discharge relation. Therefore, the regulation of CRBC may be undertaken strictly through application of hydraulic formula, developed in the present study.

3. Similarly, the regulation of Chashma Jhelum Link at head regulator may also be undertaken through application of hydraulic formula, developed in the present study.

4. The newly developed equation downstream of Thal cross regulator at RD 36+000 of CJ Link is recommended for use as it yielded comparatively less percentage difference with measured values compared to PID reported values.

Taunsa and Guddu Barrage

1. For Taunsa and Guddu Barrages, the best results were obtained by applying the regression equation developed in the present study for Main Weir to whole Barrage.
2. The newly developed equations based on flow measurements downstream of head regulators and PID's discharge sites for the canals off-taking from Taunsa and Guddu barrages were recommended for use as they yielded comparatively less percentage difference with measured values compared to PID reported values.

Pat Feeder Canal at RD-109+000

As per the additional scope of services, one flow measurement was carried out in July 2015. The measurement fitted well over the developed stage-discharge relationship (Kharif 2015). Therefore, the additional flow measurement at Pat Feeder canal passed the validation test as shown in Figure 2-29(a). Therefore, the rating tables for Pat Feeder Canal at RD 109+000, developed using the flow measurements carried out in 2014 is valid and can be used for regulation purposes during Rabi 2015-16 and Kharif 2016.

Kirther Canal at Garang Cross-Regulator

1. The stage-discharge relations of Kirther Canal at Garang Cross-Regulator for Rabi and Kharif seasons differ considerably; in Rabi the Manning values of the canal bed appear to be significantly higher, leading to lower flows for selected water levels.
2. The discharge ratings for Kirther Canal at Garang Cross-Regulator, being used by PIDs strongly underestimate the canal discharge, particularly in Rabi season.
3. Separate discharge rating for Rabi and Kharif seasons were developed, in the study.
4. Making use of the head difference across the regulator for discharge computations, is theoretically possible, but practically not feasible in view of reading inaccuracies in the very small head differences.
5. As per the additional scope of services two flow measurements were carried out in July, 2015. The measurements fitted well over the developed stage-discharge relationship. Therefore, the additional flow measurements at Kirther canal downstream Garang gross regulator passed the validation test as shown in Figure 2-30(a). Therefore, the rating tables for Kirther Canal at Garang Cross-Regulator, developed using the flow measurements carried out in 2014 is valid and can be used for regulation purposes during Rabi 2015-16 and Kharif 2016.

Marala Barrage

1. The best results for Marala Barrage were obtained by applying the three distinct regression equations developed for main weir. It is however important to mention that in real time operation, it is hard to fix the gate settings at a uniform opening during flood days.

2. The newly developed equations based on flow measurements downstream head regulator of Marala Ravi Link was recommended for use as they yield comparatively less percentage difference with measured values compared to PID reported values.

2.4 DEVELOPMENT OF STANDARDISED FLOW MEASUREMENT SYSTEM AT FIVE PILOT SITES

The standardised Flow Measurements System (FMS) would be necessary to promote harmony and good faith amongst the provinces by demonstrating that the water is distributed equitably in accordance with the WAA of 1991.

The salient features of the standardised system would comprise:
(iii) calibrated discharge coefficients at barrages and canal heads
(iv) standard procedure for revision of stage-discharge relationships at canals

The steps involved in devising a standardised flow measurement system includes;

1. Use of standard formulas at each site for respective flow conditions (Free Orifice, Submerged Orifice, Free Weir or Submerged Weir)

During the course of the study, it was observed that existing formulas being used to estimate discharges at 5 pilot locations varies with respect to definition of parameters and including/excluding constants in discharge coefficients. (See Table 2-4 to Table 2-19). For different flow conditions, the formulas defined by ISO along with recommended methodology and definition of parameters should be implemented at 5 pilot sites to keep uniformity in computational methodologies.

2. Use of standard coefficients, as available in literature, in formulas corresponding to respective flow conditions.

Based on various visits, meetings and discussions with concerned operators of 5 pilot sites, it was assumed that existing discharge coefficients being used at 5 pilot sites were extracted either from original design manual or from physical model studies. The original design manuals and physical model studies were not available at 5 pilot sites for review and expert judgment on use of coefficients. The weir shape of each site is unique (see Figure 2-32) and coefficients for use in discharge formulas are not available in standard hydraulic literature. Therefore, in the absence of information in hydraulic literature, design manual and physical model studies the only options available to calibrate coefficients is either physically measure flow at each structure or estimate through physical model studies.

The first option was employed by the Consultants under current studies to calibrate discharge coefficients at each of 5 pilot site with flow ranges available during course of the studies. However, the calibration of coefficients and its subsequent use is limited for the flow range used in analysis and the extrapolation of coefficients from developed equations for the flow range other than measured range is not advisable.

The second option, to use physical model studies to estimate coefficients is generally recommended for non-standard weir shapes. With this option, all possible flow ranges expected at barrage can be reproduced and corresponding coefficients can be estimated without extrapolation.

As a first step, use of calibrated discharge coefficients as estimated under current studies (see Section 2.3) were advised to be implemented for the flow ranges corresponding to which they were calibrated for each of 5 pilot sites. The flow ranges covered in the study were the dominant flow range covering flows of more than 95% of the time. The remaining flow ranges either correspond to flood flows in rivers or low flows in canals which are rare to encounter. Therefore, could not be captured during the study duration.

3. Shifting of canal measurements form rating curve method to structure formula method.

At 5 pilot sites, the estimation of discharge from canals is being carried out from rating curves established at some distance downstream of head regulator. The rating curves need continuous adjustment/ correction due to morphological changes in the channel and annual desilting activity at each canal. Since upstream water levels, downstream water levels and gate openings data is available at each canal head regulator (except Garang regulator) for 5 pilot sites, therefore, uncertainties and efforts involved in adjustments/correction of ratings may get substantially reduced if the discharge estimation is carried out on head regulator instead of at some distance downstream of head regulator using rating curve. Structure based computations (which are not affected by morphological aspects) are more accurate, reliable and efficient method for discharge estimation at canals. Improvements in discharge estimation of canals would directly improve net inflow figures and equity in distribution at each of 5 pilot sites.

4. Observation and transmission of real-time gauge and gate opening data

For an efficient, reliable and standardised flow measurement system at each site, accurate measurement of required parameters (upstream water levels, downstream water levels, gate openings and flow velocity) and its transmission is an essential part. To achieve this objective, existing telemetry system was analysed for its performance (see Section 2.5) and certain recommendations were made for automated sensing of levels and transmission of data.

It is recommended that existing telemetry system should be replaced with latest technology available for transparent and efficient data communication. The new/improved system may be installed at the 5 pilot sites, initially, to monitor the performance for at least two seasons before implementing the same to whole system of 23 sites.

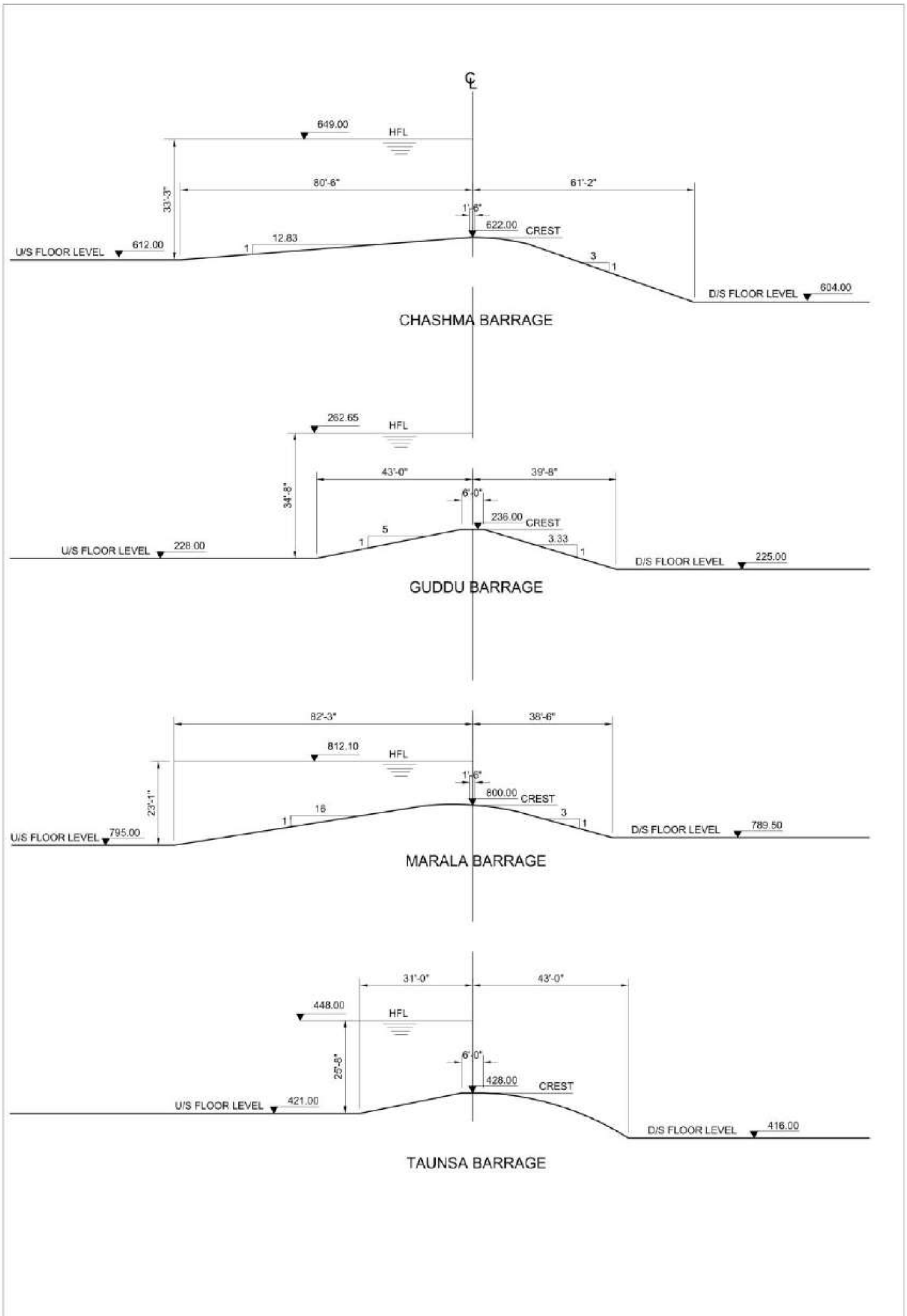

Figure 2-32 Main Weir Shapes of 4 Pilot Sites/Barrages

2.5 REVIEW AND GIVE RECOMMENDATIONS FOR UPGRADING/DEVELOPMENT OF WATER DISTRIBUTION MONITORING SYSTEM

The Consultants conducted a comprehensive condition survey of the existing telemetry network by the electronics engineers of Consultants and the staff of WAPDA telemetry directorate on all the 23 sites of IBIS. The visits were conducted from November 25 to December 27, 2014. This survey provided basis for giving recommendations to upgrade/develop a comprehensive system of monitoring of water distribution. The survey report has been annexed as Annexure-K.

A brief on findings of survey are given below,

1. Spares required time to time during operation of the system are unavailable.
2. Power backup is the real bottleneck in efficient operation of the system which is running without backup protection. If any equipment fails, it causes disruption of service. While at some places locally manufactured (unreliable) power supplies are being used in order to keep the system working.
3. Due to lack of funds for O&M activities, the aged batteries are replaced and the system is working without any battery backup causing extended outage during power cuts. Under such circumstances, telemetry staff has to physically record the gate positions on each location which results in incorrect calculation of discharges being transmitted to the monitoring sites.
4. The computers used at the sites are outdated having low processing speeds and RAM capacities. The spares of these computers are also no longer available in the market. No antivirus program is installed making the system highly vulnerable to virus threats.
5. Low AC Utility Power Supply Voltage ~170V was observed at some of the sites which may damage the survived aged equipment.
6. The Gate Positioning Sensors (GPSs) Calibration window does not have any protection to avoid erroneous data entry in the tabs having “counts values” for Gate Fully Closed and Gate Fully Open that would result in inaccurate values for gate opening.
7. No alarm is being generated in the Human Machine Interface (HMI) to indicate swapping of GPSs signal wire.
8. Water Level Sensors (WLSs) in place at most of the sites were in working condition, WLSs at some of the locations require relocation for ease of maintenance, chocking of stilling wells due to deposition of silt in front of the sensor. Despite other technical/operational reasons, these also pose incorrect water level measurements.
9. Voice quality was found to be poor during speech communication with the WAPDA main monitoring site at Lahore. Fuse protection of GPSs is partially implemented, due to failure of gaskets and damaged locks, the Ingress protection capability of Data Acquisition Unit (DAU) cabinets installed in the field are compromised exposing the sensitive electronic hardware to moisture and dust.

10. No indication or notification appears on SCADA software (iFix) home window on the generation of an alarm. Thus, when an alarm is generated the Operator is not aware of it, unless he himself check the alarm window, Labelling of all DAUs and GPS junction boxes is not the same as that shown on the HMI.

11. No safety equipment is available at any of the sites, only one Programming (PG) device is available with WAPDA Telemetry Staff making it difficult to efficiently maintain the entire telemetry system.

12. Inconsistent color coding of the grounding wires was observed. At some points improper grounding or grounding without proper wire termination was observed. Thimbles is not used for wire termination. At many sites breakers of incorrect rating are used in the DAU cabinets, cable glands and flexible conduits are not being used where required.

13. Discharge formulae from which the discharge is being calculated by the telemetry system are not being displayed on the HMI to check the discrepancy in discharges measured by Irrigation Department and Telemetry system.

14. The year-wise budget for O&M provided by WAPDA Telemetry department (since 2005-2006) is inadequate for O&M of the existing Telemetry System.

15. Normally two semi-skilled site personnel are deputed at a site. They cannot properly handle corrective and preventive maintenance.

On the basis of outcome of above observations, following options have been proposed to make the data communication system reliable and efficient.

2.5.1 Rehabilitate the Existing System

To make the existing system functional, necessary equipment/spares need to be procured. Repair/replace the faulty UPSs in the Control Room and install new batteries with at least 8 hour autonomy. In addition to above, following are the various recommendations to minimize/improve O&M of the system.

a. Instead of processing of data at the site, all data of the site may be sent to the Main Monitoring Site for processing. This will eliminate the use of Operator work station at the site and thus UPS of lesser rating will be required for powering the remaining equipment. In this case, more bandwidth through VSAT may be required to transmit the raw data.

b. Replace the existing GPSs with Absolute Sensors (Potentiometer based) or Optical Sensors with modification in coupling arrangement for proper operation. These GPSs will retain calibration on restoration of power after mains failure thereby eliminating human intervention. Powering the GPSs directly from the AC mains power needs to be explored to reduce the sizing of UPS.

c. Same recommendations as mentioned in "b" above, but instead of implementing on all sites, the replacement to be done on one pilot site of highest priority. On successful experience at pilot site, gradually implement the same on other sites of higher priority. Make use of the removed equipment from the pilot site to replenish the equipment on other sites. Use of Solar power supplies may be explored as an additional means of compensation against long power outages.

d. VSAT communication be replaced with GPRS/GSM to reduce the recurring annual costs.

It may be noted that if implemented none of the above alternatives would be a long term solution as the refurbished system would have an active life span of 3 years stretchable to about 5 years. This is because in another five years, a totally new operating system would have been introduced by Microsoft ® which in turn would mandate a new hardware platform. Thus above Alternatives are only proposed for the short term and in case of paucity of funds.

2.5.2 Installation of New Data Communication System:

The existing telemetry system commissioned in 2004-5 has outlived its useful service life. While the data acquisition and processing hardware and software has long since been rendered obsolete, the water level and gate position sensors are salvageable. It may be noted that many new technologies have emerged since the system was designed. These include efficient telecommunication media and micro power hardware.

For a reliable and obsolescence proof long term solution which enjoys the full confidence of all the stakeholders, a completely new system shall need to be designed procured and commissioned from scratch. Thus for the best techno economical solution, it is imperative that an independent yet comprehensive design exercise be conducted. Herein all present day, state of art available technologies and equipment should be studied culminating in the proposal of a new system.

Lastly it may be noted that no system, no matter how well designed and technologically sophisticated, can function successfully without the will and ownership. The existing system while originally conceived to be operated by IRSA was outsources to WAPDA as per Prime Minister Inspection Committee (PMIC) directions as the system was not operational. Therefore if the new system is to be successful it must be operated not a by a third party agency such as WAPDA, but by the owner (IRSA) itself.

2.5.2.1 Various Options for New Telemetry System for Indus Basin Irrigation System

The healthy way forward to restore the Telemetry System has already been presented to IRSA in previous section of the report. The following paragraphs puts forth budgetary cost estimate for a totally new Telemetry System from scratch. Keeping in view the lessons learnt from the existing Telemetry System, following improvements have been considered while arriving at the three options.

- Absolute gate positioning sensors have been considered to avoid recalibration of sensors, in case of power outage and human intervention
- Power backup of 8 hours have been considered supported by solar power for remote sites
- Micro power PLCs have been taken for energy efficient system
- Available computer technology has been considered for efficient processing

- Various options for newer better communication technology have been taken for data communication from remote site to central monitoring site and data display centers
- Video surveillance has also been considered an option to monitor any planned and unusual IBIS operation
- Communication of raw data (water level and gate openings) has been considered from each site to central monitoring site (IRSA) for further processing to arrive at discharge estimations; processed data will be transmitted from central monitoring center to other monitoring sites (PIDs/WAPDA).

Keeping in view the above requirements, three possible options have been studied. These are as follows:

Option A

The first option is SMS/ GSM/GPRS based WAN whereby raw data (water levels and gate positions) from 24 remote sites is transmitted to IRSA Control Room/Main Monitoring Site for processing and final data (Water Discharges) will be shared with other 7 Monitoring Sites by WAN deploying GSM/GPRS/SMS protocols. In this case the data will be received at the Main Monitoring Site no later than five minutes of initiating the data request. Additional equipment such as GSM modems, and or router/switches will be procured for the project. The GSM/GPRS/SMS services will be acquired from the third party service providers by paying monthly recurring charges.

Option B

The second option deploys point to point Digital Radio System (DRS) based data transmission solution. Radio towers shall have to be installed at the Remote Sites and the raw data from the Remote Sites will be transmitted to the nearest node of the Cellular Telecommunications Provider. This data will then be forwarded to IRSA Control Room/Main Monitoring Site for processing via MPLS or suitable protocols. Once processed, it will be shared with the other 7 Monitoring Sites. This solution is reliable and robust. Video Surveillance feature can also be added to this solution. The video cameras will be fed into Network Video Recorders (NVR) at each Remote Site. Field based video cameras will constantly record high resolution videos at the Remote Sites. When motion will be detected, alarm will be raised and an “event clip”, which is typically lower resolution will be sent back to Main Monitoring Site based on predetermined triggers.

Option C

The third option also comprises point to point Digital Radio System (DRS) based data transmission. Infrastructure requirement is the same that is Radio Towers along with associated equipment will be installed at each Remote Site. However, IP Sec Tunnel will be established instead of MPLS and the raw data will be transmitted through this virtual tunnel as IP packets.

There are further possible variants to above options in order to implement redundancy to ensure continuous connectivity and availability of telecom medium for transfer of raw data between Sites.

For Option A, GSM service can be availed through two service providers so in case of loss of service from one service provider the raw data can be transferred through the other GSM modem connected to the second service provider. Similarly, for Option B and Option C, either duplicated arrangement can be used or Option A can be used with Option B and Option C to provide redundancy. The cost for opting redundancy will depend on the chosen option which shall be addressed at the detailed design stage since it has significant cost impact which needs to be evaluated along with performance enhancement.

Approximate cost to replace the existing field instruments/equipment and data communication is listed below in Table 2-40:

Table 2-40: New IRSA Telemetry Project Cost for Various Options (cost in Million Rs)

Sr. No.	Description	Option-A	Option-B	Option-C
1	Field equipment	331.38	331.38	331.38
2	Control & Communication System	498.61	883.79	534.29
3	Civil Works	36.00	36.00	36.00
	Total	**865.99**	**1,251.17**	**901.67**

The above estimates have been prepared on the basis of real-time bids for similar projects wherefrom prices were obtained and processed using our in-house knowledge base, and applicable escalation factors.

It needs to be appreciated that to generate an accurate cost estimate, a detailed design must be conducted. Only then can the exact quality and quantity of individual subsystems and components be determined. Once so determined, actual prices of the components are obtained from the market and added to the service charges for activities such as design and installation and testing to arrive at a realistic cost estimate. Note however that design is a time and resource intensive exercise requiring numerous man months. Nevertheless to fulfill IRSA's requirement for allocating budget for the said works the above estimate shall suffice.

Site-wise cost breakup is also given in Tables 2-41 to 2-43.

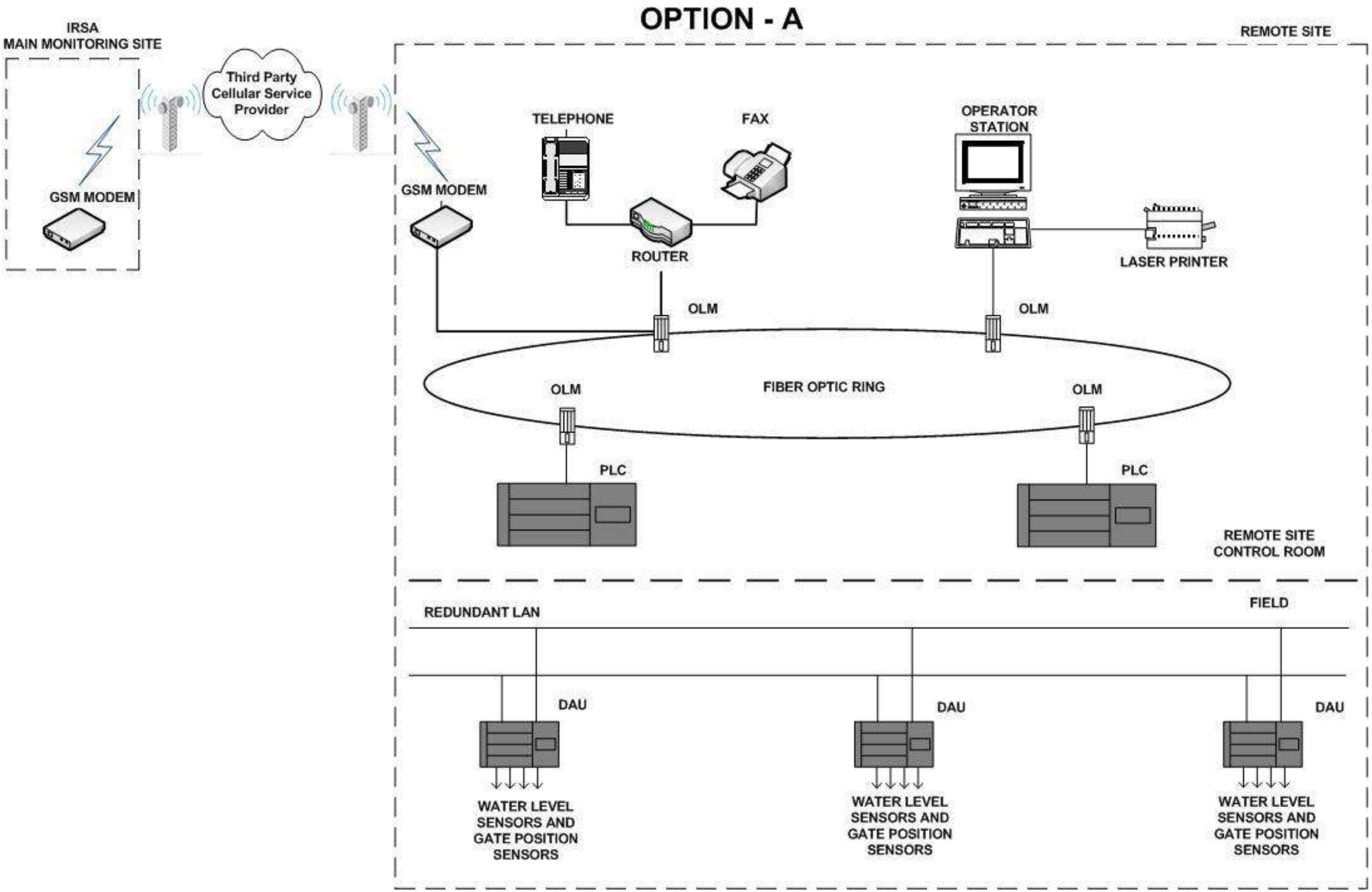

Figure 2-33: New Telemetry System – Option-A

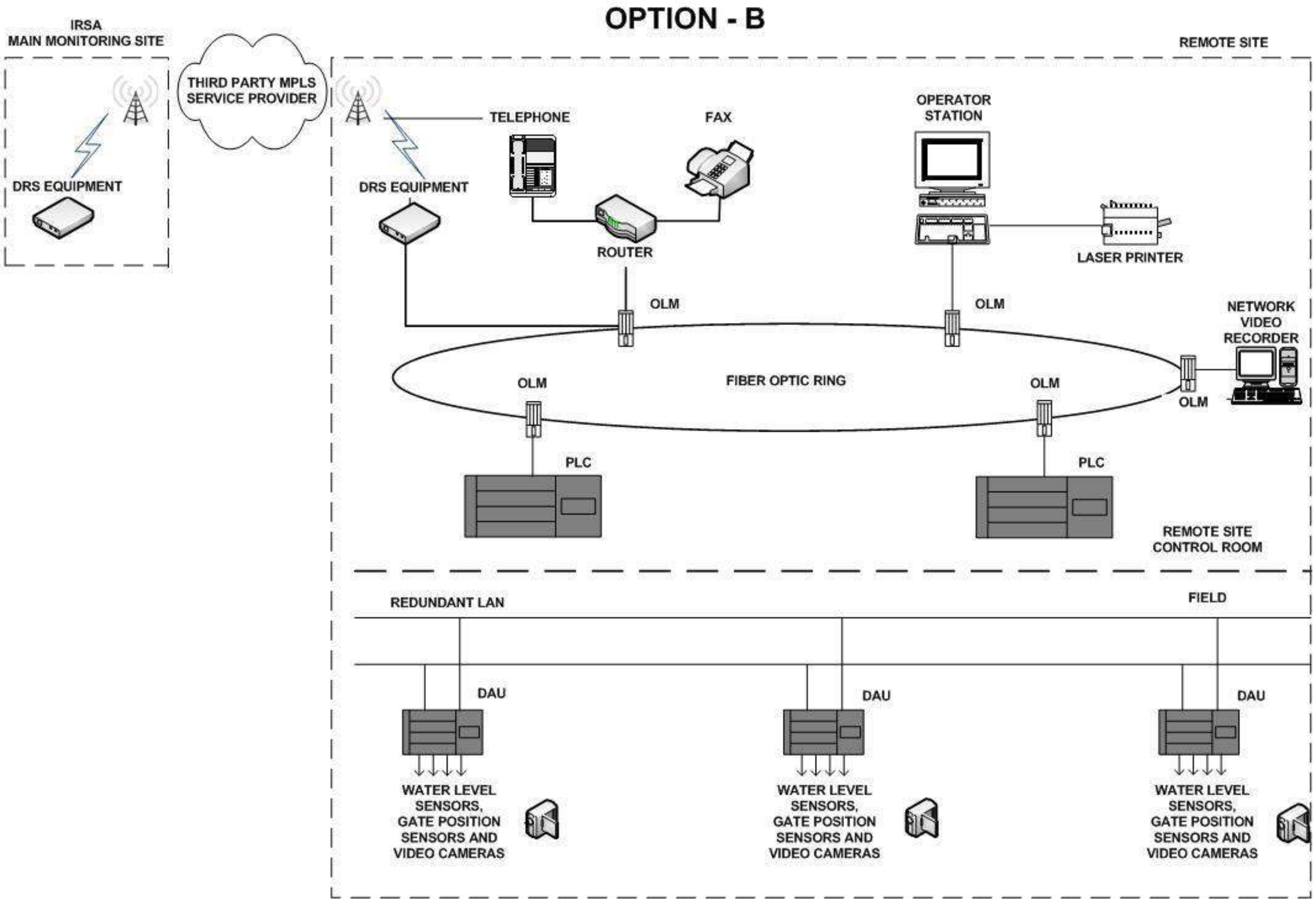

Figure 2-34: New Telemetry System – Option-B

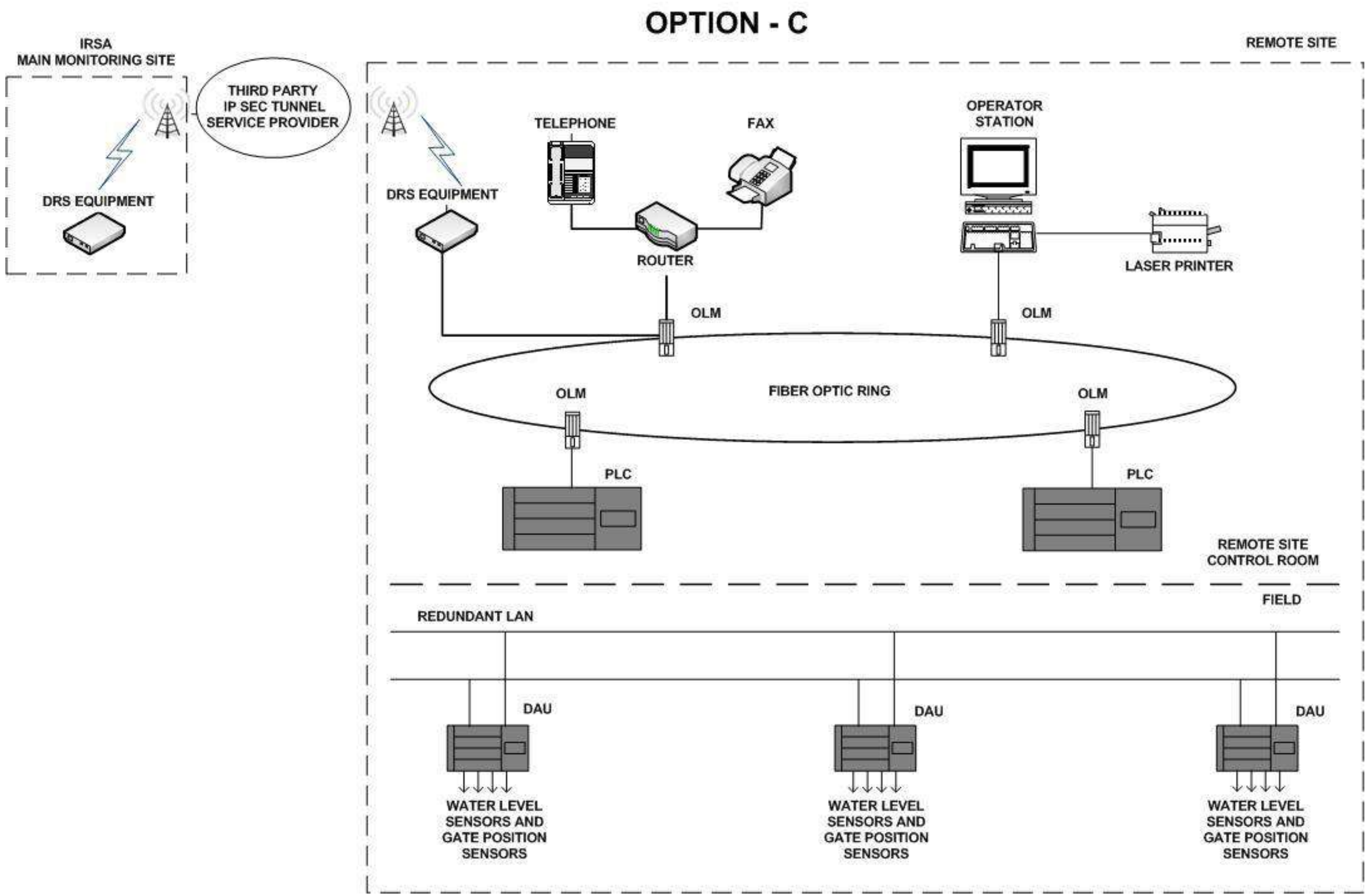

Figure 2-35: New Telemetry System – Option-C

Table 2-41: Telemetry Site-Wise Detail Cost Breakup – Option A

All costs are in Pak Rupees

Telemetry Site	Field Equipment	Control & Communication System	Cost of civil works	Total
Sulemanki Barrage	18,538,000	19,988,000	1,500,000	40,026,000
Jinnah Barrage	23,213,000	20,722,000	1,500,000	45,435,000
Balloki Barrage	15,182,000	19,322,000	1,500,000	36,004,000
Marala Barrage	13,689,000	29,059,000	1,500,000	44,248,000
Tarbela Dam	6,413,000	22,462,000	1,500,000	30,375,000
Panjnad Barrage	15,662,000	21,457,000	1,500,000	38,619,000
Taunsa Barrage	21,006,000	26,982,000	1,500,000	49,488,000
Kotri Barrage	20,881,000	22,902,000	1,500,000	45,283,000
Sidhnai Barrage	10,638,000	15,280,000	1,500,000	27,418,000
Rasul Barrage	11,741,000	21,306,000	1,500,000	34,547,000
Islam Barrage	10,897,000	19,445,000	1,500,000	31,842,000
Ghazi Barrage	9,923,000	18,942,000	1,500,000	30,365,000
Qadirabad Barrage	10,528,000	22,239,000	1,500,000	34,267,000
Trimmu Barrage	15,227,000	23,426,000	1,500,000	40,153,000
Mangla DAM	10,723,000	12,313,000	1,500,000	24,536,000
Sukkur Barrage	43,000,000	34,250,000	1,500,000	78,750,000
Manuthy Canal	2,427,000	9,665,000	1,500,000	13,592,000
Garang Regulator	5,893,000	10,128,000	1,500,000	17,521,000
Khanki Barrage	11,956,000	19,229,000	1,500,000	32,685,000
Guddu Barrage	20,356,000	27,635,000	1,500,000	49,491,000
Noshera	3,251,000	11,245,000	1,500,000	15,996,000
Pat feeder	5,763,000	10,622,000	1,500,000	17,885,000
UCH	4,854,000	9,777,000	1,500,000	16,131,000
Chashma Barrage	19,622,000	25,017,000	1,500,000	46,139,000
IRSA Monitoring sites	-	15,660,000	-	15,660,000
7 Monitoring sites	-	9,536,000	-	9,536,000
Total Cost	**331,384,000**	**498,608,000**	**36,000,000**	**865,992,000**

Table 2-42: Telemetry Site-Wise Detail Cost Breakup – Option B

All costs are in Pak Rupees

Telemetry Site	Field Equipment	Control & Communication System	Cost of civil works	Total
Sulemanki Barrage	18,538,000	42,557,000	1,500,000	62,595,000
Jinnah Barrage	23,213,000	53,290,000	1,500,000	78,003,000
Balloki Barrage	15,182,000	37,030,000	1,500,000	53,712,000
Marala Barrage	13,689,000	43,573,000	1,500,000	58,762,000
Tarbela Dam	6,413,000	28,366,000	1,500,000	36,279,000
Panjnad Barrage	15,662,000	35,554,000	1,500,000	52,716,000
Taunsa Barrage	21,006,000	54,828,000	1,500,000	77,334,000
Kotri Barrage	20,881,000	43,526,000	1,500,000	65,907,000
Sidhnai Barrage	10,638,000	23,267,000	1,500,000	35,405,000
Rasul Barrage	11,741,000	31,654,000	1,500,000	44,895,000
Islam Barrage	10,897,000	27,988,000	1,500,000	40,385,000
Ghazi Barrage	9,923,000	25,402,000	1,500,000	36,825,000
Qadirabad Barrage	10,528,000	32,309,000	1,500,000	44,337,000
Trimmu Barrage	15,227,000	38,912,000	1,500,000	55,639,000
Mangla DAM	10,723,000	22,800,000	1,500,000	35,023,000
Sukkur Barrage	43,000,000	99,870,000	1,500,000	144,370,000
Manuthy Canal	2,427,000	11,680,000	1,500,000	15,607,000
Garang Regulator	5,893,000	14,921,000	1,500,000	22,314,000
Khanki Barrage	11,956,000	32,355,000	1,500,000	45,811,000
Guddu Barrage	20,356,000	54,092,000	1,500,000	75,948,000
Noshera	3,251,000	12,705,000	1,500,000	17,456,000
Pat feeder	5,763,000	15,137,000	1,500,000	22,400,000
UCH	4,854,000	12,348,000	1,500,000	18,702,000
Chashma Barrage	19,622,000	47,586,000	1,500,000	68,708,000
IRSA Monitoring sites	-	20,893,000	-	20,893,000
7 Monitoring sites	-	21,145,000	-	21,145,000
Total Cost	**331,384,000**	**883,789,000**	**36,000,000**	**1,251,173,000**

Table 2-43: Telemetry Site-Wise Detail Cost Breakup – Option C

All costs are in Pak Rupees

Telemetry Site	Field Equipment	Control & Communication System	Cost of civil works	Total
Sulemanki Barrage	18,538,000	20,930,000	1,500,000	40,968,000
Jinnah Barrage	23,213,000	21,664,000	1,500,000	46,377,000
Balloki Barrage	15,182,000	20,264,000	1,500,000	36,946,000
Marala Barrage	13,689,000	30,001,000	1,500,000	45,190,000
Tarbela Dam	6,413,000	23,404,000	1,500,000	31,317,000
Panjnad Barrage	15,662,000	22,399,000	1,500,000	39,561,000
Taunsa Barrage	21,006,000	27,924,000	1,500,000	50,430,000
Kotri Barrage	20,881,000	23,844,000	1,500,000	46,225,000
Sidhnai Barrage	10,638,000	16,222,000	1,500,000	28,360,000
Rasul Barrage	11,741,000	22,248,000	1,500,000	35,489,000
Islam Barrage	10,897,000	20,387,000	1,500,000	32,784,000
Ghazi Barrage	9,923,000	19,884,000	1,500,000	31,307,000
Qadirabad Barrage	10,528,000	23,181,000	1,500,000	35,209,000
Trimmu Barrage	15,227,000	24,368,000	1,500,000	41,095,000
Mangla DAM	10,723,000	13,255,000	1,500,000	25,478,000
Sukkur Barrage	43,000,000	35,192,000	1,500,000	79,692,000
Manuthy Canal	2,427,000	10,607,000	1,500,000	14,534,000
Garang Regulator	5,893,000	11,070,000	1,500,000	18,463,000
Khanki Barrage	11,956,000	20,171,000	1,500,000	33,627,000
Guddu Barrage	20,356,000	28,577,000	1,500,000	50,433,000
Noshera	3,251,000	12,187,000	1,500,000	16,938,000
Pat feeder	5,763,000	11,564,000	1,500,000	18,827,000
UCH	4,854,000	10,719,000	1,500,000	17,073,000
Chashma Barrage	19,622,000	25,959,000	1,500,000	47,081,000
IRSA Monitoring sites	-	20,422,000	-	20,422,000
7 Monitoring sites	-	17,848,000	-	17,848,000
Total Cost	**331,384,000**	**534,287,000**	**36,000,000**	**901,671,000**

2.6 REVIEW AND DEVELOPMENT OF WATER ACCOUNTING AND AUDITING MECHANISM

2.6.1 The Current Practice - Existing Flow Distribution System

Forecasting and Planning

The existing system of flow distribution is preceded by a flow forecasting and planning phase by IRSA. This planning requires forecasting of river flows at the following 4 rim stations:

- Indus river at Tarbela;
- Jhelum river at Mangla;
- Chenab river at Marala; and,
- Kabul river at Noshera.

Average of historic flows, received from eastern rivers (Sutlej at Sulemanki and Ravi at Balloki after excluding the contributions from the Marala-Ravi and Qadirabad-Balloki Link canals) are used as contributions from the eastern rivers. Normally last 5-10 years averages of flows received from eastern rivers are used. The forecasting and subsequently seasonal planning is described in Final Report of MIS/GIS and DSS for Capacity Building of IRSA (NESPAK/AHT, 2014), and has 5 major steps. The procedure is summarized and visualized in the flowchart (Figure 2-36).

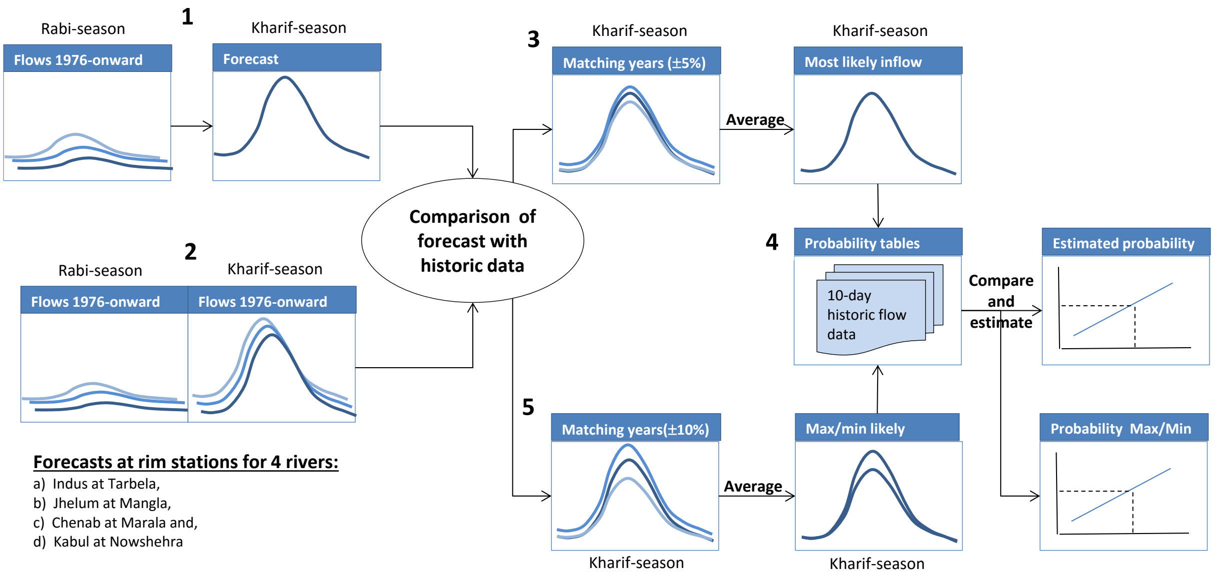

Figure 2-36: Flowchart Forecast and Planning Process of Water Supply for Kharif Season in the IBIS

The process as visualized above follows the same steps when planning is to be made for the Rabi season. In that case, the historic flows and probability tables from the Kharif season are to be taken.

2.6.2 Probability Tables

At step 4 of the forecasting input the probability tables are utilized. The probability tables are prepared by the Hydrology and Water Management (H&WM) Directorate of WAPDA for each river at the rim stations. Post Tarbela (April 1976 onward) 10-day observed flow data is used. WAPDA has developed a FORTRAN program (Prob.exe) to calculate flows of various probabilities (5%-95% at the interval of 5%) at 10-day. IRSA uses these probability tables in their flow forecasting with a lag of one season.

2.6.3 Reservoir Contents

At the start of each season, the actual reservoir level and storage for Tarbela and Mangla reservoirs are used as input for the planning process. This provides the storage available in the reservoirs for irrigation releases in Rabi season (low flow season) and storage to fill during the Kharif season (high flow season). The storage content at the start of season does influence the water availability for the following seasonal planning.

2.6.4 Losses/Gains of the System

Losses and gains in the system below rim stations are estimated based on the historic losses and gains data. History of IRSA operational planning shows that normally 15%-20% losses are taken in Indus zone in the Kharif season while 10%-15% in Rabi season. The range is 5%-10% for the Kharif season and 0%-5% for the Rabi season in the Jhelum-Chenab (J-C) Zone.

Provincial irrigation departments report daily observed gauge and discharge data at key distribution/water regulation sites (Table 1-1) to IRSA. Besides other uses, IRSA estimates daily loss and gain in various river reaches of IBIS using these as daily observed discharges.

A worksheet was used to compute the daily losses and gains in the system. The Worksheet also accounts for lag times in various river reaches. The loss and gain data was further compiled on monthly and seasonal basis for use in seasonal planning.

2.6.5 Reservoir Operations

In view of the above inputs of inflows, initial reservoir contents and losses/gains of the system, Tarbela and Mangla reservoirs are operated on 10-day interval in such a way that the shortages in the Indus and Jhelum-Chenab zones are met by filling/depletion of the reservoirs. During this, the reservoir operations are made within their operational constraints. The reservoir operation for the two reservoirs result in the canal diversions for J-C and Indus Zones with sharing of surface flows as per WAA of 1991.

2.7 EXISTING WATER AUDIT AND ACCOUNTING SYSTEM

The existing audit and account of the system depend upon the observed flow data reported by provincial irrigation departments. The data includes the upstream/downstream discharges at dams and barrages along with canal diversions. The data is communicated to IRSA on daily basis who is maintaining the observed data in various worksheets for their further use in seasonal planning and operation of IBIS.

The Consultants collected all the observed flow data from IRSA since 1993-2014 and compiled in a database, developed in another WCAP study “MIS/GIS for IRSA”. The same data was used to develop audit and account system.

2.8 DATA: ACQUISITION, ASSESSMENT AND INTERPRETATION

2.8.1 Assessment of Available Data on Discharges at the Reservoirs and Barrages

The database developed for IRSA in MIS/GIS project, contain discharge data of 3 reservoirs and 16 barrages. The data concerns the mean daily value of the upstream and downstream discharges along with diversions (if any) in cusecs. The data was available from April 1993 to September 2014. Table 2-44 below shows an overview of the availability of the mean daily inflows data at the selected structures. Before drawing the table, a consistency check was performed to eliminate erroneous data, such as typing errors or wrong data types.

Table 2-44: List of Structures with Available Inflow/Outflow Data (Source IRSA)

Structure	Years (1993 - 2015)																					
	93-94	94-95	95-96	96-97	97-98	98-99	99-00	00-01	01-02	02-03	03-04	04-05	05-06	06-07	07-08	08-09	09-10	10-11	11-12	12-13	13-14	14-15
Kabul at Noshera																						
Tarbela																						
Mangla																						
Marala Barrage																						
Balloki Headworks																						
Chashma Barrage																						
Guddu																						
Islam Headworks																						
Kalabagh/Jinnah Barrage																						
Khanki Headworks																						
Kotri																						
Panjnad Headworks																						
Qadirabad Barrage																						
Rasul Barrage																						
Sidhnai Barrage																						
Sukkur Barrage																						
Sulemanki Headworks																						
Taunsa Barrage																						
Trimmu Headworks																						

	Data available
➊	Partial data available
	Data not available

The data concerns the mean daily value of the upstream discharges for the period 1993-2014; the start is at April 01, 1993 and it ends at September 30, 2014. Table 2-44 shows that the inflow data is complete for the period of 1994-2014 while 1993-94 is missing for few structures.

A similar representation was drawn for the downstream daily discharges. The same is given in Table 2-45.

Table 2-45: List of Structures with Available Outflow Data (Source IRSA)

Structure	Years (1993 - 2015)																					
	93-94	94-95	95-96	96-97	97-98	98-99	99-00	00-01	01-02	02-03	03-04	04-05	05-06	06-07	07-08	08-09	09-10	10-11	11-12	12-13	13-14	14-15
Kabul at Noshera																						
Tarbela																						
Mangla																						
Marala Barrage																						
Balloki Headworks																						
Chashma Barrage																						
Guddu																						
Islam Headworks																						
Kalabagh/Jinnah Barrage																						
Khanki Headworks																						
Kotri																						
Panjnad Headworks																						
Qadirabad Barrage																						
Rasul Barrage																						
Sidhnai Barrage																						
Sukkur Barrage																						
Sulemanki Headworks																						
Taunsa Barrage																						
Trimmu Headworks																						

	Data available
0	Partial data available
	Data not available

Table 2-45 shows a similar data availability for the mean daily outflows as for the mean daily inflows. Based on the observations of data availability of mean daily inflows and outflows, it was concluded that the suitable period for analysis was from April 01, 1994 up to September 30, 2014.

The data availability of mean daily flows for the downstream canals and link intakes of the structures the overview is given in Table 2-46. The earliest date of the available continuous data was April 1st 1994.

Based on observed data (Tables 2-44 to 2-46) a proper check on the water accounting and a water audit was performed with the data starting at 01-01-2002 and ending at 30-09-2014.

2.8.2 Water Availability

Water availability of the system was estimated by considering the inflows received at rim stations i.e. Indus at Tarbela, Jhelum at Mangla, Kabul at Noshera and Chenab at Marala. In addition to these inflows at rim stations, eastern river component i.e. contribution of Ravi and Sutlej rivers was also considered. The water availability was computed from daily available data for the period April 01, 1994 to September 30, 2014. Water (April-March) years were classified to Wet, Average and Dry according to mean and standard deviation of the inflows. Mean + standard deviation (Stdev) was considered as wet while mean - standard deviation was taken as dry; remaining years as Average. Table 2-47 to Table 2-52 give the water availability at rim stations during Kharif and Rabi.

Table 2-46: List of Structures with Available Flow Data at Canal Structures (source IRSA)

Canal/Links	94-95	95-96	96-97	97-98	98-99	99-00	00-01	01-02	02-03	03-04	04-05	05-06	06-07	07-08	08-09	09-10	10-11	11-12	12-13	13-14	14-15
Balloki																					
B.S Link	■	■	■	■	■	■	■	■	■	■	■	■	■	■	■	■	■	■	■	■	■
LBDC	■	■	■	■	■	■	■	■	■	■	■	■	■	■	■	■	■	■	■	■	■
Chashma																					
C.J Link	■	■	■	■	■	■	■	■	■	■	■	■	■	■	■	■	■	■	■	■	■
CRBC	■	■	■	■	■	■	■	■	■	■	■	■	■	■	■	■	■	■	■	■	■
Guddu																					
Pat Feeder RD109	■	■	■	■	■	■	■	■	■	■	■	■	■	■	■	■	■	■	■	■	■
WDLS	■	■	■	■	■	■	■	■	■	■	■	■	■	■	■	■	■	■	■	■	■
Islam																					
WDLS	■	■	■	■	■	■	■	■	■	■	■	■	■	■	■	■	■	■	■	■	■
Kalabagh																					
Thal Canal	■	■	■	■	■	■	■	■	■	■	■	■	■	■	■	■	■	■	■	■	■
Khanki																					
L.C.C	■	■	■	■	■	■	■	■	■	■	■	■	■	■	■	■	■	■	■	■	■
Kotri																					
WDLS	■	■	■	■	■	■	■	■	■	■	■	■	■	■	■	■	■	■	■	■	■
Mangla																					
Mean Jari Dis								⓿	■	■	■	■	■	■	■	■	■	■	■	■	■
Mean Power (MPH)								⓿	■	■	■	■	■	■	■	■	■	■	■	■	■
Mean S. Way								⓿	■	■	■	■	■	■	■	■	■	■	■	■	■
U.J.C Gaggu	⓿	■	■	■	■	■	■	■	■	■	■	■	■	■	■	■	■	■	■	■	■
Marala																					
M.R Link	■	■	■	■	■	■	■	■	■	■	■	■	■	■	■	■	■	■	■	■	■
U.C.C	■	■	■	■	■	■	■	■	■	■	■	■	■	■	■	■	■	■	■	■	■
Panjnad																					
Abbasia canal	■	■	■	■	■	■	■	■	■	■	■	■	■	■	■	■	■	■	■	■	■
Abbasia Link	■	■	■	■	■	■	■	■	■	■	■	■	■	■	■	■	■	■	■	■	■
Panjnad Canal	■	■	■	■	■	■	■	■	■	■	■	■	■	■	■	■	■	■	■	■	■
Qadirabad																					
L.C.C Feeder	■	■	■	■	■	■	■	■	■	■	■	■	■	■	■	■	■	■	■	■	■
Q.B Link	■	■	■	■	■	■	■	■	■	■	■	■	■	■	■	■	■	■	■	■	■
Rasul																					
L.J.C	■	■	■	■	■	■	■	■	■	■	■	■	■	■	■	■	■	■	■	■	■
R.Q Link	■	■	■	■	■	■	■	■	■	■	■	■	■	■	■	■	■	■	■	■	■
R.P.C										■	■	■	■	■	■	■	■	■	■	■	■
Sidhnai																					
S.M Link							■	■	■	■	■	■	■	■	■	■	■	■	■	■	■
Sidhnai Canal				■	■	■	■	■	■	■	■	■	■	■	■	■	■	■	■	■	■
Sukkur																					
Kirther Below Garang	■	■	■	■	■	■	■	■	■	■	■	■	■	■	■	■	■	■	■	■	■
WDLS	■	■	■	■	■	■	■	■	■	■	■	■	■	■	■	■	■	■	■	■	■
Sulemanki																					
WDLS	■	■	■	■	■	■	■	■	■	■	■	■	■	■	■	■	■	■	■	■	■
Tarbela																					
AUX S.Way							⓿	■	■	■	■	■	■	■	■	■	■	■	■	■	■
Indent						⓿	■	⓿													
Mean Power (MPH)							⓿	■	■	■	■	■	■	■	■	■	■	■	■	■	■
S. S Way							⓿	■	■	■	■	■	■	■	■	■	■	■	■	■	■
Tunnel 4/5							⓿	■	■	■	■	■	■	■	■	■	■	■	■	■	■
Tunnel 5																					
Unit 11-13							⓿	■	■	■	■	■	■	■	■	■	■	■	■	■	■
Taunsa																					
D.G.K canal	■	■	■	■	■	■	■	■	■	■	■	■	■	■	■	■	■	■	■	■	■
MZGH Canal	■	■	■	■	■	■	■	■	■	■	■	■	■	■	■	■	■	■	■	■	■
T.P Link Canal	■	■	■	■	■	■	■	■	■	■	■	■	■	■	■	■	■	■	■	■	■
Trimmu																					
Haveli Head	■	■	■	■	■	■	■	■	■	■	■	■	■	■	■	■	■	■	■	■	■
Rangpur Canal	■	■	■	■	■	■	■	■	■	■	■	■	■	■	■	■	■	■	■	■	■
T.S Link	■	■	■	■	■	■	■	■	■	■	■	■	■	■	■	■	■	■	■	■	■

■	Data available for complete year
⓿	Partial data available
	Data not available

Table 2-47: Water Availability of Indus at Tarbela (MAF)

Water	Indus at Tarbela					
Year	Early Kharif	Late Kharif	Total Kharif	Rabi	Total	Class
1994-95	9.5	55.6	65.1	8.8	74.0	Wet
1995-96	8.5	44.6	53.2	9.4	62.6	Average
1996-97	9.8	49.8	59.6	9.1	68.6	Wet
1997-98	7.2	39.0	46.2	9.0	55.1	Average
1998-99	10.2	44.7	54.9	8.9	63.8	Average
1999-00	12.7	43.4	56.2	8.8	65.0	Average
2000-01	9.4	36.2	45.6	7.2	52.8	Dry
2001-02	7.9	35.9	43.8	6.6	50.4	Dry
2002-03	9.8	38.5	48.3	7.9	56.2	Average
2003-04	12.0	43.1	55.1	8.5	63.6	Average
2004-05	9.1	33.0	42.1	9.5	51.6	Dry
2005-06	9.1	46.9	56.0	9.5	65.5	Average
2006-07	12.1	42.9	55.1	10.0	65.0	Average
2007-08	10.6	38.5	49.2	8.2	57.4	Average
2008-09	9.1	37.8	46.9	9.1	56.0	Average
2009-10	9.7	37.0	46.8	9.3	56.0	Average
2010-11	8.5	53.7	62.3	10.0	72.3	Wet
2011-12	10.8	38.0	48.8	8.9	57.7	Average
2012-13	6.6	38.4	45.0	9.0	54.0	Average
2013-14	8.5	44.7	53.3	9.6	62.9	Average
2014-15	6.5	36.4	43.0	8.2	51.2	Dry
Average	**9.4**	**41.8**	**51.2**	**8.8**	**60.1**	
Stdev	**1.7**	**6.0**	**6.5**	**0.8**	**6.9**	

Table 2-48: Water Availability of Jhelum at Mangla (MAF)

Water	Jhelum at Mangla					
Year	Early Kharif	Late Kharif	Total Kharif	Rabi	Total	Class
1994-95	8.0	12.8	20.8	5.7	26.5	Wet
1995-96	8.3	13.6	21.9	6.5	28.4	Wet
1996-97	9.6	15.3	24.9	4.1	29.0	Wet
1997-98	6.5	10.4	17.0	7.1	24.0	Average
1998-99	9.6	8.5	18.1	3.6	21.7	Average
1999-00	5.9	5.4	11.2	3.2	14.4	Dry
2000-01	4.7	5.6	10.3	2.3	12.5	Dry
2001-02	3.6	4.6	8.2	3.7	11.9	Dry
2002-03	6.2	6.1	12.3	5.1	17.4	Average
2003-04	9.4	8.3	17.7	5.0	22.7	Average
2004-05	6.1	5.6	11.7	6.7	18.5	Average
2005-06	7.7	10.0	17.7	5.5	23.2	Average
2006-07	7.4	9.0	16.4	6.8	23.2	Average
2007-08	6.8	6.7	13.5	4.2	17.7	Average
2008-09	6.5	6.9	13.4	5.9	19.2	Average
2009-10	8.0	8.5	16.5	4.6	21.0	Average
2010-11	6.8	12.9	19.7	5.4	25.1	Average
2011-12	8.4	6.9	15.3	4.2	19.4	Average
2012-13	6.0	8.7	14.7	5.4	20.1	Average
2013-14	6.4	8.8	15.2	5.1	20.3	Average
2014-15	7.8	12.2	19.9	5.3	25.2	Average
Average	**7.1**	**8.9**	**16.0**	**5.0**	**21.0**	
Stdev	**1.5**	**3.0**	**4.1**	**1.2**	**4.7**	

Table 2-49: Water Availability of Chenab at Marala (MAF)

Water	Chenab at Marala					
Year	Early Kharif	Late Kharif	Total Kharif	Rabi	Total	Class
1994-95	4.1	20.5	24.6	5.6	30.2	Wet
1995-96	5.6	20.8	26.4	5.5	31.9	Wet
1996-97	5.2	22.3	27.5	4.4	31.9	Wet
1997-98	4.0	17.7	21.7	6.6	28.3	Average
1998-99	6.3	16.9	23.2	4.8	27.9	Average
1999-00	4.4	14.3	18.7	4.3	23.1	Average
2000-01	4.3	12.9	17.2	2.7	19.9	Dry
2001-02	3.4	12.6	16.0	2.9	18.9	Dry
2002-03	4.7	13.3	18.0	5.5	23.5	Average
2003-04	5.9	15.6	21.5	4.4	25.9	Average
2004-05	3.9	11.0	14.9	6.4	21.3	Average
2005-06	4.5	16.6	21.1	4.0	25.1	Average
2006-07	5.1	16.3	21.4	6.3	27.7	Average
2007-08	4.8	12.2	17.0	3.6	20.6	Average
2008-09	3.8	12.5	16.2	3.6	19.8	Dry
2009-10	3.4	11.0	14.5	3.4	17.9	Dry
2010-11	3.9	16.5	20.4	4.8	25.2	Average
2011-12	5.2	13.6	18.8	3.6	22.5	Average
2012-13	3.5	13.6	17.1	4.4	21.6	Average
2013-14	3.8	14.9	18.7	4.5	23.1	Average
2014-15	4.7	16.4	21.1	4.5	25.7	Average
Average	**4.5**	**15.3**	**19.8**	**4.6**	**24.4**	
Stdev	**0.8**	**3.2**	**3.6**	**1.1**	**4.1**	

Table 2-50: Water Availability of Kabul at Noshera (MAF)

Water	Kabul at Noshera					
Year	Early Kharif	Late Kharif	Total Kharif	Rabi	Total	Class
1994-95	5.8	13.2	18.9	3.3	22.2	Average
1995-96	6.3	12.9	19.2	4.4	23.6	Average
1996-97	5.5	11.3	16.8	3.7	20.5	Average
1997-98	6.0	11.7	17.8	5.1	22.9	Average
1998-99	8.2	11.4	19.6	5.2	24.8	Average
1999-00	5.3	7.5	12.8	2.5	15.2	Dry
2000-01	3.2	6.0	9.2	1.7	11.0	Dry
2001-02	3.7	6.4	10.1	2.3	12.4	Dry
2002-03	4.5	7.5	12.0	2.6	14.6	Dry
2003-04	5.3	10.3	15.7	3.2	18.9	Average
2004-05	4.3	6.8	11.1	5.9	17.0	Average
2005-06	6.6	16.4	23.0	5.0	28.0	Wet
2006-07	5.3	9.0	14.4	5.7	20.1	Average
2007-08	9.0	11.1	20.1	3.9	24.0	Average
2008-09	5.3	8.7	14.1	3.8	17.9	Average
2009-10	7.0	11.4	18.3	4.4	22.7	Average
2010-11	5.3	17.1	22.4	6.2	28.6	Wet
2011-12	6.2	7.9	14.1	4.0	18.1	Average
2012-13	5.2	11.0	16.2	5.4	21.6	Average
2013-14	8.0	12.2	20.3	4.4	24.7	Average
2014-15	7.6	11.4	18.9	4.6	23.6	Average
Average	**5.9**	**10.5**	**16.4**	**4.2**	**20.6**	
Stdev	**1.5**	**3.0**	**4.0**	**1.2**	**4.7**	

Table 2-51: Water Availability of Eastern Rivers (MAF)

Water	Eastern Rivers					
Year	Early Kharif	Late Kharif	Total Kharif	Rabi	Total	Class
1994-95	0.0	12.1	12.1	0.8	12.8	Wet
1995-96	0.3	13.4	13.7	1.5	15.1	Wet
1996-97	0.1	7.1	7.3	0.7	8.0	Average
1997-98	0.3	5.4	5.6	3.6	9.2	Wet
1998-99	2.4	5.3	7.6	5.7	13.3	Wet
1999-00	0.4	1.6	2.1	0.5	2.6	Average
2000-01	0.0	1.0	1.0	0.1	1.1	Average
2001-02	0.0	0.9	1.0	0.4	1.3	Average
2002-03	0.0	0.6	0.6	0.4	1.0	Average
2003-04	0.0	0.9	0.9	0.1	1.1	Average
2004-05	0.0	0.4	0.4	0.4	0.8	Average
2005-06	0.0	1.0	1.0	0.1	1.1	Average
2006-07	0.0	1.2	1.2	0.4	1.7	Average
2007-08	0.6	0.7	1.3	0.3	1.6	Average
2008-09	0.0	3.7	3.8	0.3	4.1	Average
2009-10	0.0	0.1	0.1	0.2	0.3	Dry
2010-11	0.0	3.2	3.3	0.7	3.9	Average
2011-12	0.1	5.0	5.1	1.3	6.4	Average
2012-13	0.1	1.0	1.1	0.7	1.9	Average
2013-14	0.0	6.0	6.1	1.0	7.1	Average
2014-15	0.3	0.9	1.2	0.0	1.2	Average
Average	**0.2**	**3.4**	**3.6**	**0.9**	**4.6**	
Stdev	**0.2**	**3.0**	**3.2**	**0.9**	**4.2**	

Table 2-52: Water Availability of IBIS (MAF)

Water	Indus Basin Irrigation System					
Year	Early Kharif	Late Kharif	Total Kharif	Rabi	Total	Class
1994-95	27.4	114.1	141.5	24.2	165.7	Wet
1995-96	29.1	105.3	134.4	27.2	161.6	Wet
1996-97	30.2	105.9	136.0	22.0	158.1	Wet
1997-98	24.1	84.2	108.3	31.2	139.5	Average
1998-99	36.7	86.7	123.4	28.1	151.5	Wet
1999-00	28.8	72.2	101.0	19.3	120.3	Average
2000-01	21.5	61.8	83.3	14.0	97.3	Dry
2001-02	18.6	60.4	79.0	15.9	94.9	Dry
2002-03	25.2	66.0	91.2	21.5	112.7	Average
2003-04	32.6	78.3	110.9	21.3	132.2	Average
2004-05	23.4	56.8	80.2	28.9	109.1	Dry
2005-06	28.0	90.8	118.9	24.1	143.0	Average
2006-07	30.0	78.5	108.5	29.2	137.7	Average
2007-08	31.8	69.3	101.1	20.3	121.4	Average
2008-09	24.7	69.6	94.3	22.7	117.0	Average
2009-10	28.1	68.0	96.1	21.8	118.0	Average
2010-11	24.6	103.5	128.1	27.1	155.1	Wet
2011-12	30.7	71.4	102.0	22.0	124.0	Average
2012-13	21.5	72.7	94.1	24.9	119.1	Average
2013-14	26.9	86.7	113.5	24.6	138.1	Average
2014-15	26.9	77.3	104.2	22.6	126.8	Average
Average	**27.2**	**80.0**	**107.1**	**23.5**	**130.6**	
Stdev	**4.2**	**16.2**	**18.1**	**4.3**	**20.3**	

Perusal of the above tables show that average annual flows to IBIS (1994-20014) are 131 MAF. During the time series (1994-95 to 2014-15), the system received three dry years (flows <110 MAF) and five wet years (flows>151 MAF).

Water availability for provincial diversion of surface flows are regarded as the sum of the inflows into the province minus the sum of the outflows from the province. Table 2-53 below gives the water availability definition for each province.

Table 2-53: Provincial Water Availability

Province	Water availability definition
Sindh	Guddu inflow – Kotri outflow-Balochistan canals
Punjab	Kabul inflow + Tarbela outflow + Mangla outflow + Marala inflow + Eastern Rivers Flow-CRBC (KPK) – Taunsa outflow – Panjnad outflow
Balochistan	PAT Feeder discharge+Kirther discharge+Uch discharge+Manuthi discharge
KPK	CRBC (KPK) discharge

Note: Tarbela and Mangla reservoirs outflows are the input for the water availability, since these are the flows which are released keeping in view the inflows and storages and thus are available to the users.

2.8.3 Provincial Utilization

Table 2-54 reflects the calculation adopted by IRSA, as per WAA 1991, while arriving at the actual provincial utilization.

Table 2-54: Actual Water Utilization for Sindh, Punjab, Balochistan and KPK

Province	Actual Water utilization definition
Sindh	Guddu Withdrawals+Sukkur Withdrawals+Kotri Withdrawals - Balochistan canals
Punjab	FLC+MR(INT)+CBDC+SVC(U)+CRBC(PB)+SVC(L)+TMU+PNJD+THAL+GreaterThal+TSA
Balochistan	PAT Feeder discharge+Kirther discharge+Uch discharge+Manuthi discharge
KPK	KPK releases - KPK escapages-4.6% Water losses

For actual provincial utilization, following data (Table 2-55) was available in the database.

Table 2-55: Available Data of 10-day Actual Provincial Canal Withdrawals

Structure	Years (1993 - 2015)																					
	93-94	94-95	95-96	96-97	97-98	98-99	99-00	00-01	01-02	02-03	03-04	04-05	05-06	06-07	07-08	08-09	09-10	10-11	11-12	12-13	13-14	14-15
Punjab																						
CRBC									●	■	■	■	■	■	■	■	■	■	■	■	■	■
FLC							■	■	■	■	■	■	■	■	■	■	■	■	■	■	■	■
MR_INT							■	■	■	■	■	■	■	■	■	■	■	■	■	■	■	■
CBDC							■	■	■	■	■	■	■	■	■	■	■	■	■	■	■	■
SVC_U							■	■	■	■	■	■	■	■	■	■	■	■	■	■	■	■
SVC_L							■	■	■	■	■	■	■	■	■	■	■	■	■	■	■	■
TMU							■	■	■	■	■	■	■	■	■	■	■	■	■	■	■	■
PNJD							■	■	■	■	■	■	■	■	■	■	■	■	■	■	■	■
THAL							■	■	■	■	■	■	■	■	■	■	■	■	■	■	■	■
GREATER_THAL																		●	■	■	■	■
TSA							■	■	■	■	■	■	■	■	■	■	■	■	■	■	■	■
Sindh																						
Guddu		■	■	■	■	■	■	■	■	■	■	■	■	■	■	■	■	■	■	■	■	■
Sukkur		■	■	■	■	■	■	■	■	■	■	■	■	■	■	■	■	■	■	■	■	■
Kotri		■	■	■	■	■	■	■	■	■	■	■	■	■	■	■	■	■	■	■	■	■
KPK																						
KPK Canals									■	■	■	■	■	■	■	■	■	■	■	■	■	■
Balochistan																						
PAT FEEDER												■	■	■	■	■	■	■	■	■	■	■
Kirther												■	■	■	■	■	■	■	■	■	■	■
UCH												■	■	■	■	■	■	■	■	■	■	●
Manuthi												■	■	■	■	■	■	■	■	■	■	●

■	Data available
●	Partial data available
	Data not available

Actual historic provincial utilizations for Kharif season are presented in Table 2-56.

Table 2-56: Actual Provincial Utilizations – Kharif Season

Kharif	Punjab	Sindh	KPK*	Balochistan
2004	30.35	27.82	0.98	2.17
2005	36.46	33.33	0.99	2.16
2006	34.94	27.12	1.05	2.03
2007	37.68	32.04	1.09	1.75
2008	34.25	31.63	1.01	2.13
2009	34.58	31.68	1.12	2.11
2010	29.17	23.81	0.81	1.21
2011	34.23	25.14	1.10	1.85
2012	29.76	27.03	1.10	1.61
2013	33.50	30.76	1.00	1.61
2014	35.17	33.19	0.98	1.88
Average	**33.64**	**29.41**	**1.02**	**1.86**
Para-14b	**34.65**	**28.79**	**0.82**	**2.57**
Para-2	**37.07**	**33.94**	**0.82**	**2.85**
Shortage (Para-14b)	3%	0%	**N/A**	**N/A**
Shortage (Para-2)	9%	13%	**N/A**	**N/A**

* Only CRBC diversions have been considered

Perusal of the above table shows that the actual diversions are always less than the allocations as per Para-2. The system shortages were 3% and nil, respectively for Punjab and Sind while comparing with Para-14b i.e., actual average system uses of 1977-82. The same were 9% and 13% as compared to Para-2. The variation in shortages are complex in nature and difficult to quantify. The allocations made by IRSA on daily basis are strictly following the provisions of WAA 1991 in view of water availability at rim stations and at dams. However, the contributions from intervening streams/nullahs/hill torrents in various river reaches make the distribution erratic i.e. sometime different than WAA allocations. The other important factor is rainfall in the southern command areas of IBIS particularly in Sind where canal diversions are reduced in view of rainfall moisture in agriculture fields and the full share remains unutilized.

Shortages are not relevant to Khyber Pakhtunkhwa and Balochistan as their allocations are as per their demands without shortage. The variation in diversion is due to varying demands.

The actual historic provincial utilizations for Rabi season are presented in Tables 2-57.

Table 2-57: Actual Provincial Utilizations – Rabi Season

Rabi	Punjab	Sindh	KPK*	Balochistan
2003-2004	17.02	13.74	0.75	0.43
2004-2005	11.55	11.12	0.50	0.72
2005-2006	16.40	13.02	0.70	0.89
2006-2007	16.30	14.48	0.50	0.73
2007-2008	15.17	12.00	0.67	0.79
2008-2009	13.29	10.89	0.75	0.59
2009-2010	13.37	11.04	0.75	0.80

Rabi	Punjab	Sindh	KPK*	Balochistan
2010-2011	18.74	15.38	0.47	0.87
2011-2012	17.63	11.26	0.75	1.12
2012-2013	17.15	14.23	0.55	0.64
2013-2014	17.37	14.63	0.53	1.08
Average	**15.82**	**12.89**	**0.63**	**0.79**
Para-14b	**19.75**	**14.91**	**0.70**	**1.02**
Shortage (Para-14b)	**20%**	**14%**	**N/A**	**N/A**

* Only CRBC diversions have been considered

The shortages in Rabi were 20% and 14% in Punjab and Sind, respectively comparing with Para-14b i.e. actual average system uses of 1977-82; variations have already been discussed while explaining the Kharif diversions.

2.8.4 System Loss/Gain

Table 2-58 To Table 2-61 present the formulae to estimate the system loss and gains for Indus and Jhelum-Chenab Commands for the two seasons.

Table 2-58: Definition of Various Data used in Estimation of Loss and Gain for Indus Command – Kharif Season

Sr.	Field Title	Formula
1	Kalabagh	Tarbela Inflow – Tarbela Outflow- PHLC + THAL + Chashma Inflow
2	Tarbela Sto/Rel	Tarbela Outflow – Tarbela Inflow- PHLC
3	Chashma Sto/Rel	Chashma Mean Outflow + CJ Link + CRBC – Chashma Mean Inflow
4	Carry Rabi	Tarbela LIVE Content (on March 31) + Chashma LIVE Content (on March 31)
5	J C Outflow	Rasul Discharge Downstream + Qadirabad Discharge Downstream + Balloki Discharge Downstream + Sulemanki Discharge Downstream
6	System Inflow	Kalabagh + Tarbela Sto/Rel + Chashma Sto/Rel + Carry Rabi +JC Outflow
7	Kotri Below	Kotri Discharge Downstream
8	System Utilization	System Inflows – Kotri Below
9	Canal WDLS	CRBC (PB) + SVC(L) + TMU + PNJD + THAL + Greater Thal + TSA+ Guddu Withdrawals + Sukkur Withdrawals +Kotri Outflow+ (KPK releases - KPK escapages-4.6% Water losses)
10	Losses/Gain	Canal WDLS – System Utilization
11	Percentage	((Loses/Gain) / System Inflows) * 100

Table 2-59: Definition of Various Data used in Estimation of Loss and Gain for Indus Command – Rabi Season

Sr.	Field Title	Formula
1	Kalabagh	Tarbela Inflow – Tarbela Outflow- PHLC + THAL + Chashma Inflow
2	Tarbela Sto/Rel	Tarbela Outflow – Tarbela Inflow- PHLC
3	Chashma Sto/Rel	Chashma Mean Outflow + CJ Link + CRBC – Chashma Mean Inflow
4	J-C Outflow	Rasul Discharge Downstream + Qadirabad Discharge Downstream + Balloki Discharge Downstream + Sulemanki Discharge Downstream
5	System Inflow	Kalabagh + Tarbela Sto/Rel + Chashma Sto/Rel + JC Outflow
6	Kotri Below	Kotri Discharge Downstream
7	System Utilization	System Inflows – Kotri Below
8	Canal WDLS	CRBC (PB) + SVC(L) + TMU + PNJD + THAL + Greater Thal + TSA+ Guddu Withdrawals + Sukkur Withdrawals +Kotri Outflow+ (KPK releases - KPK escapages-4.6% Water losses)
9	Carry Over	Tarbela LIVE Content (on March 31) + Chashma LIVE Content (on March 31)
10	Total Requirement	Canal WDLS – Carry Over
11	Losses/Gain	Canal WDLS – System Utilization
12	Percentage	((Loses/Gain) / System Inflows) * 100

Table 2-60: Definition of Various Data used in Estimation of Loss and Gain for J-C Command – Kharif Season

Sr.	Field Title	Formula
1	Jhelum @ Mangla	Mangla Mean Inflow
2	Mangla Sto/Rel	Mangla MEAN OUT FLOW - Mangla MEAN IN FLOW)*24*3600/43560000000
3	Chenab @ Marala	Marala DISCHARGE UP STREAM*24*3600/43560000000
4	Eastern River	(Balloki Discharge U/S - UCC Tail - MR Tail - QB Tail) + (Sulemanki Discharge U/S - BSI Tail – BSII Tail)
5	Carry Rabi	Mangla LIVE Content (on March 31)
6	System Inflows	Jhelum @ Mangla + Chenab @ Marala + Mangla Sto/Rel + Eastern River + Carry Rabi
7	J-C Outflow	Rasul Discharge Downstream + Qadirabad Discharge Downstream + Balloki Discharge Downstream + Sulemanki Discharge Downstream
8	System Utilization	System Inflows – J-C Outflows
9	Canal WDLS	FLC + MR (INT) + CBDC + SVC (U)
10	Losses/Gain	Canal WDLS – System Utilization
11	Percentage	((Losses/ Gain) / System Inflows) * 100

Table 2-61: Definition of Various Columns used in Estimation of Loss and Gain for J-C Command – Rabi Season

Sr.	Field Title	Formula
1	Jhelum @ Mangla	Mangla Mean Inflow
2	Mangla Sto/Rel	Mangla MEAN OUT FLOW - Mangla MEAN IN FLOW)*24*3600/43560000000
3	Chenab @ Marala	Marala DISCHARGE UP STREAM*24*3600/43560000000
4	Eastern River	(Balloki Discharge U/S - UCC Tail - MR Tail - QB Tail) + (Sulemanki Discharge U/S - BSI Tail – BSII Tail)
5	System Inflows	Jhelum @ Mangla + Chenab @ Marala + Mangla Sto/Rel + Eastern River
6	J-C Outflow	Rasul Discharge Downstream + Qadirabad Discharge Downstream + Balloki Discharge Downstream + Sulemanki Discharge Downstream
7	System Utilization	System Inflows – J-C Outflows
8	Canal WDLS	FLC + MR (INT) + CBDC + SVC (U)
9	Losses/Gain	Canal WDLS – System Utilization
10	Percentage	((Losses/ Gain) / System Inflows) * 100

The estimated loss and gain of Indus and J-C Commands are given in Tables 2-62 to Table 2-65.

Table 2-62: Indus Zone – Estimation of Kharif Loss and Gain

Year	Kalabagh	Tarbela Storage Release	Chashma Storage Release	Carry Rabi	J-C Outflow	System Inflows	Kotri Spills	System Utilization	Canal Withdrawals	Loss/gain	%age Loss/Gain
2004	55.5	-3.1	0.0	0.0	6.4	58.7	0.2	58.5	43.5	-15.1	-25.7
2005	82.4	-3.7	0.0	2.6	17.6	99.0	24.4	74.6	52.9	-21.7	-22.0
2006	74.0	-6.1	-0.1	0.1	18.3	86.2	20.2	66.1	45.6	-20.5	-23.8
2007	75.4	-4.3	0.0	1.6	11.9	84.7	15.8	68.9	52.6	-16.3	-19.3
2008	66.3	-3.5	-0.1	0.0	13.0	75.8	5.7	70.1	49.4	-20.7	-27.3
2009	68.1	-4.3	0.0	0.3	8.2	72.3	4.0	68.3	49.9	-18.4	-25.4
2010	91.4	-6.9	-0.2	0.0	24.7	109.0	50.5	58.5	37.4	-21.1	-19.4
2011	65.9	-6.6	-0.2	0.3	18.6	77.9	12.0	65.9	43.5	-22.5	-28.8
2012	66.3	-6.9	-0.1	0.0	12.4	71.7	5.3	66.4	42.1	-24.4	-34.0
2013	82.4	-5.3	0.0	0.6	17.6	95.3	18.1	77.1	48.1	-29.0	-30.5
2014	65.9	-6.2	0.1	0.8	22.1	82.6	5.0	77.6	52.7	-24.9	-30.1
Average	**72.1**	**-5.2**	**0.0**	**0.6**	**15.5**	**83.0**	**14.6**	**68.4**	**47.1**	**-21.3**	**-26.0**
Last 5-year	**74.3**	**-6.4**	**-0.1**	**0.3**	**19.1**	**87.3**	**18.2**	**69.1**	**44.8**	**-24.4**	**-28.5**
Last 10-year	**73.8**	**-5.4**	**0.0**	**0.6**	**16.5**	**85.5**	**16.1**	**69.4**	**47.4**	**-21.9**	**-26.0**

Table 2-63: Indus Zone – Estimation of Rabi Loss and Gain

Year	Kalabagh	Tarbela Storage Release	Chashma Storage Release	J-C Outflow	System Inflows	Kotri Spills	System Utilization	Canal Withdrawals	Carry Rabi	Total Requirement	Loss/gain	%age Loss/Gain
2004-05	17.43	0.69	-0.22	8.08	25.98	0.08	25.89	17.22	2.60	14.62	-8.67	-33.39
2005-06	14.45	5.90	0.21	3.15	23.71	0.14	23.56	20.71	0.13	20.59	-2.85	-12.03
2006-07	17.73	4.78	-0.13	7.37	29.74	1.56	28.18	22.98	1.58	21.40	-5.20	-17.47
2007-08	12.39	5.57	0.18	1.96	20.10	0.05	20.05	18.90	0.01	18.89	-1.15	-5.74
2008-09	13.51	3.46	-0.12	3.93	20.78	0.15	20.63	17.19	0.26	16.93	-3.44	-16.56
2009-10	13.22	4.24	0.09	2.61	20.16	0.06	20.09	16.89	0.01	16.87	-3.21	-15.91
2010-11	14.51	6.41	0.14	4.51	25.57	4.03	21.54	24.05	0.28	23.78	2.52	9.84
2011-12	10.93	6.02	0.25	4.08	21.28	2.28	19.00	19.25	0.01	19.24	0.25	1.19
2012-13	15.37	5.71	-0.11	5.11	26.08	0.70	25.38	22.69	0.63	22.06	-2.69	-10.33
2013-14	14.88	4.39	-0.04	6.54	25.77	0.13	25.64	22.74	0.76	21.98	-2.90	-11.26
2014-15	15.54	4.58	-0.05	9.82	29.89	1.86	28.04	22.46	1.67	20.78	-5.58	-18.67
Average	14.54	4.70	0.02	5.20	24.46	1.00	23.46	20.46	0.72	19.74	-2.99	-11.85
Last 5-year	14.25	5.42	0.04	6.01	25.72	1.80	23.92	22.24	0.67	21.57	-1.68	-5.85
Last 10-year	14.25	5.11	0.04	4.91	24.31	1.10	23.21	20.79	0.54	20.25	-2.43	-9.69

Table 2-64: J-C Zone – Estimation of Kharif Loss and Gain

Year	Mangla U/S	Marala U/S	Mangla Storage Release	Eastern Component	Carry Rabi	System Inflows	J-C Outflows	System Utilization	Canal Withdrawals	Loss/gain	%age Loss/Gain
2004	11.74	14.90	-2.56	0.39	0.01	24.48	6.41	18.07	15.66	-2.42	-9.87
2005	17.72	21.12	-3.77	1.01	0.58	36.66	17.39	19.27	17.91	-1.37	-3.72
2006	16.44	21.38	-4.20	1.19	0.28	35.09	18.28	16.82	17.50	0.69	1.96
2007	13.52	16.95	-1.70	1.33	2.22	32.32	11.94	20.38	18.16	-2.22	-6.88
2008	13.36	16.21	-3.48	3.76	0.04	29.89	13.04	16.85	17.49	0.64	2.15
2009	16.48	14.47	-2.71	0.11	0.79	29.14	8.22	20.92	17.35	-3.57	-12.25
2010	20.37	21.03	-4.61	3.25	0.13	40.17	24.74	15.43	16.15	0.72	1.78
2011	15.28	18.84	-4.46	5.06	0.57	35.29	18.62	16.67	16.84	0.17	0.48
2012	14.70	17.12	-4.70	1.12	0.04	28.29	12.40	15.89	15.66	-0.23	-0.81
2013	15.22	18.69	-5.86	6.06	0.65	34.76	17.62	17.14	17.06	-0.08	-0.24
2014	19.94	21.14	-6.14	4.73	1.21	40.88	22.07	18.81	16.57	-2.24	-5.48
Average	**15.89**	**18.35**	**-4.02**	**2.55**	**0.59**	**33.36**	**15.52**	**17.84**	**16.94**	**-0.90**	**-2.99**
Last 5-year	**17.10**	**19.36**	**-5.15**	**4.04**	**0.52**	**35.88**	**19.09**	**16.79**	**16.45**	**-0.33**	**-0.85**
Last 10-year	**16.30**	**18.69**	**-4.16**	**2.76**	**0.65**	**34.25**	**16.43**	**17.82**	**17.07**	**-0.75**	**-2.30**

Table 2-65: J-C Zone – Estimation of Rabi Loss and Gain

Year	Mangla U/S	Marala U/S	Mangla Storage Release	Eastern Component	System Inflows	J-C Outflows	System Utilization	Canal Withdrawals	Loss/gain	%age Loss/Gain
2004-05	6.72	6.41	1.77	0.36	15.27	8.08	7.18	6.05	-1.14	-7.46
2005-06	5.47	4.02	4.06	0.13	13.68	3.15	10.53	9.35	-1.19	-8.66
2006-07	6.77	6.33	2.21	0.43	15.75	7.37	8.38	8.19	-0.19	-1.18
2007-08	4.18	3.62	3.88	0.24	11.92	1.96	9.96	8.91	-1.05	-8.82
2008-09	5.88	3.61	2.74	0.31	12.54	3.93	8.61	7.90	-0.71	-5.66
2009-10	4.56	3.39	3.38	0.18	11.52	2.61	8.90	8.11	-0.80	-6.94
2010-11	5.42	4.78	4.12	0.67	14.99	4.51	10.47	10.54	0.06	0.43
2011-12	4.17	3.60	4.90	1.33	14.00	4.08	9.92	10.10	0.19	1.32
2012-13	5.38	4.42	4.09	0.75	14.64	5.11	9.53	9.32	-0.21	-1.44
2013-14	5.07	4.45	5.30	1.04	15.86	6.54	9.32	9.72	0.40	2.52
Average	**5.36**	**4.46**	**3.64**	**0.54**	**14.01**	**4.73**	**9.28**	**8.82**	**-0.46**	**-3.59**
Last 5-year	**4.92**	**4.13**	**4.36**	**0.79**	**14.20**	**4.57**	**9.63**	**9.56**	**-0.07**	**-0.82**
Last 10-year	**5.36**	**4.46**	**3.64**	**0.54**	**14.01**	**4.73**	**9.28**	**8.82**	**-0.46**	**-3.59**

Perusal of the above tables show that average Indus system losses are about 10% and 25% for Rabi and Kharif seasons, respectively while the same are 0-5% for Jhelum-Chenab Zone.

2.9 CONSULTATIVE MEETINGS

The Consultants organized various meetings to get the stakeholders on board and provide an interactive environment in which they can freely provide their observations/suggestions on the overall activities associated to the flow measurements. These meetings were aimed to assist in development of consensus and to present the transparency of the ongoing activities.

The first consultative meeting was convened at Islamabad within first week of mobilization of consultants. Subsequent involvement of representatives of the stakeholders, identified in the Terms of Reference was in the form of active participation in each flow measurement mission. The stakeholders were involved in all flow measurement as well as outcome of the study, presented in various workshops/meetings. Details of consultative meetings has been discussed in Section 1.5 of the report.

2.10 PROPOSAL FOR IMPLEMENTATION OF FINDINGS OF STUDY

To implement findings of the study, through provincial irrigation departments (PIDs), following key tasks were being proposed.

2.10.1 Standardization of Flow Measurements for 5 Pilot Sites

i. Estimate discharges at 5 pilot sites using developed formulas, improved coefficients and procedures recommended under current studies.

ii. Developed stage discharge ratings be implemented at canal locations for discharge estimations. Season-wise rating be used at Kirther canal i.e. for Kharif and Rabi. The flow measurements to be made frequently at least fortnightly basis, to verify the validity of ratings.

iii. PIDs to follow the flow measurement methodology (mid-section with at least 25 verticals) for carrying out discharge measurements at canals/barrages at different discharges to have a complete stage-discharge relationship. Future measurements should be carried out through ADCP to minimize the physical efforts and increase the measurement accuracy.

2.10.2 Standardization of Flow Measurements for 18 Remaining Sites

i. Based on the consensus developed among the stakeholders for flow measurement procedure, methodologies used in development of stage-discharge rating and calibration of discharge coefficients, as agreed in the consultative meetings, the same approaches be initiated for remaining sites.

ii. As agreed, the flow measurements at the remaining 18 sites be carried out using ADCP for the reasons noted above.

iii. Flow measurement through ADCP will also enhance the capacity of stakeholders in using latest tools of discharge measurement. This is possible only, if the flow measurement programmes are carried out with active participation of stakeholders, as practiced in the current studies.

iv. Stage-discharge ratings at canals and calibration of discharge coefficients at barrages be developed using the procedures developed in the present study.

v. In parallel, model studies be initiated at barrages and canal head regulators for better estimation of discharge coefficients under various flow ranges.

vi. Validate results of sectional model formulas through physical flow measurements covering flow ranges up to high flood level at barrage locations.

vii. Possibility of constructing permanent flow measurement structures e.g. flume and weir etc. should be explored so that impact of morphology and channel roughness in stage discharge rating be eliminated. This would result in reduced frequency of flow measurement in the long run.

2.10.3 Water Distribution Monitoring System

i. To assure the transparency in the water distribution and thereby increasing the confidence of the stakeholders in the overall water accounting and water auditing mechanism, it is inevitable to restrict the real-time communication to only the basic parameters viz. water level and the gate openings rather than the derived quantities i.e., discharges which involves empirical coefficients which vary from structure to structure and even at the same structure under different flow conditions i.e., hydraulic conditions.

ii. To have full confidence in the discharges being calculated on the basis of real-time basic parameters, it is essential to get all the hydraulic formula along with the respective coefficients corresponding to various geometric and hydraulic conditions be signed-off from all the stakeholders before implementation. It is important to mention that the signing off of the hydraulic formulae can only be done once the discharge coefficients at all the barrages, other than the four studied in the current project, be calibrated through the implementation of sectional model studies and subsequent field verification by conducting a rigorous flow measurement covering full range of discharges being encountered on the respective barrages.

iii. The selected Telemetry solution be implemented, initially, on five pilot sites to monitor the accuracy, efficiency and reliability.

2.11 CAPACITY BUILDING OF IRSA

i. Establish new flow monitoring unit at IRSA for sporadic discharge measurements to ascertain the discharges reported by provincial irrigation departments and WAPDA on barrages and canal head regulators. The field teams should be trained through on-job flow measurements of proposed 18 remaining sites. Procure ADCP, vehicles and allied equipment for flow measurements.

ii. To keep the above facility operational on long-term basis IRSA should also create a calibration unit for discharge measuring equipment.

iii. The above mentioned proposed recommendations be implemented out of the water charges being available through provinces.

2.11.1 Training of Upper Indus Flow forecasting Model and updated MIS/GIS and DSS Application

The trainings to IRSA professionals were initiated upon completion of the forecasting model and updated MIS/WebGIS applications. Presentation on Snow and glacier melt Runoff was delivered in order to demonstrate the basics of the model, its parameters and inputs. SRM+G requires daily input of temperature, precipitation, snow cover area and glacier exposed area. These inputs were prepared via R-Scripts (R-lanGauge), developed to download and process daily satellite data which was used to forecast flows on seasonal as well as on 10-day basis.

Different software were installed for which Client was trained how to download and execute them successfully. Moreover, seasonal and 10-day forecast procedures were also demonstrated. To execute R-Scripts for input data preparation, an exercise was conducted for Client to understand these scripts and produce required inputs for SRM+G.

Furthermore, hands-on practice of seasonal and 10-day forecast for the current year (2015) on Tarbela was also made by the Client.

IRSA professionals were also given demonstration of the updated MIS/WebGIS applications with all the new features incorporated. The following modules were demonstrated to Client:

- Seasonal Losses/Gains
- Seasonal Flow Data
- Water Audit
- Inflow Forecasting (Statistical & SRM Method)

Training with hands-on practice sessions was conducted; details of the training programmes were as follows:

Attendees:

IRSA: Muhammad Azam Khan, Rabia Faqir, Sumble Ghani

NESPAK: Muhammad Rizwan Alvi, Muhammad Umar, Ghulam Mohyyud Din

Dates	Day	Agenda
02-09-2015 (Wednesday)	1	MIS & DSS Demonstration of Command based Seasonal Losses/Gains. Demonstration of Reach based Seasonal Losses/Gains. Hands-on practice of Seasonal Losses/Gains.
03-09-2015 (Thursday)	2	MIS & DSS Overview of Water Audit Report Hands-on practice of Seasonal Losses/Gains and Water Audit Report. Web GIS Demonstration of Web-GIS IRSA-II component. SRM+G Presentation on SRM+G Overview of SRM+G Model and its parameters Installation of software (R, RStudio, MRT, Java)
04-09-2015 (Friday)	3	MIS & DSS Presentation on Inflow Forecasting (Statistical method & Snow Melt Run-Off method) Downloading, save and view IRSA manuals according to user's roles. Hands-on practice of Inflow Forecasting. Web GIS Hands-on practice of Web-GIS (Seasonal flow). SRM+G Use of R-Programming for downloading and processing of model data. SRM Input Preparation (Temperature, Precipitation, Snow and Glacier).
07-09-2015 (Monday)	4	MIS & DSS Overview and hands-on practice of Seasonal Flow Data of Rivers, Dams, Canals and Barrages. Web GIS Hands-on practice of Web-GIS (Loss and Gain). SRM+G Overview of forecasting procedures on seasonal and 10-day basis. Hands-on practice of execution of Model and input preparations.
08-09-2015 (Tuesday)	5	MIS & DSS Demonstration on Daily Losses/Gains and Editing of Daily Reports Footnotes Web GIS Hands-on practice of Web-GIS (Audit and Account). SRM+G Hands-on practice of execution of Model and input preparations. Hands-on practice of forecasting of current (2015) year seasonally and 10-day basis. Seasonal Forecasting of 2015 year on Tarbela.

2.12 LINKING WITH INDUS BASIN DECISION SUPPORT SYSTEM

According to TOR, study outcome was planned to be linked with the MIS/WebGIS and Decision Support System (DSS), developed in a separate study "Development of GIS/MIS Centre and Decision Support System to Enhance the Capacity of Indus River System Authority (IRSA), funded by WCAP.

The detailed functional requirement specification (DRS) document was submitted to Client which stated all the linkage requirements of seasonal flow data; water audit and accounts; upper Indus Flow Forecasting in MIS/WebGIS portals. The DRS document is attached as Annexure-L.

The application has also been updated in view of DRS, User Acceptance Testing (UAT) phase successfully completed with IRSA/WCAP professionals, before final deployment at IRSA data centre.

The Following screens elicit the newly added functionality:

Seasonal Losses/Gains

Losses/Gains are calculated in volumes (MAF) with respect to command and reach. All calculations are based upon individual season (Rabi, Early Kharif, Late Kharif & Kharif)

Year	Kalabagh	Tarbela Sto/Rel	Chashma Sto/Rel	J-C Outflow	System Inflow (2...5)	Kotri Below	System Utilization (6-7)	Canal Wdls	Losses/Gains (9-8)	%age (10/6)
1	2	3	4	5	6	7	8	9	10	11
2006-2007	17.726	4.792	-0.131	7.356	28.743	1.564	27.178	22.994	-5.185	-17.8
2007-2008	12.388	5.570	0.184	1.960	20.100	0.048	20.052	18.983	-1.069	-5.3
2008-2009	13.512	3.456	-0.123	3.930	20.775	0.145	20.630	17.085	-3.545	-17.1
2009-2010	13.216	4.242	0.088	2.611	20.157	0.064	20.093	16.886	-3.207	-16.0
2010-2011	14.607	6.409	0.140	4.514	25.670	4.091	21.580	24.064	2.515	9.8
2011-2012	10.628	6.020	0.281	4.051	21.280	2.280	19.000	19.280	0.280	1.3
2012-2013	15.371	5.710	-0.105	5.106	26.082	0.702	25.380	22.580	-2.800	-10.7
2013-2014	14.683	4.394	-0.044	6.539	25.772	0.131	25.641	22.739	-2.902	-11.3
2014-2015	15.540	4.581	-0.050	9.821	29.892	1.856	28.036	24.544	-3.492	-11.7
Average	14.230	5.018	0.023	5.103	24.375	1.202	23.172	21.027	-2.145	-8.8
Last 5 Years Average	14.246	5.423	0.038	6.012	25.719	1.800	23.919	22.661	-1.258	-4.9
Last 10 Years Average	14.252	5.105	0.042	4.907	24.308	1.097	23.211	20.995	-2.216	-9.1

Figure 2-37: Seasonal Losses/Gains (Command based)

Seasonal Loss and Gain at jhelum-Chenab Command in Rabi From 2007-2008 TO 2013-2014

Year	Jhelum at Mangla	Chenab at Marala	Mangla Sto/Rel	Eastern River	System Inflow	JC Outflow	System Utilization	Canal Wdls	Loss/Gain	%age
2007-2008	4.179	3.618	3.879	0.285	11.961	1.959	10.002	8.969	-1.033	-8.64
2008-2009	5.875	3.614	2.741	0.304	12.534	3.931	8.603	7.836	-0.767	-6.12
2009-2010	4.561	3.394	3.376	0.191	11.522	2.611	8.911	8.105	-0.806	-7
2010-2011	5.423	4.783	4.116	0.686	15.008	4.514	10.494	10.538	0.044	0.29
2011-2012	4.167	3.602	4.901	1.298	13.968	4.081	9.887	10.167	0.28	2
2012-2013	5.376	4.424	4.085	0.737	14.622	5.106	9.516	9.276	-0.24	-1.64
2013-2014	5.068	4.449	5.302	1.036	15.855	6.538	9.317	9.721	0.404	2.55
Avg	4.95	3.983	4.057	0.648	13.639	4.106	9.533	9.23	-0.303	-62.43
Avg_Five	4.919	4.13	4.356	0.79	14.195	4.57	9.625	9.561	-0.064	-64.84
Avg_Ten	5.361	4.464	3.645	0.547	14.017	4.733	9.283	8.818	-0.466	-70.86

Export Print

Headworks for Irrigation Diversion

Figure 2-38: Seasonal Losses/Gains (Command based) from WebGIS

Command Reach

Season Rabi From 2006-2007 To 2014-2015 Command Indus Reach Tarbela-Kalaba View Export

Tarbela-Kalabagh

LOSSES/GAINS (RABI)

Period	Flows (MAF)	L/G (MAF)	L/G (Percentage)
2006-2007	20.550	1.405	6.8
2007-2008	17.907	1.692	9.5
2008-2009	16.504	-0.064	-0.4
2009-2010	18.070	-0.394	-2.2
2010-2011	22.633	-1.172	-5.2
2011-2012	18.538	-0.471	-2.5
2012-2013	20.359	1.303	6.4
2013-2014	18.696	1.068	5.7
2014-2015	18.416	0.993	5.4
Average	19.075	0.484	2.5
Last 5 Years Average	19.726	0.344	1.7
Last 10 Years Average	19.225	0.412	2.1

(All figures in MAF)

Figure 2-39: Seasonal Losses/Gains (Reach based)

Figure 2-40: Selection Criteria for Seasonal Losses/Gains (Reach based) from WebGIS

Period	Flows (MAF)	L/G (MAF)	Percentage
2011-2012	10.493	-0.379	-3.61
2012-2013	14.066	-0.806	-5.73
2013-2014	13.115	-0.742	-5.66
2014-2015	16.914	-1.166	-6.89
Avg	13.647	-0.773	-5.67
Avg_Five	13.588	-0.711	-5.24
Avg_Ten	12.527	-0.601	-4.8

Figure 2-41: Seasonal Losses/Gains (Reach based) from WebGIS

Seasonal Flow Data

Inflow and outflow data for all Dams, Barrages, Canals and Rivers were computed in volumes (MAF) on seasonal basis (Rabi, Early Kharif, Late Kharif & Kharif)

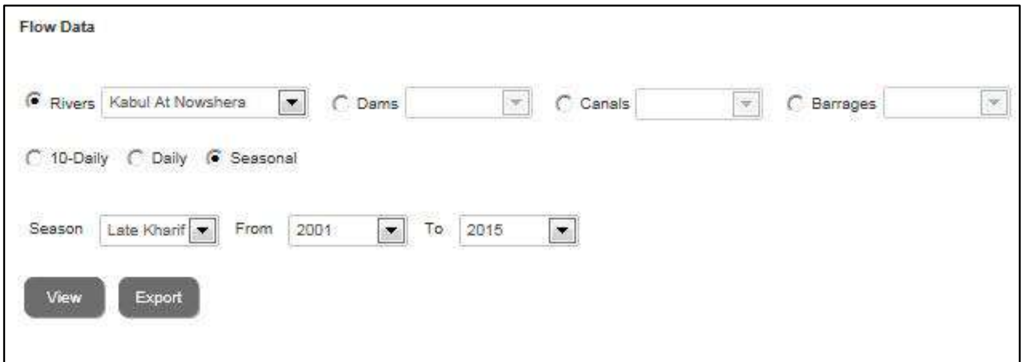

KABUL AT NOWSHERA

Year	Discharge	Average
2001	6.816	6.816
2002	7.492	7.492
2003	10.323	10.323
2004	6.803	6.803
2005	16.406	16.406
2006	9.052	9.052
2007	11.083	11.083
2008	8.747	8.747
2009	11.386	11.386
2010	17.381	17.381
2011	7.901	7.901
2012	10.983	10.983
2013	12.238	12.238
2014	11.395	11.395

Note:-

1- All volumes are in MAF.

Figure 2-42: Seasonal Flow Data of River

TARBELA

Year	Inflow	Outflow
2001	35.889	30.109
2002	38.506	34.169
2003	43.121	37.614
2004	32.980	29.852
2005	46.850	42.720
2006	42.941	38.065
2007	38.538	33.830
2008	37.791	34.647
2009	37.042	33.079
2010	53.739	46.874
2011	38.024	32.268
2012	38.367	31.856
2013	44.716	40.608
2014	36.428	30.168

Note:-

1- All volumes are in MAF.

Figure 2-43: Seasonal Flow Data of Dam

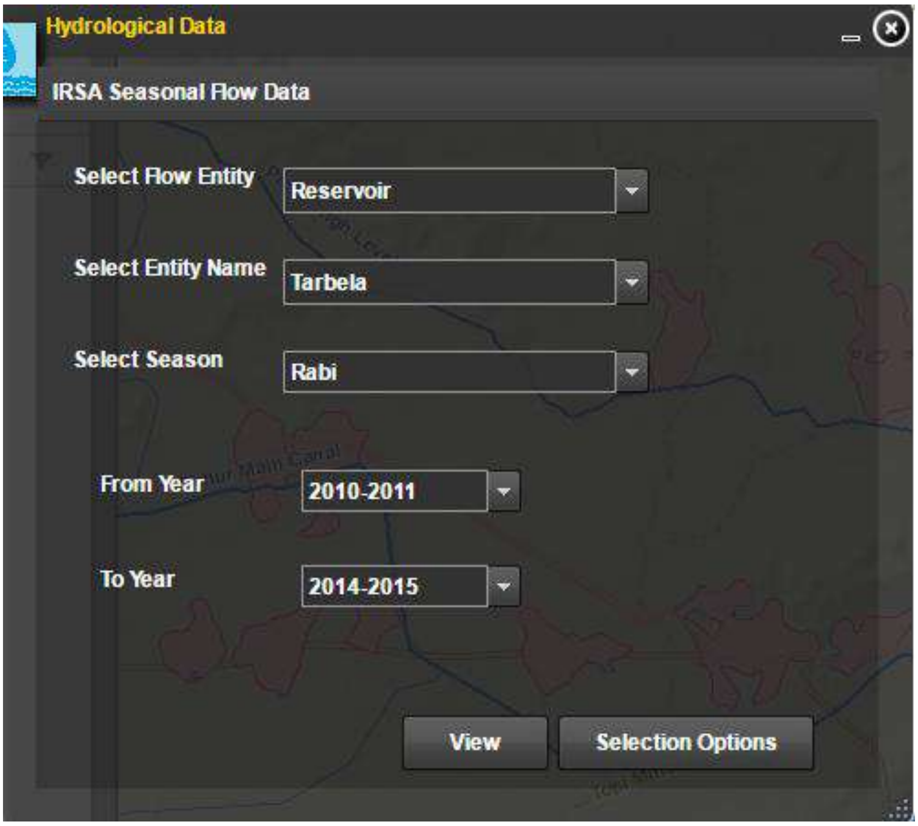

Figure 2-44: Selection Criteria for Seasonal Flow Data of Dam WebGIS

Figure 2-45: Seasonal Flow Data of Dam WebGIS

Water Audit

A special report was prepared to compare total water inflows in the system with the actual system withdrawals on seasonal basis (Rabi, Early Kharif, Late Kharif & Kharif). This report provides the overall picture of total water availability and its usage.

INDUS RIVER SYSTEM AUTHORITY (IRSA)
Water Accounting & Audit
Rabi 2005-2006 to 2014-2015

All values are in MAF

Period Rabi	Inflow at Rim Stations	Punjab			Sindh	KPK(Below)	Balochistan	Total
		J-C	Indus	Total				
2005-2006	34.385	9.349	7.048	16.397	12.132	0.643	0.889	30.061
2006-2007	39.425	8.194	8.089	16.283	13.755	0.414	0.726	30.137
2007-2008	29.393	8.908	6.248	15.156	11.167	0.698	0.785	28.606
2008-2009	29.597	7.897	5.484	13.381	10.356	0.752	0.597	26.650
2009-2010	29.515	8.105	5.257	13.362	10.245	0.587	0.796	26.781
2010-2011	37.814	10.538	8.194	18.732	14.509	0.478	0.873	33.446
2011-2012	31.365	10.103	7.516	17.619	10.069	0.555	1.115	28.890
2012-2013	35.527	9.318	7.897	17.215	13.660	0.486	0.642	31.154
2013-2014	35.378	9.721	7.643	17.364	13.553	0.466	1.077	31.865
2014-2015	39.424	8.889	8.499	17.388	14.447	0.573	1.025	31.982
Avg	34.182	9.102	7.188	16.290	12.389	0.565	0.853	29.957

Note:-
Rim Stations Include:
1-Indus @ Tarbela
2-Jhelum @ Mangla
3-Chenab @ Marala
4-Kabul @ Nowshera
5-Eastern(Ravi+Satluj)

Figure 2-46: Seasonal Water Audit Report

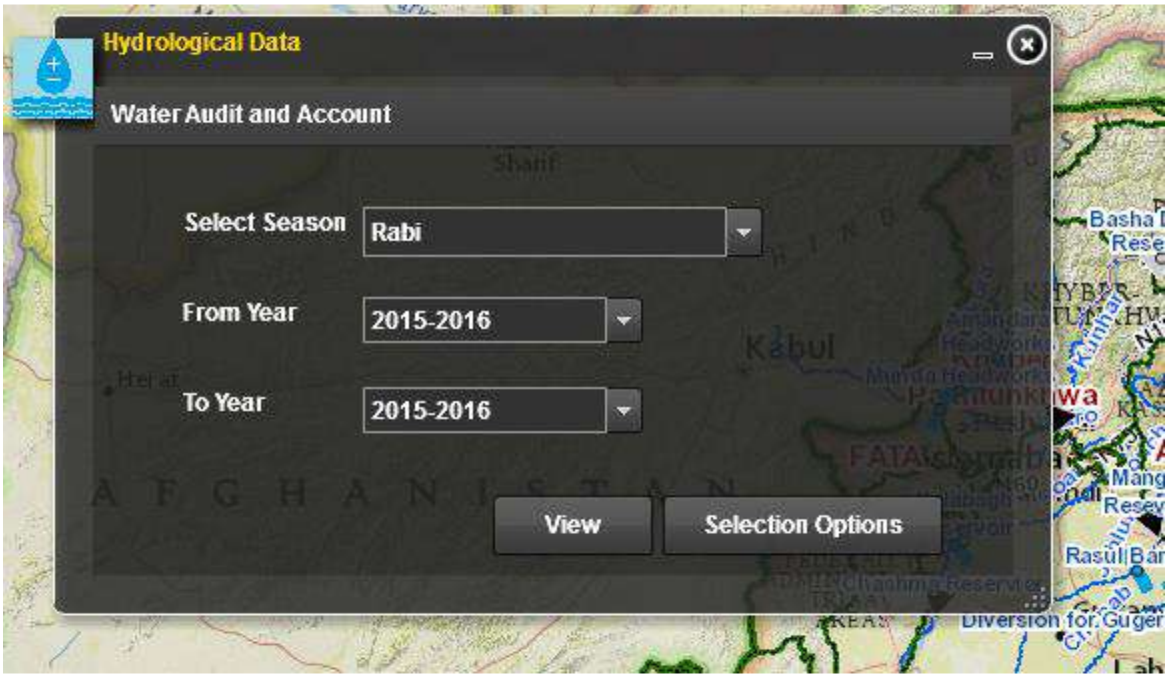

Figure 2-47: Selection Criteria for Seasonal Water Audit Report WebGIS

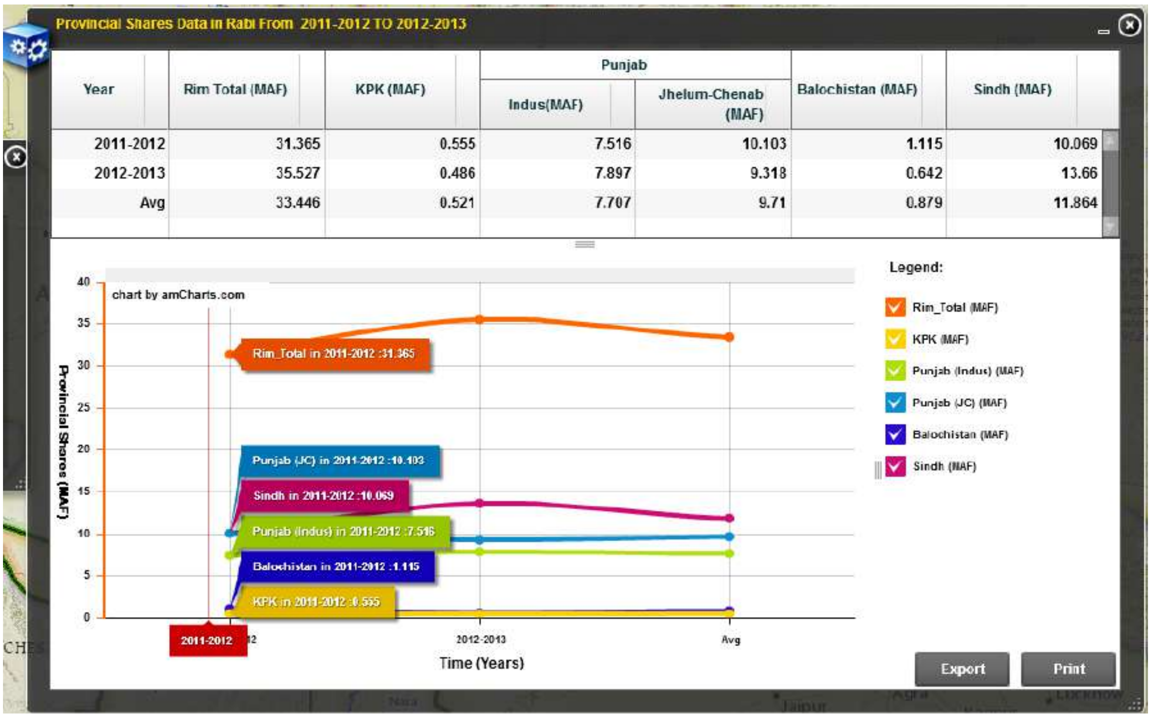

Figure 2-48: Seasonal Water Audit Report WebGIS

Inflow Forecasting (Statistical & SRM Method)

The system has the capability to provide two methods of inflow forecasting namely statistical and SRM forecast. In seasonal planning a combination of statistical and SRM forecast can now be utilized in planning a certain season (preferably Kharif season)

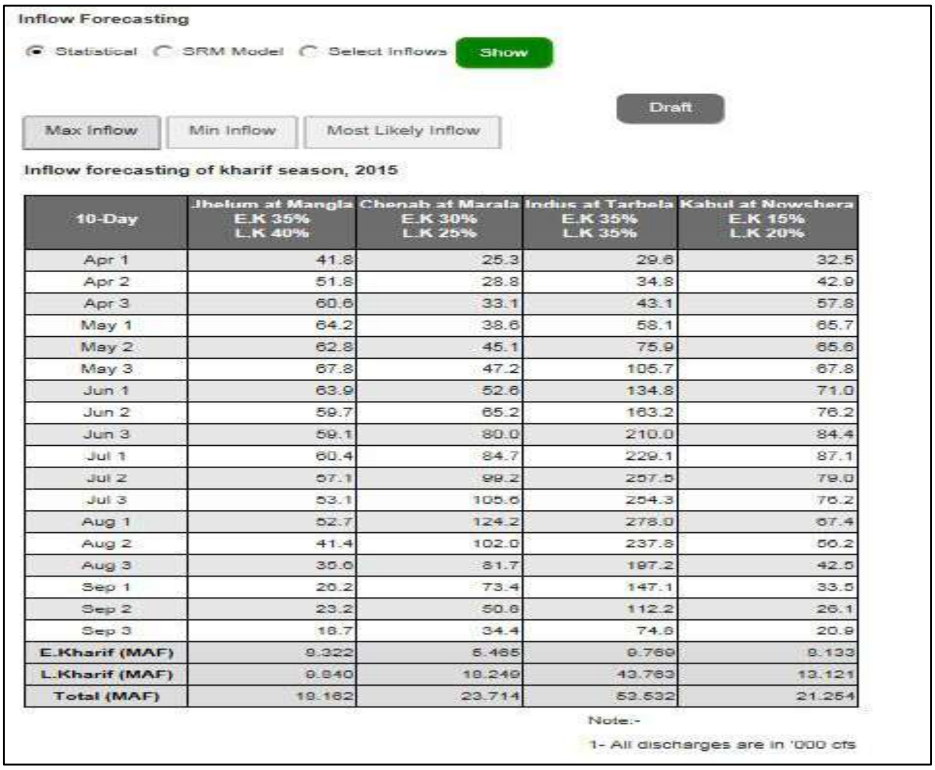
Inflow Forecasting

Statistical SRM Model Select Inflows Show

Draft

Max Inflow | Min Inflow | Most Likely Inflow

Inflow forecasting of kharif season, 2015

10-Day	Jhelum at Mangla E.K 35% L.K 40%	Chenab at Marala E.K 30% L.K 25%	Indus at Tarbela E.K 35% L.K 35%	Kabul at Nowshera E.K 15% L.K 20%
Apr 1	41.8	25.3	29.6	32.5
Apr 2	51.8	28.8	34.8	42.9
Apr 3	60.6	33.1	43.1	57.8
May 1	64.2	38.6	58.1	65.7
May 2	62.8	45.1	75.9	65.6
May 3	67.8	47.2	105.7	67.8
Jun 1	63.9	52.6	134.8	71.0
Jun 2	59.7	65.2	163.2	76.2
Jun 3	59.1	80.0	210.0	84.4
Jul 1	60.4	84.7	229.1	87.1
Jul 2	57.1	99.2	257.5	79.0
Jul 3	53.1	105.6	254.3	76.2
Aug 1	52.7	124.2	278.0	67.4
Aug 2	41.4	102.0	237.8	56.2
Aug 3	35.0	81.7	197.2	42.5
Sep 1	26.2	73.4	147.1	33.5
Sep 2	23.2	50.6	112.2	26.1
Sep 3	16.7	34.4	74.6	20.9
E.Kharif (MAF)	9.322	5.465	9.769	9.133
L.Kharif (MAF)	9.840	18.249	43.763	13.121
Total (MAF)	19.162	23.714	53.532	21.254

Note:-

1- All discharges are in '000 cfs

Figure 2-49: Statistical Inflow Forecast

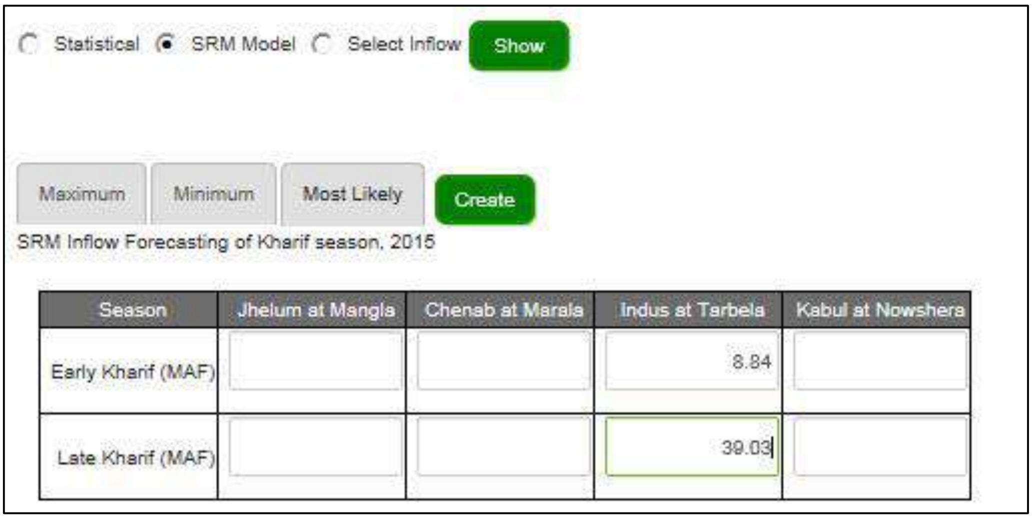

Season	Jhelum at Mangla	Chenab at Marala	Indus at Tarbela	Kabul at Nowshera
Early Kharif (MAF)			8.84	
Late Kharif (MAF)			39.03	

Figure 2-50: Input Screen for adding SRM Draft

10-Day	Jhelum at Mangla EK % LK %	Chenab at Marala EK % LK %	Indus at Tarbela EK 25% LK 45%	Kabul at Nowshera EK % LK %
Apr 1			30.3	
Apr 2			36.1	
Apr 3			48.3	
May 1			62.9	
May 2			86.9	
May 3			110.8	
Jun 1			145.7	
Jun 2			151.3	
Jun 3			200.1	
Jul 1			217.2	
Jul 2			242.4	
Jul 3			247.5	
Aug 1			261.1	
Aug 2			227.2	
Aug 3			190.2	
Sep 1			140.6	
Sep 2			103.1	
Sep 3			72.2	
Early Kharif (MAF)			10.555	
Late Kharif (MAF)			41.588	
Total (MAF)			52.143	

Figure 2-51: Screen for SRM Draft

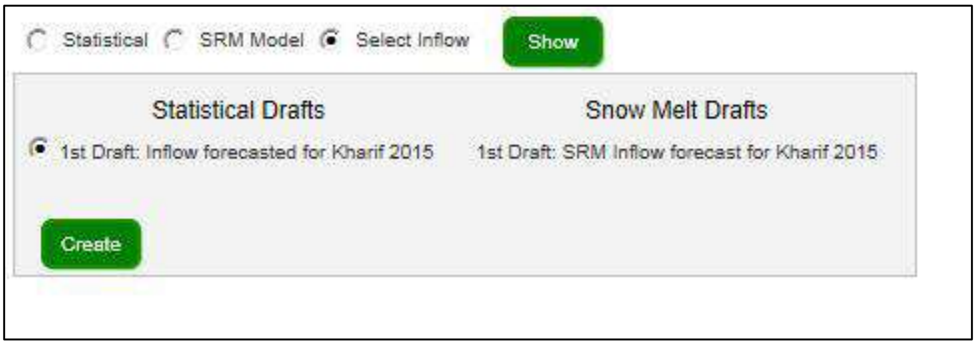

Figure 2-52: Screen for Selecting Flow Forecasts

Maximum | Minimum | Most Likely | Save

Selected Inflow Forecasting of Kharif season, 2015

10-Day Max	Jhelum at Mangla EK 35% LK 40%	Chenab at Marala EK 30% LK 25%	Indus at Tarbela EK 35% LK 35%	Kabul at Nowshera EK 15% LK 20%
Apr 1	41.8	25.3	29.6	32.5
Apr 2	51.8	28.8	34.8	42.9
Apr 3	60.6	33.1	43.1	57.8
May 1	64.2	38.6	58.1	65.7
May 2	62.8	45.1	75.9	65.6
May 3	67.8	47.2	105.7	67.8
Jun 1	63.9	52.6	134.8	71.0
Jun 2	59.7	65.2	163.2	76.2
Jun 3	59.1	80.0	210.0	84.4
Jul 1	60.4	84.7	229.1	87.1
Jul 2	57.1	99.2	257.5	79.0
Jul 3	53.1	105.6	254.3	76.2
Aug 1	52.7	124.2	278.0	67.4
Aug 2	41.4	102.0	237.8	56.2
Aug 3	35.6	81.7	197.2	42.5
Sep 1	26.2	73.4	147.1	33.5
Sep 2	23.2	50.8	112.2	26.1
Sep 3	18.7	34.4	74.8	20.9
E.Kharif (MAF)	8.322	5.465	9.769	8.133
L.Kharif (MAF)	9.840	18.249	43.763	13.121
Total (MAF)	18.162	23.714	53.532	21.254

10-Day Max	Jhelum at Mangla EK % LK %	Chenab at Marala EK % LK %	Indus at Tarbela EK 25% LK 45%	Kabul at Nowshera EK % LK %
Apr 1			30.3	
Apr 2			36.1	
Apr 3			48.3	
May 1			62.9	
May 2			86.9	
May 3			110.8	
Jun 1			145.7	
Jun 2			151.3	
Jun 3			200.1	
Jul 1			217.2	
Jul 2			242.4	
Jul 3			247.5	
Aug 1			261.1	
Aug 2			227.2	
Aug 3			190.2	
Sep 1			140.6	
Sep 2			103.1	
Sep 3			72.2	
E.Kharif (MAF)			10.554	
L.Kharif (MAF)			41.588	
Total (MAF)			52.142	

Figure 2-53: Screen for Selecting Flows from the two Methods

3 TASK-II HYDROLOGIC MODELLING FOR FLOW FORECASTING OF INDUS RIVER BASIN

3.1 INTRODUCTION

The flow regime of the upper catchments of the Indus Basin is a combination of i) a glacial regime at very high altitudes, ii) a nival regime at middle altitudes where flow is dependent on the melting of seasonal snow accumulated during the preceding winter and spring, and iii) a rainfall regime dependent on runoff from concurrent rainfall mainly during the monsoon season that dominates on the southern foothills. Although the Upper Indus Basin as situated in the high mountain ranges of the Western Himalaya – Karakoram – Hindu Kush region contains the greatest area of perennial ice outside the Polar Regions[10], the area of winter snow cover is an order of magnitude greater than the glacier area. Thus, the major contribution to flow comes from the nival regime, whereas the runoff originating from rainfall is the smallest component volume-wise.

As irrigated agriculture is of vital importance for Pakistan's economy, even small improvements to the planning and management of water releases from the two major reservoirs Tarbela and Mangla and in the forecasting of flows in unregulated rivers could create significant economic benefits to the country. Although, seasonal and 10-day flow forecasts are provided for the major river basins by several institutions, e.g. the Pakistan Meteorological Department PMD, the Water Resources Management Directorate WRMD and the Snow and Ice Hydrology Project SIHP of WAPDA, recent available Remote Sensing Snow Products promise a higher forecast precision in particular for snowmelt dominated flows.

It is necessary to develop an improved river flow forecasting system to assess the variability in river flows due to climate change impacts in upper catchments and there corresponding effects on the water availability for agriculture as well as for other usage. The new improved snow and glacial melt flow forecasting system will help in assessing the early melt flows in Tarbela in accordance with the climate change impacts on water availability on short and long term basis.

3.2 BRIEF DESCRIPTION OF THE STUDY AREA

Of the entire UIB area, approximately measuring 173,411km^2, about 10% or 16.750km^2 are covered by glaciers. The watershed is under the influence of two different climatic systems – the South West Indian Monsoon and the Westerlies – bringing in moisture from different sources, during different times of the year and affecting different areas in the UIB. The utmost east and the southern slopes are primarily influenced by the Monsoon while precipitation in the north and the west of the basin is controlled by the Westerlies.

Temperatures are strongly controlled by topographic elevation and submitted to a seasonal cycle that reaches maximum temperatures during July and minimum temperatures in January. This spatio-temporal temperature pattern prevails in all of the UIB. The difference in topographic elevation (lowest: 475m at Tarbela, highest: 8611m K^2) is reason for a huge vertical temperature range. In some areas mean temperatures never drop below zero, others

[10] > 20,000 km^2

show permanent frost. Figure 3-1 shows the extent of the study area. While the distribution of monthly inflows to Tarbela is shown in Figure 3-2.

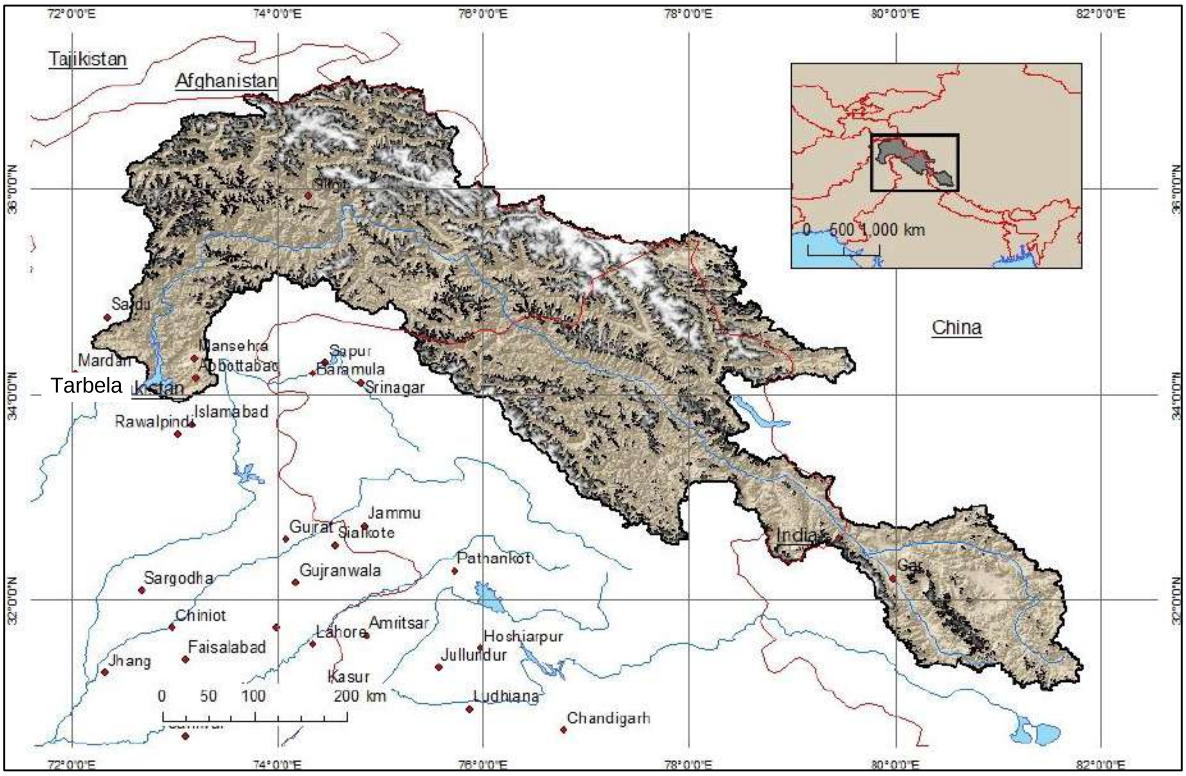

Figure 3-1: Extent of Study Area (Upper Indus Basin)

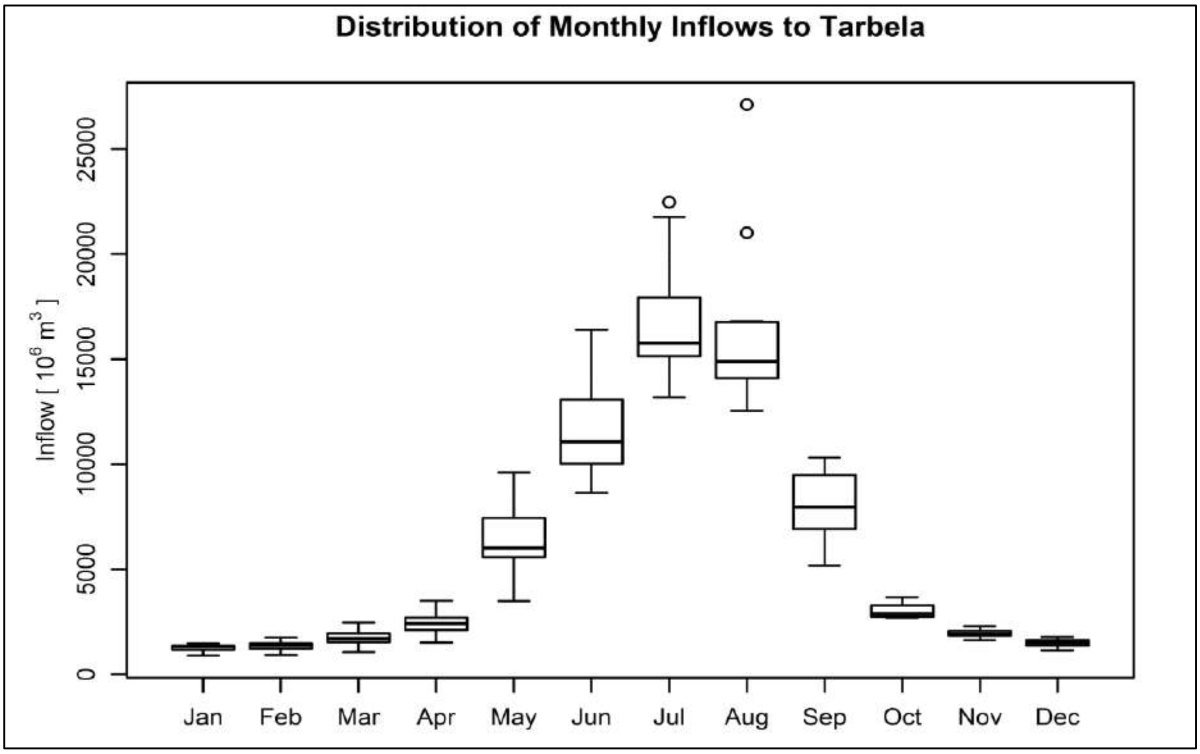

Figure 3-2: Box Plot for Monthly Inflow to Tarbela Reservoir

3.3 REVIEW OF EXISTING FLOW FORECASTING PROCEDURES

3.3.1 Presently used Methods for Flow Forecasting

This section describes the existing state of the work and research being carried out on snow and ice hydrology in Pakistan. The various departments and their methods used to forecast the flows in the rivers and mainly to the two major reservoirs of Pakistan Tarbela and Mangla are described below.

3.3.2 The Upper Indus Basin (UIB)

The upper catchments of the Indus river basin feed two major reservoirs of Pakistan, Tarbela and Mangla, which are located such that the snowmelt in these catchments becomes the major source of flows especially in early summer. At the end of most winters nearly the entire basin above 2 200 m asl, is covered with snow, which spreads over some 173,345 km^2. More than half of the snow-cover is thin and melts and evaporates before the main rise of the rivers occurs. About 20% of the snow covered area is glacierized.

From May to July melting of seasonal snow cover contributes to the bulk of the flow of the Upper Indus streams. These flows tend to rise progressively, as melting temperatures advance into areas of deeper snowpack at higher elevations. By the end of June the flows reduce due to diminished snow cover. At this time the glacierized basins become important contributors to the flows due to melting of their seasonal snow cover and then the ice (glaciated snow). Most of the water-yield is from higher elevations and hence, mainly part of the contribution of the heavily glacierized basins, especially of the Hindu Kush and Karakoram. Overall glacial melt dominates the flows of the largest tributaries of Indus river; Chitral, Gilgit, Hunza, Braldu and Shyok rivers.

3.3.3 Estimation & Forecasting of Flows from Melting of Snow and Ice

The forecasting of flows due to snow and ice melt in the UIB is being carried out by the following departments:

- Pakistan Snow and Ice Hydrology Project (PSIHP) of Hydrology and Research Directorate (H&RD), Water and Power Development Authority (WAPDA)
- Flood Forecasting and Warning Centre, Lahore of Pakistan Meteorological Department (PMD)
- Water Resources Management Directorate (WRMD) of WAPDA
- Indus River System Authority (IRSA)

A brief description of the methodology of the above mentioned departments is given in the following sections.

3.3.4 Estimation and Flow Forecasting by PSIHP of H&RD of WAPDA

Pakistan Snow and Ice Hydrology Project (PSIHP) was established in 1985 by H&RD of WAPDA in collaboration with two universities of UK and Canada in which research was carried out on the UIB. Its second phase was started in 1989 in which several high altitude stations were established for the measurement of snow water equivalent and meteorological parameters. The data transmission to a master station was established and thus estimating and forecasting the flows using a computer model became possible.

3.3.5 Flow Forecasting by Pakistan Meteorological Department (PMD)

The Pakistan Meteorological Department (PMD) undertook the preparation of a model "Hydromet Model 1" in early 90's for forecasting the seasonal and 10-day flows in to the Mangla reservoir. The model uses the meteorological approach to forecast the snowfall/rainfall and thus estimating the flows from the upper catchments to the Mangla reservoir. This model is being used to forecast the seasonal and 10-day flows, but results are only available late in May or June.

3.3.6 Flow Forecasting by WRMD of WAPDA

The Water Resources Management Directorate uses the statistical approach to predict the seasonal flows to Tarbela and Mangle reservoirs.

3.4 SNOWMELT RUNOFF FORECASTING

3.4.1 By PSIHP of H&RD (WAPDA)

The Development of the System - Phase-1

In the first five years phase (1985-89), "Pakistan Snow and Ice Hydrology Project" (PSIHP) research was conducted into glacio-hydrologic aspects of the Upper Indus Basin (UIB) relevant to water resource development and forecasting of flows. It also included defining the terms of a monitoring and flow forecasting system for the snow and ice regime basins.

In the first phase, studies were conducted for the glaciers of following sub-basins:

- Hunza River Basin
- Braldu River Basin
- Rakhiot River Basin
- Jhelum River Basin

The above mentioned research basins are shown in Figure 3-3. The studies carried out under this project included the following:

i. Glacier accumulation, movement, ablation and mass balance and runoff
ii. Effect of facets on the ablation of debris covered glaciers
iii. Snowmelt runoff
iv. Hydromet variables and transient snowline retreat
v. Relationships between topography, climate, snowmelt and runoff
vi. Rock avalanches on selected glaciers
vii. Dammed lake and its potential hazards in selected basins
viii. Effect of monsoon air-mass penetration in Upper Indus Basin
ix. Sediment yields of selected glaciers
x. Avalanches along with their hazards in snow basins

xi. Flow forecasting for Jhelum river basin using University of British Columbia (UBC) Watershed Model.

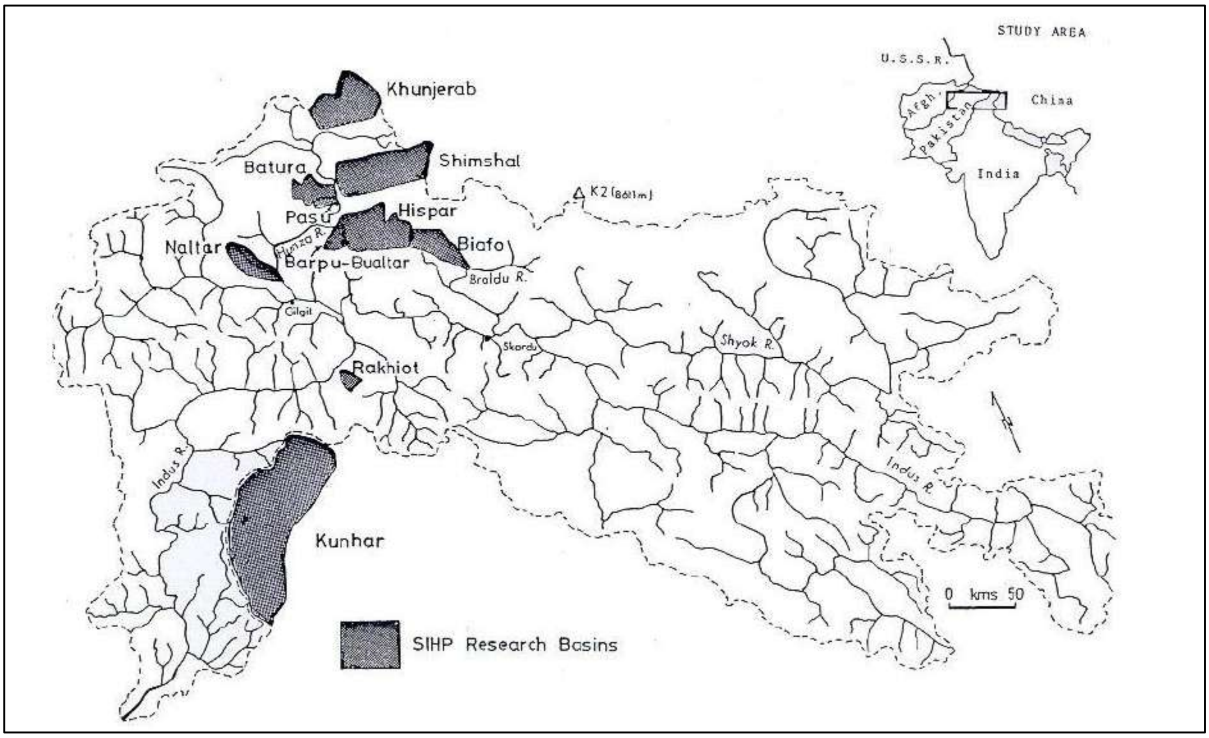

Figure 3-3: Pakistan Snow and Ice Hydrology Research Basins

Development of System - Phase-2 (Flow Forecasting System)

In the second phase of the PSIHP project (1989 to 1997), a system was setup for the collection of high altitude data and flow forecasting with the collaboration of IDRC Canada. Technical assistance was provided by the British Columbia Hydro International and University of British Columbia (UBC), Canada.

This phase aimed at producing forecasts for inflows to Mangla and Tarbela reservoirs and for Kabul river at Noshera on 10-day and seasonal basis. This data helps improving the operation of the two reservoirs for meeting the irrigation demands and optimizing the hydropower generation.

System for Collecting and Communicating the Remote Data

Twenty Data Collection Platforms (DCP) have been set up in the Upper Indus Basin located at elevations of 2 500 to 5 000 m asl., as shown on the map in Figure 3-4. The instruments/sensors are mounted over a 4.5 to 6.0 meter high steel tower. A snow pillow made of neoprene rubber (3.0 m diameter) is placed about 3 meters away from the tower.

A master station was set up at Badoki near Lahore, where the following hydro-meteorological parameters are transmitted from the field observation stations:

i) Temperature
ii) Precipitation
iii) Snow Water Equivalent
iv) Wind Speed

v) Wind Direction and
vi) Relative Humidity

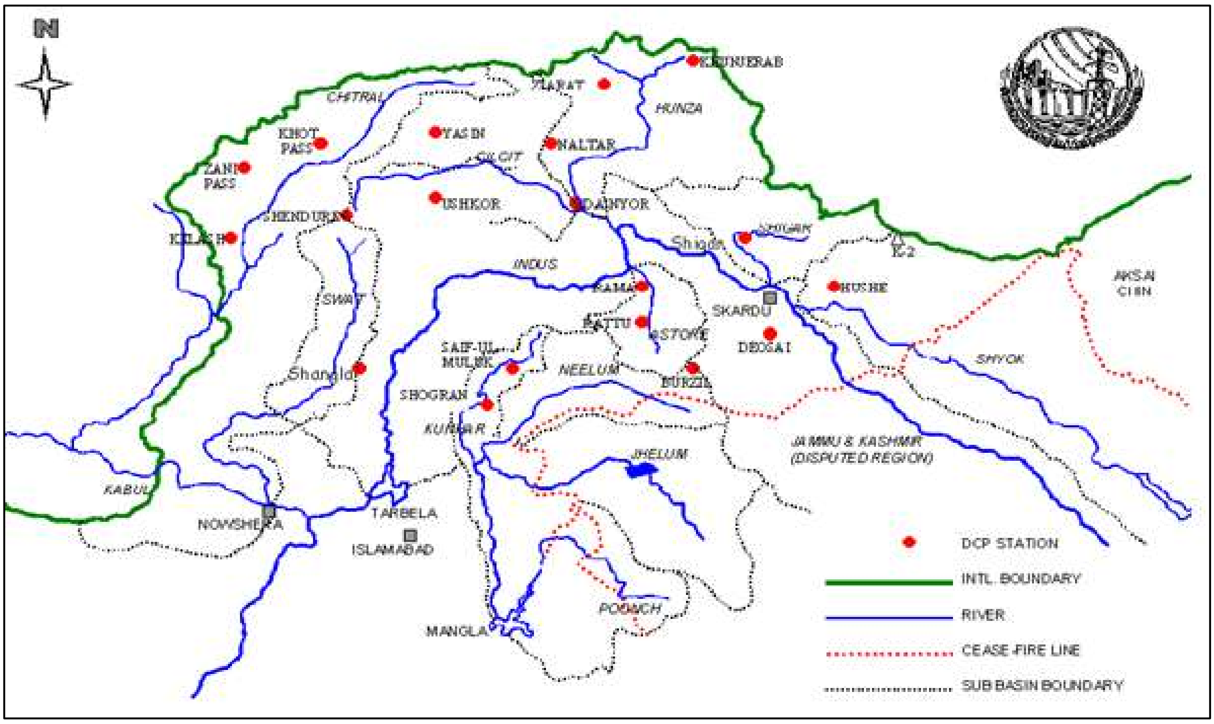

Figure 3-4: High - Altitude Weather Stations in the Upper Indus Basin

University of British Columbia's UBC Watershed Model

The UBC Watershed Model (UBCWM), developed by University of British Columbia, Canada is being used for the forecasting of flows in major reservoirs/rivers of the Indus basin. UBCWM is a hydrologic deterministic model designed primarily for mountainous watersheds, which calculates the total contribution from snow and glacial melt as well as rainfall runoff. The model can be used for the watersheds areas ranging from a few square kilometres to several thousand square kilometres.

Calibration of UBC Watershed Model

The UBCWM was calibrated for all the UIB catchments using 10 high elevation stations with coefficient of efficiency (monthly volume matching) and coefficient of determination (shape matching) of more than 85%.

Forecasting of Flows

For the forecasting of flows, the following inputs are given to the model:

- Physical Description of the Watersheds
- Hydrologic Features of the Watersheds
- Daily temperature data (max and min)
- Precipitation data

The historic data of observed mean daily river flows is also used for the comparison with results. For given continuous meteorological data, the model gives the outputs as listed below:

- Estimates of river flows
- Accumulation and depletion of snowpack
- Soil moisture budget
- Soil and groundwater storage values
- Contributions to runoff from various parts of watershed
- Surface and subsurface components of runoff

In Pakistan, the model is being used for the forecasting of flows at the following locations:

- River Indus at Tarbela
- River Jhelum at Mangla
- River Kabul at Noshera

The Flow forecast procedure includes the calibration, validation of the model on historic weather and flow data. The calibrated model is primed for the recent past (last season) available weather and flows. The primed model is tuned to develop a file for forecast. This forecast file is subjected to several weather patterns experienced by the basin in the past, thus generating several hydrographs corresponding to each weather pattern.

The output is in the form of hydrographs whose volumes are calculated and statistics such as probability of exceedance, 95% confidence limit on average and maximum, average and minimum is reported in the forecasting bulletin which also includes the historic average values and a comparison of forecasted and observed values.

3.5 HYDROMET MODEL BY PAKISTAN METEOROLOGICAL DEPARTMENT (PMD)

The Ministry of Science and Technology, through Pakistan Council of Research in Water Resources (PCRWR), conducted a study on “Forecasting of Seasonal and 10 Daily Inflows into Mangla Reservoir” in early 90’s. This model was based basically on study of meteorological systems developing in the region and estimation of rain/snow fall in the upper catchments of river Jhelum. Catchment of Jhelum River at Mangla dam is shown in Figure 3-5.

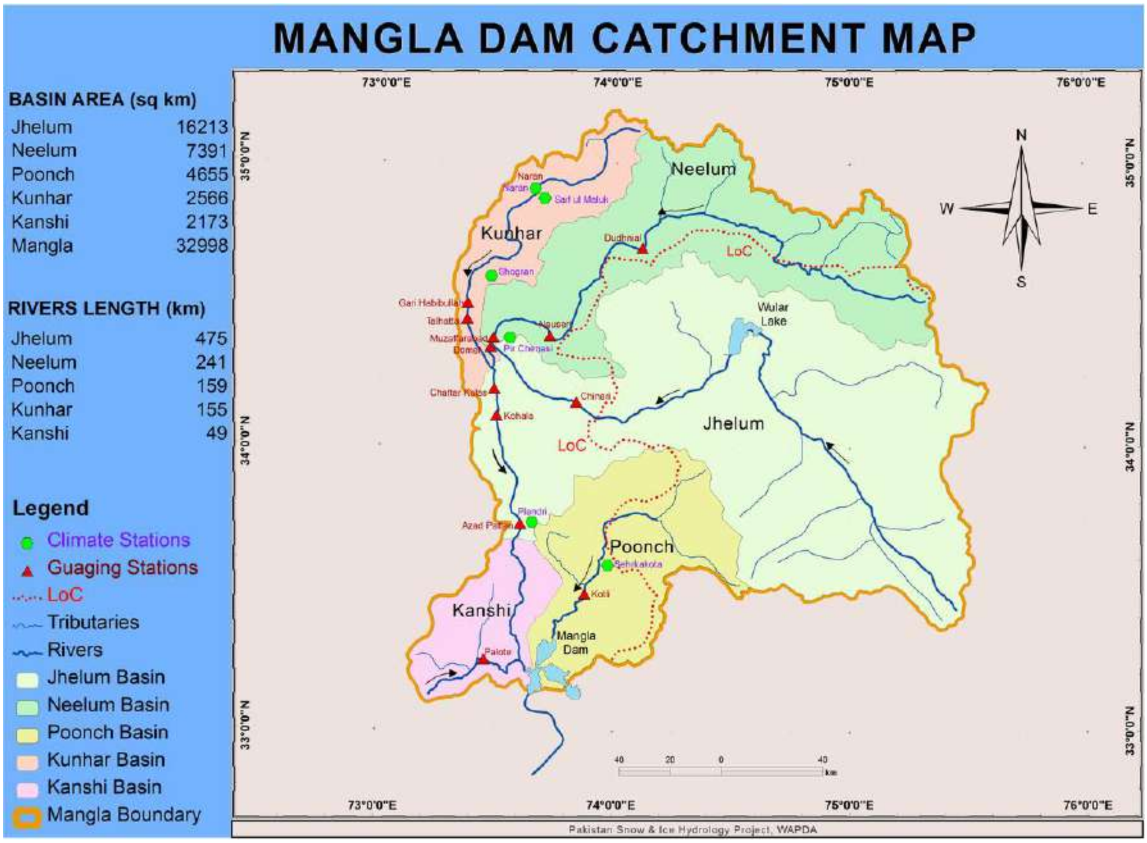

Figure 3-5: Mangla Catchment and Sub-Catchments

The basic source of runoff into Mangla reservoir is the precipitation, both as snow as well as rain. Snowmelt constitutes the base flow upon which the rainstorms create the surface runoff resulting in sharp fluctuations as short duration peaks.

The model gives two types of forecasts:

- The seasonal inflow forecast
- The 10-day inflow forecast

The salient hydro-meteorological characteristics of the catchment which provide basic infrastructure upon which the two forecasting procedures are based are given below.

- Extreme seasonal variability in precipitation occurs both in winter as well as in summer therefore the knowledge of available winter precipitation/snow pack is essential for a reasonable forecast
- The westerly waves responsible for deposition of snow during winter are more intense along the upper part of catchment, where they may continue depositing snow till as late as May
- The intensity and frequency of the westerly waves and thus the winter snowfall over the catchment can be indirectly inferred from the precipitation record of the meteorological stations within the catchment
- The thermal conditions can be adequately represented in terms of maximum temperatures recorded at the available meteorological stations
- The belt of maximum temperature shifts gradually northwards with the season and reaches the upper catchment of river Neelum during July and August

- During winter months the runoff is mostly due to the groundwater contribution and to some extent due to the snowmelt. The rainfall contribution is relatively insignificant, which is about 10 to 20% (which occasionally may reach to 35%).
- The contribution of snowmelt starts reducing by the middle of August and gets almost completely cut off by early October.
- Rainfall contribution is significant in Poonch and lower part of the Jhelum catchment which causes major peaks in to Mangla reservoir.
- The effect of rainfall is significant on 10-day forecast making the rainfall forecast a prerequisite to the hydrological forecast.
- Each 10-day period requires a unique and separate relationship due to temperatures and snowpack variability.

Seasonal Forecast

The historical data for the years 1976 to 1989 was used for the model formulation of the snowmelt component of the seasonal runoff. The model was tested for the years 1971 to 1975, 1990 and 1991.

Assessment of the model accuracy was done by computing the forecasts for all the years individually. The reported average error is less than 5%, while the error is less than 2% for the year 1971 and 1972. Only for the year 1975, the error was high (about 23%).

Ten Daily Forecast

The model formulation for 10-day forecast computation was based upon the data for the years 1980 to 1987. The data of 1988 to 1990 was used for the model validation. The reported error in the forecast in 64% of the cases is below 10% while overall it is within 25%.

3.6 FORECASTING BY WRMD OF WAPDA

The Water Resources Management Directorate (WRMD) of WAPDA applies a statistical approach to forecast the seasonal flows in to Tarbela, Mangla and Chashma reservoirs.

The historical data of Rabi (October to March) and Kharif (April to September) is used to carry out flow duration analysis. If the flows of Rabi season are to be forecasted, the flows of previous Kharif season are matched with the flow duration curve of historical Kharif flows. Then the flows of following Rabi season nearest to the historical flows are forecasted with confidence limits of 75% as maximum 85% as likely and 95% as minimum.

3.7 STATISTICAL FORECASTING BY IRSA

Indus River System Authority (IRSA) is also using a statistical approach in forecasting the inflows at rim stations. The seasonal forecasts are made for Jhelum river at Mangla and Indus river at Tarbela, 20-day in advance of the season. The forecasts are used to develop upper and lower operational rule curves at Mangla and Tarbela reservoirs. The reservoirs are operated keeping in view the water availability of the system and share of each province based on Water Apportionment Accord (1991).

IRSA uses 10-day inflow volume for 01-10 March of the Rabi season to forecast the subsequent Kharif (April-September) inflows. The observed inflows volume of 01-10 March is compared with the historic data for the same period. Matching years are identified having the similar inflow volume within a variation of ±5%. Kharif inflow volume of the matching years are averaged to estimate the expected Kharif volume. The estimated Kharif volume are looked into the probability tables of Kharif season, prepared by WAPDA using historic 10-day flow data, to find the most likely probability of estimated flows. ±10% of the most likely probability is used as the minimum and maximum probability of Kharif flows. Distribution of Kharif volume within the season is taken from the 10-day probability tables.

Rabi inflows are estimated similar to Kharif season by comparing the observed inflows from 01-10 September with the historic data for finding the matching years.

3.8 AVAILABLE SNOW & GLACIER MELT RUNOFF MODELS

A great number of snow and glacier melt runoff models have been developed in the last decades; some of them specially designed for nival and glacial flow regimes, some being minor components of broader hydrological precipitation-runoff modelling systems. The choice of a suitable model is a multi-criteria decision taking into account not only the accuracy of model results, but also the purpose of modelling, e.g. research, flood forecasting or water management, the availability of operation and calibration data as one of the a key constraints, as well as number of successful applications worldwide and existing experiences in the geographic region, and last but not least the terms of software licensing.

This chapter highlights just a brief introduction of models and SRM+G has been selected as an appropriate snow and glacier melt model for Upper Indus Basin.

SRM model can be run at variable spatial resolutions and temporal intervals. It uses the temperature index approach for producing the snowmelt runoff. It is a freeware software. The main reason for rejection of SRM is because it doesn't have any glacier melt component which is very important feature of model selection.

CREST model can be run at variable spatial resolutions and temporal intervals. It uses the energy balance approach for producing the snowmelt and glacialmelt runoff. It can run on the windows platform. It also provide the separate output in the form of snow, glacialmelt runoffs as well as rainfall runoff. It is a freeware. The main reason for not selecting the CREST model is because there is no online help available to use the model. Moreover, during the model running there were a lot of issues faced by the consultants. There is also another reason for rejection of CREST model as this model was applied only once for Hunza catchment and there are no results available for that.

TOPKAPI model can be run at variable spatial resolutions and temporal intervals. It uses the energy balance approach for producing the snowmelt and glacialmelt runoff. It can run on the windows platform. It also provides the separate output in the form of snow, glacialmelt runoffs as well as rainfall runoff. It is a licensed software. The main reason for not accepting the TOPKAPI model is because there were a lot of issues for preparing the model input data. It also uses a separate Map Window GIS programme which had caused problems during the input data preparation. Moreover during the model running there were issues faced by the consultants and to remove these errors took much time and to remove these errors may take longer time. Hence, the model was not selected for the modelling purposes.

SRM+G model was developed by the Consultants using the open source code/equations of SRM. The SRM+G is a customised application for snow runoff + glacier modelling of upper Indus Basin. The model can be run at variable spatial resolutions and temporal intervals. It uses the temperature index approach for producing the snowmelt and glacialmelt runoff. It can run on the windows platform. It also provide the separate output in the form of snow, glacialmelt runoffs as well as rainfall runoff.

Weighting carefully all the aspect of the above discussion, SRM+G was finalized as the best choice of an operational flow forecasting model for the Upper Indus Basin (UIB). SRM+G completely takes into account of both snow and glacial melt components. It fulfils the model selection criteria defined by the consultants.

3.9 FLOW FORECASTING PROCEDURES FOR UPPER INDUS BASIN

3.9.1 Introduction

The methodology of flow forecasting is very closely related to the snowmelt runoff model being used, as data requirements, data preparation, and the post-processing of simulation results are defined by the model approach and its implementation in the computer program. The following sections present a focused review of the approach, important features, operation and application of the Snow & Glacier Runoff Model to real time flow forecasts as presented in the WinSRM User's Manual (Martinec et al. 2008).

3.9.2 General Characteristics of the Snow & Glacier melt Runoff Model

The Snow & Glacier Runoff Model (SRM+G) was designed to simulate and forecast daily stream flow in mountain basins where snowmelt and glacialmelt is a major runoff factor.

This model is a further development of the snowmelt runoff model (SRM) and can calculate the glacial melt (G) as well. The model works with the remote sensing derived daily snow and glacier cover areas, temperature and precipitation measurements and a set of 10 physically derived parameters. The model is tested in several basins and found high accuracy even in basins with 67% glacier areas on three alpine basins Rhine-Felsberg, Rhône-Sion and Ticino-Bellinzona in Switzerland (K. Seidel et al., 2001). The accuracy of runoff modelling in high alpine basins is considerably improved by evaluating separately the snow coverage over glaciers and over glacier-free areas of each elevation zone. This approach takes into account the specific melt factors of glacier and the actual elevation of glaciers within the respective elevation zones. Following a test in a small experimental basin (K. Seidel et al., 1999), the paper demonstrates that the method can be applied in basins of several thousand km. Apart from the improvement of the runoff modelling, the independent computation of glacier melt is an important step towards evaluations of glacier behaviour with regard to global warming.

3.9.3 Range of Conditions for Model Application

SRM+G can be used for the following purposes:

i) Simulation of daily flows in a snowmelt season, in a year, or in a sequence of years

The results can be compared with the measured runoff in order to assess the performance of the model and to verify the values of the model parameters. Simulations can also serve to evaluate runoff patterns in un-gauged basins using satellite monitoring of snow covered areas and extrapolation of temperatures and precipitation from nearby stations.

ii) Short term and seasonal runoff forecasts

The computer program WinSRM+G includes a derivation of modified depletion curves which relate the snow covered areas to the cumulative snowmelt depths as computed by SRM. These curves enable the snow coverage to be extrapolated manually by the user several days ahead by temperature forecasts so that this input variable is available for discharge forecasts. The modified depletion curves can also be used to evaluate the snow reserves for seasonal runoff forecasts. The model performance may deteriorate if the forecasted air temperature and precipitation deviate from the observed values, but the inaccuracies can be reduced by periodic updating.

3.10 MODEL STRUCTURE

Each day, the water produced from snowmelt, glacialmelt and from rainfall is computed, superimposed on the calculated recession flow and transformed into daily discharge from the basin according to the Equation given below:

$$Q_{n+1} = Q_n k_{n+1} + (1 - k_{n+1}) \, . \sum_{i=1}^{n} \left(\mathrm{Q_{rain,n,i}} + \mathrm{Q_{newsnow,n,i}} + \mathrm{Q_{snowmelt,n,i}} + \mathrm{Q_{glaciermelt,n,i}}\right)$$

$$Q_{rain,n,i} = A_{total,i}\ c_r\ P_r\ \left(\frac{10000}{86400}\right)$$

$$Q_{newsnow,n,i} = A_{total,i}\ c_s\ a_{n,i}\ T_i(1 - S_{total,i})\left(\frac{10000}{86400}\right)$$

$$Q_{snowmelt,n,i} = A_{nogal,i}\ c_s\ a_{n,i}\ T_i(S_{nogla,i}) + A_{gl,i}\ C_s\ a_{n,i}\ T_i(S_{gl,i})\left(\frac{10000}{86400}\right)$$

$$Q_{glaciermelt,n,i} = A_{gla,i}\ c_{gl}\ a_{n,i}\ T_i(1 - S_{gla,i})\ \left(\frac{10000}{86400}\right)$$

$$\mathrm{k_{n+1}} = x.(Q_n)^{-y}$$

Where,

- Q = average daily discharge [m^3/s]
- c = runoff coefficient expressing the losses as a ratio (runoff/precipitation), with c_s & c_g referring to snowmelt and glacial melt, and c_R to rain
- a = degree-day factor [cm/°C/d] indicating the melt depth resulting from 1 degree-day
- a_s = Degree-day factor for snow [cm $°C^{-1}$ d^{-1}]
- a_g = Degree-day factor for glacier [cm $°C^{-1}$ d^{-1}]
- T = number of degree-days [°C d]
- ΔT = the adjustment by temperature lapse rate when extrapolating the temperature from the station to the average hypsometric elevation of the basin or zone [°C d]

S = ratio of the snow covered area to the total area

S_{gla} = ratio of the glacier exposed area to the total area

P = Precipitation contributing to runoff [cm]. A preselected threshold temperature, T_{Crit}, determines whether this contribution is rainfall and immediate. If precipitation is determined by T_{Crit} to be new snow, it is kept on storage over the hitherto snow free area until melting conditions occur.

A_{total} = Total area of the catchment or zone [km^2]

A_{gla} = Glacier exposed area or zone [km^2]

A_{nogla} = Snow covered area or zone [km^2]

k = recession coefficient indicating the decline of discharge in a period without snowmelt, glacial melt or rainfall

n = sequence of days during the discharge computation period. Above equation is written for a time lag between the daily temperature cycle and the resulting discharge cycle of 18 hours. In this case, the number of degree-days measured on the nth day corresponds to the discharge on the n + 1 day. Various lag times can be introduced by a subroutine.

$\frac{10000}{86400}$ = conversion from [cm·km^2/d] to [m^3/s]

T, S and P are variables to be measured or determined each day, c_S, c_g , c_R, lapse rate to determine ΔT, T_{Crit}, k and the lag time are parameters which are characteristic for a given catchment or, more generally, for a given climate. If the elevation range of the basin exceeds 500 m, it is recommended that the basin be subdivided into elevation zones of about 500 m each. The glacier melt supply a higher amount of melt water, if the temperature keeps rising.

3.11 MODEL APPLICATIONS FOR REAL TIME FORECASTS

In order to be applied for real-time discharge forecasts, a model should be able to simulate the runoff not only in selected test basins with good data but also in basins where such forecasts are required by the user. SRM+G has relatively modest requirements as that of SRM for input variables (temperature, precipitation, and snow covered area) with an additional glacier feature and therefore, it was easily possible to shift the runoff simulations to the basins delivering water for various purposes.

SRM+G can be used for short term (for example weekly) forecasts of daily flows as well as for longer time period forecasts such as monthly runoff volumes or seasonal runoff volumes. For short term forecasts, temperature, precipitation and snow covered area must be forecasted or predetermined for the coming days and entered into the model. From the extrapolation of SCA, the glacier exposed area will be forecasted. Temperature and even precipitation forecasts are becoming increasingly available from meteorological services, but the snow covered areas must be extrapolated by the model user. The forecasts of input variables are still an important challenge for all snow and glacier runoff models. The model simulations for the catchments of hydroelectric stations Sedrun and Tavanasa are shown in Figure 3-6 and Figure 3-7, respectively.

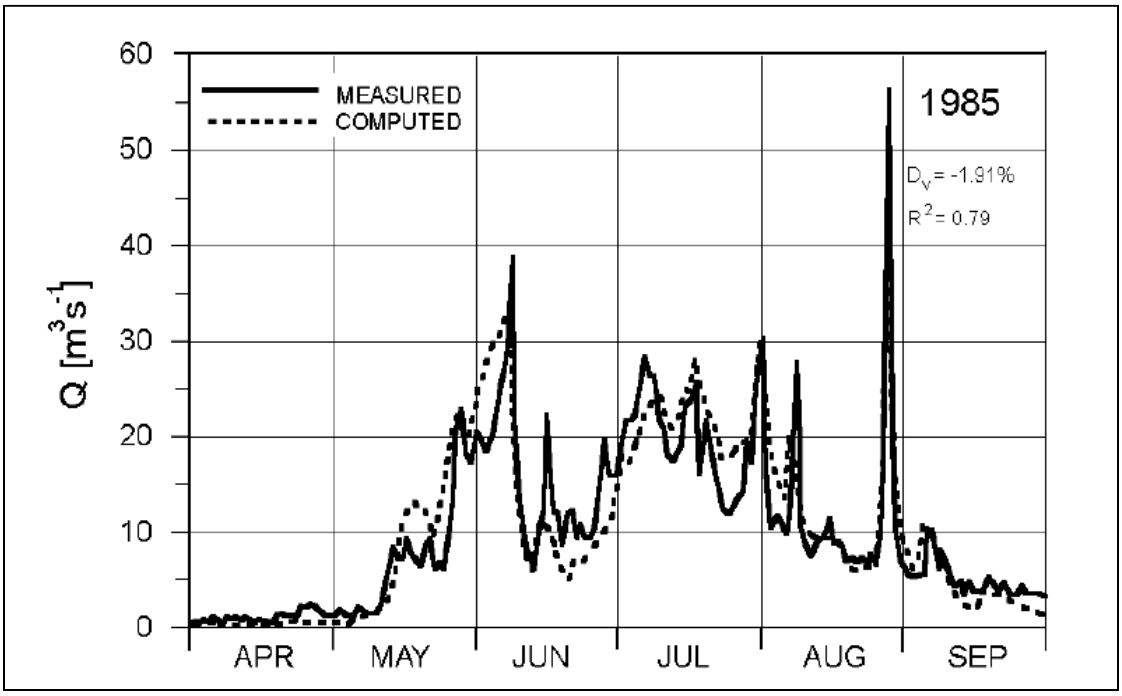

Figure 3-6: Runoff Simulation in the Catchment Area of the Hydroelectric Station Sedrun
Swiss Alps, 108 km^2, 1 840 - 3 210 m asl. (Baumann et al. 1990 in: Martinec et al. 2008)

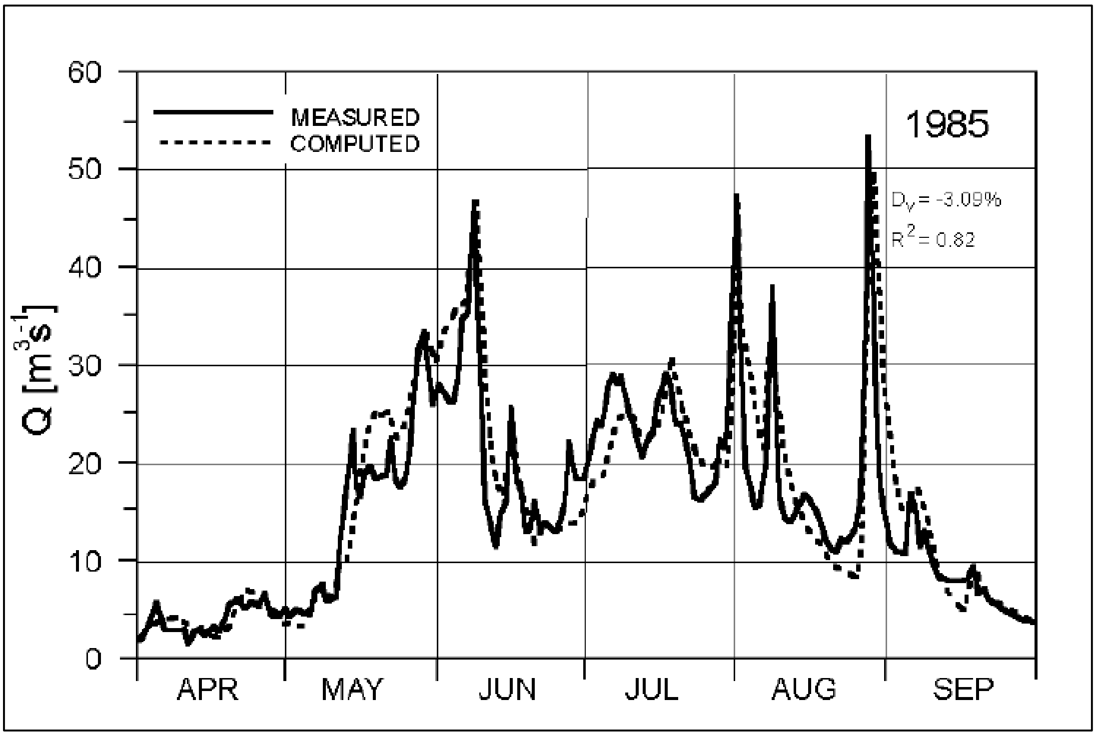

Figure 3-7: Runoff Simulation in the Catchment Area of the Hydroelectric Station Tavanasa
Swiss Alps, 215 km^2, 1 277 - 3 210 m asl. (Baumann et al. 1990 in: Martinec et al. 2008)

3.11.1 Extrapolation of Snow Coverage

The future course of the depletion curves of the snow coverage can be evaluated from the so-called modified depletion curves (MDC). These curves are automatically derived by SRM+G from the conventional curves (CDC) by replacing the time scale with cumulative daily snowmelt depths as computed by the model. Consequently, if SRM+G is run in a whole hydrological year, the derivation of MDC from CDC starts with the summer half year and not earlier. The decline of the modified depletion curves depend on the initial accumulation of snow and not on the climatic conditions, as is the case with the conventional depletion curve. The computer program also provides an option for plotting a modified depletion curve in which the totalized melt depth includes new snow that falls occasionally during the snowmelt period.

3.11.2 Extrapolation of Glacier Exposed Area

The future course of the depletion curves of the glacier coverage can be evaluated from the MDC as developed in extrapolation of snow coverage. These exposed areas are then entered in the model to incorporate the glacier melt expected in the season. The computer program also provides an option for plotting a modified depletion curve for glacier.

Static glacier map of 2013 was used for the interpretation of glacier exposed area but it is recommended to update glacier map every 5 years.

3.11.3 Periodic Updating

The model performance in the forecasting mode is naturally affected by the reduced accuracy and reliability of temperature and precipitation forecasts. The propagation of errors can be avoided by periodical updating. The updating can be divided into 3 categories:

i. Updating the computed discharge by the measured discharge when it becomes known, i.e. checking with the measured discharge to avoid carry-over of errors when the next forecast is issued.
ii. Adjustment of model parameters in the process of forecast.
iii. Correction of temperature, precipitation, snow cover and glacier exposed forecasts according to actual observations.

The computed discharge can be replaced every 1 - 9 days by the measured discharge which becomes known for the corresponding day so that each subsequent forecast period is computed by using a correct discharge value.

Figure 3-8 (a) shows a model runoff simulation starting with computed discharge of only one half of the correct value. Updating by actual discharge improves the simulation as shown in Figure 3-8 (b) Even without updating, however, the initial discrepancy is soon eliminated automatically.

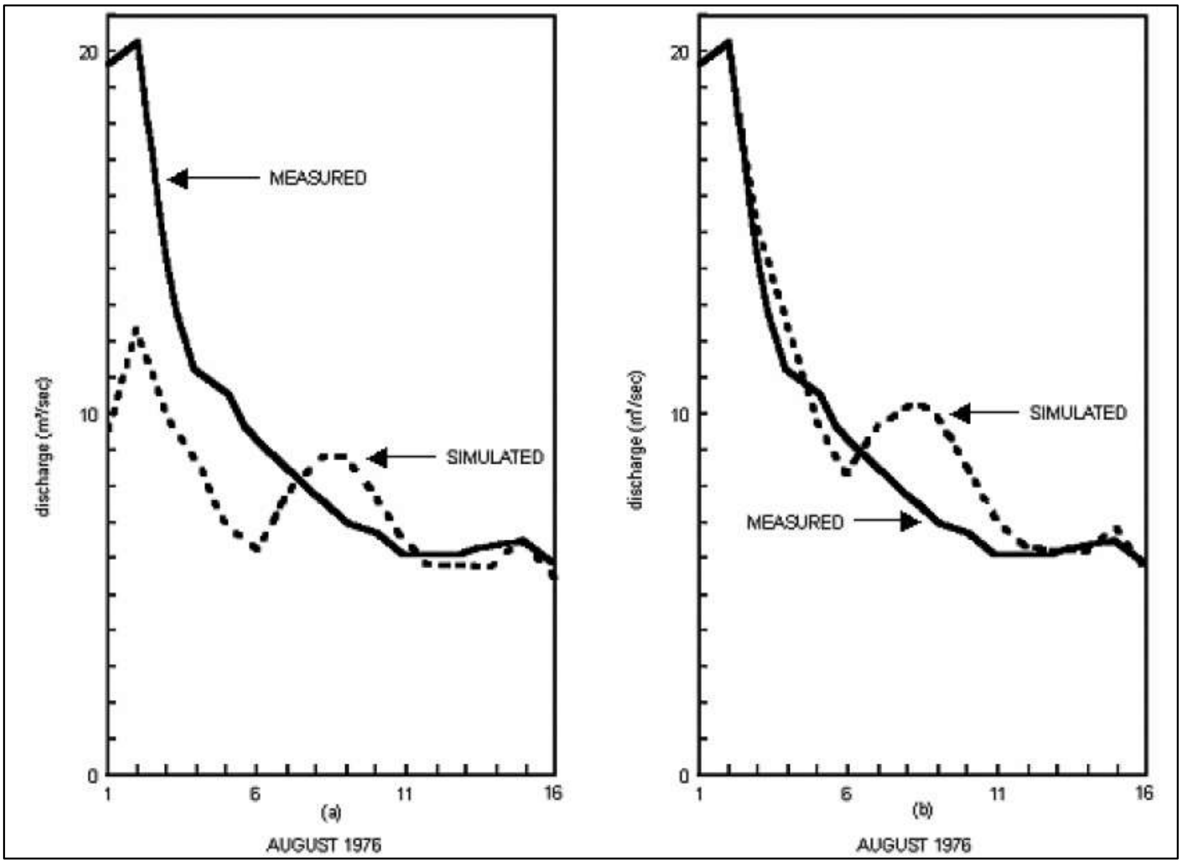

Figure 3-8: Discharge Simulation in the Dinwoody Creek Basin

Wyoming, 228 km^2, 1 981 - 4 202 m asl.,

(a) without updating, and **(b)** with updating by actual discharge on 1 August

3.11.4 Seasonal Forecasts

As seasonal[11] meteorological forecasts still only give a rough indication of "warmer" or "cooler" respectively "drier" or "wetter" compared to the average conditions, for the Kharif season flow volume forecasts a scenario approach will be used. This forecast will be issued by the end of March each year. At that date, the snow-covered area, temperature and precipitation for the following[6] Kharif month April – September have to be forecasted.

In order to predict at the end of March, the depletion of the snow-covered area in each elevation zone of the catchment in the following 6 month, SRM+G's "Modified Depletion Curve" approach will be applied. The observed snow-cover depletion in relation to the minimal and maximal historical depletion at the actual number of degree-days of this key zone will be applied as the characteristic depletion curve for all zones in that specific year.

3.11.5 Scenario Approach

The scenario approach for 10-day flow forecasts is very much similar to the methodology used for the seasonal forecasts. In order to forecast the daily flows for example during the period July-III 2014, separate simulation runs have been carried out with temperature and precipitation data of the same period July-III of each scenario year[12].

[11] Falls into the meteorological classification "long-range"

[12] At present the years 2003 – 2012

The only difference to seasonal forecasts is the prediction of the snow-covered area during the 10-days forecast period. While seasonal forecasts use one single “key zone” for all elevation zones, for 10-day forecasts an individual Modified Depletion Curve is determined for each elevation zone based on its actual snow-cover depletion at the beginning of every forecast period .In addition, the start of the degree-day factor function increase is determined by the actual 10-day average temperature for each individual zone.

3.12 SOFTWARE ENVIRONMENT AND INPUT DATA PREPARATION

The present version of WinSRM uses MS-Access database objects for storage and manipulation of variables, parameters and simulation results. As a consequence of the daily based database structure, all parameters are stored in daily records. Although WinSRM provides some tools for multiple days edits, data manipulation for weekly or 10-day periods is quite tiresome especially as it has to be done for all elevation zones separately. A direct manipulation in the MS-Access database file is also not convenient, as it requires specific database queries and permanent opening/closing of WinSRM and MS-Access. Thus, WinSRM is not particularly suited for parameter calibration which requires a frequent change of parameters and an immediate comparison of its effects.

In order to facilitate parameter calibration, MS-Excel implementation of the governing equation used in the Snowmelt + Glacier Runoff Model has been developed. The graphical User Interface (GUI) of Excel SRM+G is shown in Figure 3-9. As a major feature, the set of crucial parameters can be defined for arbitrary time periods. All parameters are applied basin-wide, while variables like temperature, snow-covered area, glacier exposed area and precipitation are given zone-wise. Special features of SRM+G like the handling of new snow[13] and glacier melt or the adjustment of the recession coefficient for heavy rainfall[14] were realised by VBA functions.

3.13 DATA PREPARATION

3.13.1 Data Acquisition

SRM is a model which uses observed data (like precipitation) called “variables” and model parameters (like runoff coefficients).

The observed data which have to be acquired are:

- Terrain elevation (time independent)
- Snow cover (daily snapshot)
- Precipitation (daily total)
- Temperature (daily mean)
- Discharges (for comparison only)

The ultimate purpose of SRM+G is to forecast flows for the coming snow-melt and glacialmelt season i.e. months March to July. It appears logical, that the same data sources should be used both for the ongoing season (for which flow forecast estimates are to be calculated) and the historical years for which the model parameters were obtained through calibration.

[13] SRM User’s Manual Chap. 5.2.2
[14] SRM User’s Manual Chap. 5.3.6.1

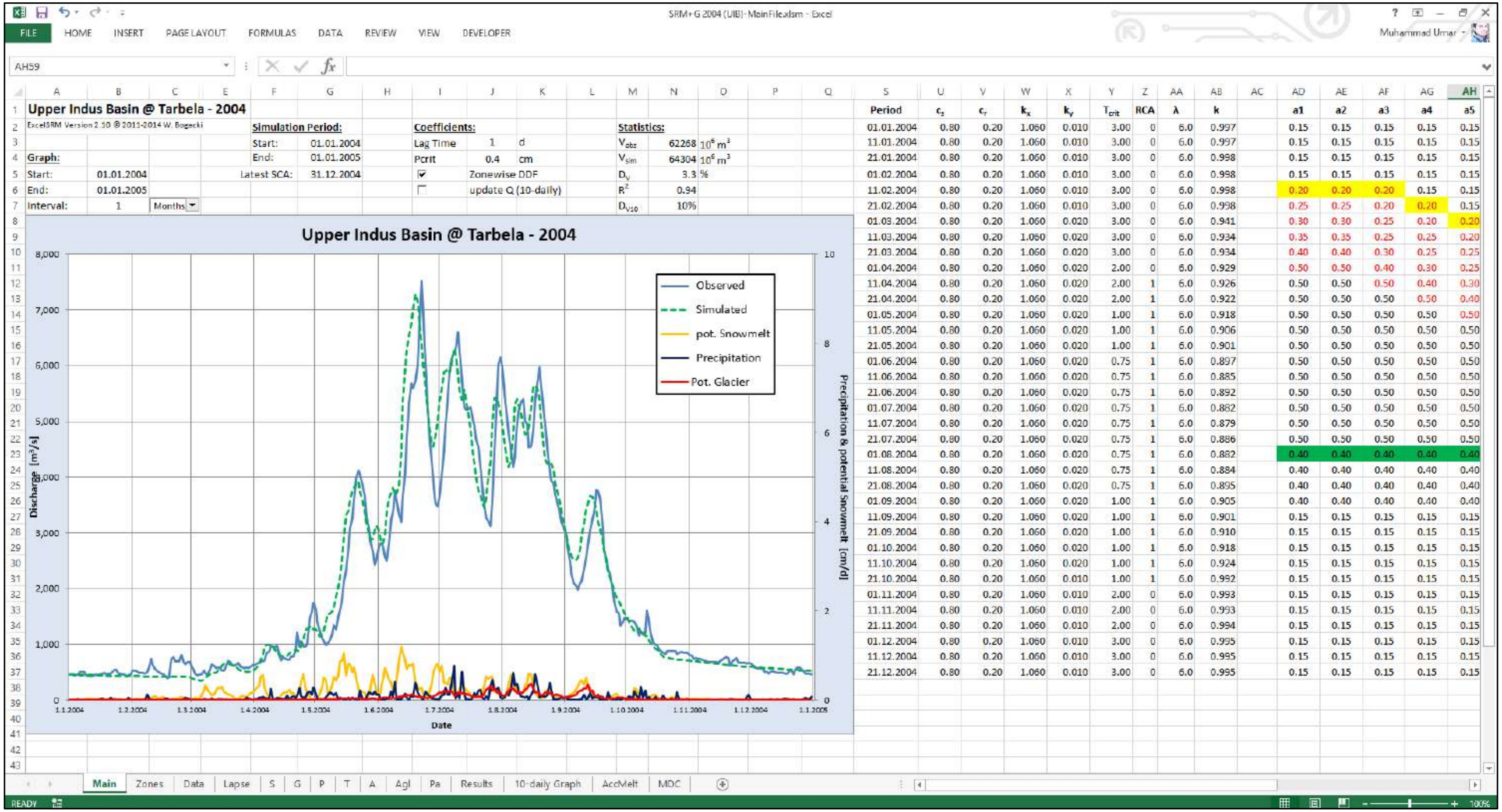

Figure 3-9: Excel SRM+G Graphical User Interface

Processed satellite data on snow cover become usually available with a delay of 2 to 3 days after original recording. This sets the standard for other data: they should also be available preferably within 3 days. For precipitation and temperature data suitable and freely available online data sources from NOAA (USA National Oceanic and Atmospheric Administration) were found and will be used. For discharges, Mangla inflow data, available to SIHP on daily basis is utilised.

All data sources identified above are in general accessible through the internet at all times. At some occasions however, it was found that the server was down one or two days for maintenance or internet access was limited. In order to have the most actual data available when issuing seasonal or 10-day flow forecasts, it is highly recommended to download all operational data i.e., snow cover, temperature and precipitation on a daily basis.

3.13.2 Digital Elevation Model

A digital elevation model is necessary to calculate catchment and sub-catchment boundaries and to construct the different elevation zones which the SRM+G is using. The extent of SRTM tiles for the UIB is shown in Figure 3-10.

While now a days, elevation data with 1 arc-second resolution (~ 30m) are available from Aster, the SRTM data with 3 arc-second resolution (~ 90m) have proved to have less errors ("Comparison and validation of recent DEMs over Australia", C. Hirt, M.S. Filmer and W.E. Featherstone, *www.cage.curtin.edu.au/~will/final_AJES_DEM_v15012010.pdf*). As with all other RS-based elevation models, the elevation is an average over the cell extends and relates not necessarily to the ground surface but may be affected by buildings or vegetation. While originally obtained in year 2002, the quality of the original data has been continuously improved. The Project uses data version 4.1.

Data citation: "Jarvis A., H.I. Reuter, A. Nelson, E. Guevara, 2008, Hole-filled seamless SRTM data V4, International Centre for Tropical Agriculture (CIAT), available from http://srtm.csi.cgiar.org."

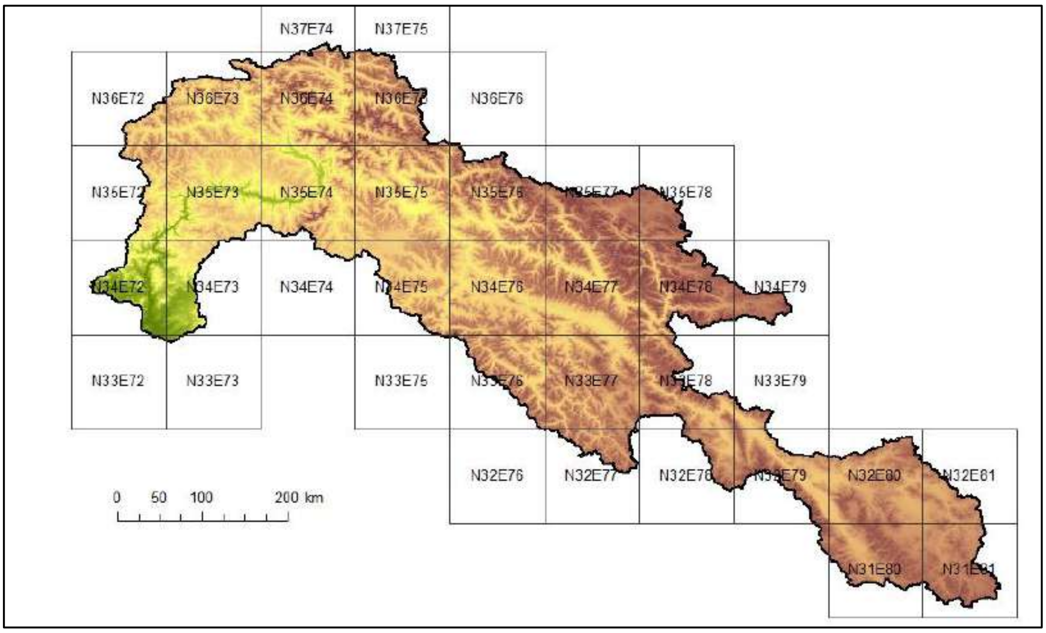

Figure 3-10: Extents of SRTM Tiles Required for Upper Indus Basin

3.13.3 Snow Cover

Daily snow cover can be obtained from MODIS (Moderate-resolution Imaging Spectroradiometer). There are two satellites equipped with these sensors, Aqua and Terra, which pass at different times of the day. Furthermore, there are different data products available, like values for individual bands, data on geolocation etc. The Project uses readily processed data by the "MODIS Snow & Sea Ice Global Mapping Project" of NASA (http://modis-snow-ice.gsfc.nasa.gov), where the geo-correction and classification has already been made.

The MODIS snow cover image is a coded raster. Those coded integer values include
- 0 (sensor data missing),
- 1 (no decision),
- 11 (darkness, terminator or polar),
- 25 (land-no snow detected),
- 37 (inland water),
- 39 (ocean),
- 50 (cloud),
- 100 (snow-covered lake ice),
- 200 (snow),
- 254 (saturated MODIS sensor detector), and
- 255 (fill ? no data expected for pixel)

(Riggs et al., 2006).

The spatial resolution (cell size) is about 500m. Both daily products (MOD10A1 for Terra respectively MYD10A1 for Aqua) and 8-days maximum products (MOD10A2 respectively MYD10A2) can be downloaded free of charge from NASA.

After a comparison of the daily and the 8-day maximum products, the daily products were chosen. The reasons were: faster availability and better suitability for automated removal of clouds and other data errors. The Project developed a script for automated download of data products obtained from the Terra satellite from the following FTP-Site: ftp://n5eil01u.ecs.nsidc.org/SAN/MOST/MOD10A1.005/

The last directory is date in yyyy.mm.dd

The following file naming convention (Table 3-1) is common to all Level 3 MODIS Land products: MOD10A1.A2003138.h24v05.005.2006.143062148.hdf

Table 3-1: Variable Explanation for MODIS File Naming Convention

Variable	Explanation
MOD	MODIS/Terra
10A1	Type of product
A	Acquisition date
2003	Year of data acquisition
138	Day of year of data acquisition (In this case, day 138)
h23v05 h24v05 h25v05	Horizontal tile number and vertical tile number (tile relevant for UIB)
005	Version number
2006	Year of production (2006)
143	Day of year of production (Day 143)
062148	Hour/minute/second of production in Greenwich Mean Time (GMT) (06:21:48)
hdf	HDF-EOS data format

The files are in compressed HDF-EOS format, their size varies between 0.5 and 2.5 MB. Three (3) tiles (Figure 3-11) were mosaiked to cover the whole UIB.

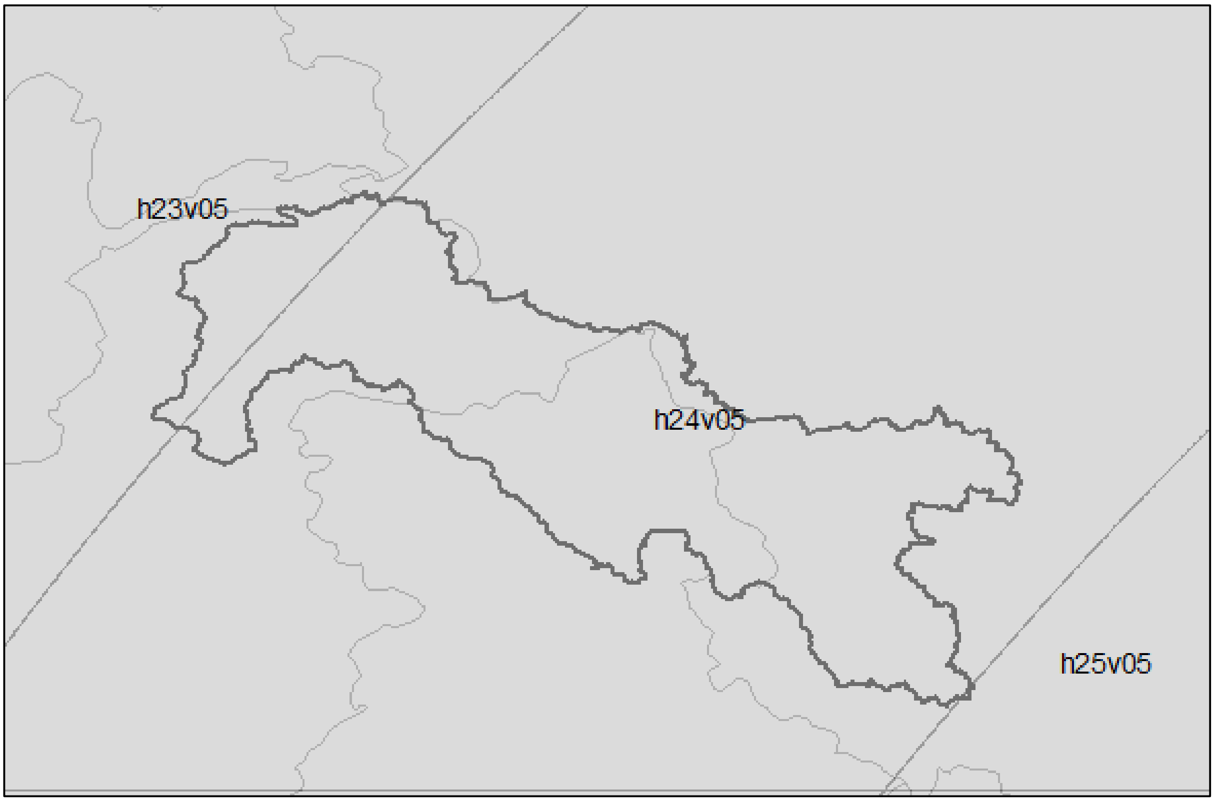

Figure 3-11: Three (3) HDF Tiles Mosaiked to Cover UIB

3.13.4 Glacier Exposed Area

Existing data on global glacier distribution are limited to those from the GLIMS data archive. A major source for their interpretation (GLIMS) is visually interpreted aerial photographs, giving a detailed view on spatial glacier distribution. Though highly accurate in spatial detail, existing GLIMS interpretations do not provide a complete coverage of the UIB that is needed for modelling purposes.

Necessary information on glaciers therefore was interpreted from Landsat8 images of the year 2013. With 30m spatial resolution the spatial accuracy of Landsat data is certainly less, but from its data a continuous map with glacier coverage could be created that is spatially comparable. Also, at an envisaged spatial modelling resolution of 1000m, the difference in spatial detail is insignificant.

For a full coverage of the UIB, a total of 19 Landsat8 scenes were interpreted as shown in Figure 3-12. Since snow and glaciers display similar spectral characteristics in satellite acquired multispectral images, only scenes acquired during late summer to early fall were processed and interpreted. This assumes that the snow pack accumulated during the previous winter, has completely melted or whatever of it is left can be considered as permanent snow.

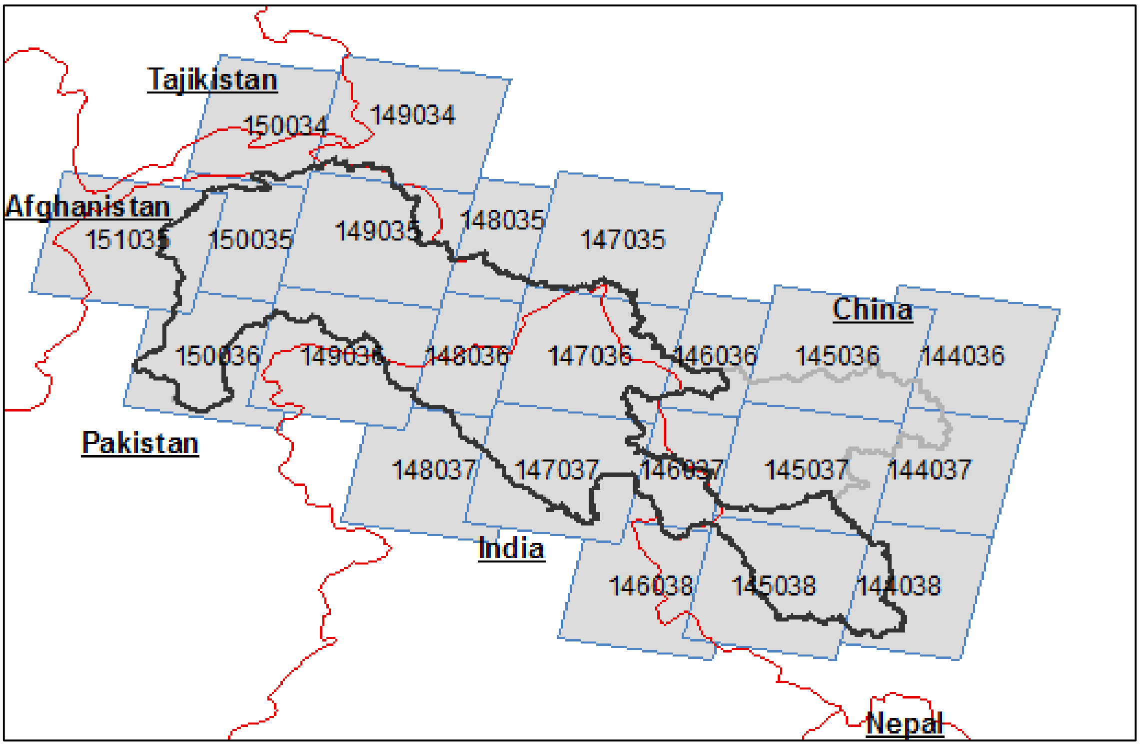

Figure 3-12: Landsat 8 Coverage of the UIB and the Pangong Tso Watershed (grey-coloured)

To avoid misinterpretations due to cloud coverage, only data with less than 10% clouds were used. In the few cases where clouds still obscured glaciers, gaps were filled through interpolation from neighbouring areas. Areas affected were exclusively located along the little glaciated south-eastern UIB watershed boundary (scene p148 r036). Processed Landsat scenes are given in Table 3-2.

Table 3-2: Processed Landsat Scenes

No	Path/Row	Acquis. date	Scene Id	No	Path/Row	Acquis. date	Scene Id
1	144/36	2013-07-02	LC81440362013215LGN00	12	147/37	2013-06-21	LC81470372013300LGN00
2	144/37	2013-07-02	LC81440372013199LGN00	13	148/35	2013-07-14	LC81480352013211LGN00
3	144/38	2013-07-02	LC81440382013247LGN00	14	148/36	2013-07-14	LC81480362013195LGN00
4	145/36	2013-07-09	LC81450362013270LGN00	15	148/37	2013-07-14	
5	145/37	2013-07-09	LC81450372013270LGN00	16	149/34	2013-06-19	LC81490342013282LGN00
6	145/38	2013-07-09	LC81450382013270LGN00	17	149/35	2013-06-19	LC81490352013282LGN00
7	146/36	2013-06-30	LC81460362013261LGN00	18	149/36	2013-06-19	LC81490362013282LGN00
8	146/37	2013-06-30	LC81460372013261LGN00	19	150/34	2013-06-10	LC81500342013209LGN00
9	146/38	2013-06-30	LC81460382013261LGN00	20	150/35	2013-06-10	LC81500352013209LGN00
10	147/35	2013-06-21	LC81470352013268LGN00	21	150/36	2013-06-10	LC81500362013289LGN00
11	147/36	2013-06-21	LC81470362013268LGN00	22	151/34	2013-06-01	LC81510342013280LGN00

This data sets provides the information on glacier exposed area when snow cover is depleted and is used by the model.

3.13.5 Precipitation

Precipitation records measured at rain-gauge stations were not used in the preparation of model inputs as these stations are too widely spaced to reliably describe precipitation characteristics. Station records were only used for verifying precipitation data produced from satellite measurements (RFE product).

Rainfall estimates (RFE) prepared from different satellite acquired data is used in hydrological model. RFE data are only available starting from 2003, setting further limits to the temporal coverage of calibration runs.

Monthly averages shown in Figure 3-13, visualize the different climate patterns influencing the different parts of the UIB at different times. The westerlies primarily influence the Western and the Northern UIB during January to March but bring little moisture to other parts of the UIB. The summer monsoon (July, August) has a stronger impact on the Eastern, but only bringing little moisture to the Eastern UIB.

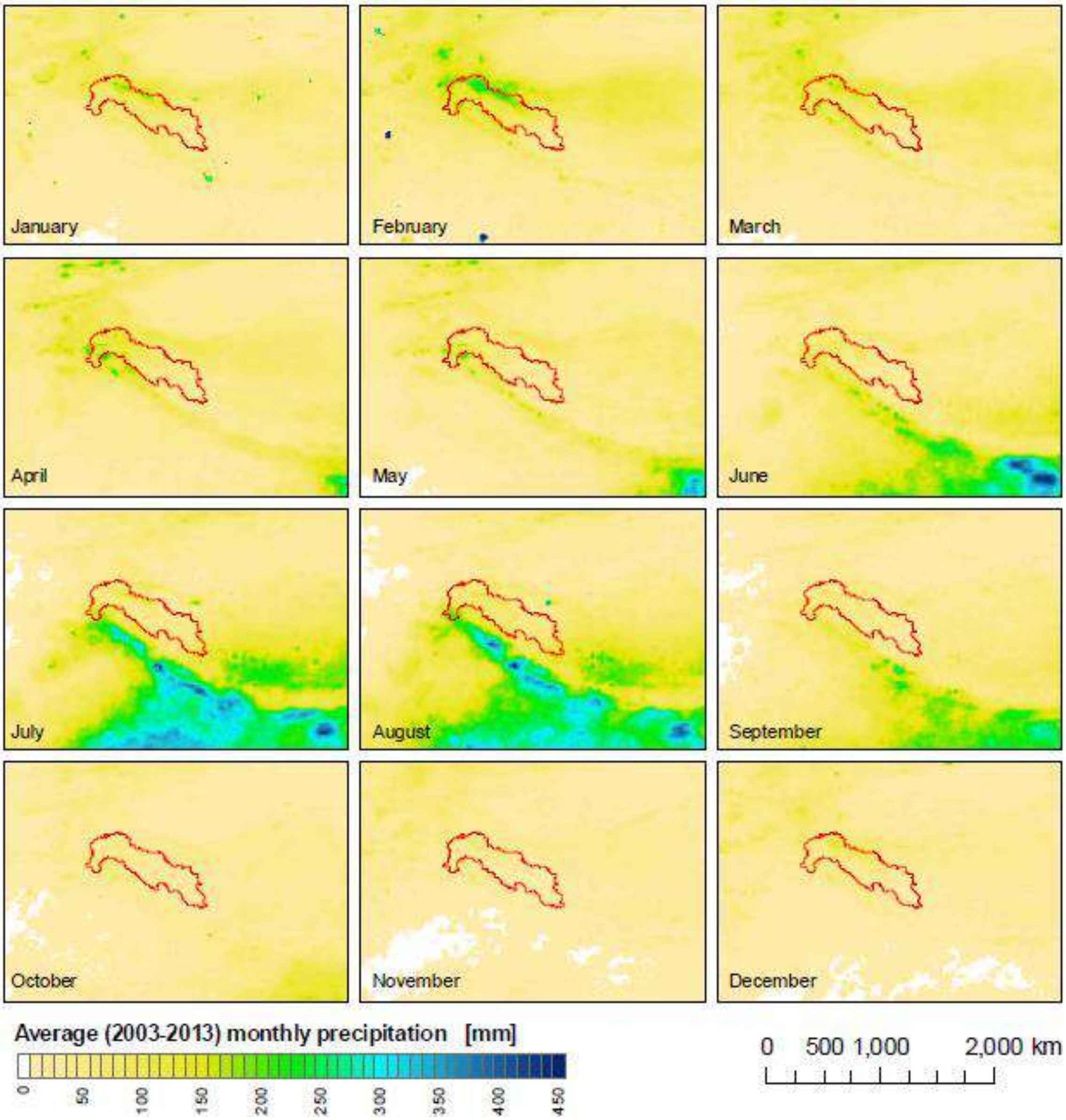

Figure 3-13: Average Monthly Precipitation (2003-2013), Daily Meteosat Data (RFE Data)

3.13.6 Temperatures

Daily temperature data is an important climatic variable used by SRM+G, it is needed to decide if precipitation falls as snow or as rain and also to simulate the melting process. Twenty-two (22) stations are found, out of which eight (8) stations are operated by Pakistan Meteorological Department (PMD) and fourteen (14) maintained by Pakistan Snow and Ice Hydrology Project (PSIHP), WAPDA (see Table 3-3). A geostatistical method (Kriging) was applied for regionalization of temperature values observed at the stations, and through masking daily average temperatures were obtained for each elevation zone and used as an input to SRM+G. Figure 3-14 shows the comparison of temperature data from the different stations.

Table 3-3: Meteorological Stations used in UIB

Station	***Lat.***	***Long.***	***Altitude***	***Station***	***Lat.***	***Long.***	***Altitude***
Pakistan Meteorological Department (PMD)				**Pakistan Snow & Ice Hydrology Project (PSIHP)**			
SKARDU	35.30	75.68	2317	KHUNJRAB	35.84	75.42	4730
ASTORE	35.33	74.90	2168	BURZIL	34.90	75.17	4310
GUPIS	36.17	73.40	2156	DEOSAI	35.09	75.54	4240
HUNZA	36.32	74.65	2156	ZIARAT	36.22	74.43	3669
GILGIT	35.92	74.33	1460	SHENDURE	36.09	72.55	3560
BUNJI	35.67	74.63	1372	RAMA	35.36	74.81	3344
CHILAS	35.42	74.10	1250	HUSHEY	35.42	76.35	3245
BABUSAR	35.15	74.05	4160	YASIN	36.45	73.30	3150
				NALTAR	36.17	74.18	3075
				USHKORE	36.05	73.40	2970
				RATTU	35.15	74.80	2920
				SHIGAR	35.63	75.53	2560
				SHANGLA	34.88	72.59	2160
				DAINYOR (GILGIT)	35.93	74.37	1550

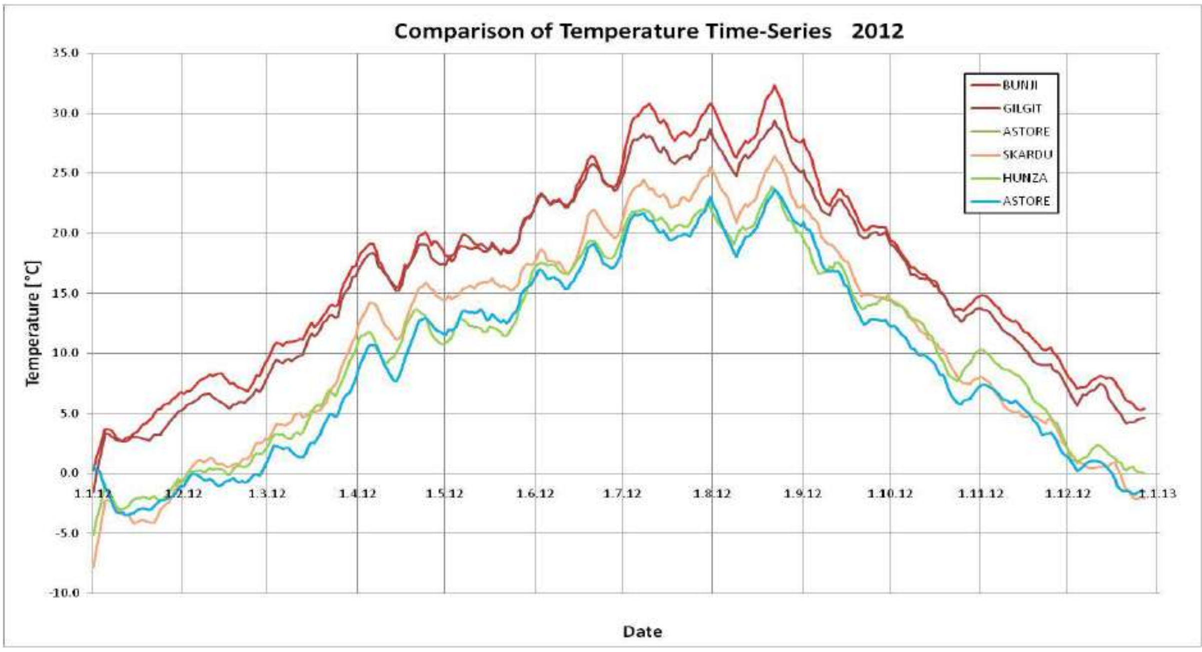

Figure 3-14: Comparison of Temperature Data from Different Stations (Year 2012)

3.14 DATA PROCESSING

For input to the SRM+G model, the following data needs to be processed:

- Catchment characteristics
- Snow extend
- Glacier exposed area
- Precipitation and
- Mean daily temperatures

Except for the catchment characteristics which are not time independent, all other variables have to be updated regularly (preferably weekly).

Irrespective of the formats of source data, all data outputs are either compressed GeoTiff with internal meta-data (for spatial data) or plain text files (with header and column separation through single space). These two data types can be easily processed by any type of modern GIS or database software.

3.14.1 Catchment Characteristics

Calculations of catchment characteristics for SRM+G were based on the digital elevation model. The original data come in 5x5 degree tiles. For UIB tiles are required which had first to be mosaicked and then clipped to reduce the size. These two procedures were achieved under ArcGIS.

The next step, the delineation of catchment and sub-catchment boundaries had been achieved with ArcGIS with Spatial Analyst and ArcHydro extensions. It used the initial raster resolution of 3 arc seconds (approximately 90m in North-South direction).

For further work, like definition of elevation zones, the elevation raster had to be adjusted to the spatial characteristics of the most important data input, the MODIS raster data. These were produced by the 'MODIS Reprojection Tool' and are in UTM43 North, geodetic datum WGS84, cell size 500m. This standard raster has a resolution of 500x480=240,000 cells. Additionally to projection, geodetic datum and cell size, cell alignment is important. In order to ensure all these specifications, a template (a GeoTiff generated by the MODIS tool) has to be used.

After this reprojection, the DEM raster was clipped to catchment boundaries (outside cells became no-data values) and assigned to elevation classes. In order to have more flexibility (like joining two or more classes into one) uniform steps of 500m from 0 to 5,500m were used.

The total area of Upper Indus Basin is 173,345 km^2. The basin is divided into 10 elevation zones having an equal altitude difference of 500 m. The resulting area and mean hypsometric elevation of each elevation zone is given in Table 3-4 and curve is shown in Figure 3-15.

Table 3-4: Hypsometric Data of the Upper Indus Basin

Elevation Zone	Elevation [m asl.]	Area [km^2]	Mean Hypsometric Elevation [m asl.]
1	0-1000	2,822	749
2	1001-1500	3,398	1254
3	1500-2000	3,336	1755
4	2001-2500	4,395	2266
5	2501-3000	5,690	2767
6	3001-3500	9,998	3272
7	3501-4000	16,183	3769
8	4001-4500	28,845	4272
9	4501-5000	39,473	4754
10	5001-5500	37,819	5240
11	>5500	21,388	5770

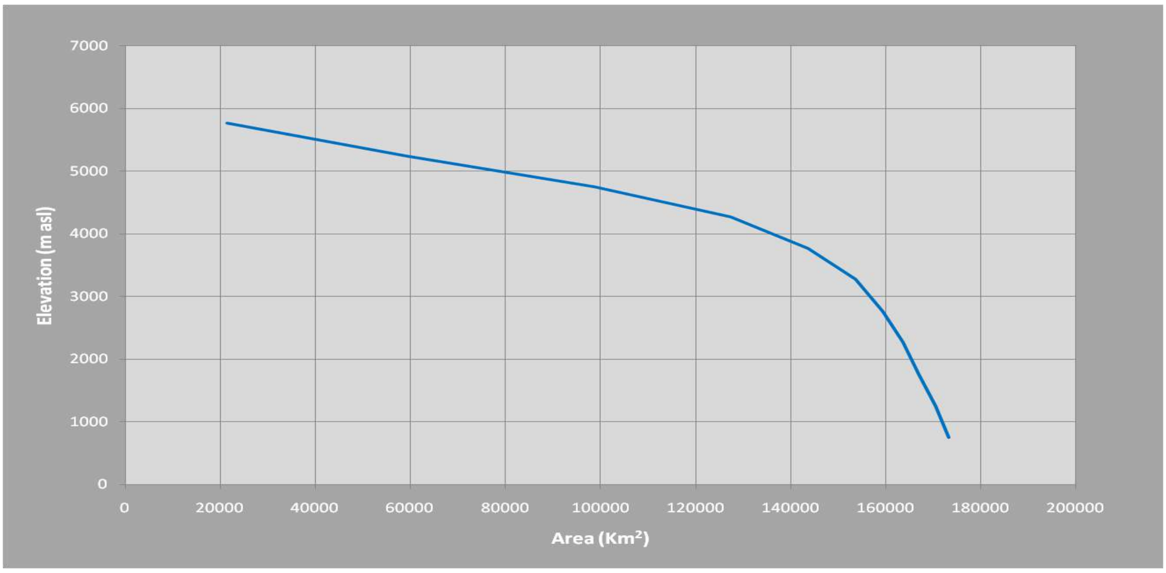

Figure 3-15: Hypsometric Curve of Upper Indus Basin Upstream of Tarbela

3.14.2 Snow Extent

Snow extent is the most important time-dependent data required by the model. In the Figure 3-16 the splined snow covered area for the different elevation zones for year 2012 is shown. While historical data (from 2001 to 2012) were downloaded and processed by the Project in order to calibrate the model, these activities need to be continued to obtain data for flow forecasting. The following steps are required:

i. Download of MODIS files from FTP-server (1 file per day) and extraction / re-projection area of interest
ii. Correction of raster cells with clouds or undefined data through temporal interpolation
iii. Analysis of corrected MODIS raster data, i.e. calculating daily statistics (snow / no-snow) per elevation zone.
iv. Filling of data gaps (missing days) through linear interpolation and calculation of snow depletion curves through spline smoothing.

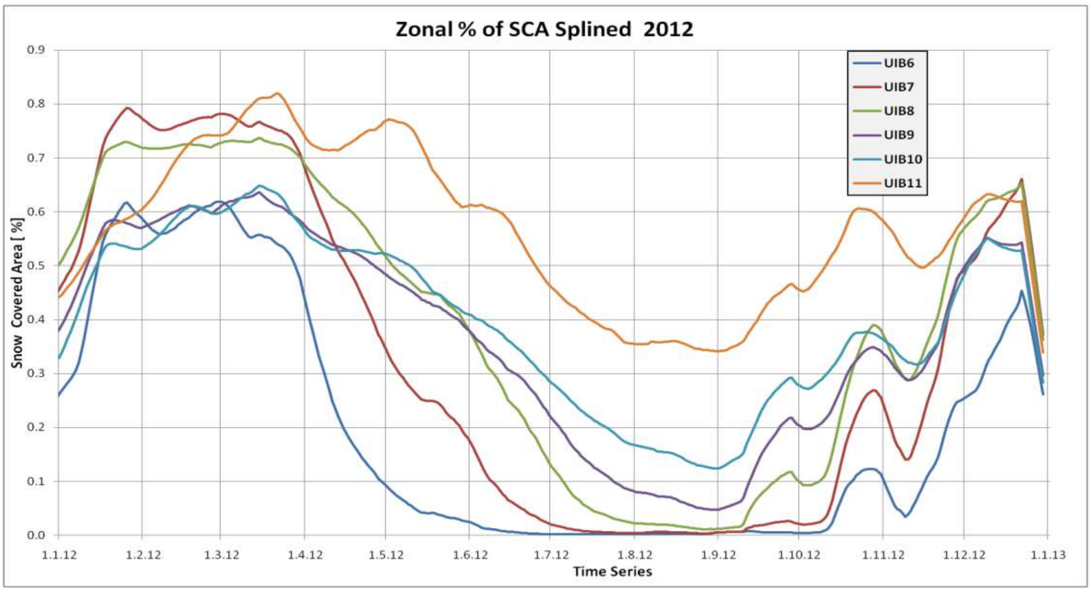

Figure 3-16: Zonal Snow Cover Area Variation in Selected Zones of UIB

3.14.3 Glacier Exposed Area

Glacier exposed area is another most important time-dependent data required by the model. In the Figure 3-17, the glacier exposed area for the different elevation zones for year 2012 is shown. Form the snow cover area depletion, the exposed glacier area is calculated by use of latest glacier data as described in earlier section. The following steps are achieved:

i. From the recent static glacier map, glacier exposed area is calculated.
ii. Correction of raster cells with clouds or undefined data through temporal interpolation
iii. Analysis of corrected raster data, i.e., calculating daily statistics per elevation zone.
iv. Filling of data gaps (missing days) through linear interpolation and calculation of glacier exposed curves through spline smoothing.

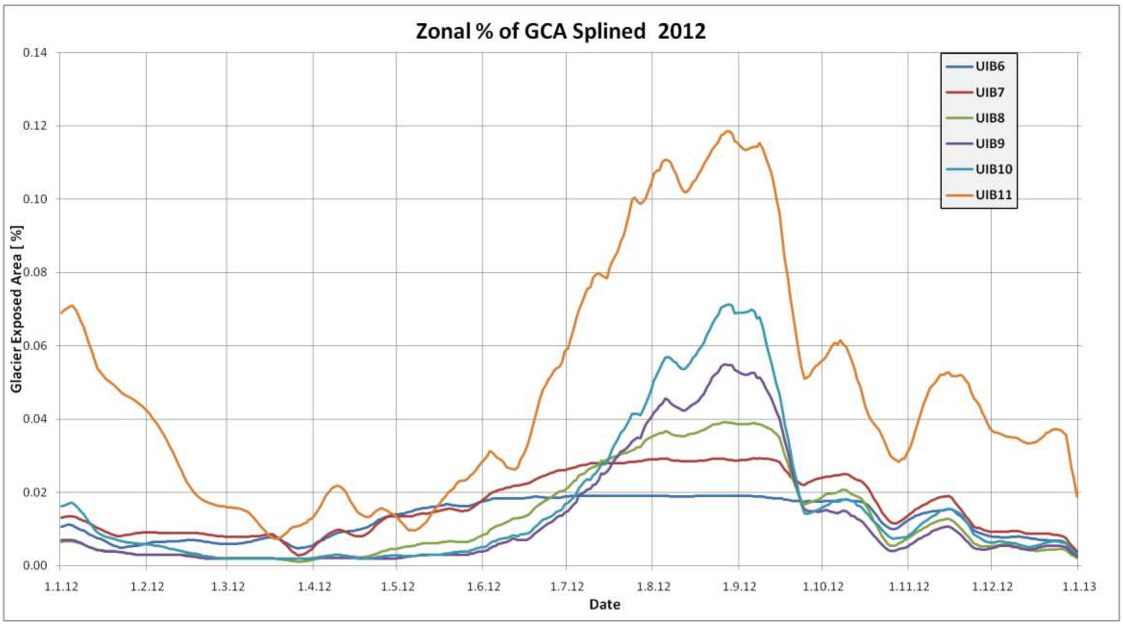

Figure 3-17: Zonal Glacier Exposed Area Variation in Upper Zones of UIB

3.14.4 Precipitation

Daily precipitation is required by the model for calculation of runoff from rainfall on snow-free surfaces. In the Figure 3-18 the daily precipitation for the 8th elevation zones for year 2012 is shown. Furthermore, it is used for estimations of snow-water-equivalent.

For the historic data, the following procedures were executed:

1. Extraction of historic daily precipitation raster data (FEWS/NOAA) from downloaded large netCDF file (reprojecting, resampling and saving as series of daily GeoTiff files).
2. Download of recent daily precipitation rasters (FEWS/NOAA) from data server, reprojecting, resampling and saving as series of daily GeoTiff files.
3. Analysis of daily precipitation raster files, calculation of mean, minimum and maximum precipitation per day and elevation zone.

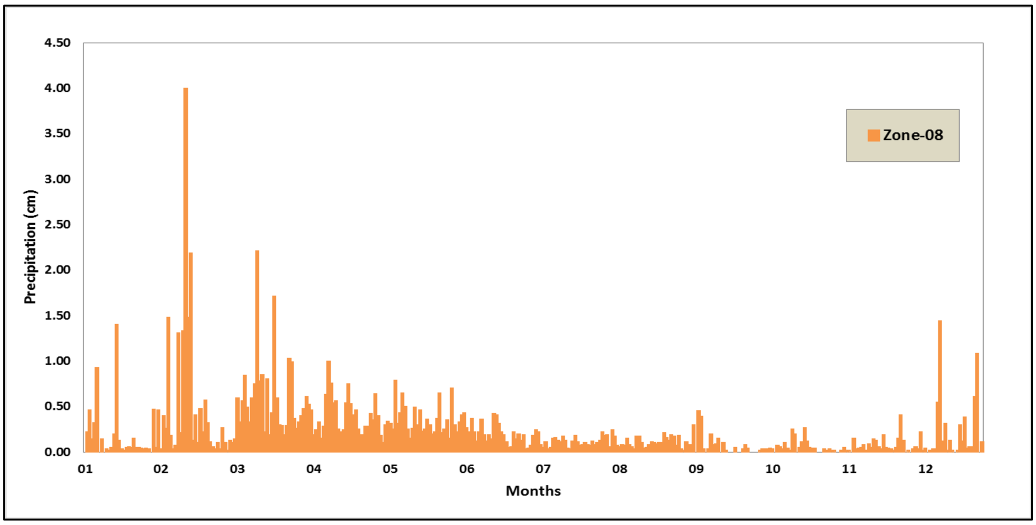

Figure 3-18: Daily Precipitation from NOAA (Year 2012, Zone-08)

3.14.5 Temperatures

Daily average temperatures of UIB stations was acquired. A geostatistical method (kriging) is applied for regionalization of temperature values observed at the stations, and through masking, daily average temperatures are then obtained for each elevation zone, which is then used as an input to SRM+G (see Figure 3-19).

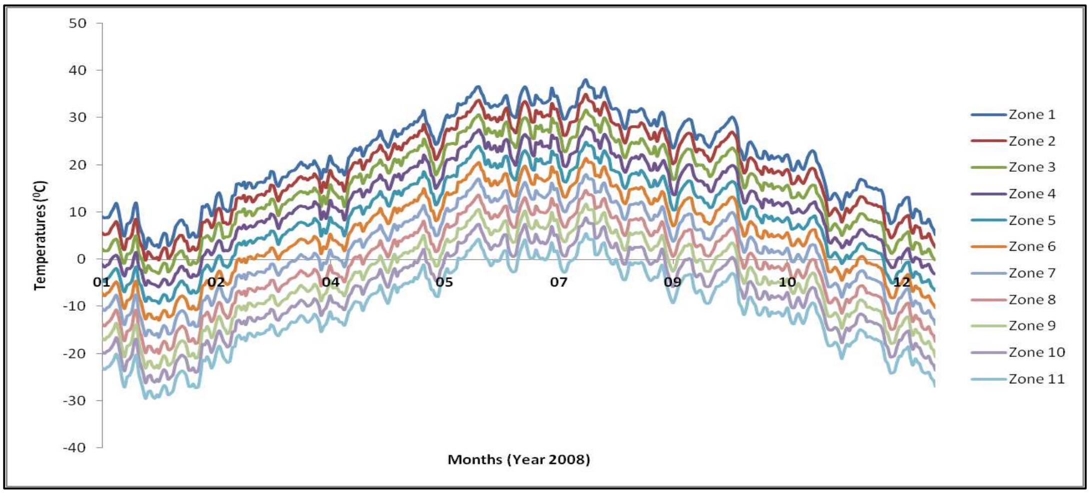

Figure 3-19: Temperature Variation in Each Elevation Zone of UIB

3.15 MODEL APPLICATION ON UIB

After having analysed and defined the input variables using the Gilgit and Hunza pilot models, the calibration of model parameters was carried out for the whole Upper Indus Basin.

In order to find a set of best fitting set of parameters for the hydrological forecast model, a two-step calibration approach was applied:

1. Find the best fitting parameters within a wide range of tolerated values, in order to identify the driving parameters in the different sections of the hydrograph, find the overall level of each parameter and establish a baseline of best-fit given the available input variables.

2. Reduce the temporal variability and restrict the parameters to reasonable values, while keeping the achieved goodness of fit as much as possible.

Model calibration was performed for all years where inflow data into the Tarbela Reservoir was available, i.e. 2003 – 2012. All calculations were carried out "year round", i.e. from 1st January to 31st December.

3.15.1 Calibrated Model Parameters

The model parameters resulting from the calibration process are discussed in the following section. All parameters were applied basin-wide, i.e. constant for all elevation zones, and with a temporal resolution of 10 days, leading to 36 individual periods in a year.

The calibration runs of this phase were carried out using ExcelSRM+G as it allows a convenient change of parameters on a 10-day basis and immediately updates the resulting hydrograph making it easy to view the effects. In the beginning of model calibration, an automatic parameter estimation procedure was applied, using Risk Solver Platform®[15] to solve the Least Squares regression between observed and simulated flow. During the course of the calibration, the procedure then was changed to manual, in order to keep parameters at smooth values and to maintain a reasonable trend in time.

At the final stage of model calibration, most parameters could be kept constant over time (Table 3-5) or were given in a fixed pattern (Figure 3-20). Finally, only the degree-day factor (a) and the runoff coefficient for rainfall c_R where adjusted period-wise in order to fit the simulated with the observed hydrograph.

[15] Risk Solver Platform® Version 11 © 1991-2011 by Frontline Systems, Inc., Incline Village, NV, USA

Table 3-5: Calibrated Values of Time-Constant Parameters

Parameter	Symbol	Value	Units	Remarks
Lag Time	L	18	h	= 1 day
Critical Precipitation	P_{crit}	0.4	cm	
Runoff Coefficient Snow	c_S	0.8	–	Constant value through out the year
Runoff Coefficient Glacier	c_g	0.8	-	Constant value through out the year
Recession Coefficient	k_x k_y	1.060 0.020	– –	Constant for UIB
Temperature Lapse Rate	γ	6.0	°C/km	Spatially interpolated by using Various temperature stations in UIB

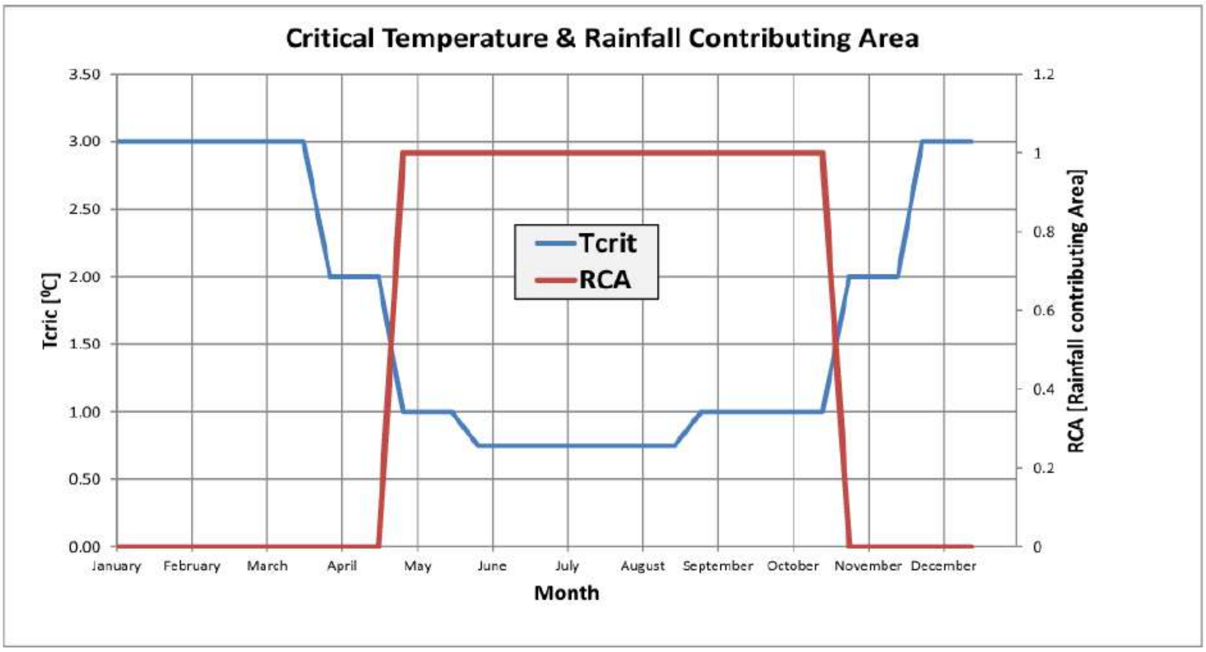

Figure 3-20: Time-Variant Pattern of Parameters RCA and T_{crit}

3.15.2 Lag Time L

The lag time L accounts for the time difference between the daily fluctuations of snowmelt, that usually starts rising around noon, lagging behind the rise of temperature by about 6 hours and the according rise in the hydrograph. Taking into account the different observation intervals of temperature and water level, a lag time of 18 h is equivalent to 1 day, i.e., snowmelt on day n will contribute to discharge on day $n+1$.

Although a close analysis of the hydrographs of certain flood events reveal a variability in the lag time of 0 – 3 days, no time related or other pattern could be identified. As a lag time of 18 h yielded the best model performance parameters D_V and R^2, this value was chosen constant for all times.

3.15.3 Critical Precipitation P_{crit}

The recession coefficient k reflects the usual conditions characterizing the base flow runoff in a given basin. However when heavy rainfall occurs, the direct runoff is concentrated in a short time interval creating an abrupt rise and subsequent decline of the hydrograph. In order to simulate such events, SRM+G adjusts the recession coefficient for a period of 5 days whenever the actual rainfall P exceeds P_{crit}.

When applying a smaller P_{crit} the hydrograph will follow more closely the flood peaks due to rainfall but also may lower the recession flow originating from snowmelt. For the Upper Indus Basin, a fairly small P_{crit} = 0.4 cm that takes account of most rainfall events showed good results[16]. It has to be noted that P_{crit} relates to the total area of the catchment thus other catchments will require different values.

3.15.4 Runoff Coefficient Snow c_S

This coefficient accounts for all losses of snow i.e. the difference between the potential snowmelt and the runoff. At the start of the snowmelt season, losses are usually very small because they are limited to sublimation from the snow surface, especially at high elevations. In the next stage, when some soil becomes exposed and vegetation grows, more losses may occur due to evapotranspiration and interception. Towards the end of the snowmelt season, direct channel flow from the remaining snowfields and glaciers may prevail and losses may again decrease.

Values of the runoff coefficient for snow vary highly from catchment to catchment and may be variable or quite constant in time[17]. As the daily runoff from snowmelt is inter alia a product of c_S and a, the coefficient c_S was given a constant value of 0.8 in order to make the calibration of the degree-day factor more transparent.

3.15.5 Runoff Coefficients Glacier c_g

Values of the runoff coefficient for glacier vary highly from catchment to catchment and may be variable or quite constant in time[18]. Constant value of 0.7 was applied that perfectly fits during the calibration phase of catchment.

The recession coefficient k is an important parameter of SRM+G since it determines strongly the daily portion of snow and glacier melt that transforms into immediate runoff. It describes the storage characteristics of the very catchment and the resulting base flow.

A quite detailed description on the calculation of the recession coefficient from historical discharge is given in the SRM User's Manual[19] [Martinec et all. 2008]. However, neither for the Upper Indus Basin nor for the sub-catchments Gilgit and Hunza, a reasonable value could be deduced that way.

---

[16] It was found that a P_{crit} = 0 leads to unpredictable results in SRM

[17] See e.g. Fig. 7 SRM User's Manual Chap. 5.3.2

[18] See e.g. Fig. 7 SRM User's Manual Chap. 5.3.2

[19] SRM User's Manual Chap. 5.3.6

The recession coefficient k, respectively its parameters x and y were therefore subject to parameter calibration. For Upper Indus Basin a good fit could be achieved with a combination of $x = 1.060$ and $y = 0.020$. But it has to be noted, that these values will differ for other catchments!

The sub-catchments of the Upper Indus basin have quite diverse topographic and hypsometric characteristics, and subsequently the recession coefficients of these several basins should be quite different.

3.15.6 Temperature Lapse Rate γ

Daily temperature data is an important climatic variable used by SRM+G; it is needed to decide if precipitation falls as snow or as rain and also to simulate the melting process. Lapse rate of 6 ^{0}C/km is applied for the calculation of temperature in each elevation zone.

Temperature is one of the two snow and glacial melt driving variables in SRM+G governing equation as it influences directly the number of degree-days and therefore the volume of available runoff from snowmelt and glacial melt.

3.15.7 Critical Temperature Tcrit

The critical temperature determines whether the measured or forecasted precipitation is rain or snow. SRM needs the critical temperature only in order to decide whether precipitation immediately contributes to runoff (rain), or, if $T < T_{crit}$, whether snowfall took place. Hence the influence of T_{crit} on the runoff is limited to short time period when temperatures incline from below 0°C to positive values, a sensible pattern following the values proposed in the SRM User's Manual[20] was chosen without further analysis.

3.15.8 Rainfall Contributing Area RCA

When precipitation is determined to be rain, it can be treated in two ways. Early in the snowmelt season, it is assumed that rain falling on the snowpack is retained by the snow which is usually dry and deep (Option 0). At some later stage, the snow cover becomes ripe and if rain falls on this snow cover, it is assumed that the same amount of water is released from the snowpack so that rainfall runoff from the entire zone area is considered (Option 1). The chosen distribution is given in Table 3-6.

3.15.9 Degree Day Factor a_s

The degree-day factor a [cm/°C/d] converts the number of degree-days T [°C·d] into the daily snowmelt depth [cm]. It absorbs a variety of inaccuracies in the determination of the snow-covered area, the zonal temperature, or the runoff coefficient for snow. As even measured degree-day factors show a great variability depending on the latitude as well as the time of the year, during model calibration this parameter was adjusted on a 10-day interval to arrive at the best fit between the simulated and observed hydrograph while trying to maintain the general increasing trend from the start to the end of the melting season.

[20] SRM User's Manual Chap. 5.3.4

The variation of degree-day factors is displayed in Table 3-6. It starts at 0.15 – 0.20 [cm/°C/d] in winter and then gradually increases to about 0.8 [cm/°C/d] towards the end of the melting season. From August onward, it was set to 0.4 [cm/°C/d] to allow for some melting of occasional new snow in the higher elevation zones.

Table 3-6: Degree-Day Factors [cm/°C/d] in the Year 2008

	Elevation Zones										
Period	**1**	**2**	**3**	**4**	**5**	**6**	**7**	**8**	**9**	**10**	**11**
JAN-1	0.15	0.15	0.15	0.15	0.15	0.15	0.15	0.15	0.15	0.15	0.15
JAN-2	0.15	0.15	0.15	0.15	0.15	0.15	0.15	0.15	0.15	0.15	0.15
JAN-3	0.15	0.15	0.15	0.15	0.15	0.15	0.15	0.15	0.15	0.15	0.15
FEB-1	0.15	0.15	0.15	0.15	0.15	0.15	0.15	0.15	0.15	0.15	0.15
FEB-2	0.15	0.15	0.15	0.15	0.15	0.15	0.15	0.15	0.15	0.15	0.15
FEB-3	0.20	0.20	0.20	0.15	0.15	0.15	0.15	0.15	0.15	0.15	0.15
MAR-1	0.25	0.25	0.20	0.20	0.15	0.15	0.15	0.15	0.15	0.15	0.15
MAR-2	0.30	0.30	0.25	0.20	0.20	0.15	0.15	0.15	0.15	0.15	0.15
MAR-3	0.35	0.35	0.25	0.25	0.20	0.20	0.20	0.15	0.15	0.15	0.15
APR-1	0.40	0.40	0.30	0.25	0.25	0.20	0.20	0.15	0.15	0.15	0.15
APR-2	0.50	0.50	0.40	0.30	0.25	0.25	0.25	0.20	0.15	0.15	0.15
APR-3	0.50	0.50	0.50	0.40	0.30	0.25	0.25	0.20	0.20	0.20	0.20
MAY-1	0.50	0.50	0.50	0.50	0.40	0.30	0.30	0.25	0.20	0.20	0.20
MAY-2	0.50	0.50	0.50	0.50	0.50	0.40	0.40	0.25	0.25	0.25	0.25
MAY-3	0.50	0.50	0.50	0.50	0.50	0.50	0.50	0.30	0.25	0.25	0.25
JUN-1	0.50	0.50	0.50	0.50	0.50	0.50	0.50	0.40	0.30	0.30	0.30
JUN-2	0.50	0.50	0.50	0.50	0.50	0.50	0.50	0.50	0.40	0.40	0.40
JUN-3	0.50	0.50	0.50	0.50	0.50	0.50	0.50	0.50	0.50	0.50	0.50
JUL-1	0.50	0.50	0.50	0.50	0.50	0.50	0.50	0.50	0.50	0.50	0.50
JUL-2	0.50	0.50	0.50	0.50	0.50	0.50	0.50	0.50	0.50	0.50	0.50
JUL-3	0.50	0.50	0.50	0.50	0.50	0.50	0.50	0.50	0.50	0.50	0.50

3.15.10 Degree Day Factor a_g

In this study, the daily glacier melt depth were computed by a uniform a_g = 0.7 cm $°C^{-1}$ d^{-1}. Naturally, this factor was applied only to the gradually increasing snow-free area of glaciers but a constant value is used to incorporate the melt coming from glaciers. The degree day factors for the glaciers are given in Table 3-7.

Table 3-7: Degree-Day Factors [cm/°C/d] in the Year 2008

	Elevation Zones										
Period	**1**	**2**	**3**	**4**	**5**	**6**	**7**	**8**	**9**	**10**	**11**
JAN-1	0.70	0.70	0.70	0.70	0.70	0.70	0.70	0.70	0.70	0.70	0.70
JAN-2	0.70	0.70	0.70	0.70	0.70	0.70	0.70	0.70	0.70	0.70	0.70
JAN-3	0.70	0.70	0.70	0.70	0.70	0.70	0.70	0.70	0.70	0.70	0.70
FEB-1	0.70	0.70	0.70	0.70	0.70	0.70	0.70	0.70	0.70	0.70	0.70
FEB-2	0.70	0.70	0.70	0.70	0.70	0.70	0.70	0.70	0.70	0.70	0.70
FEB-3	0.70	0.70	0.70	0.70	0.70	0.70	0.70	0.70	0.70	0.70	0.70
MAR-1	0.70	0.70	0.70	0.70	0.70	0.70	0.70	0.70	0.70	0.70	0.70
MAR-2	0.70	0.70	0.70	0.70	0.70	0.70	0.70	0.70	0.70	0.70	0.70
MAR-3	0.70	0.70	0.70	0.70	0.70	0.70	0.70	0.70	0.70	0.70	0.70
APR-1	0.70	0.70	0.70	0.70	0.70	0.70	0.70	0.70	0.70	0.70	0.70
APR-2	0.70	0.70	0.70	0.70	0.70	0.70	0.70	0.70	0.70	0.70	0.70
APR-3	0.70	0.70	0.70	0.70	0.70	0.70	0.70	0.70	0.70	0.70	0.70
MAY-1	0.70	0.70	0.70	0.70	0.70	0.70	0.70	0.70	0.70	0.70	0.70
MAY-2	0.70	0.70	0.70	0.70	0.70	0.70	0.70	0.70	0.70	0.70	0.70
MAY-3	0.70	0.70	0.70	0.70	0.70	0.70	0.70	0.70	0.70	0.70	0.70
JUN-1	0.70	0.70	0.70	0.70	0.70	0.70	0.70	0.70	0.70	0.70	0.70
JUN-2	0.70	0.70	0.70	0.70	0.70	0.70	0.70	0.70	0.70	0.70	0.70
JUN-3	0.70	0.70	0.70	0.70	0.70	0.70	0.70	0.70	0.70	0.70	0.70
JUL-1	0.70	0.70	0.70	0.70	0.70	0.70	0.70	0.70	0.70	0.70	0.70
JUL-2	0.70	0.70	0.70	0.70	0.70	0.70	0.70	0.70	0.70	0.70	0.70
JUL-3	0.70	0.70	0.70	0.70	0.70	0.70	0.70	0.70	0.70	0.70	0.70

3.15.11 Runoff Coefficient Rain c_R

Like the runoff coefficient for snow, the runoff coefficient for rain accounts for all losses due to interception and evapotranspiration of rainfall in the catchment. It mainly effects the flood peaks due to intense precipitation, i.e. is most important during the monsoon period. SRM+G uses a quite simple (constant) approach for this parameter, while in reality it is, inter alia, a function of land-use, condition of vegetation, type of soil, actual soil-moisture content, etc.

In order to arrive at a decent fit between simulated and observed hydrographs with special focus on the flood peaks, c_R had to be adjusted quite frequently and without a recognisable rule for the calibration. In the forecast mode these parameters are fixed.

3.16 UPPER INDUS BASIN MODEL CALIBRATION AND VALIDATION

3.16.1 Calibration Results

The two error norms widely used to characterise the accuracy of model results compared to observed hydrographs, sometimes also referred to as the “model performance”, are:

1. the Coefficient of Determination:

$$R^2 = 1 - \frac{\sum_{i=1}^{n} (Q_i - Q_i')^2}{\sum_{i=1}^{n} (Q_i - \overline{Q})^2}$$

where

Q_i = measured daily discharge

Q_i' = computed daily discharge

$\overline{Q}$ = average measured discharge of the given year or snowmelt season

n = number of daily discharge values

2. and the Volume Difference:

$$D_V = \frac{V_R - V_R'}{V_R} \cdot 100 \qquad [\%]$$

where

V_R = measured yearly or seasonal runoff volume

V_R' = computed yearly or seasonal runoff volume

Table 3-8 gives the respective values for all “year round” simulations 2003 – 2012. The absolute value of the total volume difference $|D_V|$ ranges from 0.3 – 4.7 % being an excellent estimation of total annual discharge. The coefficient of determination R^2, that represents the goodness of fit between the simulated and observed hydrographs ranges from 0.94 – 0.97 which also indicates a close fit of the two graphs[21].

Table 3-8: Model Accuracy of UIB SRM+G after Calibration

UIB	D_V	R^2
2003	-3.81	97%
2004	-0.34	94%

Besides the two error norms, a visual judgement of the goodness of fit is of very importance. As an example, the hydrograph of the best (2003) fitting year is given in Figure 3-21 together with a comparison of 10-day flow volumes.

[21] R^2 = 1 would indicate a 100% fit

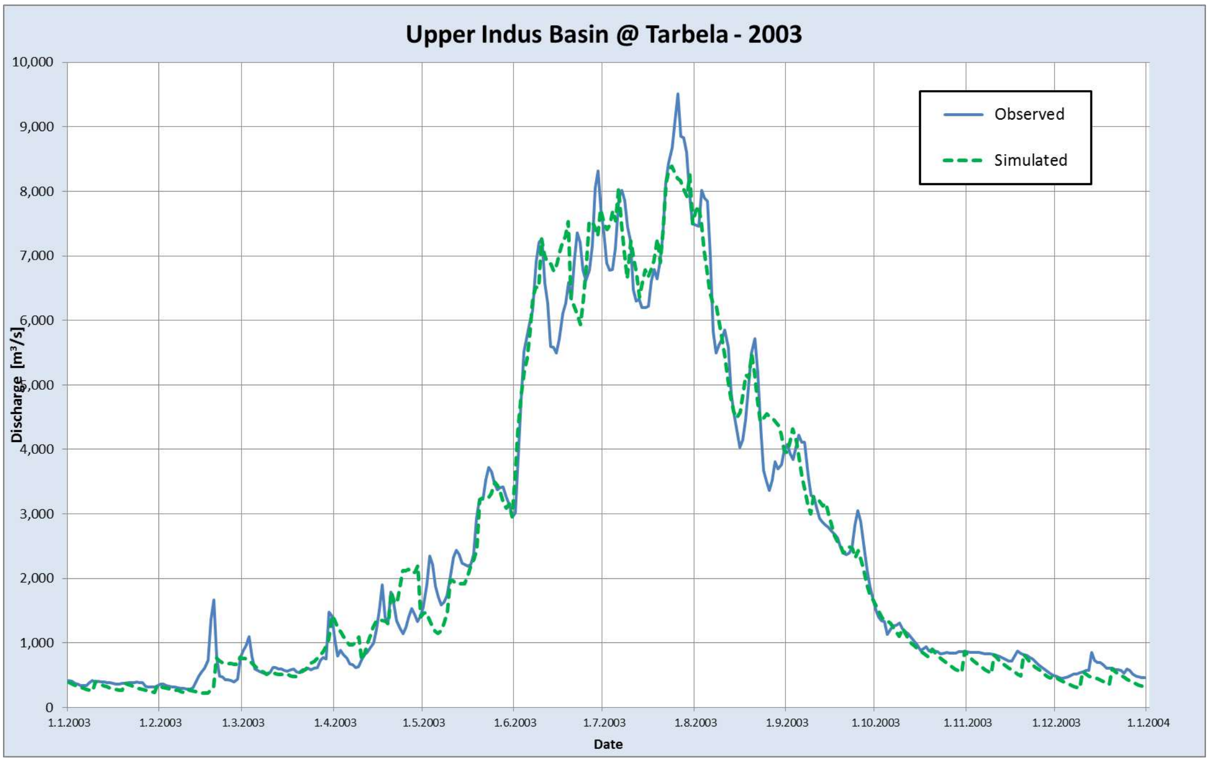

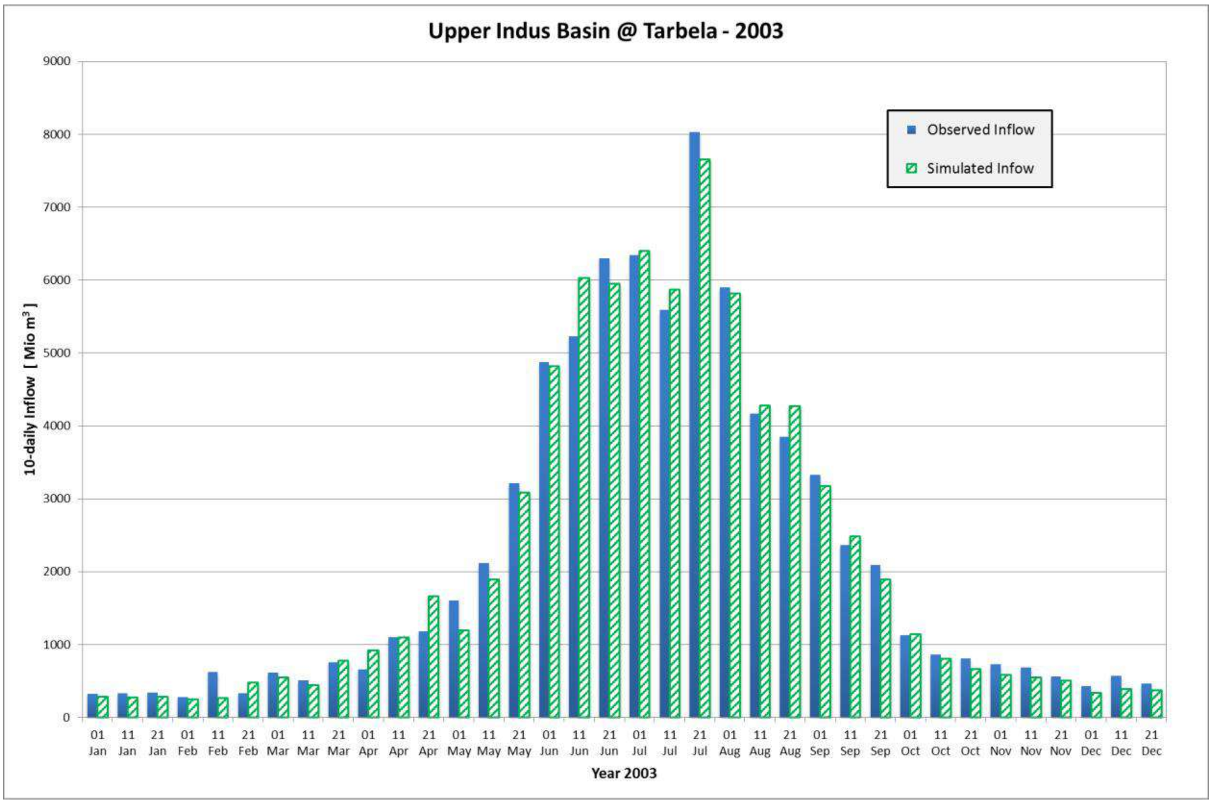

Figure 3-21: Simulated vs. Observed Hydrograph and 10-day Volume 2003

3.16.2 Validation of the Forecast Model

Applying the previously calibrated model parameters as well as the above described parameters and rules, the forecast model was validated against observed Tarbela inflows for the years 2005-2012. A comparison of the respective observed vs. simulated hydrographs can be found in Table 3-9.

The results of the forecast model validation using the common error norms D_V (Volume Difference) and R^2 (Coefficient of Determination) are given in Table 3-9. Although the model accuracy is not as extraordinary as for the model calibration (see Table 3-9), it still can be regarded as excellent taking the meteorological variance in the simulated years, in particular the extreme flood in 2010.

Table 3-9: Validation Results of the Forecast Model

UIB	D_V (MAF)	R^2
2005	1.09	96%
2006	-0.36	95%
2007	-2.51	94%
2008	-4.14	97%
2009	-3.82	96%
2010	-2.03	95%
2011	-1.01	94%
2012	-4.74	94%

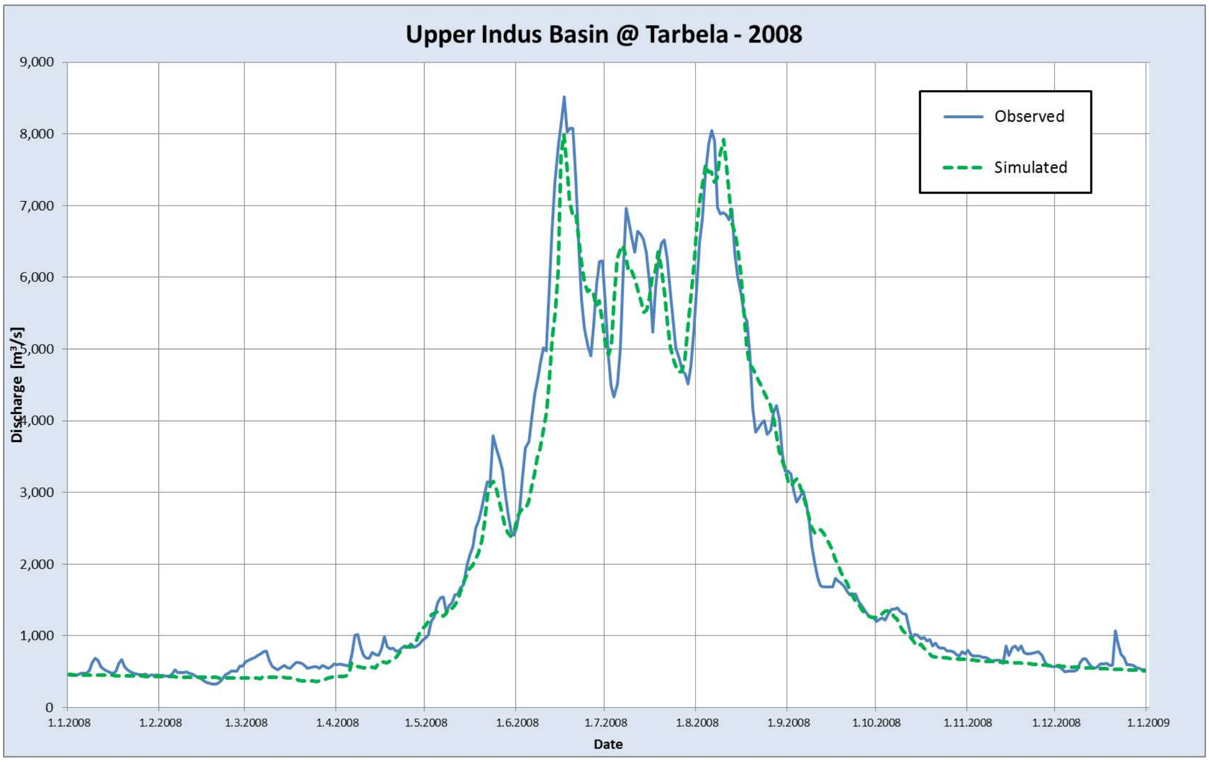

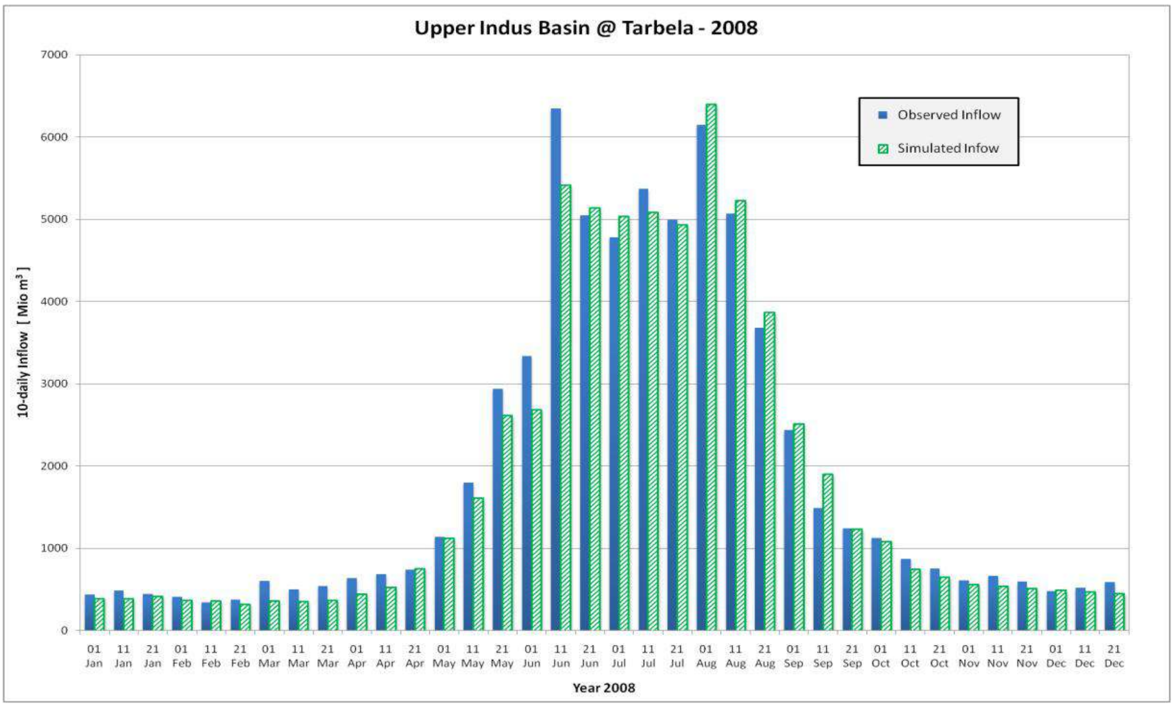

Figure 3-22: Simulated vs. Observed Hydrograph and 10-day Volume 2008

3.17 INTERMEDIATE RESULTS (SHORT AND MEDIUM TERM FORECASTS)

SRM+G can be used for the following purposes:

i. Simulation of daily flows in a snowmelt season, in a year, or in a sequence of years. The results can be compared with the measured runoff in order to assess the performance of the model and to verify the values of the model parameters. Simulations can also serve to evaluate runoff patterns in un-gauged basins using satellite monitoring of snow covered areas and extrapolation of temperatures and precipitation from nearby stations.

ii. For short term and seasonal runoff forecasts, the computer program SRM+G includes a derivation of modified depletion curves which relate the snow covered areas to the cumulative snowmelt depths as computed by SRM. These curves enable the snow coverage to be extrapolated manually by the user several days ahead by temperature forecasts so that this input variable is available for discharge forecasts. The modified depletion curves can also be used to evaluate the snow reserves for seasonal runoff forecasts. The model performance may deteriorate if the forecasted air temperature and precipitation deviate from the observed values, but the inaccuracies can be reduced by periodic updating.

3.18 FORECASTING MODEL PARAMETER SET AND RULES

While during model calibration the parameters can be adjusted against the observed hydrograph, for forecasting a pre-defined set of parameters and/or rules is necessary as the hydrological conditions lie in the future. As basically the degree-day factors and the runoff coefficients for rain have been subject to calibration, special effort was made to arrive at a fixed set and/or fixed rules for these two parameters.

3.18.1 Runoff Coefficient

For the calibration of the SRM+G model, initially effort has been made to arrive at the best possible fit of the simulated flow data to the (calculated) inflow hydrograph of Tarbela Reservoir. Although it has not been allowed to let the model parameters reach values that are unrealistic, in the particular case of the runoff coefficient c_R, which is the principle parameter to adjust the runoff values from rainfall in SRM+G, this procedure did let to rather haphazard changes in the values over the year (Figure 3-23). Furthermore, values in the same 10-day period change noticeably from year to year making them not well suited for forecasting.

Thus, in order to arrive at reliable flow forecasts especially during monsoon season, it is not only required to define a single set of values, but also this set should have logic values that can be understood in physical terms and still reproduce reasonable modelling results. For this reason, a forecasting set of c_R values was derived that comply with both these criteria.
The derivation of the forecasting set of c_R values was based on two criteria:

- A logical set of values that can easily be explained by the physical processes the parameter is supposed to represent.
- Maintain a calibration model result that results in a reasonable fit of the simulated hydrograph to the Tarbela inflow hydrograph, especially in terms of total flow volume**.**

For the latter, it was assumed that it would not be reasonably possible to simulate well the flood hydrographs associated with extreme rainfall events as both the rainfall data as well as the calculated inflow hydrograph does not always fit together and SRM+G on the other hand does only have a basic routine for the rainfall-runoff process.

It was judged that the original sets of parameters were not only haphazardly looking, but were also too extreme both on the low and high sites. Values of c_R = 0.8 would mean that there is only little loss to the groundwater during a flood or any other losses. On the other hand, extremely low values as 0.2 would imply that nearly all the water (80%) is lost. Investigation of rainfall events shows a very little impact with values reaching to 0.8 in July while for the rest of the year it remains constant as 0.2. For this reason, the values for the forecasting set are supposed to vary between 0.2 and 0.4.

A trial-and-error procedure was used to arrive at a set of values that both comply with these assumptions as well as manage to reproduce satisfactorily well the overall average inflow hydrograph at Tarbela Reservoir, especially in the Early Kharif (April – June) that is very important for the water availability for irrigation. Values were only allowed to change between months, not within a month as this would lead to a much longer trial-and-error procedure that is not reasonable given the quality of the available data.

In Figure 3-24, both the calibrated values of the runoff coefficient per year are shown as well as the final forecasting set of values. It is evident that the calibrated values varied widely, both in time and between simulation years. The forecasting set on the other hand has a smooth form, representing the slow decrease in runoff percentage from rainfall in the basin due to the increase in losses due to evaporation in the summer. The overall values, between 0.2 and 0.4, represent the expected losses due to infiltration and retention in the total basin.

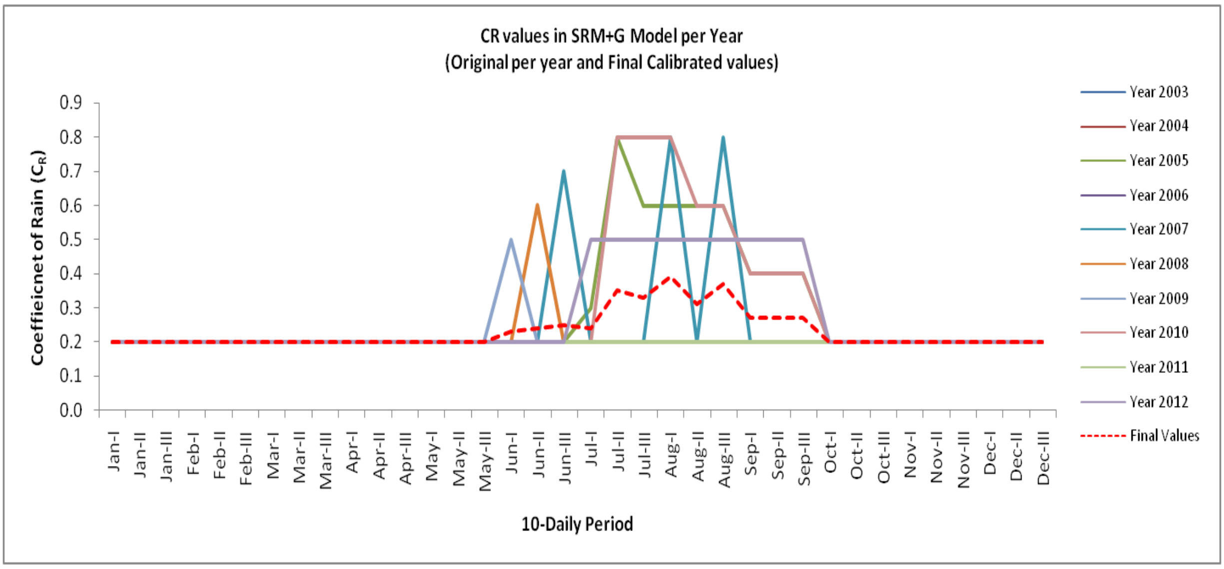

Figure 3-23: Calibrated Values and Forecasting Set of Runoff Coefficient

The impact of the choice of the final forecasting set of c_R values on the simulation results can be dramatic. An extreme example is the year 2005 (See Figure 3-24), for which also originally extreme values of c_R have been used although the overall line of the hydrograph is still reasonable, the model does not reproduce the peak flow hydrographs as was expected. However, although the peaks are not reproduced, leading to a higher volume error, the overall predicted inflow hydrograph, important for water availability from Tarbela Reservoir, is well reproduced.

With the final forecasting set of c_R values the model is expected to give more reliable results for the total inflow *volume* towards Tarbela. Nevertheless, when using the fixed pattern of monthly runoff coefficients c_R over the year, the model does not sufficiently reproduce the peak flow hydrographs, especially during the month of July & August and in case of high rainfall intensities over the whole Tarbela catchment. Thus, a special rule was developed in order to automatically arrive at runoff coefficients for high intensity rainfall events, which better match the observed Tarbela inflow hydrograph.

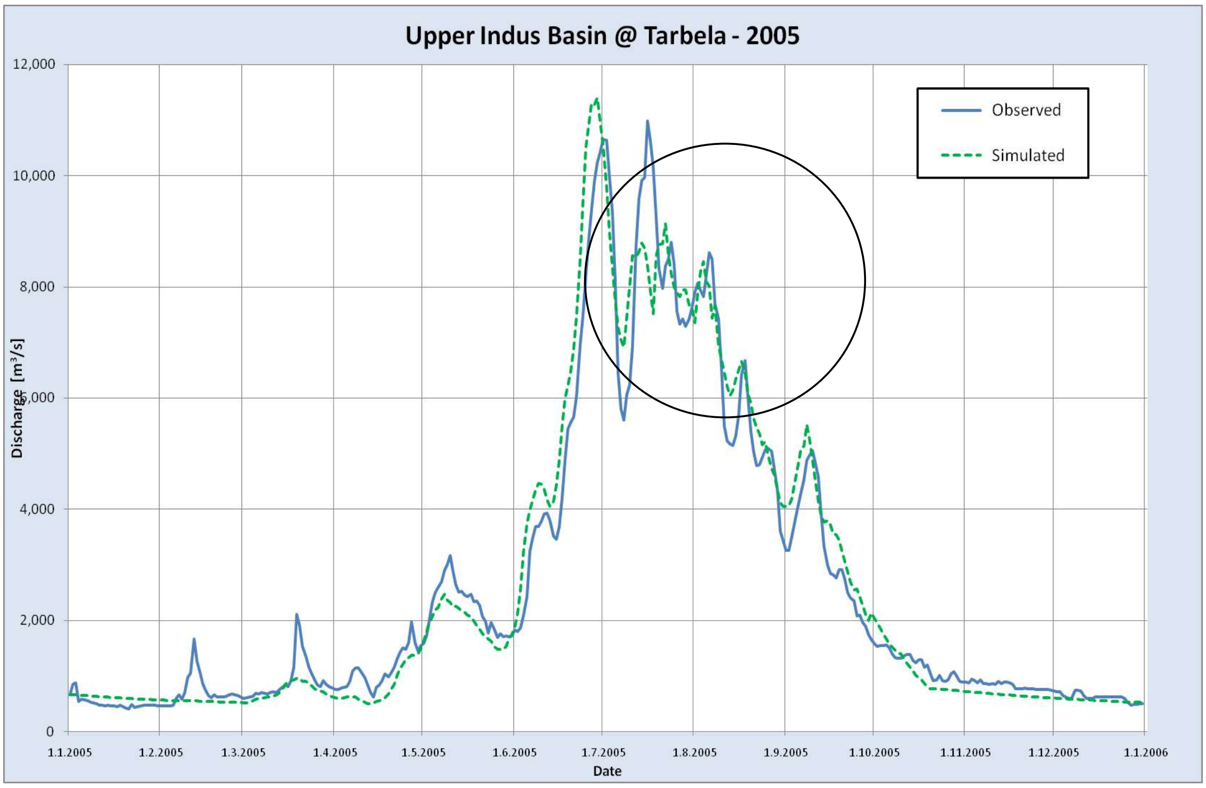

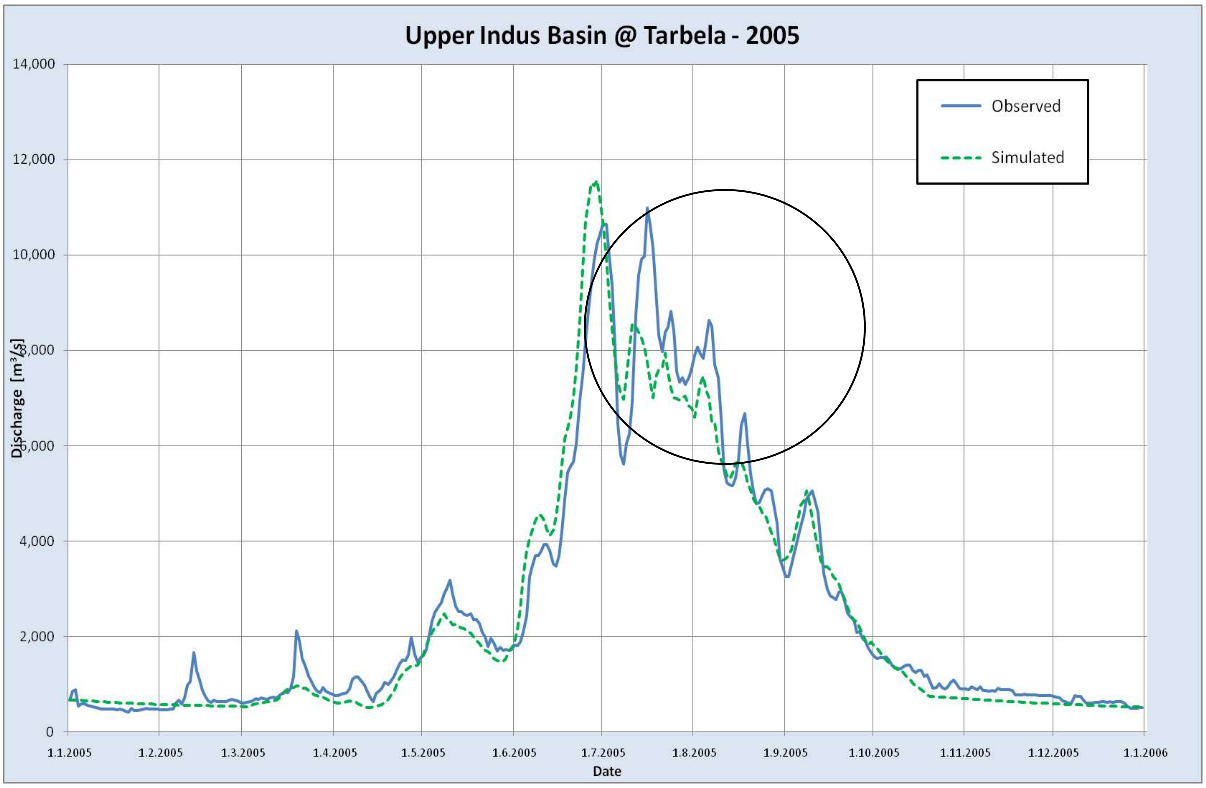

Figure 3-24: Simulation Results of Calibrated (above) and Final Forecasting Set of Runoff Coefficient Cr (below) – 2005

3.18.2 Degree-Day Factor

The most important parameter for the snow-melt component in SRM+G is the degree-day factor. During model calibration, for the sake of transparency the degree-day factors were applied basin-wide. The degree-day factor generally increases during melt season, as the snowpack becomes "ripe" with increasing temperature (Martinec et al. 2011). It is obvious, that this process happens later at higher elevation zones as temperatures are lower up there. In order to find a common increase pattern of the degree-day factors as well as a rule when this pattern starts in each elevation zone, zone-wise degree-day factors were introduced trying to keep the simulation results as good as during the model calibration phase.

In order to determine a common function for each zone, all the graphs commence at the same point, although the actual start may differ from year to year. Then, linear interpolation was applied to obtain the number of periods needed to arrive at a degree-day factor of 0.5 [cm/°C/d] which was set as the maximum value. Finally, the values of periods in-between were determined by linear interpolation (Table 3-10).

Table 3-10: Zone-wise Degree-Day Factor Functions

Periods	1	2	3	4	5	6	7
Zone 1-2	0.20	0.25	0.30	0.35	0.40	0.50	0.60
Zone 3-11	0.20	0.20	0.25	0.25	0.30	0.40	0.50

When the degree-day factors have reached their maximum value of 0.5 [cm/°C/d], this value is kept constant until end of July. Starting from October onward, when the new snow-pack is build up during the winter, degree-day factors in all zones are set to the minimum value of 0.15 [cm/°C/d] until again the degree-day factor functions are applied in the following year. In August and September the degree-day factors in all zones are set to 0.4 [cm/°C/d] as the snow falling in the first snow events after summer, which often is melted immediately, is expected to be "wetter" than under temperatures well under the freezing point.

It has to be noted, that the degree-day factor functions, i.e. the increase of the degree-day factors, do not start at the same date for all zones. Obviously, the start is related to the rise of temperature, especially when the mean daily temperature advances above 0°C. On basis of the above functions, a general rule has been developed when to start with the increase of the degree-day factors at each zone. For this purpose, the average daily mean temperature of each 10-days period for each elevation zone is calculated. If that value is higher than the specific temperature threshold given in Table 3-11, the degree-day factor function for the respective zone is applied.

Table 3-11: Start Temperature Threshold [°C] for Degree-Day Factor Functions

	Zone 1	Zone 2	Zone 3-4	Zone 5	Zone 6	Zone 7-8	Zone 9	Zone 10	Zone 11
T_{10d} [a)]	12	9	6	4	2	1	1	1	1

[a)] T_{10d} = average daily mean temperature of the preceding 10-days period

An example for the start period rule and the application of the degree-day factor functions is given for the year 2003. Table 3-12 shows the average 10-day temperature for each zone with an indication of the temperature threshold and Table 3-13 the resulting zone-wise degree day factors.

Table 3-12: Average 10-day Temperature [°C] in the Year 2003

Period	Elevation Zones										
	1	2	3	4	5	6	7	8	9	10	11
Jan-I	11.3	7.8	4.1	0.3	-3.3	-6.6	-9.9	-13.2	-16.2	-19.1	-22.5
Jan-II	14.2	10.4	6.7	2.8	-0.5	-3.7	-6.9	-10.1	-13.0	-15.9	-19.3
Jan-III	11.4	8.4	5.3	2.1	-1.3	-4.8	-8.2	-11.6	-14.8	-17.9	-21.3
Feb-I	10.9	7.7	4.4	0.9	-2.7	-6.3	-9.8	-13.1	-16.2	-19.2	-22.5
Feb-II	10.7	7.4	4.3	1.5	-1.6	-4.8	-8.0	-11.3	-14.3	-17.4	-20.7
Feb-III	12.8	9.6	6.6	3.8	0.8	-2.4	-5.6	-8.9	-12.0	-15.1	-18.5
Mar-I	10.8	7.7	4.4	1.3	-2.3	-5.8	-9.3	-12.7	-15.8	-18.8	-22.2
Mar-II	15.5	12.3	9.0	5.7	2.2	-1.3	-4.7	-8.1	-11.1	-14.1	-17.5
Mar-III	18.0	14.9	11.9	9.0	5.7	2.3	-1.0	-4.4	-7.5	-10.5	-13.9
Apr-I	19.7	16.7	13.5	10.0	6.3	2.5	-1.1	-4.5	-7.7	-10.6	-14.0
Apr-II	20.5	17.7	14.8	11.9	8.5	4.9	1.4	-2.0	-5.1	-8.1	-11.5
Apr-III	22.5	19.3	16.0	13.0	9.6	6.4	3.1	-0.2	-3.3	-6.2	-9.6
May-I	19.9	16.6	13.3	9.9	6.5	3.0	-0.3	-3.6	-6.7	-9.7	-13.1
May-II	24.3	21.2	17.8	14.4	10.9	7.4	3.9	0.6	-2.5	-5.4	-8.8
May-III	24.8	21.9	18.8	15.8	12.4	8.9	5.5	2.1	-1.0	-4.0	-7.3
Jun-I	29.7	26.6	23.3	19.9	16.4	12.7	9.3	6.0	2.9	-0.1	-3.5
Jun-II	29.7	26.7	23.6	20.5	17.1	13.6	10.1	6.8	3.6	0.6	-2.8
Jun-III	30.1	27.6	24.9	22.0	18.7	15.2	11.7	8.4	5.1	2.0	-1.4
Jul-I	30.6	27.9	25.2	22.6	19.5	16.1	12.7	9.3	6.1	3.0	-0.4
Jul-II	31.0	28.5	25.9	23.8	21.0	17.7	14.4	11.0	7.8	4.6	1.3
Jul-III	31.7	29.3	27.0	25.1	22.2	18.9	15.5	12.1	8.8	5.7	2.3
Aug-I	29.7	27.2	24.6	22.4	19.3	15.9	12.6	9.2	5.9	2.7	-0.7
Aug-II	29.0	26.4	23.8	21.3	18.3	14.9	11.6	8.2	4.9	1.8	-1.6
Aug-III	29.4	26.6	23.6	20.9	17.8	14.6	11.3	8.0	4.8	1.7	-1.6
Sep-I	27.4	24.4	21.2	18.6	15.6	12.6	9.3	6.1	3.0	0.0	-3.4
Sep-II	28.6	25.4	22.2	19.4	16.5	13.5	10.3	7.0	4.1	1.1	-2.3
Sep-III	23.1	20.3	17.3	14.5	11.3	7.9	4.5	1.2	-2.0	-5.1	-8.5
Oct-I	22.6	19.4	16.1	12.8	9.4	6.0	2.7	-0.7	-3.8	-6.8	-10.2
Oct-II	22.0	18.6	15.2	11.7	8.2	4.9	1.5	-1.8	-4.8	-7.8	-11.2
Oct-III	22.8	19.5	16.0	12.6	9.3	6.1	2.9	-0.4	-3.5	-6.5	-9.9
Nov-I	17.5	14.4	11.3	8.5	5.2	1.9	-1.4	-4.8	-7.9	-10.9	-14.2
Nov-II	14.3	11.2	8.0	5.1	1.7	-1.7	-5.1	-8.5	-11.7	-14.6	-18.0
Nov-III	15.1	11.5	7.8	4.2	0.6	-2.7	-6.0	-9.3	-12.2	-15.1	-18.5
Dec-I	15.7	12.0	8.3	4.7	1.4	-1.8	-5.1	-8.3	-11.2	-14.2	-17.5
Dec-II	10.9	7.6	4.2	1.1	-2.2	-5.5	-8.8	-12.1	-15.0	-18.0	-21.3
Dec-III	9.4	6.1	2.7	-0.7	-3.9	-7.2	-10.4	-13.8	-16.8	-19.8	-23.1

Table 3-13: Degree-Day Factors [cm/°C/d] in the Year 2003

Period	Elevation Zones										
	1	2	3	4	5	6	7	8	9	10	11
Jan-I	0.15	0.15	0.15	0.15	0.15	0.15	0.15	0.15	0.15	0.15	0.15
Jan-II	0.15	0.15	0.15	0.15	0.15	0.15	0.15	0.15	0.15	0.15	0.15
Jan-III	0.15	0.15	0.15	0.15	0.15	0.15	0.15	0.15	0.15	0.15	0.15
Feb-I	0.15	0.15	0.15	0.15	0.15	0.15	0.15	0.15	0.15	0.15	0.15
Feb-II	0.15	0.15	0.15	0.15	0.15	0.15	0.15	0.15	0.15	0.15	0.15
Feb-III	0.20	0.20	0.20	0.15	0.15	0.15	0.15	0.15	0.15	0.15	0.15
Mar-I	0.25	0.25	0.20	0.15	0.15	0.15	0.15	0.15	0.15	0.15	0.15
Mar-II	0.30	0.30	0.25	0.20	0.15	0.15	0.15	0.15	0.15	0.15	0.15
Mar-III	0.35	0.35	0.25	0.20	0.20	0.20	0.15	0.15	0.15	0.15	0.15
Apr-I	0.40	0.40	0.30	0.25	0.20	0.20	0.15	0.15	0.15	0.15	0.15
Apr-II	0.50	0.50	0.40	0.25	0.25	0.25	0.20	0.15	0.15	0.15	0.15
Apr-III	0.50	0.50	0.50	0.30	0.25	0.25	0.20	0.15	0.15	0.15	0.15
May-I	0.50	0.50	0.50	0.40	0.30	0.30	0.25	0.15	0.15	0.15	0.15
May-II	0.50	0.50	0.50	0.50	0.40	0.40	0.25	0.15	0.15	0.15	0.15
May-III	0.50	0.50	0.50	0.50	0.50	0.50	0.30	0.20	0.15	0.15	0.15
Jun-I	0.50	0.50	0.50	0.50	0.50	0.50	0.40	0.20	0.20	0.15	0.15
Jun-II	0.50	0.50	0.50	0.50	0.50	0.50	0.50	0.25	0.20	0.15	0.15
Jun-III	0.50	0.50	0.50	0.50	0.50	0.50	0.50	0.25	0.25	0.20	0.15
Jul-I	0.50	0.50	0.50	0.50	0.50	0.50	0.50	0.30	0.25	0.20	0.15
Jul-II	0.50	0.50	0.50	0.50	0.50	0.50	0.50	0.40	0.30	0.25	0.20
Jul-III	0.50	0.50	0.50	0.50	0.50	0.50	0.50	0.50	0.40	0.25	0.20
Aug-I	0.40	0.40	0.40	0.40	0.40	0.40	0.40	0.50	0.50	0.30	0.25
Aug-II	0.40	0.40	0.40	0.40	0.40	0.40	0.40	0.40	0.40	0.40	0.25
Aug-III	0.40	0.40	0.40	0.40	0.40	0.40	0.40	0.40	0.40	0.50	0.30
Sep-I	0.40	0.40	0.40	0.40	0.40	0.40	0.40	0.40	0.40	0.40	0.40
Sep-II	0.15	0.15	0.15	0.15	0.15	0.15	0.15	0.15	0.15	0.15	0.50
Sep-III	0.15	0.15	0.15	0.15	0.15	0.15	0.15	0.15	0.15	0.15	0.15
Oct-I	0.15	0.15	0.15	0.15	0.15	0.15	0.15	0.15	0.15	0.15	0.15
Oct-II	0.15	0.15	0.15	0.15	0.15	0.15	0.15	0.15	0.15	0.15	0.15
Oct-III	0.15	0.15	0.15	0.15	0.15	0.15	0.15	0.15	0.15	0.15	0.15
Nov-I	0.15	0.15	0.15	0.15	0.15	0.15	0.15	0.15	0.15	0.15	0.15
Nov-II	0.15	0.15	0.15	0.15	0.15	0.15	0.15	0.15	0.15	0.15	0.15
Nov-III	0.15	0.15	0.15	0.15	0.15	0.15	0.15	0.15	0.15	0.15	0.15
Dec-I	0.15	0.15	0.15	0.15	0.15	0.15	0.15	0.15	0.15	0.15	0.15
Dec-II	0.15	0.15	0.15	0.15	0.15	0.15	0.15	0.15	0.15	0.15	0.15
Dec-III	0.15	0.15	0.15	0.15	0.15	0.15	0.15	0.15	0.15	0.15	0.15

3.19 FORECASTING PROCEDURES

While a validated model with a fixed set of parameters and rules is a pre-requisite, for real time forecasts however, additional information about the future state of the system variables is required. In SRM+G there are four major system variables, viz. temperature, precipitation, snow-covered area and glacier-exposed area.

While temperature and precipitation have to be obtained from external sources, i.e. medium to long range weather prediction from meteorological services or a statistical approach based on historical weather conditions WinSRM offers an inherent approach to predict the future depletion of the snow-covered area. This “Modified Depletion Curve” method[22] is also adopted in ExcelSRM. Nevertheless, the forecast of input variables is still an important challenge for all snow & glacier melt runoff models.

3.19.1 Extrapolation of the Snow-Covered Area

The future course of the depletion curves of the snow coverage can be estimated from the so-called “Modified Depletion Curve” (Martinec et al. 2011). These curves are derived from the conventional depletion curves by replacing the time scale with the cumulative daily snow-melt depth. Consequently, the modified depletion curves start with the maximum snow cover during the winter half year[23]. The decline of the modified depletion curves depends on the initial accumulation of snow and not on the climatic conditions. These curves therefor are a representation the initial snow-water equivalent.

For the Tarbela Basin, modified depletion curves have been calculated for each of the 11 elevation zones for the years 2003 – 2012, as snow-covered areas from MODIS snow-cover products are available since 26th February 2000. An example of these curves for elevation zone 7 (3,769 m asl.)[24] and zone 10 (5,240 m asl.)**[19]** can be found in Figure 3-25 and Figure 3-26. While in zone 7 in most years, the snow is totally melted after 650 accumulated degree-days, in zone 10 up-to 15%-35% of the area remains covered by snow all over the summer. On basis of these observed modified depletion curves, a statistical analysis was performed for each elevation zone in order to identify the upper (90%) and lower (10%) limiting depletion curves. The limiting modified depletion curves for all zones can be found in Table 3-14. Given the actual snow cover at a certain cumulated melt-depth of an elevation zone, the position in-between the limiting curves can be determined by linear interpolation. This position is an indicator of the initial snow depth, or the snow-water equivalent respectively, and defines the characteristic modified depletion curve for this zone in the actual year. This characteristic curve can be used to extrapolate the future depletion in this elevation zone according to the following degree-days.

The limiting modified depletion curves given in Table 3-14 are included into ExcelSRM+G. According to the observed daily temperatures, the accumulated degree-days, since the latest maximum snow-cover in the winter half-year, are calculated for each elevation zone. When the intended simulation run ends later than observed snow-cover area data exists, which is usually the case when forecasting, the characteristic modified depletion curve for that year is

[22] SRM User’s Manual Chap. 7.1

[23] In SRM the modified depletion curves start at the beginning of the summer half year (1st April)

[24] Mean hypsometric elevation of the elevation zone

determined using the most recent snow-covered area. The further decline of the snow-covered area until the end of the simulation run, is extrapolated by that characteristic curve.

The above procedure is applied until end of August, when usually all snow is melted or the minimum snow cover is experienced in the higher zones. From September onward the snow cover can start building up again in the higher altitudes. As the increase of the snow cover cannot be predicted by the modified depletion curve approach, the most actual snow-covered area is used for the following forecasting period.

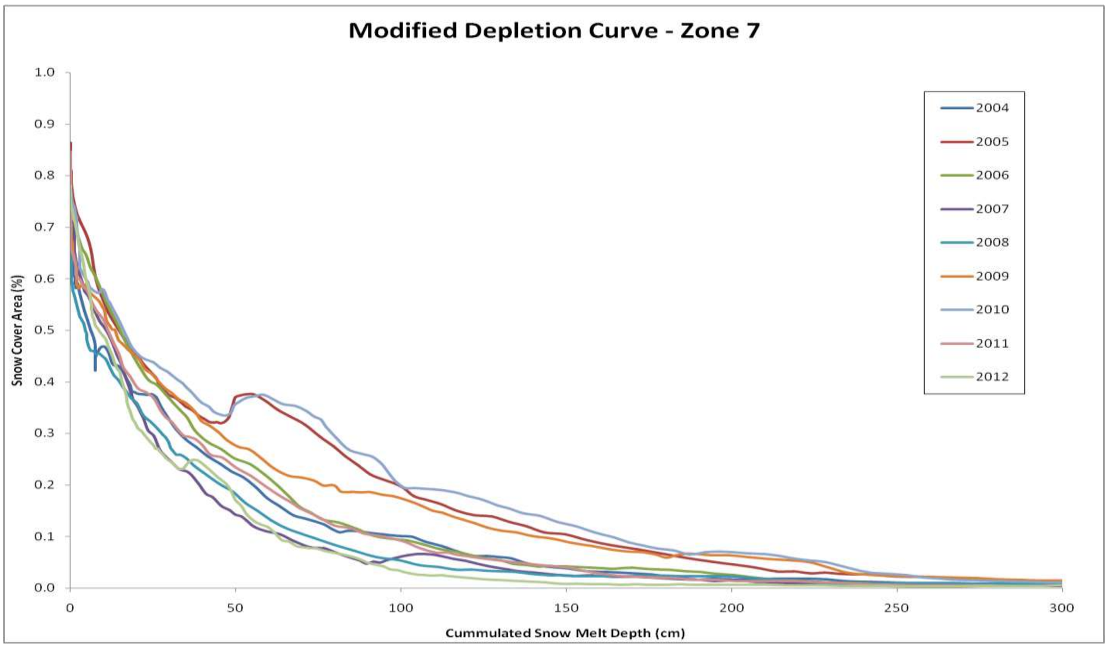

Figure 3-25: Modified Depletion Curves of Elevation Zone 7

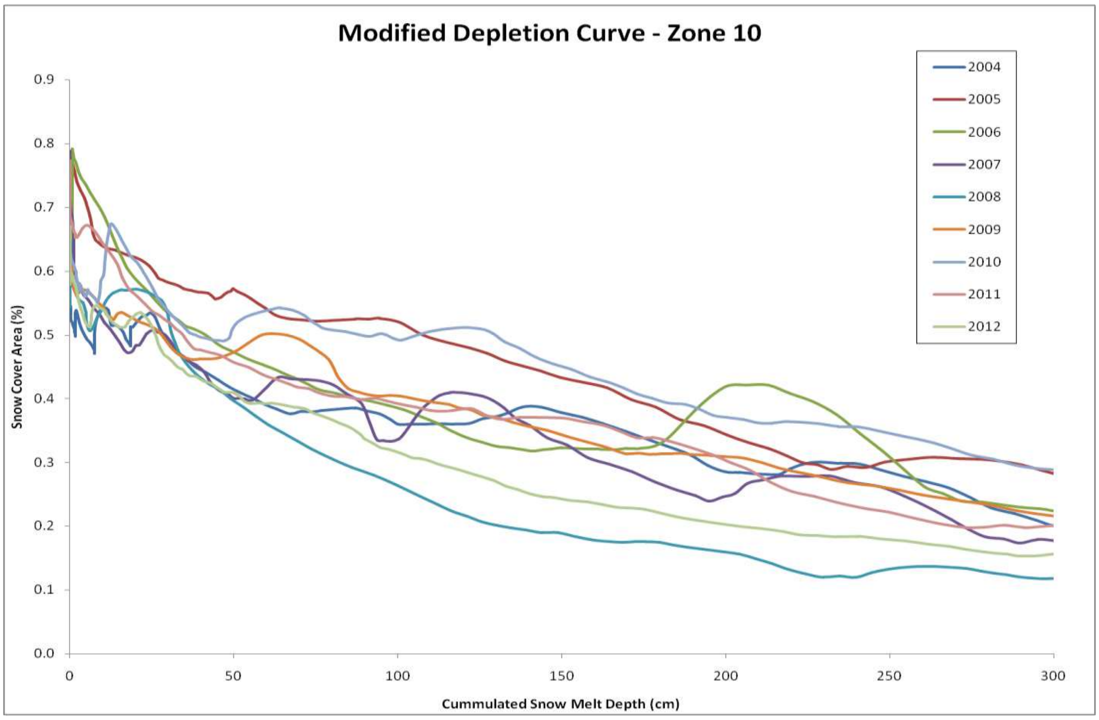

Figure 3-26: Modified Depletion Curves of Elevation Zone 10

Table 3-14: Limiting Modified Depletion Curves for the Upper Indus Basin

Accumulated Melt Depth (cm)	Lower (10%) and Upper (90%) Limiting Depletion Curves for Each Elevation Zone																					
	Zone 1		Zone 2		Zone 3		Zone 4		Zone 5		Zone 6		Zone 7		Zone 8		Zone 9		Zone 10		Zone 11	
	10%	90%	10%	90%	10%	90%	10%	90%	10%	90%	10%	90%	10%	90%	10%	90%	10%	90%	10%	90%	10%	90%
0	0.000	0.010	0.004	0.050	0.085	0.410	0.170	0.458	0.420	0.720	0.613	0.780	0.770	0.860	0.730	0.780	0.620	0.680	0.640	0.720	0.780	0.880
5	0.000	0.010	0.004	0.049	0.083	0.400	0.245	0.473	0.349	0.513	0.394	0.521	0.513	0.652	0.479	0.570	0.337	0.443	0.305	0.421	0.413	0.494
10	0.000	0.010	0.004	0.039	0.126	0.339	0.183	0.341	0.269	0.422	0.298	0.438	0.438	0.576	0.389	0.510	0.269	0.378	0.268	0.377	0.365	0.418
15	0.000	0.010	0.014	0.054	0.076	0.278	0.149	0.282	0.221	0.360	0.242	0.416	0.361	0.494	0.336	0.480	0.228	0.360	0.236	0.334	0.349	0.411
20	0.000	0.010	0.012	0.071	0.048	0.199	0.118	0.225	0.173	0.291	0.212	0.388	0.334	0.466	0.304	0.464	0.204	0.344	0.209	0.296		
25	0.000	0.010	0.004	0.065	0.035	0.134	0.091	0.193	0.138	0.255	0.183	0.340	0.283	0.419	0.276	0.447	0.167	0.301	0.192	0.285		
30	0.000	0.010	0.002	0.044	0.030	0.098	0.060	0.159	0.119	0.232	0.157	0.294	0.256	0.394	0.244	0.410	0.136	0.266	0.179	0.274		
40	0.000	0.010	0.001	0.011	0.020	0.057	0.037	0.110	0.078	0.199	0.107	0.226	0.204	0.340	0.192	0.356	0.118	0.233	0.171	0.235		
50	0.000	0.010	0.001	0.005	0.011	0.043	0.027	0.071	0.058	0.175	0.076	0.167	0.159	0.303	0.148	0.325	0.101	0.214	0.150	0.210		
60	0.000	0.010	0.001	0.003	0.001	0.040	0.019	0.058	0.039	0.120	0.061	0.144	0.127	0.284	0.120	0.298	0.086	0.193	0.140	0.192		
70	0.000	0.010	0.001	0.003	0.001	0.025	0.014	0.045	0.025	0.086	0.042	0.121	0.110	0.272	0.101	0.271	0.082	0.172	0.136	0.176		
80			0.000	0.002	0.001	0.017	0.010	0.032	0.014	0.069	0.030	0.100	0.089	0.244	0.081	0.240	0.079	0.148				
90			0.000	0.002	0.001	0.005	0.008	0.029	0.009	0.052	0.024	0.085	0.075	0.214	0.064	0.207	0.072	0.132				
100			0.000	0.002	0.001	0.004	0.006	0.025	0.008	0.044	0.018	0.069	0.062	0.181	0.057	0.188	0.064	0.122				
110					0.001	0.004	0.004	0.019	0.004	0.037	0.015	0.062	0.049	0.153	0.049	0.166	0.058	0.112				
120					0.001	0.003	0.002	0.010	0.003	0.036	0.013	0.058	0.039	0.140	0.042	0.153	0.055	0.100				
130					0.000	0.000	0.001	0.008	0.000	0.031	0.012	0.059	0.034	0.129	0.034	0.139	0.054	0.090				
140							0.001	0.006	0.001	0.026	0.009	0.060	0.029	0.117	0.030	0.127						
150							0.001	0.005	0.001	0.022	0.007	0.056	0.024	0.101	0.025	0.113						
175									0.001	0.011	0.005	0.034	0.017	0.076	0.022	0.072						
200											0.004	0.021	0.011	0.051	0.020	0.054						
225											0.004	0.017	0.008	0.039	0.014	0.042						
250											0.003	0.014	0.006	0.036	0.013	0.030						
275											0.003	0.010	0.004	0.026								
300											0.002	0.008	0.004	0.015								
350											0.002	0.008	0.004	0.009								
400													0.003	0.006								
450													0.002	0.005								

3.20 SEASONAL FORECASTS

As seasonal[25] meteorological forecasts still only give a rough indication of "warmer" or "cooler" respectively "drier" or "wetter" compared to the average conditions, for the Kharif season flow volume forecasts a scenario approach is used. This forecast is issued by the end of March each year. At that date, the snow-covered area, temperature and precipitation for the following six Kharif month April – September have to be forecasted.

In order to predict at the end of March the depletion of the snow-covered area in each elevation zone of the basin in the following 6 month, SRM's "Modified Depletion Curve" approach is applied. A single characteristic depletion curve is determined for all zones using the highest elevation zone with more than 60 accumulated degree-days[26] as the "key zone". The observed snow-cover depletion in relation to the minimal and maximal historical depletion at the actual number of degree-days of this key zone is applied as the characteristic depletion curve for all zones in that specific year.

According to the scenario approach, for each year to be forecasted, e.g. Kharif 2013, scenario runs are carried out for all years where historical temperature and precipitation data is available[27]. Thus for each year an ensemble of total Kharif inflows to Tarbela representing various historic weather conditions is obtained that can be evaluated by statistical means. For this purpose, an Excel application (see Figure 3-27) has been developed to perform the subsequent statistical analysis where besides the standard sample parameters, also frequency distributions are calculated, whereby the "most likely" (50% probability) flow as well as flows under "dry" (10%) or "wet" (90%) conditions can be identified. Different distribution functions can be chosen i.e. "Normal[28]", "Pearson III" or "Plotting Position" as well as the probability level (%) of "dry" and "wet" years can be defined freely.

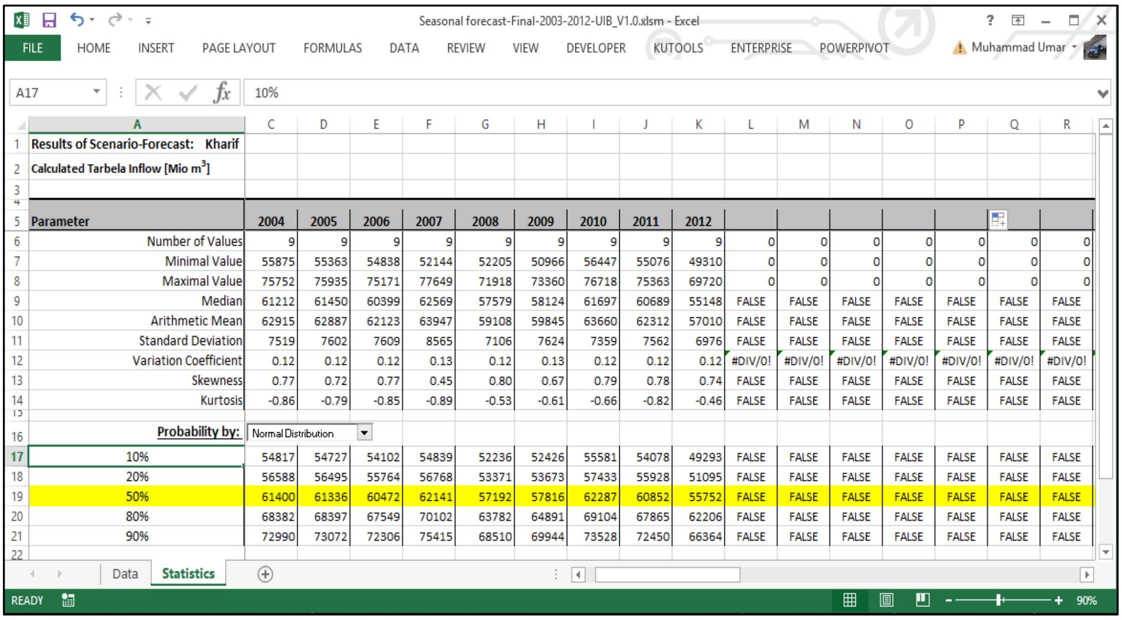

Results of Scenario-Forecast: Kharif
Calculated Tarbela Inflow [Mio m³]

Parameter	2004	2005	2006	2007	2008	2009	2010	2011	2012							
Number of Values	9	9	9	9	9	9	9	9	9	0	0	0	0	0	0	0
Minimal Value	55875	55363	54838	52144	52205	50966	56447	55076	49310	0	0	0	0	0	0	0
Maximal Value	75752	75935	75171	77649	71918	73360	76718	75363	69720	0	0	0	0	0	0	0
Median	61212	61450	60399	62569	57579	58124	61697	60689	55148	FALSE	FALSE	FALSE	FALSE	FALSE	FALSE	FALSE
Arithmetic Mean	62915	62887	62123	63947	59108	59845	63660	62312	57010	FALSE	FALSE	FALSE	FALSE	FALSE	FALSE	FALSE
Standard Deviation	7519	7602	7609	8565	7106	7624	7359	7562	6976	FALSE	FALSE	FALSE	FALSE	FALSE	FALSE	FALSE
Variation Coefficient	0.12	0.12	0.12	0.13	0.12	0.13	0.12	0.12	0.12	#DIV/0!	#DIV/0!	#DIV/0!	#DIV/0!	#DIV/0!	#DIV/0!	#DIV/0!
Skewness	0.77	0.72	0.77	0.45	0.80	0.67	0.79	0.78	0.74	FALSE	FALSE	FALSE	FALSE	FALSE	FALSE	FALSE
Kurtosis	-0.86	-0.79	-0.85	-0.89	-0.53	-0.61	-0.66	-0.82	-0.46	FALSE	FALSE	FALSE	FALSE	FALSE	FALSE	FALSE
Probability by:	Normal Distribution															
10%	54817	54727	54102	54839	52236	52426	55581	54078	49293	FALSE	FALSE	FALSE	FALSE	FALSE	FALSE	FALSE
20%	56588	56495	55764	56768	53371	53673	57433	55928	51095	FALSE	FALSE	FALSE	FALSE	FALSE	FALSE	FALSE
50%	61400	61336	60472	62141	57192	57816	62287	60852	55752	FALSE	FALSE	FALSE	FALSE	FALSE	FALSE	FALSE
80%	68382	68397	67549	70102	63782	64891	69104	67865	62206	FALSE	FALSE	FALSE	FALSE	FALSE	FALSE	FALSE
90%	72990	73072	72306	75415	68510	69944	73528	72450	66364	FALSE	FALSE	FALSE	FALSE	FALSE	FALSE	FALSE

Figure 3-27: Statistical Analysis of Kharif Inflow Scenario Ensembles

25 Falls into the meteorological classification "long-range"
26 A characteristic value for the Upper Indus Basin
27 For the time being 2003 – 2012
28 = Gaussian

In order to evaluate the accuracy of the above described scenario approach, hind-casts for the years 2004 – 2012 have been carried out. In Table 3-15 and Table 3-16 a comparison between the observed Tarbela inflow and the forecasted flows by SRM+G and IRSA forecasts is given (Comparison of Kharif and Rabi forecast is done separately). The error is calculated as the difference of simulated – observed flows, while the average error is calculated using the absolute error values. Although the prediction accuracy varies from year to year, on average of the last 8 years SRM+G forecasts show a significant improvement compared to the forecasts given by IRSA. However, this is not good as compared to the seasonal Early Kharif forecasts (see Table 3-16).

Table 3-15: Comparison of Total Kharif Season Forecast Accuracy (MAF)

Total Kharif Season [SRM+G]					Total Kharif Season [IRSA]		
Years	**Observed**	**Most Likely**	**Error**	**|Error| [ABS]**	**Most Likely**	**Error**	**|Error| [ABS]**
2004	42.1	49.8	18%	18%	49.2	17%	17%
2005	56.0	49.7	-11%	11%	56.1	0%	0%
2006	55.1	49.0	-11%	11%	55.6	1%	1%
2007	49.2	50.4	2%	2%	60.9	24%	24%
2008	46.9	46.4	-1%	1%	55.7	19%	19%
2009	46.8	46.9	0%	0%	51.8	11%	11%
2010	62.3	50.5	-19%	19%	51.5	-17%	17%
2011	48.8	49.3	1%	1%	54.6	12%	12%
2012	45.0	45.2	0%	0%	49.8	11%	11%
Bias/Mean Absolute Error			**-2.2%**	**7.2%**		**8.5%**	**12.4%**
Mean Absolute Error (Excluding Flood year-2010)				**5.8%**			**11.8%**

Table 3-16: Comparison of Early Kharif Accuracy (MAF)

Early Kharif [SRM+G]					Early Kharif [IRSA]		
Years	**Observed**	**Most Likely**	**Error**	**|Error| [ABS]**	**Most Likely**	**Error**	**|Error| [ABS]**
2004	9.1	7.4	-19%	19%	8.1	-11%	11%
2005	9.1	5.1	-45%	45%	9.5	4%	4%
2006	12.1	7.8	-36%	36%	9.5	-21%	21%
2007	10.6	8.3	-22%	22%	10.5	-2%	2%
2008	9.1	8.4	-8%	8%	9.2	1%	1%
2009	9.7	6.9	-29%	29%	8.4	-13%	13%
2010	8.6	5.2	-39%	39%	9.2	7%	7%
2011	10.8	8.6	-20%	20%	9.9	-8%	8%
2012	6.6	8.6	31%	31%	8.9	34%	34%
Bias/Mean Absolute Error			**- 20.8%**	**27.6%**		**-0.8%**	**11.3%**

Table 3-17: Comparison of Late Kharif Accuracy (MAF)

Late Kharif [SRM+G]					Late Kharif [IRSA]		
Years	**Observed**	**Most Likely**	**Error**	**|Error| [ABS]**	**Most Likely**	**Error**	**|Error| [ABS]**
2004	33.0	36.9	12%	12%	41.1	25%	25%
2005	46.9	40.0	-15%	15%	46.5	-1%	1%
2006	43.0	53.2	24%	24%	46.4	8%	8%
2007	38.5	40.7	6%	6%	50.5	31%	31%
2008	37.8	49.4	31%	31%	46.5	23%	23%
2009	37.1	43.5	17%	17%	43.4	17%	17%
2010	53.7	41.2	-23%	23%	42.3	-21%	21%
2011	38.0	45.3	19%	19%	44.7	18%	18%
2012	38.4	35.6	-7%	7%	40.9	7%	7%
Bias/Mean Absolute Error			**7.1%**	**17.1%**		**11.8%**	**16.7%**
Mean Absolute Error (Excluding Flood year-2010)				**16.3%**			**16.1%**

Result are based on Year 2004-2012 comparison
- sign indicates over estimation w.r.t observed flows
+ sign indicates under estimation w.r.t observed flows

3.21 SCENARIO APPROACH

The scenario approach for 10-day flow forecasts is very much similar to the methodology used for the seasonal forecasts. In order to forecast the daily flows, for example during the period May-III 2015, separate simulation runs are carried out with temperature and precipitation data of the same period May-III of each scenario year[29].

The only difference to seasonal forecasts is the prediction of the snow-covered area during the 10-days forecast period. While seasonal forecasts use one single “key zone” for all elevation zones, for 10-day forecasts an individual Modified Depletion Curve is determined for each elevation zone based on its actual snow-cover depletion at the beginning of every forecast period. In addition, the start of the degree-day factor function increase is determined by the actual 10-day average temperature for each individual zone.

[29] At present the years 2003 – 2014

3.22 REVISED METHODOLOGY

3.22.1 Splitting of UIB Model into Lower and Upper Sub-Catchments

ExcelSRM as well as original WinSRM follow a lumped catchment approach, i.e. although they are distributed in terms of elevation zones, they don't support a division into sub-catchments. Accordingly, in the first place the UIB was modelled as a whole and a good accuracy was achieved during model calibration (Table 3-8 and Table 3-9).

However when running hind-casts for historic years the results showed an inferior forecasting capability of the model for seasonal (Kharif) forecasts (Table 3-16 and Table 3-17). In general, forecasted flows where considerably too low in Early Kharif while being too high in Late Kharif.

An in depth analysis of the model variables, i.e. temperature, snow-covered area (SCA), and precipitation, as well as model variables, e.g. runoff and recession coefficients, degree-day factors, etc. didn't give any hint on what was causing the forecasting problems. Only when evaluating the Modified Depletion Curves, that are used to forecast the depletion of snow covered area during the melting period in each zone, some strange behaviour of the catchment was revealed.

In the Karakorum – Western Himalayas region snow usually accumulates during winter and reaches its maximum extension during February / March. Higher altitudes typically have a 90% – 100% snow cover that stays more or less constant until temperature rises above 0°C at that elevation zone and melting starts. In contrast, high elevation zones in UIB, namely zones 9 & 10 (4.500 – 5.500 m asl) in general show a maximum SCA of about 70% whereas lower zones e.g. zone 7 (3.500 – 4.000 m asl) have a higher SCA (see as an example Figure 3-28). Moreover, depletion of SCA starts generally already in February in that zones while mean daily temperature at that altitude is still well below 0°C.

As lower zones where melting already has started in March are used as key-zones for seasonal forecasting by determining the actual snow depth of that very year from Modified Depletion Curves (MDC) statistics, the above described bias between SCA respective MDC of lower and higher zones along with the depletion of SCA without according degree-days in the higher zones always leads to an under-estimation of actual snow available and is almost certainly the reason for subsequent low flow forecasts in Early Kharif.

A closer analysis of the observed unexpected behaviour of zones 9 & 10 revealed, that this is most likely due to the particular meteorological conditions of the south-eastern part of the UIB catchment, namely the Tibetan Plateau. For example Figure 3-29 and Figure 3-30 clearly demonstrate that snow is vanishing on the Tibetan Plateau from these zones during March while same zones are still nearly completely covered in the north-western part of the catchment. The snow covered for Lower UIB is shown in Figure 3-31.

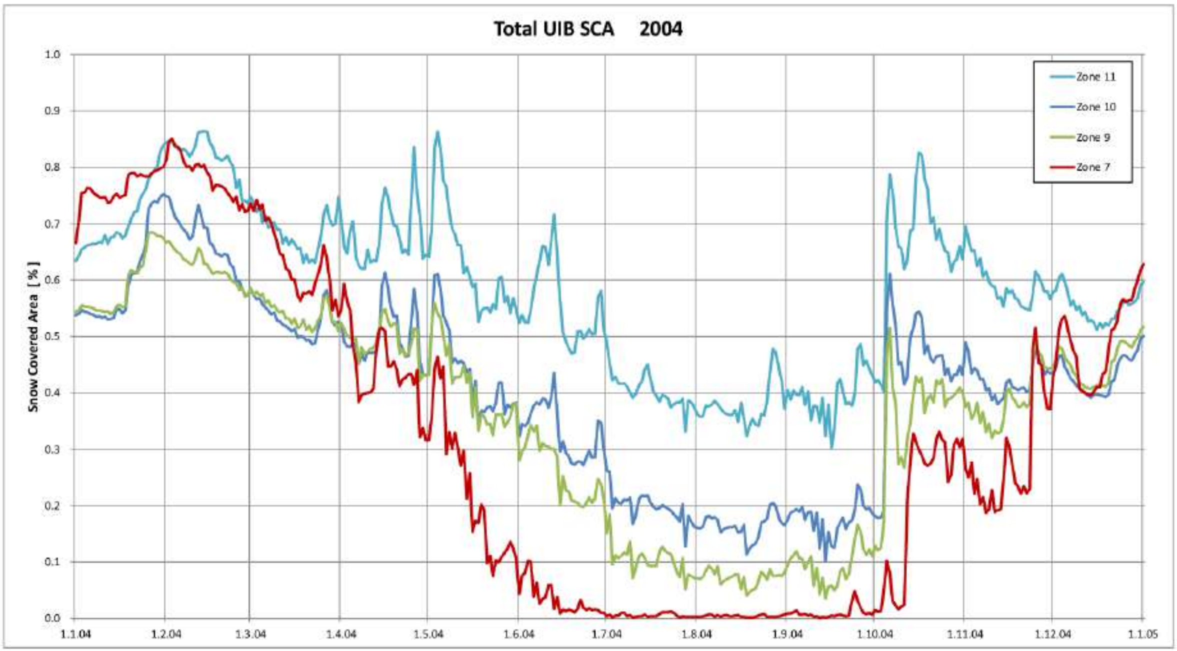

Figure 3-28: Snow-Covered Area in Higher Zones of Total UIB in 2004

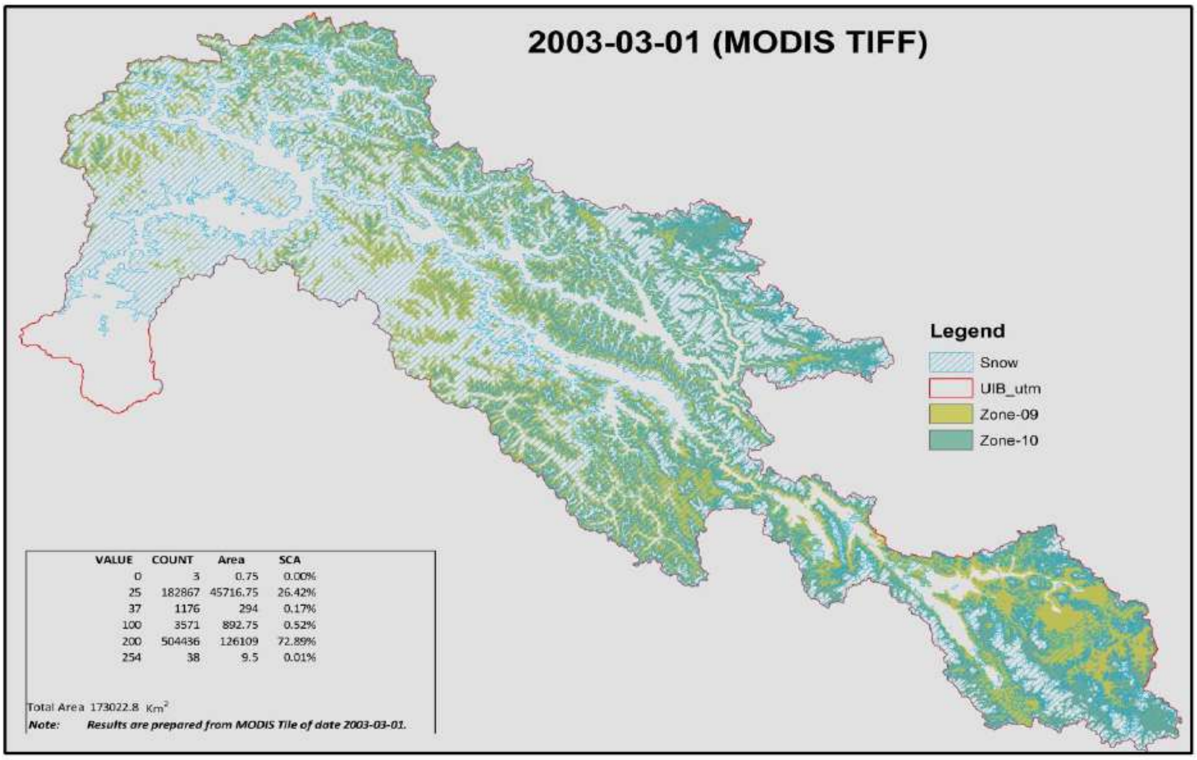

Figure 3-29: Spatial Distribution of Snow-Cover in Zones 9 & 10 on 1st March 2003

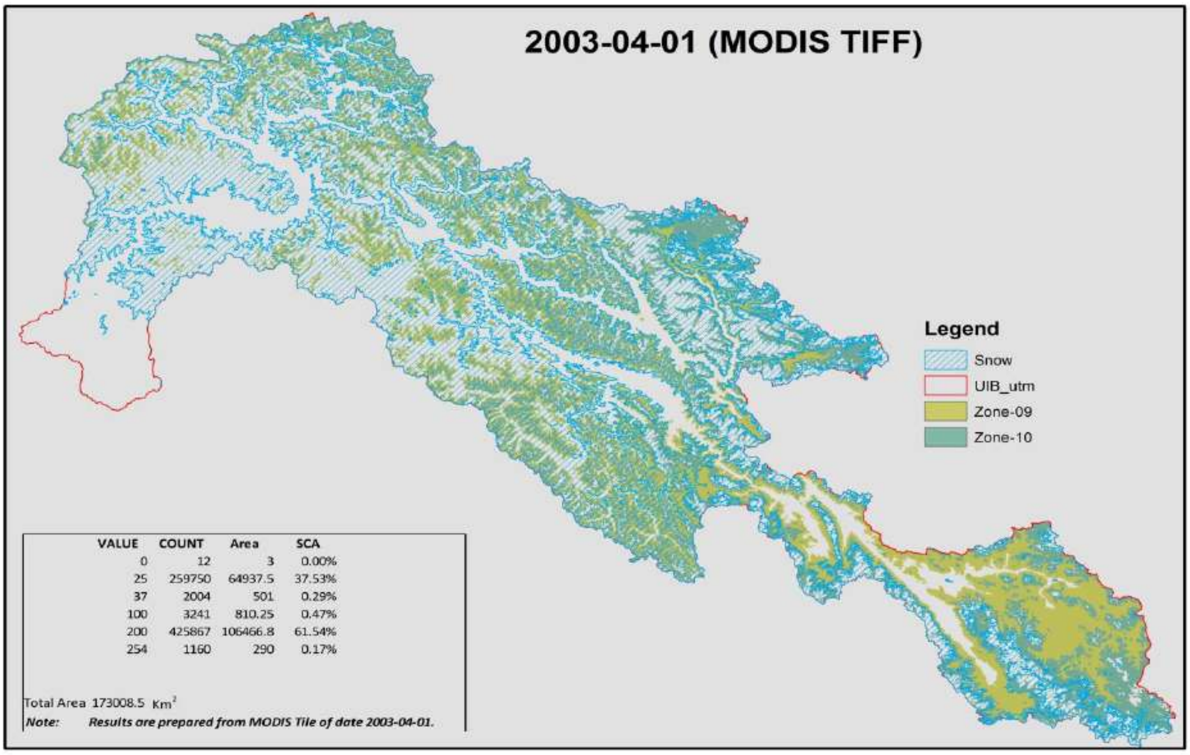

Figure 3-30: Spatial Distribution of Snow-Cover in Zones 9 & 10 on 1st April 2003

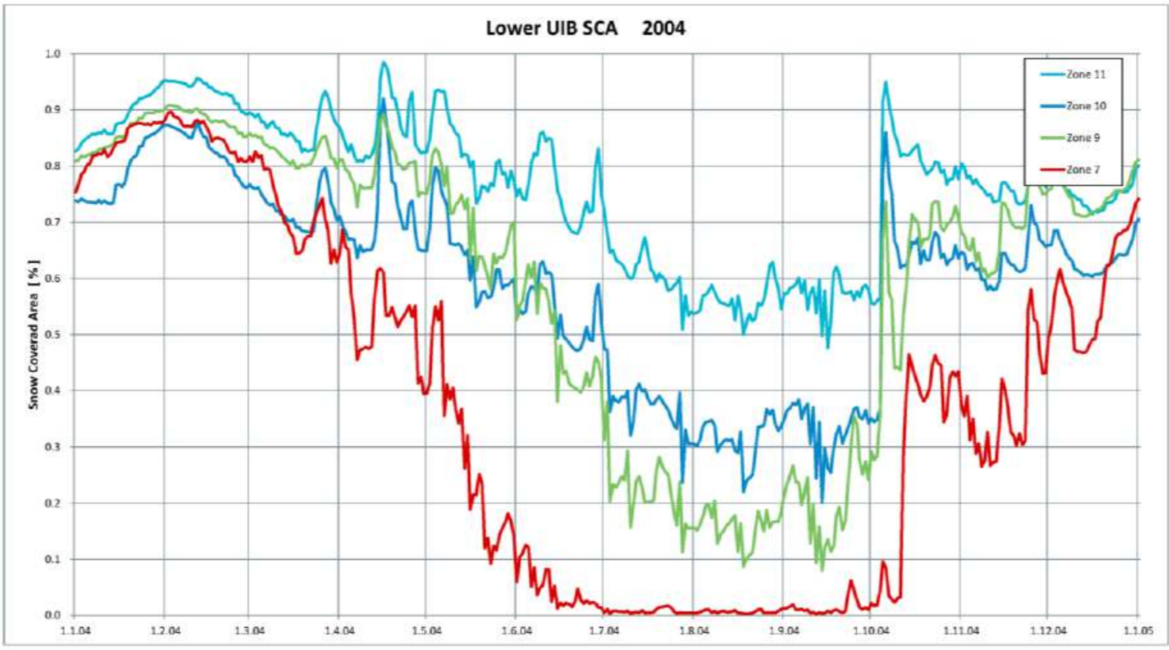

Figure 3-31: Snow-Covered Area in Higher Zones of Lower UIB in 2004

As there is no provision in a lumped model to simulate different behaviour of one elevation zone in different regions of the catchment, the only way to account for the bias between north-western and south-eastern part of UIB is to split the catchment into two, namely Lower and Upper UIB (see Figure 3-32). This measure however, inter alia requires a major modification of ExcelSRM in order to handle sub-catchments which is a basic change compared to the existing SRM approach. Nevertheless a re-calculation of SCA for the Lower UIB (see Figure

3-31 for 2004 results) shows already promising effects of the splitting, as SCA of zones 9 & 10 is significantly higher than before.

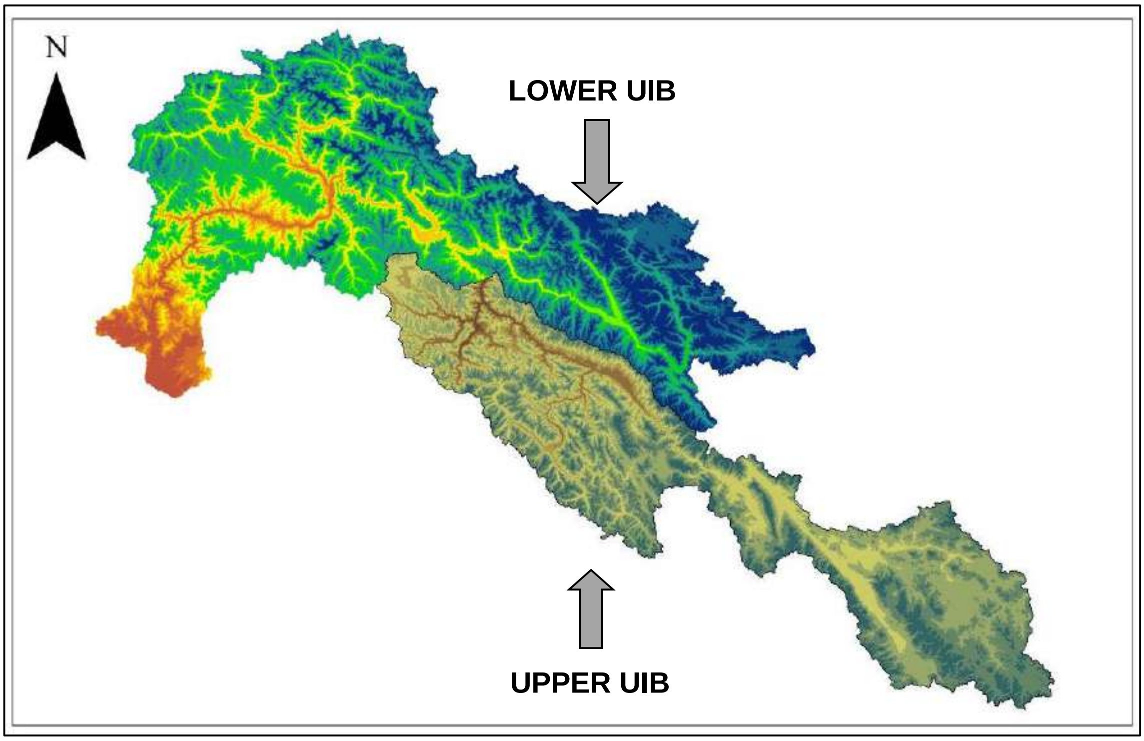

Figure 3-32: Splitting of UIB into Lower and Upper Sub-catchments

3.22.2 Lower UIB

The whole UIB has been divided into two sub-catchments as discussed in earlier sections. The total area of Lower UIB is 101,931 km^2. The Lower UIB is divided into 11 elevation zones having an equal altitude difference of 500 m. The mean hypsometric elevation curve is shown in Figure 3-33.

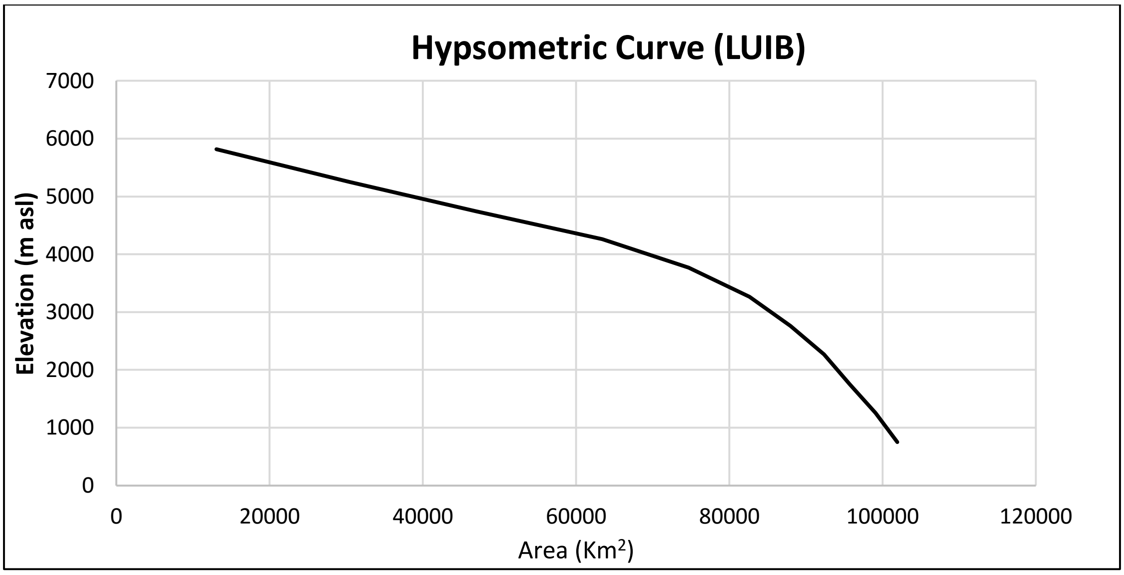

Figure 3-33: Hypsometric Curve for Lower UIB

3.22.3 Temperatures

While rainfall is mainly caused by rainfall cells moving in a certain direction, temperature, within a certain range, is primarily related to altitude. Therefore, it is common for to use station data for temperatures and obtain the regionalisation by using a terrain model and a temperature gradient.

The criteria for selecting an online source for daily temperature data were:

- Free access
- Quick data availability (not more than 2 days after recording)
- Data in downloadable data format (not HTML, PDF or graphic format)

It is a point of concern that either the ultimate user will develop a mechanism for obtaining this data on daily basis for the 22 stations. When the model will be in the forecast mode or there should be another alternative in terms of using the single temperature station which has a good representation for the UIB as well as have a long term data time series availability.

After doing the analysis for the aforementioned concern, Srinagar climatic station was selected as base station for the Lower UIB SRM+G, as this station possess all the information with 'near real-time'[30] daily data from NCDC's GSOD[31] data-set, has a long and quite complete data-series and is located at an altitude of 1,587 m asl which best possibly represents the temperature situation at higher altitudes.

Because of the high impact of temperature on model results, it should be noted that the SRM Manual expressly states that "the measurement of correct air temperatures is difficult, and therefore one good temperature station (even if located outside the basin) may be preferable to several less reliable stations". In the Figure 3-34, the mean temperatures for the Srinagar station for year 2012 to 2014 is shown.

[30] typically less than 2 days delay
[31] Global Surface Summary of the Day. Download at: ftp://ftp.ncdc.noaa.gov/pub/data/gsod/

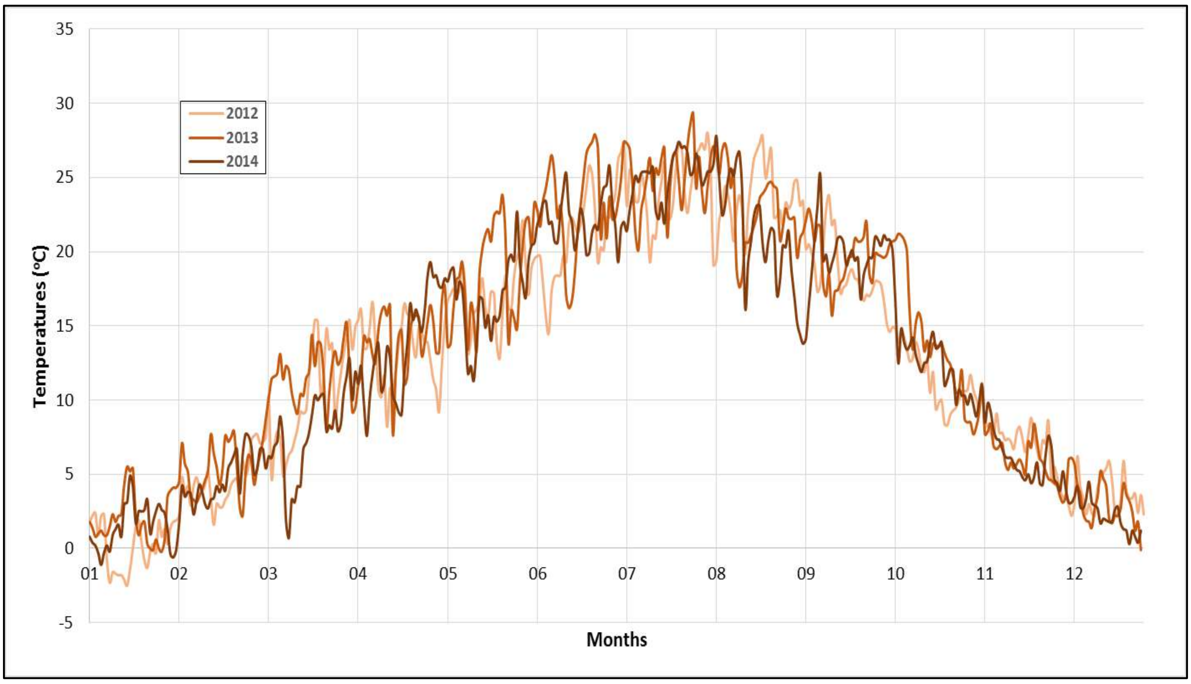

Figure 3-34: Mean Srinagar Temperatures

3.22.4 Snow Covered and Glaciers Exposed Area for Lower UIB

Snow covered as well as glacier exposed area for Lower UIB are shown in Figure 3-35 and Figure 3-36. The process adopted for data preperation and analysis has already been discussed in Section 3.14.3 and 3.14.4.

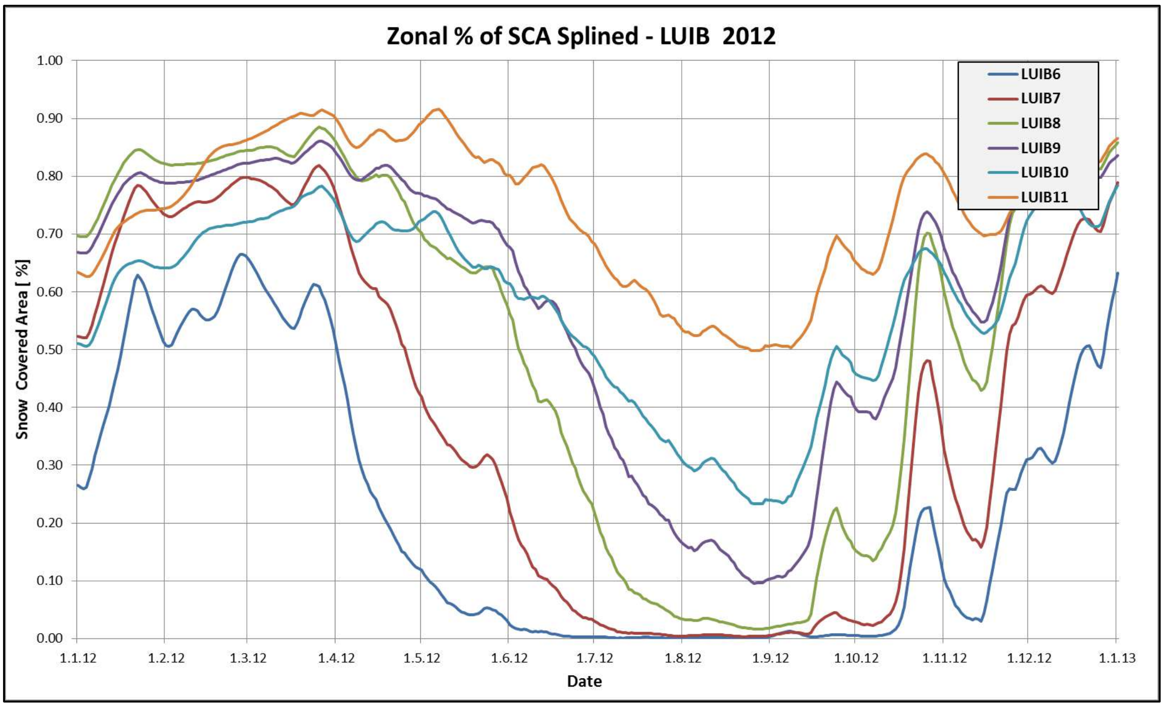

Figure 3-35: Snow Covered Area for Lower UIB

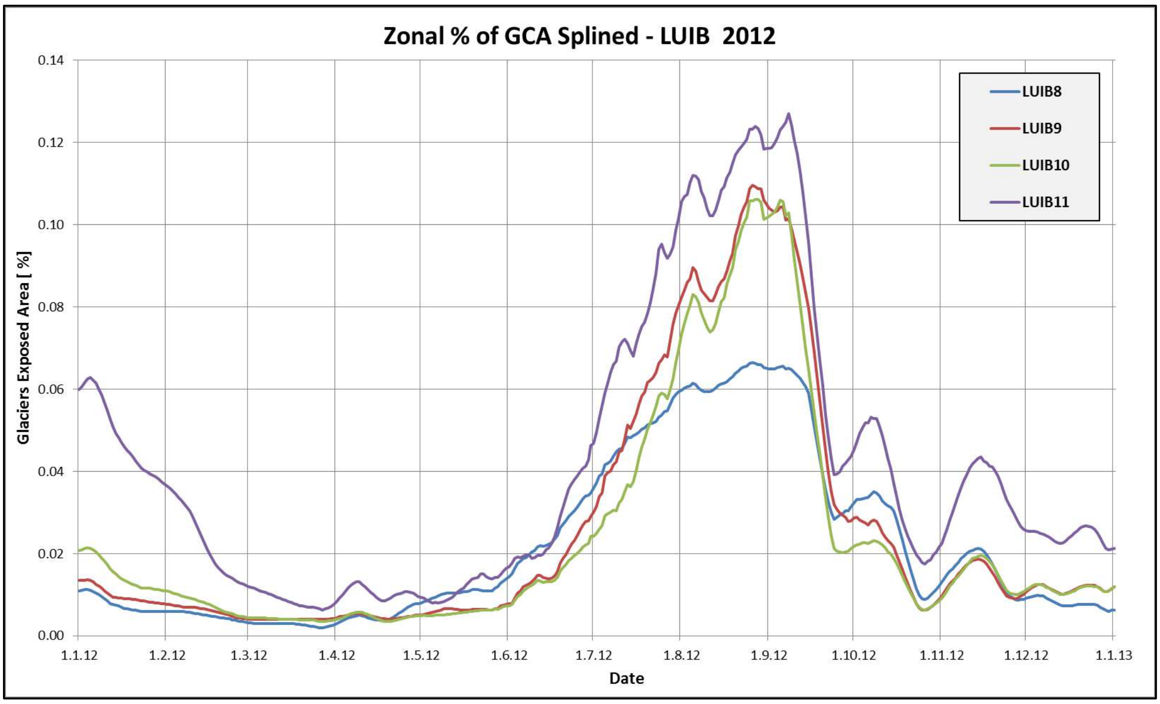

Figure 3-36: Glaciers Exposed Area for Lower UIB

3.22.5 Degree Day Factor Rule for Lower UIB

As in whole UIB case, same methodology is adopted to determine DDF as discussed in Section 5.4.2. Examples of resulting degree-day factor patterns for elevation zones 7 (3501 – 4000 m asl) and 8 (4001 – 4500 m asl) are shown in Figure 3-37. Then linear regression was applied to obtain the number of periods needed to arrive at a degree-day factor of 0.8 [cm/°C/d] which was set as the maximum value. Finally, the values of period's in-between were determined by linear interpolation. As a trend apparent from Table 3-18, the time the snowpack needs to become ripe, is shorter in higher elevations, which might be related to the setting in of monsoon.

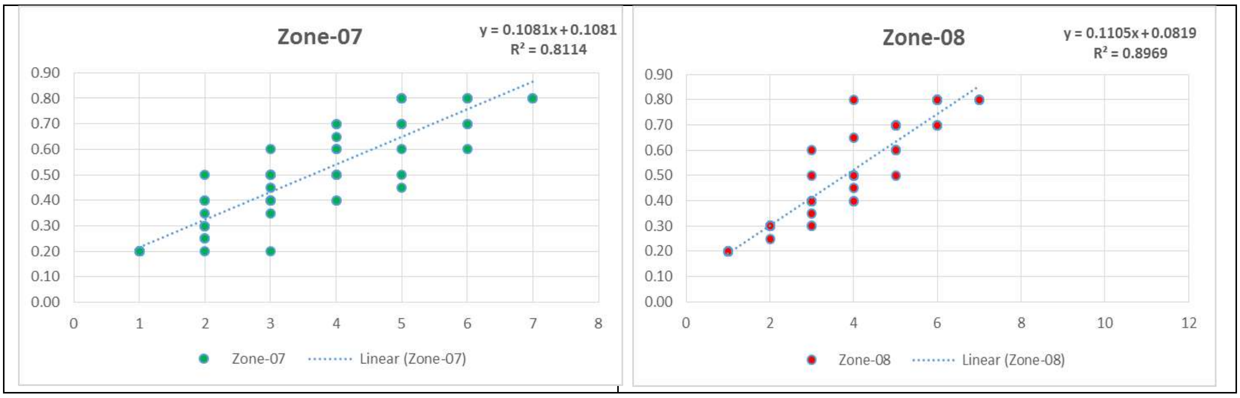

Figure 3-37: Zone-Wise Degree-Day Factor Regression Function

Table 3-18: Zonewise Degree Day Factors for Lower UIB

10-day	Zone-4	Zone-5	Zone-6	Zone-7	Zone-8	Zone-9	Zone-10	Zone-11
1	0.20	0.21	0.22	0.22	0.19	0.18	0.18	0.20
2	0.30	0.32	0.32	0.32	0.30	0.31	0.31	0.33
3	0.39	0.43	0.41	0.43	0.41	0.43	0.44	0.46
4	0.48	0.53	0.51	0.54	0.52	0.56	0.57	0.59
5	0.57	0.64	0.61	0.65	0.63	0.68	0.70	0.72
6	0.67	0.75	0.70	0.80	0.74	0.80	0.80	0.80
7	0.80	0.80	0.80	0.80	0.80			

Temperature rule for the start of DDF has also been modified and developed from mean Srinagar data. Furthermore, this rule will be used for forecasting purposes in Lower UIB. It is shown in Table 3-19.

Table 3-19: 10-day Temperature Rule for Lower UIB

	Zone 4	Zone 5	Zone 6	Zone 7	Zone 8	Zone 9	Zone 10	Zone 11
T_{10d}[32]	9.0	7.0	5.0	4.0	2.0	1.0	1.0	1.0

3.22.6 Forecast Results for Lower UIB

The forecast results for the Lower UIB are very promising and the major error which was causing problem by posing more flows in early Kharif and less flows in the late Kharif has now been eliminated. This was because of the fact that the higher elevations Zone-09 and 10 were showing the different behaviour as explained earlier. Now with the splitting of the whole UIB into two sub-catchment, have improved the results to the extent that one can rate it as a reliable flow forecast. The summarized results of Kharif (Early and Late) forecast are given in the Table 3-20 to Table 3-22.

Table 3-20: Kharif forecast for Lower UIB

KHARIF FORECAST – LUIB						
Years	**Observed [MAF][33]**	**Simulated**			**Error**	**Error [ABS]**
		Minimum [MAF]	**Most Likely [MAF]**	**Maximum [MAF]**		
2003	44	38	41	44	-7%	7%
2004	35	36	39	43	12%	12%
2005	46	36	40	43	-14%	14%
2006	44	37	40	43	-9%	9%
2007	41	36	39	42	-5%	5%
2008	39	32	35	38	-9%	9%
2009	38	38	41	44	8%	8%
2010	51	36	39	42	-22%	22%
2011	39	35	38	41	-2%	2%
2012	36	36	39	42	9%	9%
Average Error (All Years)						**9.8%**
Average Error (Excluding Flood year-2010)						**8.4%**

[32] 10-day average temperature in each elevation zone.
[33] Units = MAF (Million Acre Ft)

Table 3-21: Total Early Kharif Forecast for Lower UIB

EARLY KHARIF FORECAST - LUIB						
Years	Observed [MAF]	Simulated			Error	Error [ABS]
		Minimum [MAF]	Most Likely [MAF]	Maximum [MAF]		
2003	9.64	7.13	8.61	10.08	-11%	11%
2004	7.91	6.09	7.49	8.89	-5%	5%
2005	7.67	6.67	8.12	9.56	6%	6%
2006	9.43	6.37	7.87	9.37	-17%	17%
2007	8.77	6.31	7.72	9.14	-12%	12%
2008	7.83	5.44	6.63	7.81	-15%	15%
2009	8.74	6.87	8.43	9.99	-4%	4%
2010	7.10	6.65	8.00	9.35	13%	13%
2011	8.66	6.49	7.88	9.27	-9%	9%
2012	5.37	6.17	7.61	9.06	42%	42%
Average Error (All Years)						**13.3%**

Table 3-22: Total Late Kharif Forecast for Lower UIB

LATE KHARIF FORECAST - LUIB						
Years	Observed [MAF]	Simulated			Error	Error [ABS]
		Minimum [MAF]	Most Likely [MAF]	Maximum [MAF]		
2003	34	30	32	34	-6%	6%
2004	27	30	32	34	18%	18%
2005	38	29	31	33	-18%	18%
2006	35	30	32	35	-7%	7%
2007	32	29	31	33	-3%	3%
2008	31	26	29	31	-8%	8%
2009	29	30	32	35	11%	11%
2010	43	29	31	33	-28%	28%
2011	30	28	30	32	1%	1%
2012	30	29	31	33	3%	3%
Average Error (All Years)						**10.3%**
Average Error (Excluding Flood year-2010)						**8.4%**

3.23 UPPER UIB

The upper UIB has the total area of 71,470 km^2 and the gauging station is located at Kharmong. UUIB is divided into 07 elevation zones with an elevation band of 500m for each elevation zone. The mean hypsometric elevation curve is shown in Figure 3-38.

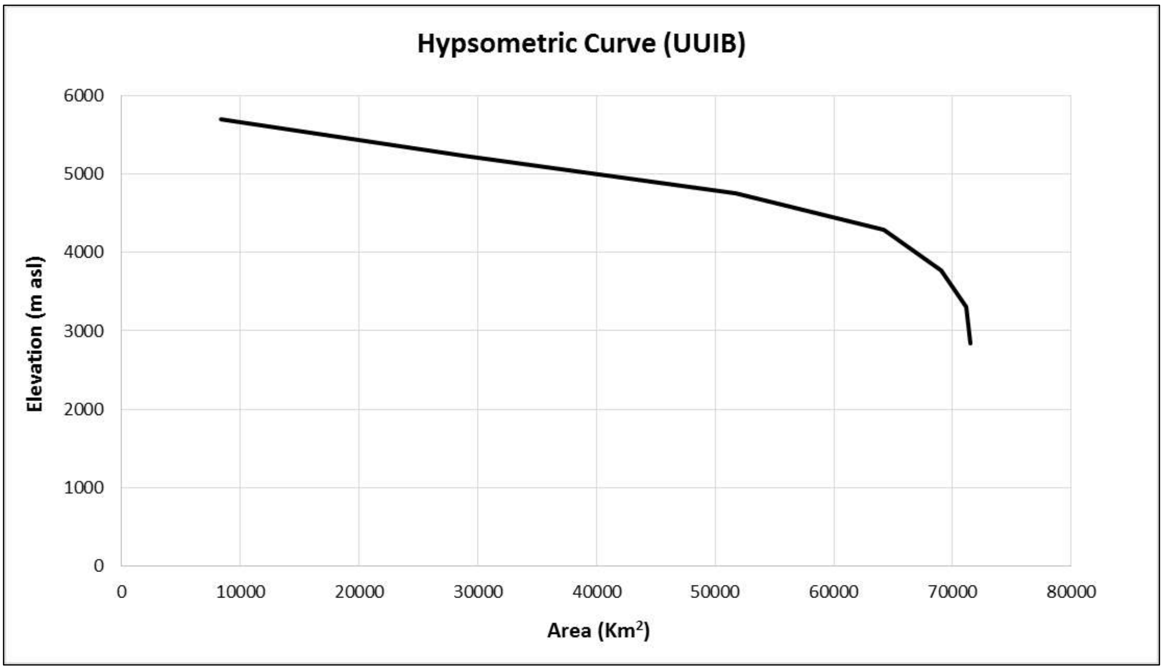

Figure 3-38: Hypsometric Curve for UUIB upstream of Kharmong

3.23.1 Temperature Data Analysis

Temperature for two different stations namely Shiquanhe and Srinagar were analysed for the upper UIB catchment. The final results show that a good representation of the actual condition is represented by the Srinagar temperature station, temperature data from this station was obtained from NCDC's GSOD[34] data-set. The temperature lapse rate of 6°C/1000m was used for the analysis. Srinagar station located at an altitude of 1,587 m asl. While Shiquanhe station is located at an elevation of 4280m asl in the UUIB.

Tibetan plateau and its climate variability as compared to the other portion of UIB has an impact on the Shiquanhe temperatures as this station in located in the Tibetan plateau, the data of this station was not found suitable to use as a base temperature station for UUIB as it over estimate the early Kharif flows for the UUIB which is nowhere close to the actual scenario. This is evident in the comparison of temperatures for these stations at the same elevation as shown in Figure 3-39.

[34] Global Surface Summary of the Day. Download at: ftp://ftp.ncdc.noaa.gov/pub/data/gsod/

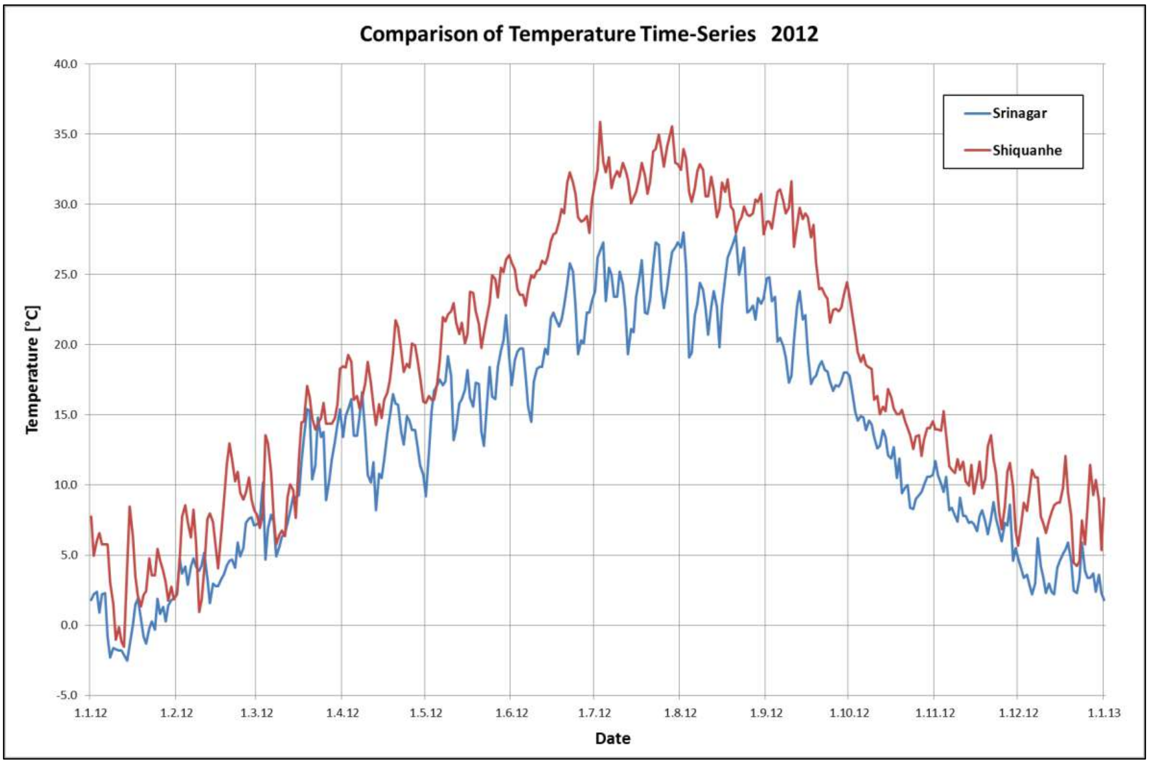

Figure 3-39 Comparison of Temperature Time Series (same elevation)

3.23.2 Snow Covered and Glaciers Exposed Area for Upper UIB

Snow covered as well as glacier exposed area for Upper UIB has been shown in Figure 3-40 and Figure 3-41. The process adopted for data preparation and analysis has already been already discussed in Section 3.14.3 and 3.14.4.

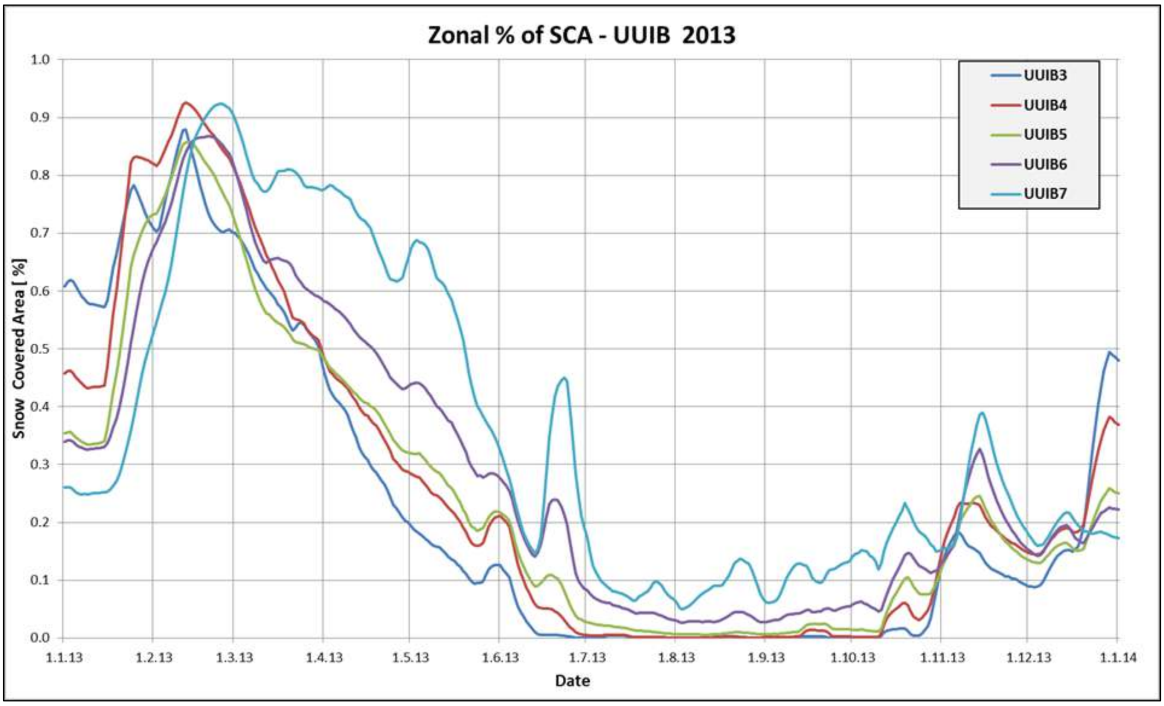

Figure 3-40 Snow Covered Area (SCA) for UUIB

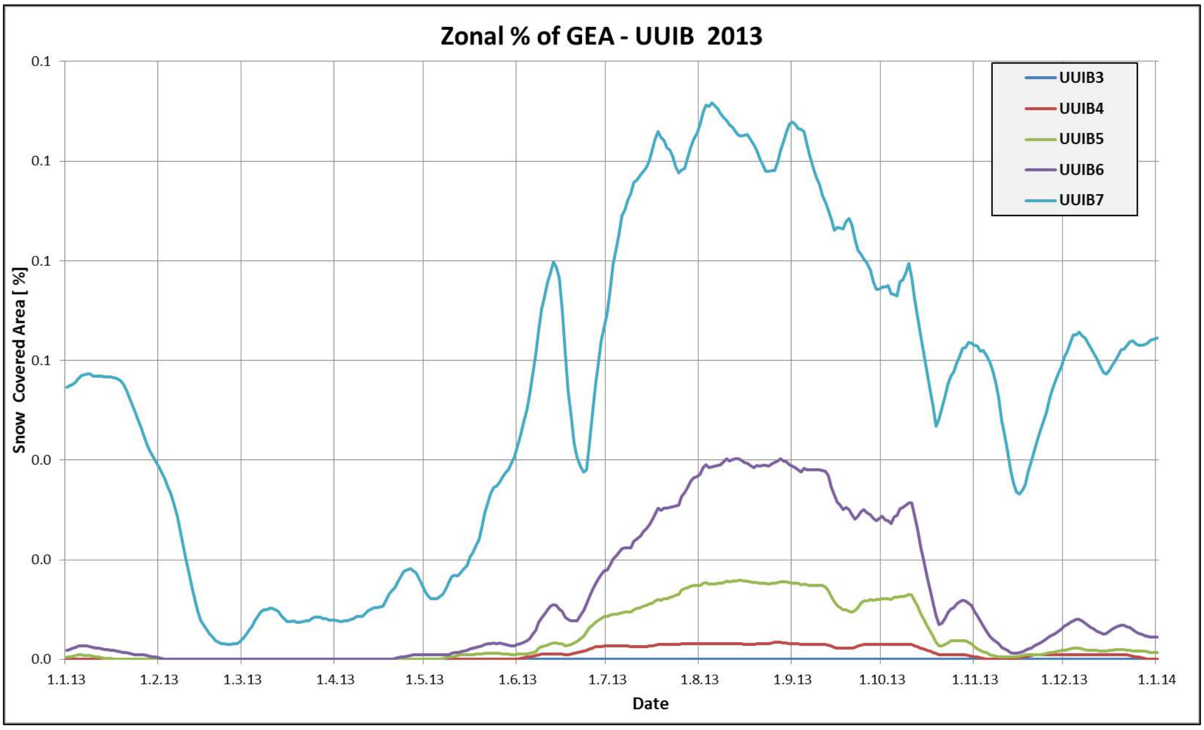

Figure 3-41 Glacier Exposed Area (GEA) for UUIB

3.23.3 Degree Day Factor Rule for Upper UIB

The same technique as described in Section 3.23.5 is being used for carrying out the analysis of DDF for the Upper UIB catchment. The graphical representation is given in Figure 3-42. While the actual values for all the zones are provided in Table 3-23.

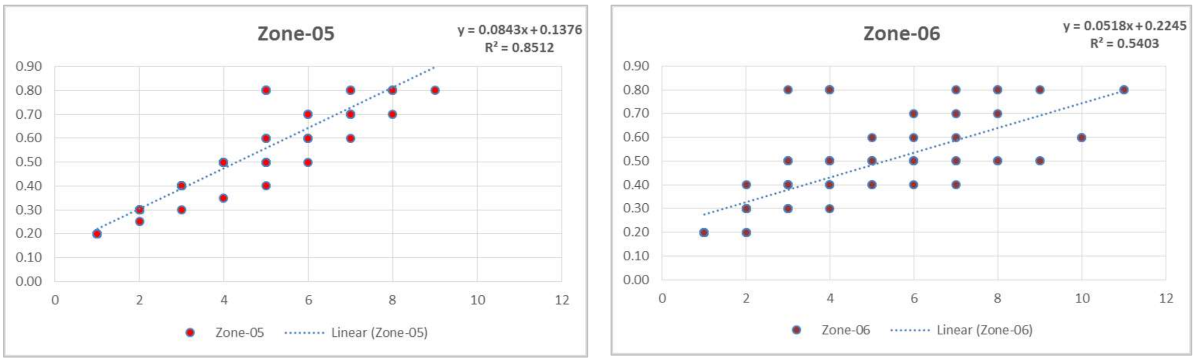

Figure 3-42 Zone-wise degree day factors for Upper UIB

Table 3-23: Elevation Zone Wise Degree Day Factors for Upper UIB

10-day	Zone-1	Zone-2	Zone-3	Zone-4	Zone-5	Zone-6	Zone-7
1	0.37	0.35	0.35	0.52	0.56	0.48	0.60
2	0.43	0.40	0.40	0.59	0.64	0.54	0.70
3	0.49	0.45	0.46	0.66	0.73	0.80	0.80
4	0.54	0.51	0.51	0.73	0.80		
5	0.60	0.56	0.56	0.80			
6	0.66	0.61	0.62				
7	0.71	0.66	0.67				
8	0.80	0.71	0.72				
9		0.80	0.80				

Temperature rule for the start of DDF has also been modified and developed from mean Srinagar data. Furthermore, this rule will be used for forecasting purposes in Upper UIB. It is given in Table 3-24

Table 3-24 10-day Temperature Rule for Upper UIB

	Zone-1	Zone-2	Zone-3	Zone-4	Zone-5	Zone-6	Zone-7
T_{10d}[35]	2.0	2.0	2.0	2.0	0.5	0.5	0.5

3.23.4 Forecast results for total UIB

The forecast results for the total UIB are obtained by combining the results of both Upper and Lower UIB. These results show an overall improvement of the model. A lag time of 3 days for water travelling from Upper UIB (Kharmong) to Tarbela is taken into account before combining the results of both catchments. The comparison of Kharif forecast results with IRSA as well as the UBCWM[36] shows that there is a close competition of forecasts. The Mean Absolute Error (MAE) for all the models are mostly in the same range, while SRM+G shows a little bit better result.

Looking at the 12 year Bias analysis for IRSA as well as WAPDA forecast shows that there is an over estimation of the flows for most of the years while on the other hand, the results generated from SRM+G shows the flows are approximately balanced.
The overall UIB results prepared from SRM+G, IRSA and UBCWM are shown in Table 3-25.

A summarized comparison of IRSA and SRM+G models results are show from Table 3-26 to Table 3-27. This comparison is provided to get an idea regarding the model behaviours during the Early and Late Kharif season. There is an overall improvement of the forecast results for the Kharif forecast of Indus @ Tarbela. SRM+G results show that the absolute average error from 12 years of available data record is approximately less than 10%. On the other hand the IRSA forecast are also nice comparing to the SRM+G results.

[35] 10-day average temperature in each elevation zone.
[36] University of British Columbia watershed model currently in use of PSIHP of WAPDA

Table 3-25: Indus @ Tarbela Kharif Results Comparison for three Models (MAF)

TOTAL KHARIF [SRM+G]					TOTAL KHARIF [IRSA]			TOTAL KHARIF [UBCWM]		
Years	Observed	Most Likely	Error	|Error| [ABS]	Most Likely	Error	|Error| [ABS]	Most Likely	Error	|Error| [ABS]
2003	55.1	51.3	-7%	7%	52.0	-6%	6%	51.6	-6%	6%
2004	42.1	49.4	17%	17%	49.2	17%	17%	51.7	23%	23%
2005	56.0	49.5	-12%	12%	56.1	0%	0%	59.6	6%	6%
2006	55.1	50.1	-9%	9%	55.6	1%	1%	59.6	8%	8%
2007	49.2	49.6	1%	1%	60.9	24%	24%	57.0	16%	16%
2008	46.9	43.8	-7%	7%	55.7	19%	19%	48.1	3%	3%
2009	46.8	50.7	8%	8%	51.8	11%	11%	54.6	17%	17%
2010	62.3	49.9	-20%	20%	51.5	-17%	17%	55.6	-11%	11%
2011	48.8	48.7	0%	0%	54.6	12%	12%	57.6	18%	18%
2012	45.0	49.1	9%	9%	49.8	11%	11%	50.2	12%	12%
2013	53.3	48.6	-9%	9%	52.8	-1%	1%	47.8	-10%	10%
2014	43.0	49.9	16%	16%	52.5	22%	22%	52.2	21%	21%
Bias/Absolute Average Error			**-0.9%**	**9.6%**		**7.7%**	**11.7%**		**8.0%**	**12.6%**
Average Error (Excluding Flood year-2010)				**8.7%**			**11.2%**			**12.8%**

Table 3-26: Indus @ Tarbela Early Kharif Results Comparison (MAF)

EARLY KHARIF [SRM+G]					EARLY KHARIF [IRSA]		
Years	Observed	Most Likely	Error	|Error| [ABS]	Most Likely	Error	|Error| [ABS]
2003	12.0	10.4	-13%	13%	8.1	-32%	32%
2004	9.1	9.0	0%	0%	8.1	-11%	11%
2005	9.1	9.8	7%	7%	9.5	4%	4%
2006	12.1	9.5	-22%	22%	9.5	-21%	21%
2007	10.6	9.5	-10%	10%	10.5	-2%	2%
2008	9.1	7.9	-14%	14%	9.2	1%	1%
2009	9.7	10.0	3%	3%	8.4	-13%	13%
2010	8.6	9.8	15%	15%	9.2	7%	7%
2011	10.8	9.7	-10%	10%	9.9	-8%	8%
2012	6.6	9.3	41%	41%	8.9	34%	34%
2013	8.6	9.2	7%	7%	9.5	11%	11%
2014	6.6	9.8	50%	50%	9.5	44%	44%
Bias/Absolute Average Error			**4.5%**	**16.0%**		**1.3%**	**15.8%**

Table 3-27: Indus @ Tarbela Late Kharif Results Comparison (MAF)

LATE KHARIF [SRM+G]					LATE KHARIF [IRSA]		
Years	**Observed**	**Most Likely**	**Error**	**|Error| [ABS]**	**Most Likely**	**Error**	**|Error| [ABS]**
2003	43.1	40.9	-5%	5%	43.9	2%	2%
2004	33.0	40.4	22%	22%	41.1	25%	25%
2005	46.9	39.7	-15%	15%	46.5	-1%	1%
2006	43.0	40.6	-5%	5%	46.1	7%	7%
2007	38.5	40.0	4%	4%	50.5	31%	31%
2008	37.8	35.9	-5%	5%	46.5	23%	23%
2009	37.1	40.7	10%	10%	43.4	17%	17%
2010	53.7	40.1	-25%	25%	42.3	-21%	21%
2011	38.0	39.0	3%	3%	44.7	18%	18%
2012	38.4	39.8	4%	4%	40.9	7%	7%
2013	44.7	39.5	-12%	12%	43.3	-3%	3%
2014	36.4	40.2	10%	10%	43.1	18%	18%
Bias/Absolute Average Error			**-1.3%**	**10.1%**		**10.2%**	**14.4%**
Average Error (Excluding Flood year-2010)				**8.7%**			**13.7%**

3.24 ASSESSMENT OF CLIMATE CHANGE IMPACT ON UIB

The study is intended to give orientation in the future development of water resources in the Upper Indus Basin under the assumption of different climate change scenarios. Particular interest is on the impact of climate change on downstream water availability e.g., needed for irrigation and how the situation of glaciers might change over the next 100 years. For reasons described below their still remain uncertainties in the reliable description of both future climate situation(s) and in the quantification of its possible impacts on water resources in the UIB. Nevertheless, presented results describe realistic, general developments of the future situation of climate, water and glaciers.

The study uses data from General Circulation Models (GCM) to describe future climate change and uses this information as an input to hydrological models to describe the situation of current, hydro-meteorological parameters as well as the changes they undergo under a B1, an A1b and an A2 climate change scenario.

Emissions Scenarios (SRES)

A1. The A1 storyline and scenario family describes a future world of very rapid economic growth, global population that peaks in mid-century and declines thereafter, and the rapid introduction of new and more efficient technologies. Major underlying themes are convergence among regions, capacity building and increased cultural and social interactions, with a substantial reduction in regional differences in per capita income. The A1 scenario family develops into three groups that describe alternative directions of technological change in the energy system. The three A1 groups are distinguished by their technological emphasis: fossil intensive (A1FI), non-fossil energy sources (A1T), or a balance across all sources (A1B) (where balanced is defined as not relying too heavily on one particular energy source, on the assumption that similar improvement rates apply to all energy supply and end-use technologies).

A2. The A2 storyline and scenario family describes a very heterogeneous world. The underlying theme is self-reliance and preservation of local identities. Fertility patterns across regions converge very slowly, which results in continuously increasing population. Economic development is primarily regionally oriented and per capita economic growth and technological change more fragmented and slower than other storylines.

B1. The B1 storyline and scenario family describes a convergent world with the same global population, that peaks in mid-century and declines thereafter, as in the A1 storyline, but with rapid change in economic structures toward a service and information economy, with reductions in material intensity and the introduction of clean and resource-efficient technologies. The emphasis is on global solutions to economic, social and environmental sustainability, including improved equity, but without additional climate initiatives.

B2. The B2 storyline and scenario family describes a world in which the emphasis is on local solutions to economic, social and environmental sustainability. It is a world with continuously increasing global population, at a rate lower than A2, intermediate levels of economic development, and less rapid and more diverse technological change than in the A1 and B1 storylines. While the scenario is also oriented towards environmental protection and social equity, it focuses on local and regional levels.

Though GCM data from current state of the art models are being used, it is important to understand that modelled parameters may not perfectly describe neither the current nor the future climate situation in all details. While there is great confidence into the general, global trends given by these data, local characteristics may be described with less accuracy with regard to their timing and their magnitude. Reasons are found in our insufficient understanding of the mechanisms and processes that drive climate. The role of ocean currents and sea surface temperatures in predicting (local) climate are not yet fully understood. For the region of the UIB, it is the role of uncertainties the El Nino and its effects on the Indian monsoon that make long term forecasts difficult and causes climate models to produce controversial results. As climate models as well as hydrological models are continuously improved, it is advisable to repeat climate and hydrological studies like this one, to further narrow the spread in predicted climate and hydrological variables, thus increasing our confidence in modelled scenarios.

To gain further trust in modelled results, the consultant simulated extreme situations to define upper and lower limits, or described identical parameters by using different approaches. This is intended to provide more planning security in making adjustments to the projected situations.

3.24.1 Data Used in Climate Analyses and Hydrologic Modelling

The process of modelling meaningful regional scale impacts of future climate change greatly depends on the quality of input data, particularly their consistency and comparability. Bringing together data from different sources, observed and modelled, require intensive pre-processing following strict processing procedures aiming at a harmonization of data inputs in the form of continuous time-series at the required spatial resolution and temporal interval.

While the process of data and model calibration/validation uses observed input parameters, future impact modelling uses outputs from General Circulation Models (GCM). To ensure a continuous modelling these data need to be spatially interpolated, composited to a desired temporal resolution (10-day interval) or down-scaled to spatial resolutions that are meaningful for the study.

Because of limited data availability in the Upper Indus basin, all available data sources/sets were evaluated, firstly to achieve reasonable data coverage and secondly to gain some confidence in data quality. Data from different data sources revealed both, good agreement between distinct climate parameters but also huge discrepancies. Where possible, corrections were applied but only to an extent that is scientifically justifiable.

Time-series were created for variables precipitation and min/max/mean temperature. For this purpose available station data from National Oceanic and Atmospheric Administration's (NOAA) National Climate Data Center (NCDC) were extracted, which includes 19 meteorological stations of the Global Summary of the Day product (GSOD), 13 stations were provided by WAPDA and 7 stations from the Pakistan Meteorological Department (PMD). The final number of useable stations is reduced to a total of 21 stations due to duplicates in stations, erratic climate records or the closure of some stations.

Furthermore, various spatial climate products were tested for their performance and their adequate reproduction of climate variables in the study area. These included precipitation products from The German Weather Service's (DWD) Global Precipitation Climate Centre (GPCC), NASA's Tropical Rainfall Mapping Mission (TRMM), NOAA's Rainfall Estimates (RFE) and temperature data (CRUTEM5 product) from the Climate Research Unit Temperature (CRUTEM) (Osborn and Jones, 2014).

Listed spatial data products cover different temporal periods or come in different spatial and temporal resolutions. They were used to judge the plausibility of data sets, to reveal regions with uncertain data records and finally to composite a best possible product.

The temporal coverage of the prepared time-series was defined by the temporal overlap of the data sets that were selected for processing and for later model input, and is therefore limited to the period from 2003 to 2008.

3.24.1.1 Temperature Data

For the compositing of a gridded, 10-day interval temperature time-series (min, max and mean), records from 21 stations were used (Figure 3-43). Daily records were first aggregated to 10-day intervals and then spatially interpolated using a weighted distance function. For the temporal aggregation, it was sufficient if there was just one measurement within a 10-day period. This is to reduce the temporal bias that is caused by using a temporally varying number of stations in the interpolations.

3.24.1.2 Data processing

Station temperatures were transferred to their sea-level equivalent using a lapse rate of 6.5°C/1000m. After applying a weighted distance interpolation, with the output grid resolution chosen as 1000x1000m^2, pixels of the interpolated grids were projected back to their specific elevation using a digital elevation model of matching spatial resolution (1km^2).

The selection of the spatial resolution as 1km^2 was driven by requirements of the terrain, the number of stations available, resolution of the DEM, and the computing effort in later model runs. Just looking at the 21 climate stations (see Figure 3-43) used in interpolations and distributed over an area of 173.500km^2, chosen spatial resolution may appear as an over-interpretation of data.

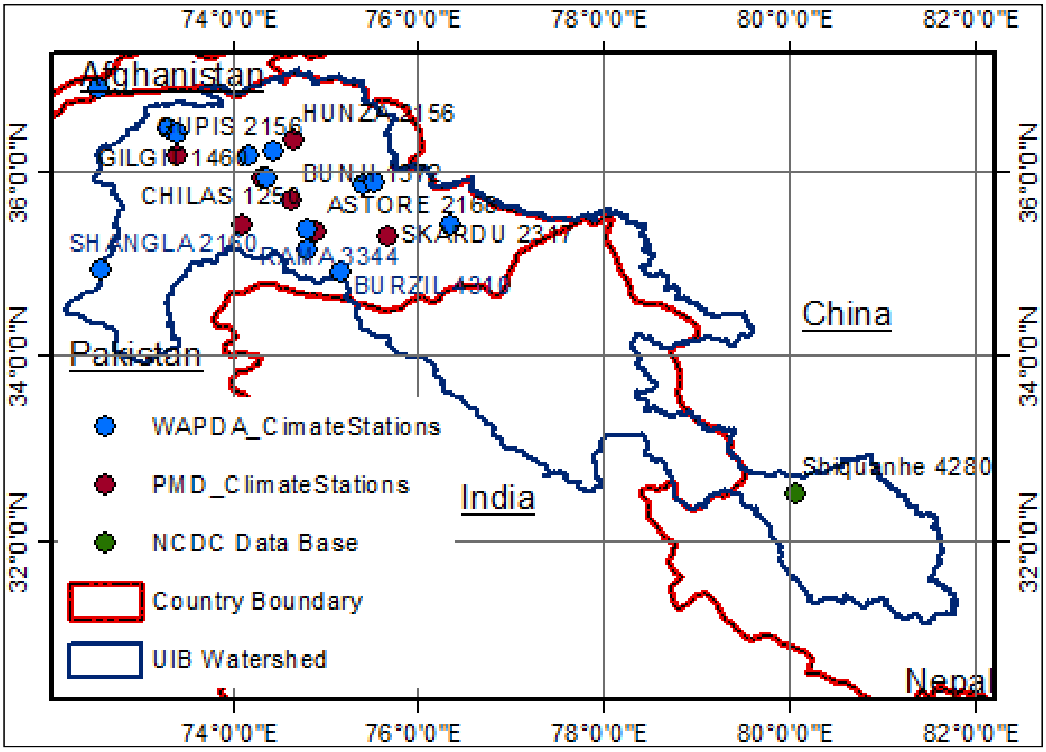

Figure 3-43: Location of Climate Stations used in Temperature Interpolation

The steep terrain however, requires a somewhat higher spatial resolution in order to capture strong vertical temperature gradients and their effects on snow/ice pack.

The procedure for down-scaling temperature data from GCMs resembles the above described steps for interpolation. GCM temperatures were projected to sea-level using the above lapse rate and a DEM degraded to a spatial resolution equivalent to the GCM data. The degraded DEM, where elevations are averaged across a GCM pixel, was prepared from GMTED2010 data. After a distance weighted resampling of the coarse resolution temperature data to a resolution of 1km^2, pixels of the high resolution output were projected back to their proper elevation using a 1km^2 resolving DEM and an identical lapse rate as used for the projection into sea level. For the conversion of monthly to 10-day interval data, a weighted temporal mean was used.

3.24.1.3 Comparison of different data sets

Temperature station data from NCDC, PMD and WAPDA show consistent agreement. After elimination of bad data and an adaptation of their units (Fahrenheit to Centigrade), they were merged and processed into 10-day interval grids.

The irregular distribution of stations across the UIB is one of the data's major weaknesses. While the Pakistani part of the UIB shows denser station coverage, there are no records available for the Indian UIB and only a single station for the Chinese UIB. In spatial interpolations, this gives the Chinese station of Shiquanhe, a strong influence on a vast area that includes all of the India possessed UIB. Because of morphological differences between these areas (Tibetan Plateau), Shiquanhe station records may not be very representative for the Indian UIB.

With climate stations limited to a maximum elevation of 4730m and most stations located between 1200 and 3300m, a prove of vertical temperature variation or vertical changes in lapse rates is not possible.

The CRUTEM4 data set is a long-term, coarse resolution data set providing monthly temperatures averaged over a 5°x5° area. It is useful for the understanding of general temperature trends in a region (Figure 3-60) but less for use in local analysis.

3.24.1.4 Precipitation

Different to temperature, which is strongly driven by topography, the relationship between precipitation and topography is not that clear. Therefore, instead of interpolating between scattered station precipitations records with unforeseeable results, preference was given to different spatial precipitation products derived from satellite measurements.

This includes the global TRMM data set (King et al., 2003), the Afghan RFE product and the South Asia RFE product (Laws et al., 2004). The monthly, station based re-analysis GPCC product (Rudolf et al., 2010) was only used for further verification of the aforementioned products (Table 3-28).

Table 3-28: Characteristics of Various Gridded Precipitation Products.

	Source	Resolution	Interval	Spatial Coverage	Temporal Coverage
GPCC	Station	0.5° (~60km)	Monthly	Global (continent)	Since 1900
TRMM	Satellite	0.25° (~30km)	3-hourly	Global (between +50° and -50° Lat)	Since 1996
RFE_Ag	Satellite, station corrected	0.1° (~12km)	Daily	Figure 3-47	Since Feb. 2002
RFE_SA	Satellite, station corrected	0.1° (~12km)	Daily	Figure 3-47	Since Sep. 2002

3.24.1.5 Data Processing (Observed Period)

Observed precipitation from data sets described in Table 3-28, do not require any particular processing other than temporal aggregation into required temporal intervals (10-day intervals).

3.24.1.6 Comparison of Different Data Sets

As a comparison of the precipitation data sets from Table 3-28 shows, they feature enormous differences in precipitation amounts (Figure 3-44). This leaves uncertainties in the judgment of what is correct and what is the best data set for this study. The two data sets (TRMM and RFE_Ag) originally selected for this study display average precipitation differences of more than 100%. (Figure 3-44). Precipitation from GPCC data confirms the lower TRMM precipitation but both produce less precipitation than the RFE_Ag data.

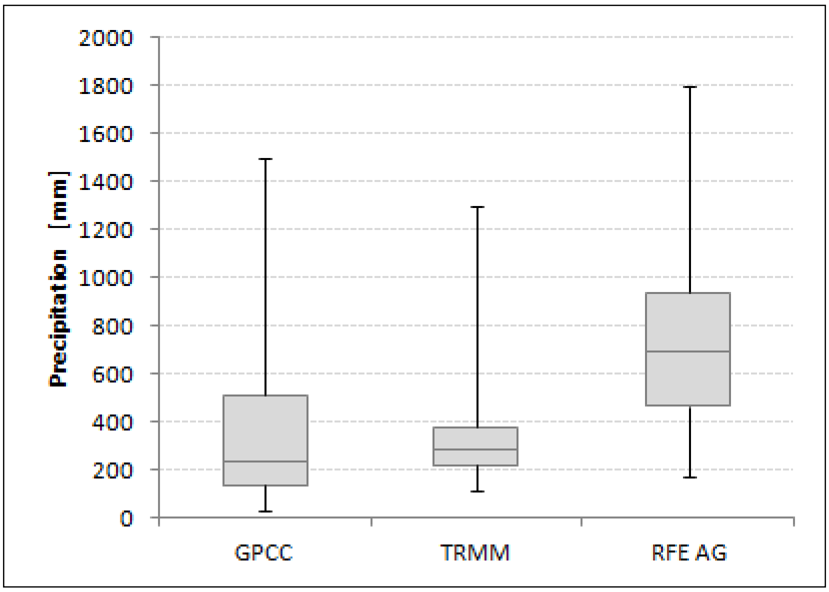

Figure 3-44: Box Plot of Average Annual UIB Precipitation (2003-2012) from Different Data Sets

To judge the validity of precipitation data, comparative analyses with river discharge data were performed. Potential sources for river discharge are precipitation, snow melt and glacier melt. Whenever precipitation in a distinct catchment is lower than the observed discharge, the difference in water must originate from snow/glacier melt, or as a second alternative, from groundwater. The latter becomes rather unlikely where precipitation amounts are consistently below observed discharge amounts for several years, as this would not allow a recharge of ground water aquifers, and the alternative assumption of an ‘endless’ ground water resource is not realistic. Alternatively, the consistent deficit water may be contributed by glacier melt, which is self-explanatory itself in a retreat of glacier tongues. To estimate potential contributions to river discharge from permanent snow/glacier melt, several multi-temporal glacier change analyses were done. The analyses used multi-temporal Landsat data for visualizing and measuring the degree of glacier retreat for several locations between 1990 and 2013. From the evaluated glacier retreat, one can conclude to the potential water amount that glacier melt contributes to river discharge.

As a second means of validation, hydrological model runs were performed using different parameter settings to produce observed discharge amounts using given precipitation data sets. Main model parameters affecting discharge are parameters controlling surface run-off and water storage at different soil levels and of different residence time. The average annual precipitation from different data sources is shown in Figure 3-45.

Neither the observed changes in glacier extent nor the various model runs carried out for different input parameters, could produce the observed river discharge for some catchments, not even in model configurations where chosen model parameters facilitate the run-off of almost all of the precipitation.

The minor losses in spatial glacier extent, also cannot explain the modelled water deficit. Model runs were performed at variable ‘critical temperatures of melting’. A lowering of T_{crit}, typically increased discharge amounts but results still showed discharge deficits. The lowering of T_{crit} cannot be done arbitrarily but has set limits that are latest reached once modelled glacier retreat exceeds observed glacier retreat.

Considering the results of multi-temporal glacier interpretations, hydrological model results and the large discrepancies between precipitation data sets, the conclusion is: erroneous precipitation data sets. Neither precipitation data set allowed the reproduction of the observed discharge amounts in various UIB sub-watersheds. The analyses suggest that in particular precipitation amounts over the western UIB are too low. Consistent results, between observed discharge and hydrological modelling outputs could only be produced for the Kharmong sub-watershed in the eastern UIB.

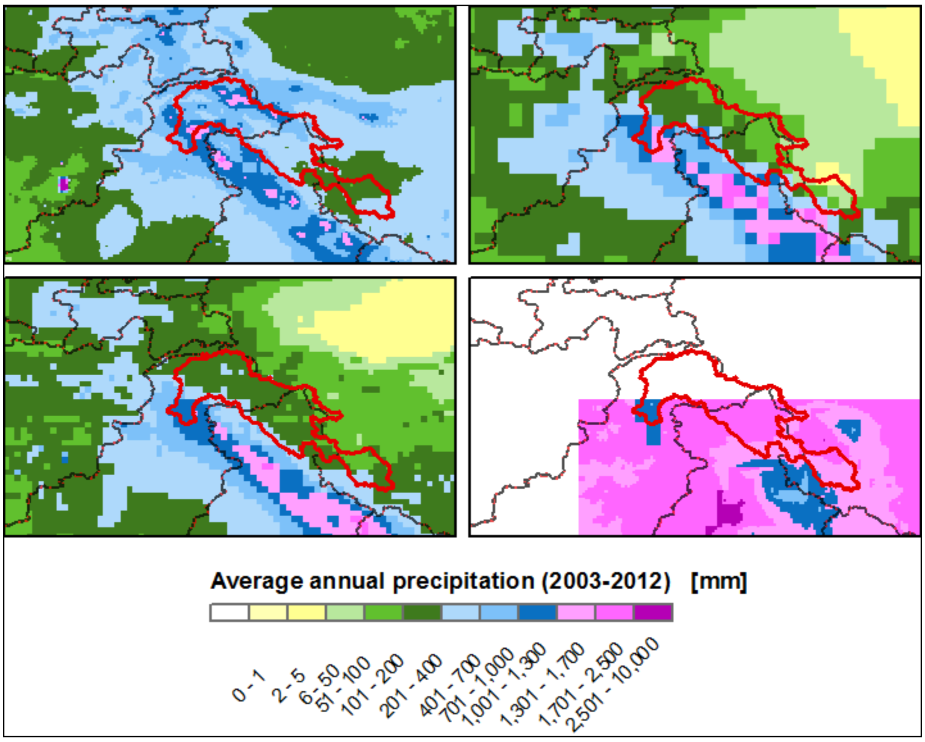

Figure 3-45: Average Annual Precipitation (2003-2012) from Different Data Sources, RFE_Ag (ul), GPCC (ur), TRMM (ll) and RFE_SA (lr).

Because of the controversial result, in an attempt for further clarification, the RFE data set for Central Asia (RFE_SA), which covers part of the UIB, was analyzed. In the comparative analyses only the UIB part of the RFE_Ag and RFE_SA overlap area was used (Figure 3-47). The result causes even more confusion: The RFE_SA data show triple the precipitation amount in comparison to RFE_Ag data (Figure 3-46). Absolute differences in precipitation amounts in the overlapping area can be explained by the use of different station records for correcting either product. However, missing seasonal and inter-annual data correlations, only allow the conclusion that used station data for at least one product are not representative for this part of the basin. This is also supported by an untypical rainfall distribution pattern along the mountain chain of the Himalayans in the case of the RFE_SA data. For this reason, attempts to transfer RFE_Ag data (entire UIB) to higher RFE_SA precipitation, based on calculated transfer functions created from the overlap area, were dismissed. Correlations between the two data sets are consistently low and do not show any significant relationship (Figure 3-48). A scientifically justifiable correction of the RFE_Ag data towards higher precipitation amounts was not feasible. As will be discussed in Section 3.25.11, this has implications for the hydrological modelling and model calibration with further impacts on snow and ice melt and on modelled discharge amounts.

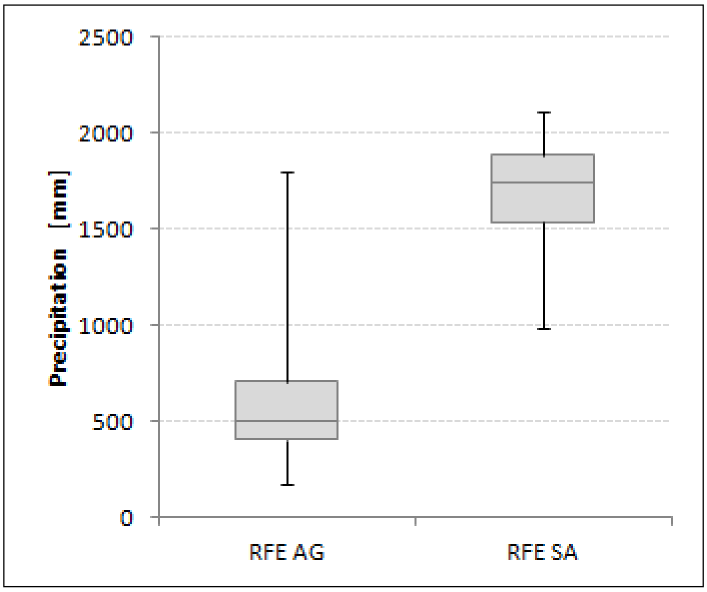

Figure 3-46: Box Plot of Average Annual Precipitation (2003-2012), created from the Afghan RFE and from the South Asia RFE data.

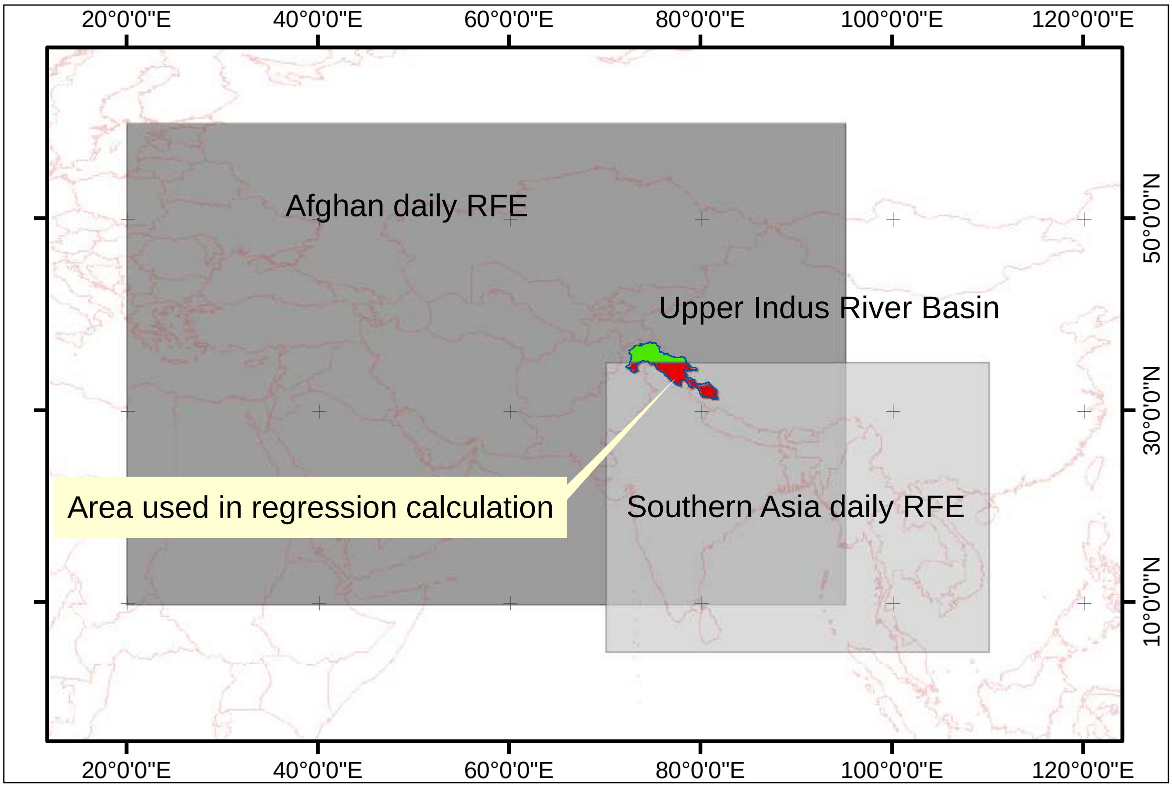

Figure 3-47: Coverage of Precipitation Products RFE_Ag and RFE_SA

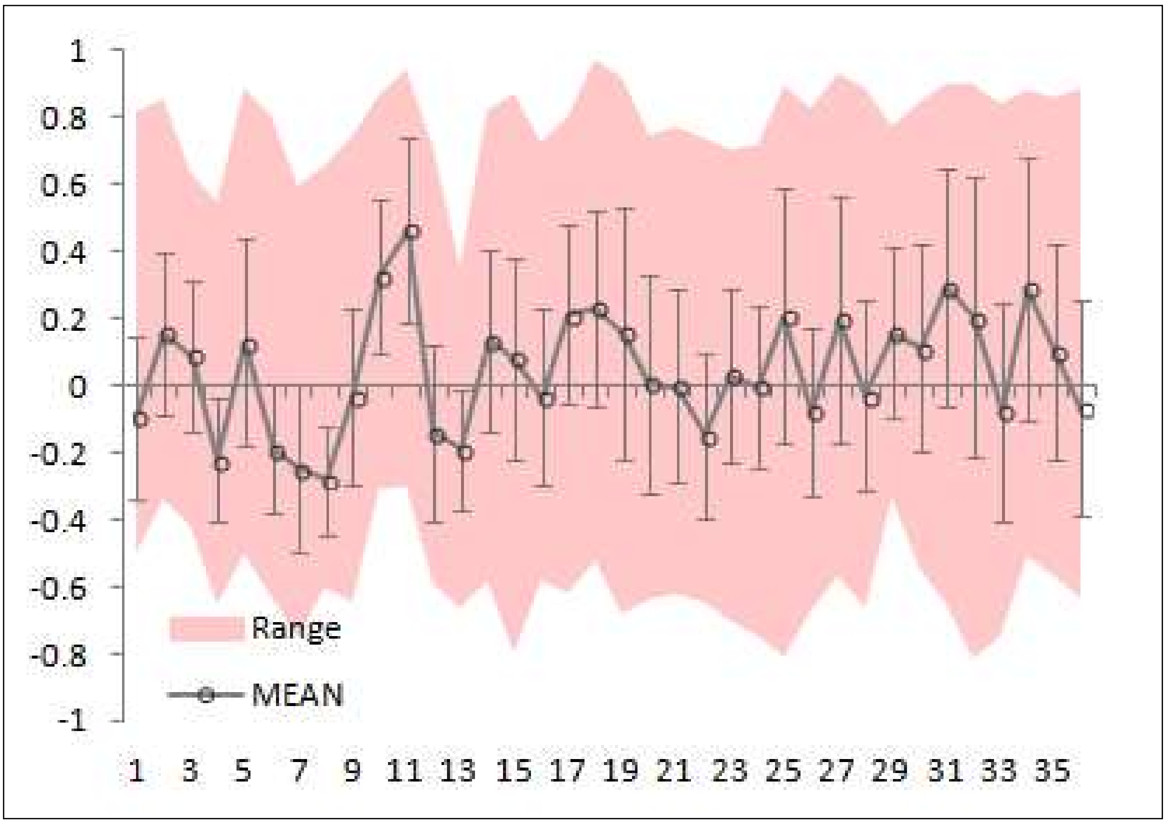

Figure 3-48: Correlations (range, standard deviation and mean) between RFE_Ag and RFE_SA in the Overlap Area (UIB overlap only) for each 10-day Period (1-36).

3.24.1.7 Precipitation Data Processing (Projected, GCM Data)

The spatio-temporal down-scaling of GCM-precipitation is based on a statistical approach (Mejia et al., 2012; Wilby et al., 1998). The conversion of 3.75° resolving GCM data to higher spatial resolution is a disaggregation process that uses observed precipitation distribution patterns determined from RFE_Ag data. For temporal downscaling to 10-day intervals, total monthly precipitation was calculated from daily RFE data. Then the decadal percentage from the monthly total was calculated for each pixel. For spatial downscaling, total precipitation within a defined spatial domain (Figure 3-49) was calculated and each location's share from the domain-total determined. Observed spatio-temporal distribution patterns were analyzed for every 10-day interval between years 2003 and 2012. The maximum achievable spatial resolution is determined by the resolution of the RFE_Ag data which is 0.1° (~12km). Observed precipitation patterns then were applied to GCM data: First, the domain total of each GCM layer was determined and in a second step the observed RFE percentages applied to disaggregate the data to higher spatial resolution.

Figure 3-49 demonstrates the good results of the down-scaling, placing high precipitation amounts along the front of the Himalayans and also emphasizing the influence of the westerlies that bring moisture into the western UIB. The statistical approach for precipitation downscaling assumes that the dominating weather patterns of the westerlies and of the monsoon continue to affect this region in the same way in the future as it does now.

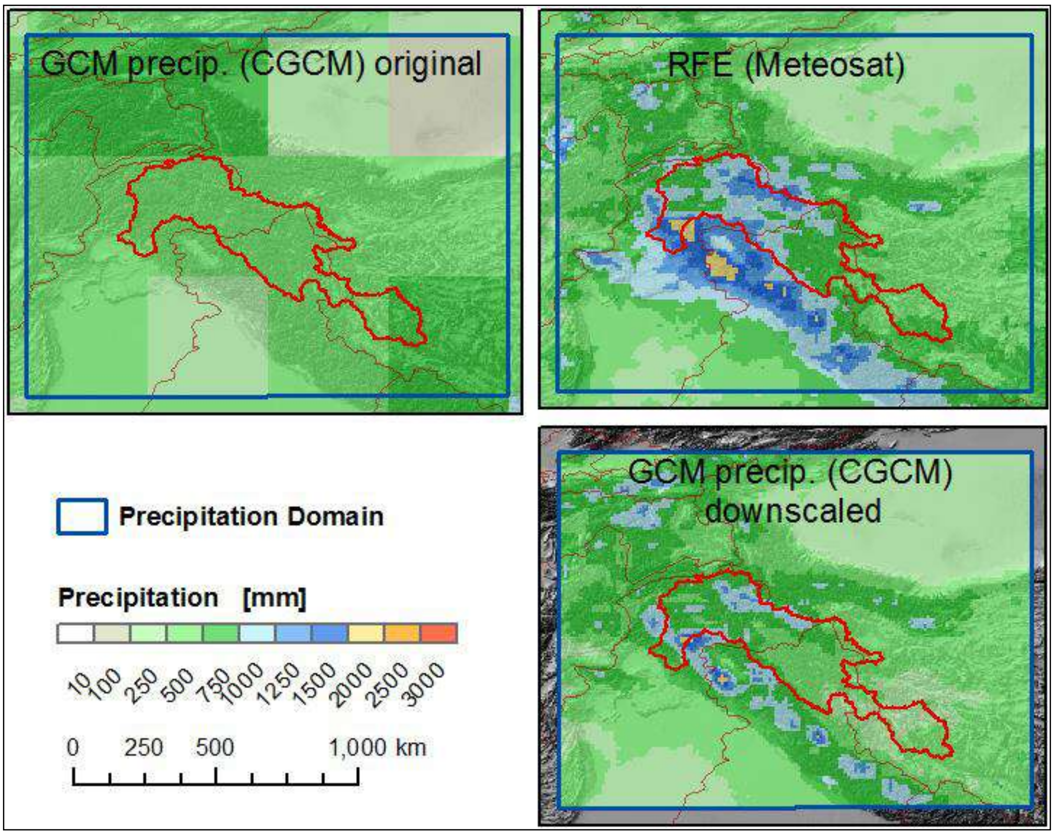

Figure 3-49: Example of Down-Scaled CGCM Precipitation Data, shown for 2003 Annual Total Precipitation:

3.24.1.8 River discharge data

Records from a total of 16 discharge stations were provided by WAPDA, measured at daily intervals and covering different periods. Latest records date from year 2006 for those stations that are still operational (Table 3-29). Records from year 2001 are missing for all stations. Out of the 16 stations, six were used in the analyses as shown in Table 3-29 and highlighted in Table 3-29. Some of the stations have been closed, others are aligned along the Indus river representing catchment areas with only minor differences to the selected stations. Primary use of discharge measurements was the verification of precipitation data and the calibration of parameters of the hydrological model. At Kachura station discharge from the Shigar- and the Shyok-Nubra sub-watersheds is recorded. The station Kharmong measures discharge from the Chinese and Indian Indus sub-watershed. Sub-watersheds of named discharge stations, as shown in Figure 3-50 and Table 3-29, were individually modelled and calibrated. Discharge measurements at the station Besham Qila were used as a reference during model runs of the entire UIB. A verification of observed discharge records was not possible. The accuracy of discharge calculations strongly depends on reliable flow velocity measurements and on the use of accurate dimensions of the river profile that may need regular, repeated measurements due to erosion and/or sedimentation processes.

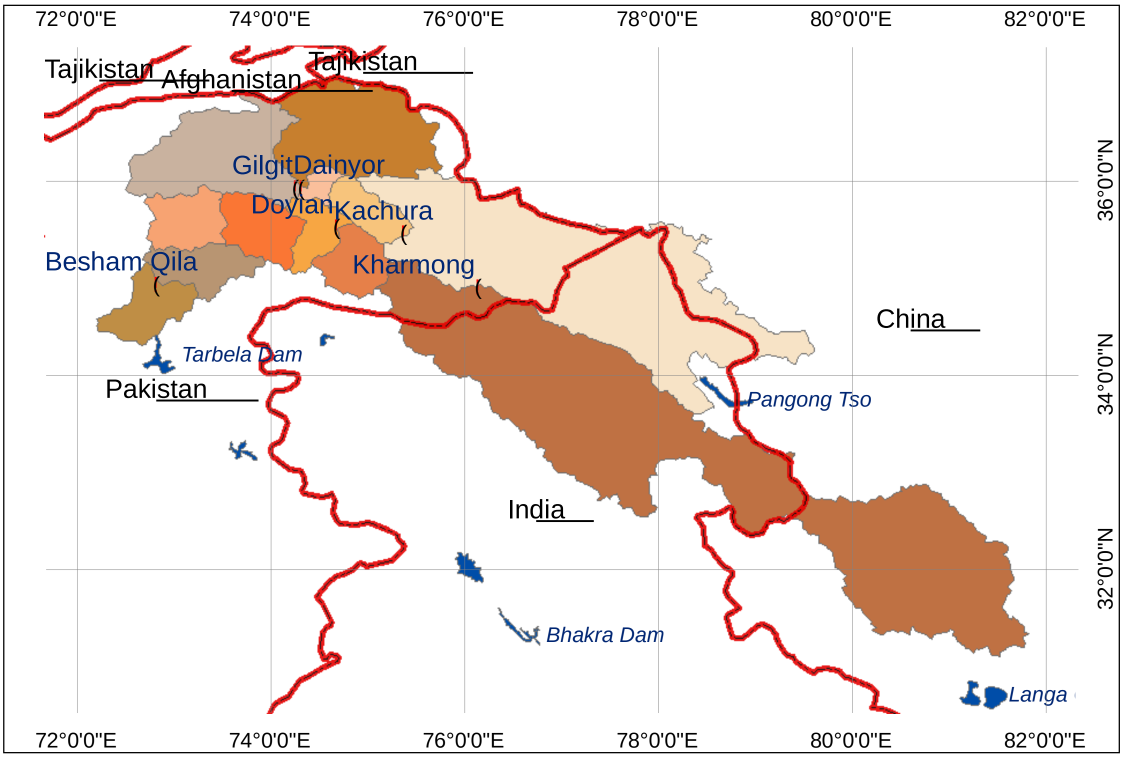

Figure 3-50: River Discharge Stations and Catchment Areas Used in Model Calibration

Table 3-29: Station Data with Period of Records

No	Station Name	River	Period recorded	Latitude	Longitude	Catchment area [km^2]	comment
1	Alam Bridge	Gilgit	1966 - 2005	35 45 00	74 37 00		
2	Barasin	Indus	1974 - 1979	35 18 00	73 16 00		Closed
3	Besham Qila	Indus	1969 - 2006	34 56 00	72 53 00		
4	Bunji	Indus	1999 - 2006	35 39 56	74 37 40		
5	Dainyor	Hunza	1966 - 2004	35 55 00	74 23 00	13592.40	
6	Darband	Indus	1960 - 1974	34 24 00	72 48 00		Closed
7	Doyian	Astor	1974 - 2006	35 31 00	74 44 00	3804.15	
8	Gilgit	Gilgit	1960 - 2006	35 56 00	74 19 00	12699.70	
9	Gunji Bridge	Indus	2003 - 2006	35 27 00	74 18 25		
10	Kachura	Indus	1970 - 2006	35 27 00	75 25 00	44263.50[37]	
11	Kharmong	Indus	1982 - 2006	34 54 00	76 13 00	71045.20	
12	Partab Bridge	Indus	1962 - 1995	35 44 00	74 37 00		Closed
13	Raikot	Indus	2003 - 2006	35 29 34	74 35 30		
14	Shatial	Indus	1983 - 2006	35 31 56	73 33 52		
15	Shigar	Shigar	1985 - 1998	35 20 00	75 25 00		
16	Yugo	Shyok	1973 - 2006	35 11 00	76 06 00		

3.24.1.9 Potential Evapotranspiration (PET)

The model input parameter ‘potential evapotranspiration’ (PET) was calculated after Hargreaves using min, max and mean temperature (Hargreaves and Allen, 2003). For the calculation of top of atmosphere radiation, a required input in the Hargreaves equation, common equations for describing daily sun orbits around the earth were used and adjusted for elevation and surface orientation (see Annexure-M). Resulting PETs were then transferred to Penman PET (Ambast et al., 2002) based on linear transfer functions measured in other alpine regions. PET layers were prepared at 10-day intervals for the observed period and for future climate change scenarios. Identical procedures were applied in PET calculations for the observed and for projected periods. Further details and equations used in PET calculations are given in the annexures.

3.24.1.10 Soils and Available Water Holding Capacities (AWC)

According to the Digital Soil Map of the World and the Harmonized World Soil Database), soil characteristics (soil type, soil depth, AWC) do not vary significantly throughout the UIB. Dominant soils are Lithosols in larger flood plains smaller areas covered by Cambisols and Acrisols are found. The distribution of glaciers and associated soil characteristics were modified according to glacier distribution, as mapped from Landsat data.

Temporary storage of water in the upper soil layer, described in the parameter ‘available water holding capacity’ (AWC) influences surface run-off, evaporation from the soil, infiltration into lower layers and base flow.

[37] Official numbers may be much larger (112,664km^2). They likely include the Pangong Tso watershed, that has however no surface connection with the UIB.

For the calculation of AWCs, information on saturated water content (ϴs) and on soil depth were taken from FAO's Digital Soil Map of the World from which a maximum water holding capacity was calculated (unit: mm). For Lithosols AWCs range between 15 to 20mm for Cambisols and Acrisols between 30 and 40mm. During calibration of the hydrological model AWCs, as given by FAO, were modified for some sub-watersheds to improve model outputs. Modifying AWCs' triggers the creation of surface run-off and thus the timing and amount of discharge. Knowing the weaknesses of the input precipitation data (too low), AWC modifications were primarily intended to achieve better matches in the timing of observed and modelled river flows, less to adjust discharge amounts. Figure 3-51, shows the digital soil map for the UIB while Figure 3-52 shows the available water holding capacity.

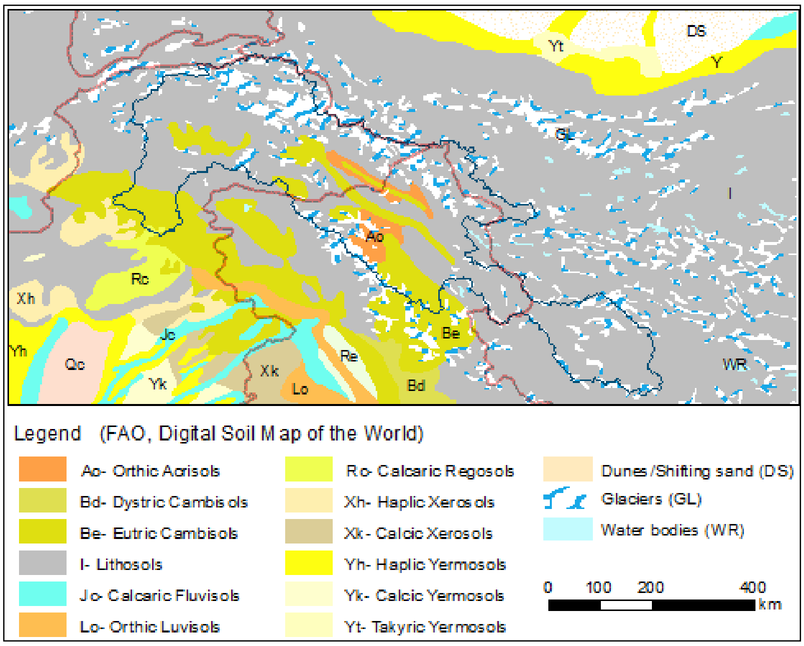

Figure 3-51: Digital Soil Map of the World (FAO)

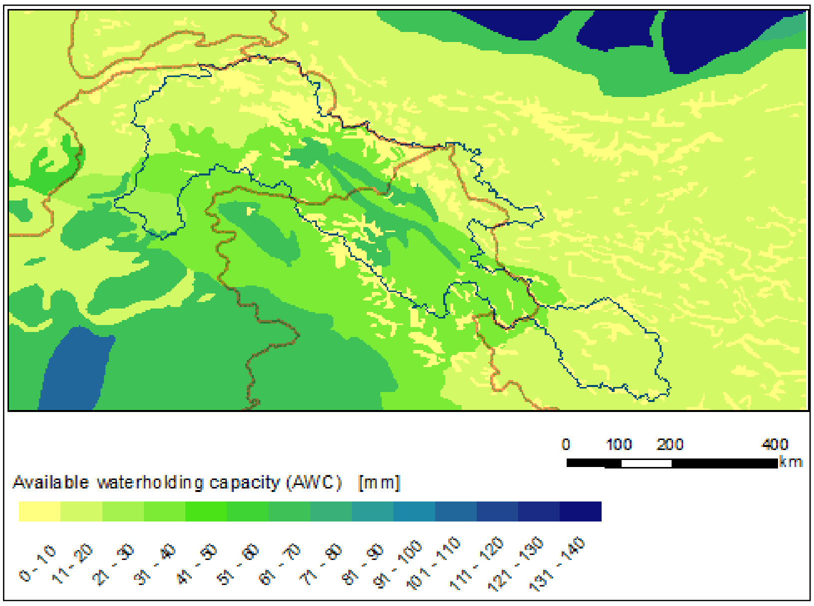

Figure 3-52: Available Waterholding Capacities Derived from FAO's DSMW.

3.24.2 Land Cover Land Use (LCLU)

The type of vegetation influences surface run off and infiltration. Vegetation type was classified from 250m resolving MODIS NDVI data (MODIS product MOD13Q1, year 2013) and resulting classes were coded according to the global land cover classification (GLCF) for hydrological modelling purposes. The classification of vegetation classes used an approach that classifies NDVI time-series according to their shape characteristic. Input to the Fourier based classifier is a one year NDVI time-series composed of 16-day interval NDVI layers (Geerken, 2009). The advantage is the distinction of vegetation types not just based on their appearance at a single time during the year but rather based on their seasonal variation. This allows a better separation of vegetation types and accounts for temporal phenological shifts due to vertical temperature gradients affecting the onset and ending of seasons or rather of vegetative periods.

The largest class forms with 47% the ‘bare soil’ class (Figure 3-53). Second largest are various ‘sparse vegetation’ classes which cover a total of 15% of the UIB area. The various bare soil classes as shown in the classification, were summarized as one single ‘sparsely vegetated’ class in the LCLU input layer to the hydrological model. The result of glacier coverage (11%) is taken from the 2013 Landsat analyses and was overlaid to the classification.

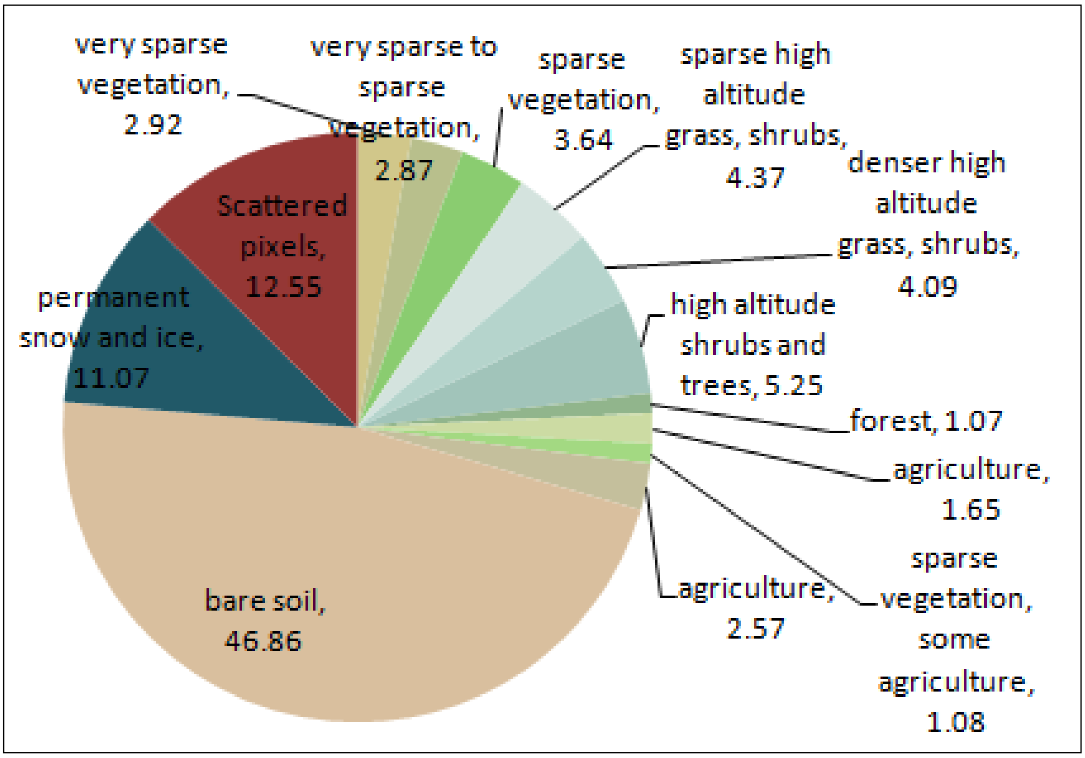

Figure 3-53: Percent Area of Vegetation Classes in the UIB

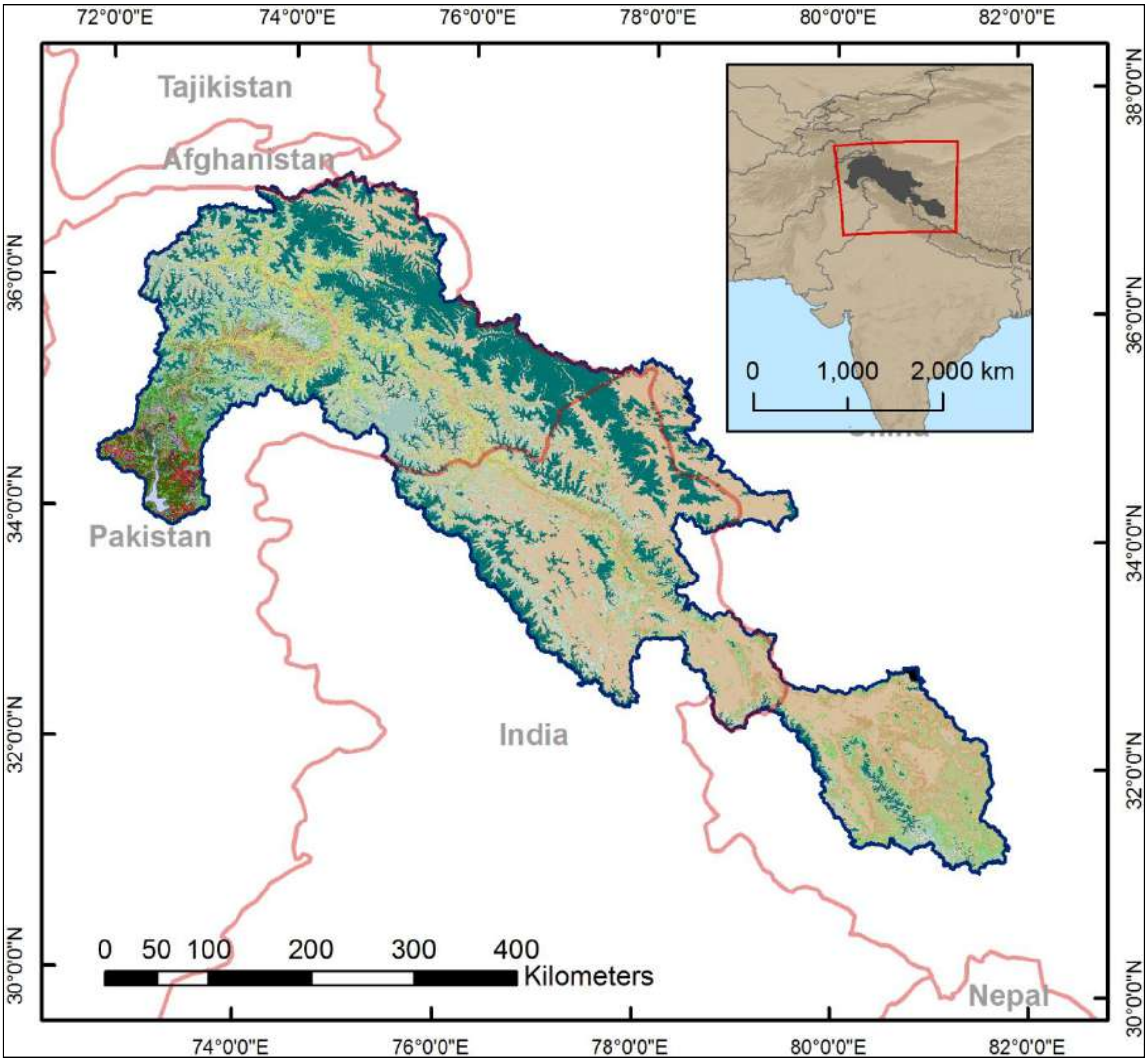

Figure 3-54: Classification of Vegetation Types

The class scattered pixels comprises isolated mixed pixels that were assigned to the dominant surrounding class. More dense vegetation covers, forests and agriculture are found in flood plains at lower altitudes. Together they only cover about 15% of the UIB area.

As an input to the hydrological model a degraded version (1,000m) of the LCLU classification was used. The necessary image degradation process causes the truncation of smaller areas and modifies percent areas as given in Figure 3-53 and in Figure 3-54.

3.24.3 Topography

All analyses that require topographic data as input use the Global Multi-resolution Terrain Elevation Data 2010 (GMTED2010). The data come in resolutions of 7.5, 15 and 30 arc-seconds (about 250m, 500m and 1,000m). GMTED2010 is derived from 11 different raster elevation sources, with SRTM data forming a primary input source. The data has been extensively corrected for errors and forms a product where all holes have been eliminated. This makes GMTED2010 the most consistent and accurate DEM currently available.

In this study different DEM resolutions were used for different purposes. The following description of watershed topography is based on 500m data. Watersheds in the UIB (Figure 3-55) differ in the spread of topographic elevation, morphology, dominant elevation level and other topographic parameters. This influences not only the extent of glaciation and the form of precipitation they receive (rain, snow) but also the discharge/precipitation ratio (rainfall index) and run-off and discharge characteristics.

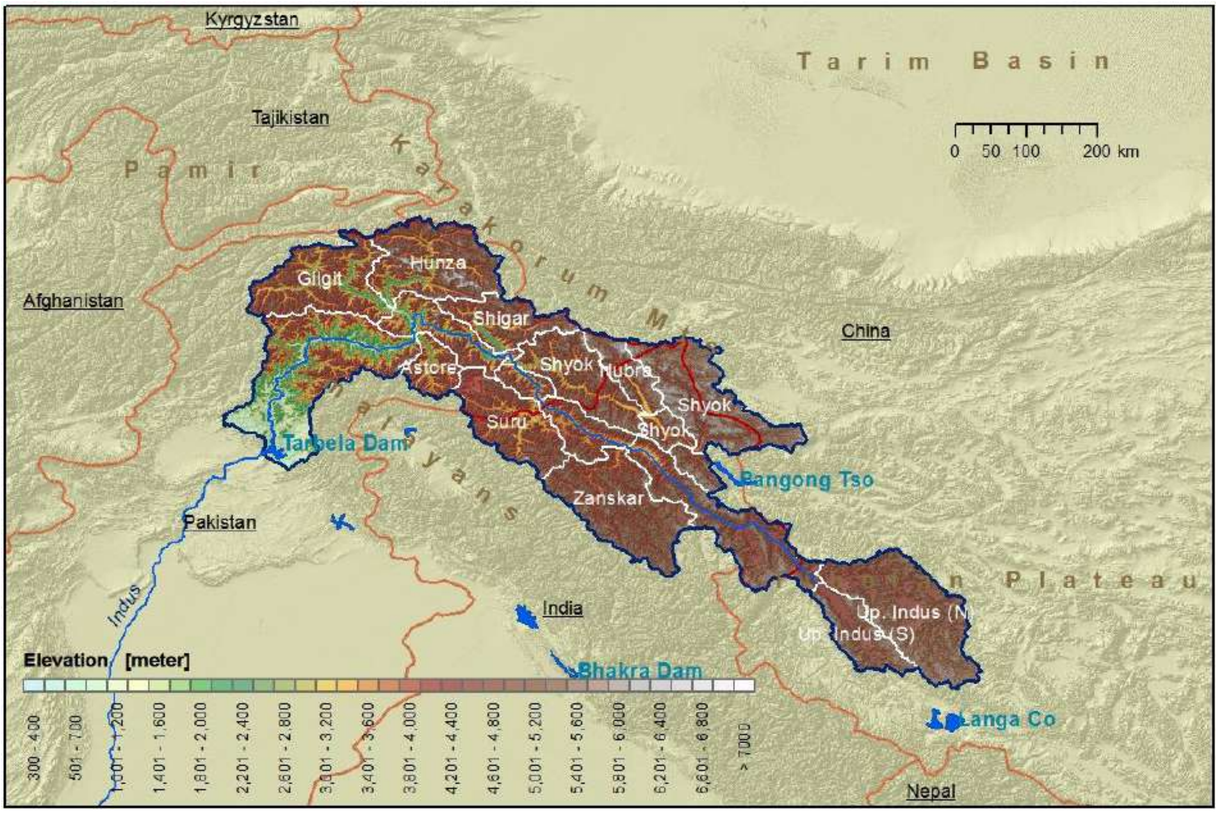

Figure 3-55: Topographic Setting of the UIB and its Sub-Watersheds (Data Source GMTED 2010 Data)

Highest average elevations are reached in the densely glacierized watershed of Shyok-Nubra where more than 50% of the area reaches elevations higher than 5000m. Similar averages but at a much lower interquartile and total range, are only reached in the upper stretches of the UIB, comprising the Upper Indus (N) and the Upper Indus (S), both forming part of the Tibetan Plateau. Minor elevation variation expresses itself in distinctive shallow slopes. These features distinguish the eastern watersheds from all other watersheds, putting them in a special position in terms of run-off and discharge characteristics. Compared to other UIB watersheds, the discharge/precipitation ratio in the Kharmong catchment is significantly lower. Despite a high average topographic elevation (around 5000m) glaciation is low. Apart from climatic causes, this is likely the result of a smooth morphology and missing deep valleys.

The Astore watershed shows lowest average elevations but the largest elevation variations. This is one reason for only small percental glacier coverage, another is the watershed's location, near the southern margins of the Himalayan Mountains. The steep Astore slopes are comparable to those in the Gilgit, Hunza and Shigar watersheds. Steep slopes together with shallow soils trigger rapid surface run-off and short discharge travel-times. Figure 3-56 shows the box plot for different sub-catchments for the elevations and slopes.

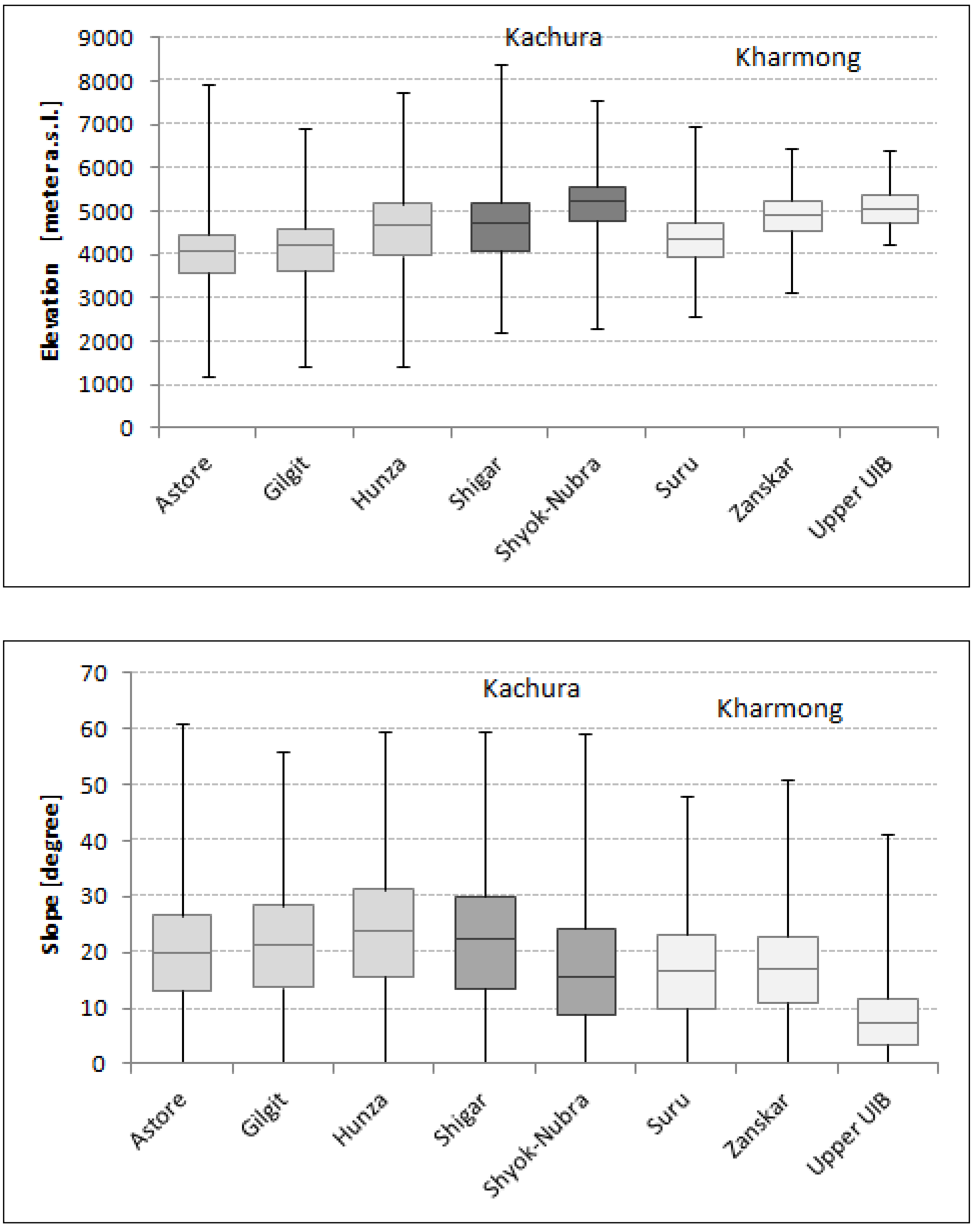

Figure 3-56: Box Plots for Topographic Elevation (top) and Slopes (Bottom) for UIB Watersheds, Prepared from GMTED2010 data (250m).

Shigar, Hunza and the somewhat less elevated watershed of Gilgit share similar topographic features. Characterized by high elevation variation, steep slopes and at least 50% of their areas ranging between 4,000 and 5,000m asl., these watersheds display substantial glacier coverage. High elevations and steep unvegetated slopes favor quick run-off and discharge and the creation of flash floods.

Areas with steep terrain as seen in Astore, Gilgit, Hunza and Shigar watersheds present ideal conditions (topography, vegetation cover) for flash flood creation. Flash flood risk and flash flood frequency may further increase for all climate change scenarios, due to changes in precipitation type that will shift towards more frequent rainfall and less snow. Climate in the UIB.

3.24.4 Climate in the UIB

The UIB is under the influence of two different climatic systems – the South West Indian monsoon and the westerlies – bringing in moisture from different sources, during different times of the year and affecting different areas in the UIB (Anders et al., 2006). The utmost east and the southern slopes are primarily influenced by the monsoon during summer while precipitation in the north and the west of the basin is controlled by the westerlies affecting the UIB during late winter.

3.24.4.1 Temperature - Seasonal Characteristics and Ongoing Trends

Temperatures are strongly controlled by topographic elevation and submitted to a seasonal cycle that reaches maximum temperatures during July and minimum temperatures in January. This temporal temperature pattern prevails in all of the UIB. The difference in topographic elevation (lowest: 475m at Tabela, highest: 8,611m K2) is reason for a huge vertical temperature range. In some areas mean temperatures never drop below zero, others show permanent frost (Figure 3-57).

Spatially dissolved seasonal temperatures are shown in Figure 3-58 and length of frost period in Figure 3-59.

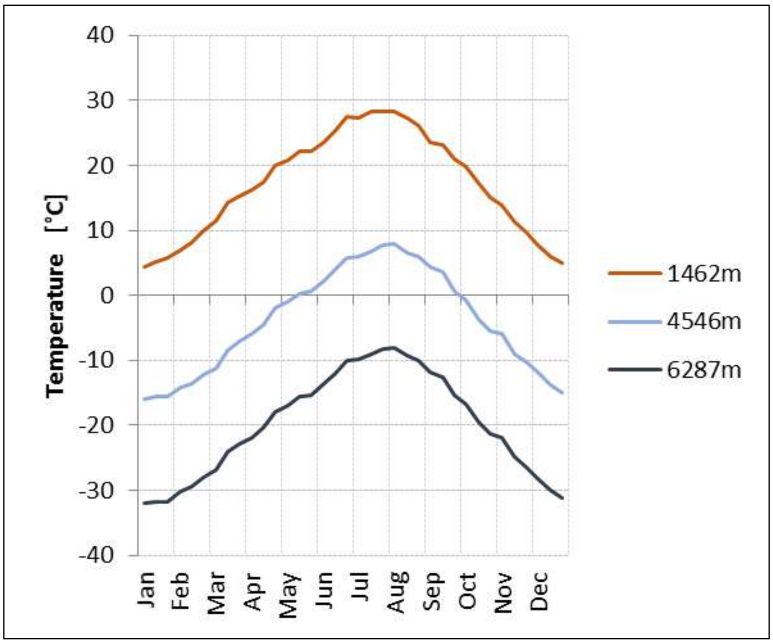

Figure 3-57: Cycles of Average (2003-2012) Mean Temperature (10-day intervals) Measured in the UIB at Different Topographic Elevations

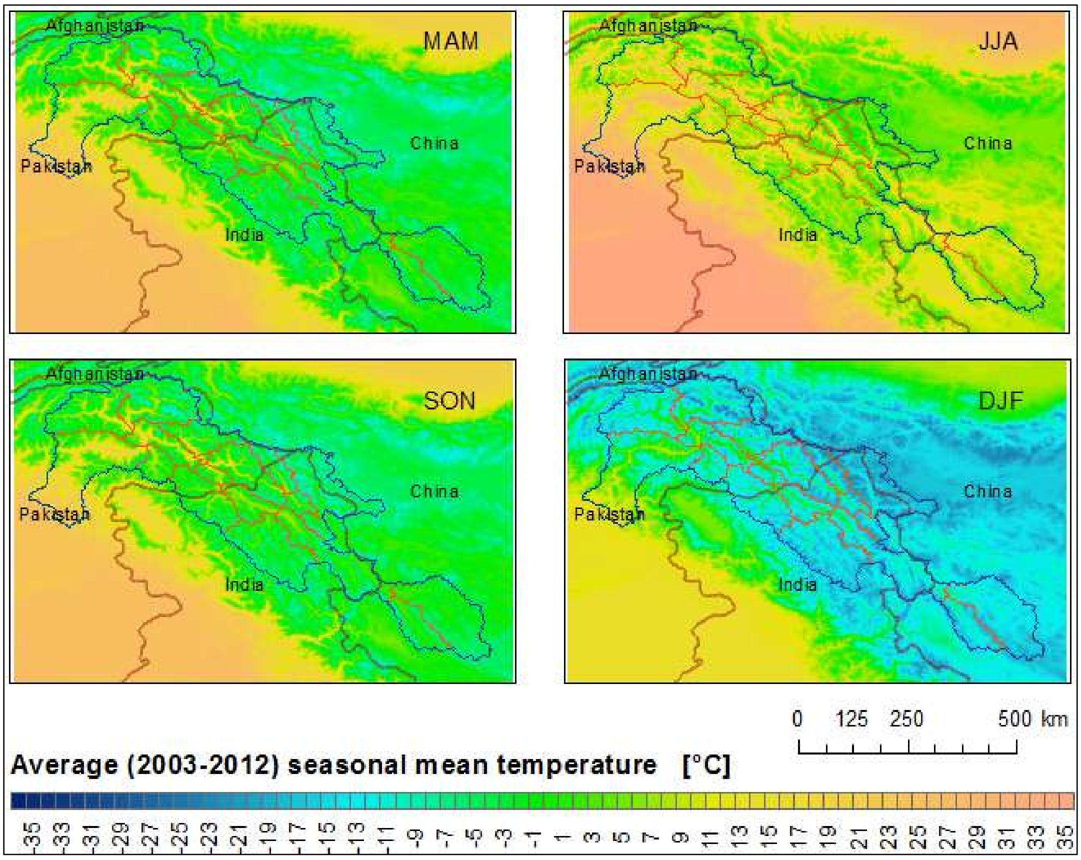

Figure 3-58: Seasonal Average (2003-2013) Mean Temperatures from Spatially Interpolated Station Data (WAPDA, PMD, NCAR/GSOD).

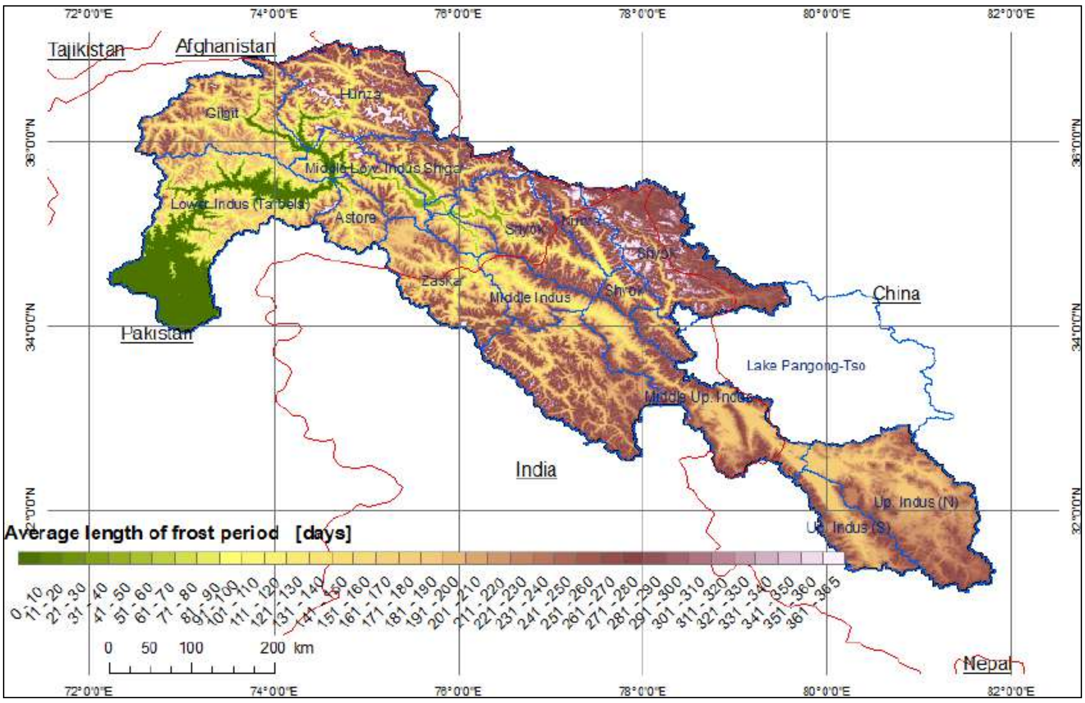

Figure 3-59: Length of Frost Periods Calculated from 10-day Interval Average Mean Temperatures

3.24.4.2 Temperature Trends

Temperature trends from different data sets of different spatial and temporal resolution were analyzed intended to learn about long term trends, and also about temporal and spatial detail.

For visualizing long term trends coarse resolution annual mean temperatures from CRUTEM5 were evaluated. Their weakness is their coarse spatial resolution (5°x5°) that may produce trends that are not necessarily representative for all UIB areas. According to experts, CRUTEM5 temperatures tend to be somewhat too high. This however is without or only little influence on trend calculations as long as temperatures have been consistently processed.

For northern UIB areas including the Tibetan plateau, CRUTEM5 temperatures show an increase between 1 to 2°C over the past 60 years (Figure 3-60). Southern UIB areas along the periphery of the Himalaya do not show any pronounced temperature tendency. A temperature drop as shown in the Indian UIB is within normal temperature variation and statistically insignificant.

Mean annual temperature variations and trends as well as measured temperature maxima, all fall within a range that does not appear unusual in comparison to temperatures reached during mid-century of the 1900s.

For more details on temperature development - spatially as well as temporally - trends were calculated for selected station records and for gridded temperatures that were created from station interpolation (see above), covering the period from 1995 to 2012. Though a period of 18 years may be too short to derive reliable trends thereof (typically a minimum of 25 years is used), temperature development over this period still is helpful to better understand and explain the development of glaciers and changes in discharge amounts.

Because of the sensitivity of glacier melt to temporal temperature changes instead of seasonal analyses, monthly intervals were chosen to better capture possible temporal shifts e.g. in the timing of the onset of melting.

Station specific trends show a diverse picture of temperature increase and decrease during different times of the year (Figure 3-61) (Bocchiola and Diolaiuti; Fowler and Archer, 2006). The months of winter and spring (January to May) are marked by temperature increases, while summer months (June to October) show drops or at least invariant temperatures. The temporal diversification of trends is likely to alleviate possible impacts on glacier melt. The moderate temperature increase during winter months is not high enough to induce substantial glacier melting, while summer decreases lead to a reduction in glacier melt. The monthly trends of temperature is shown in Figure 3-62.

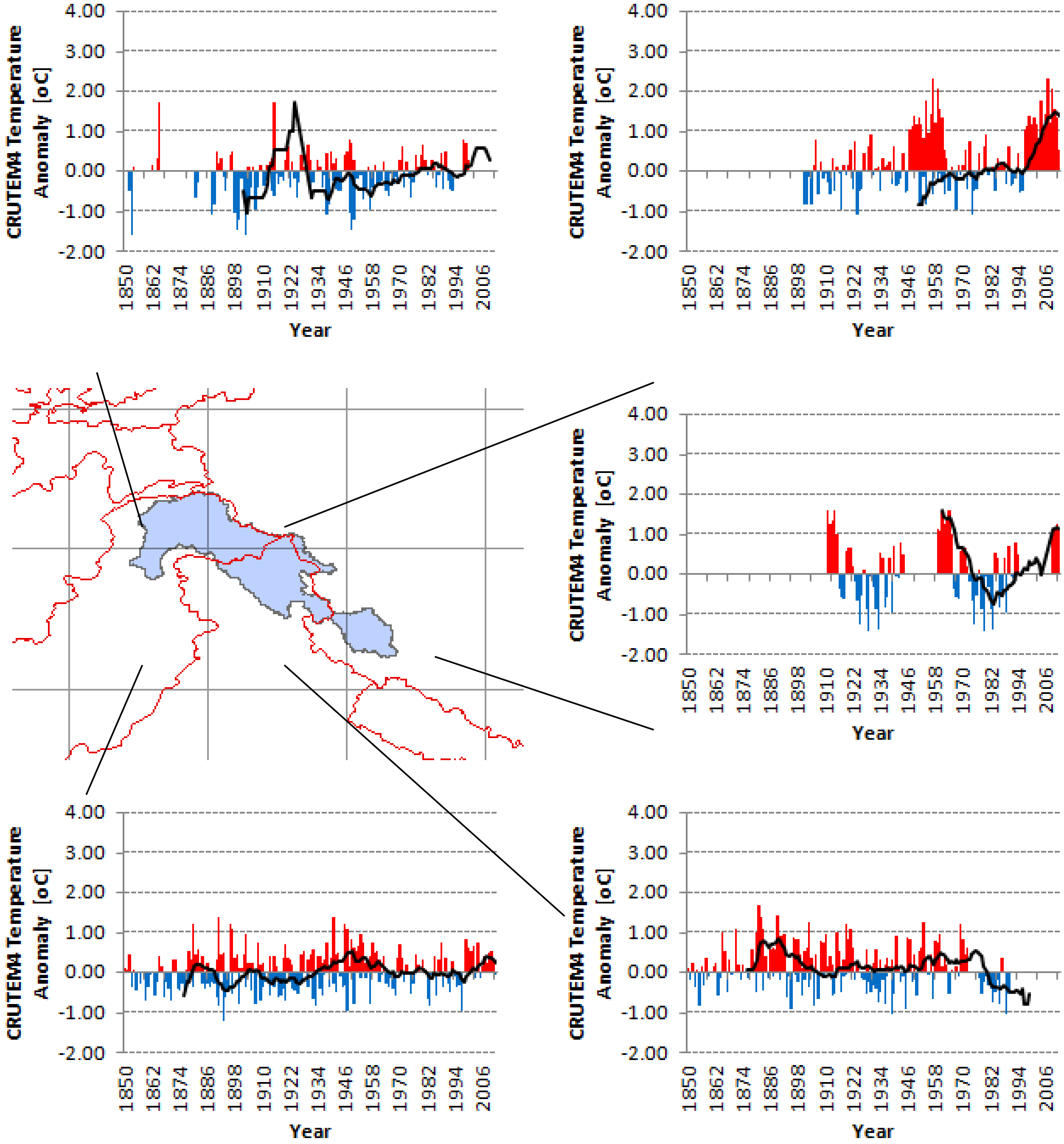

Figure 3-60: CRUTEM 4 Annual Mean Temperature

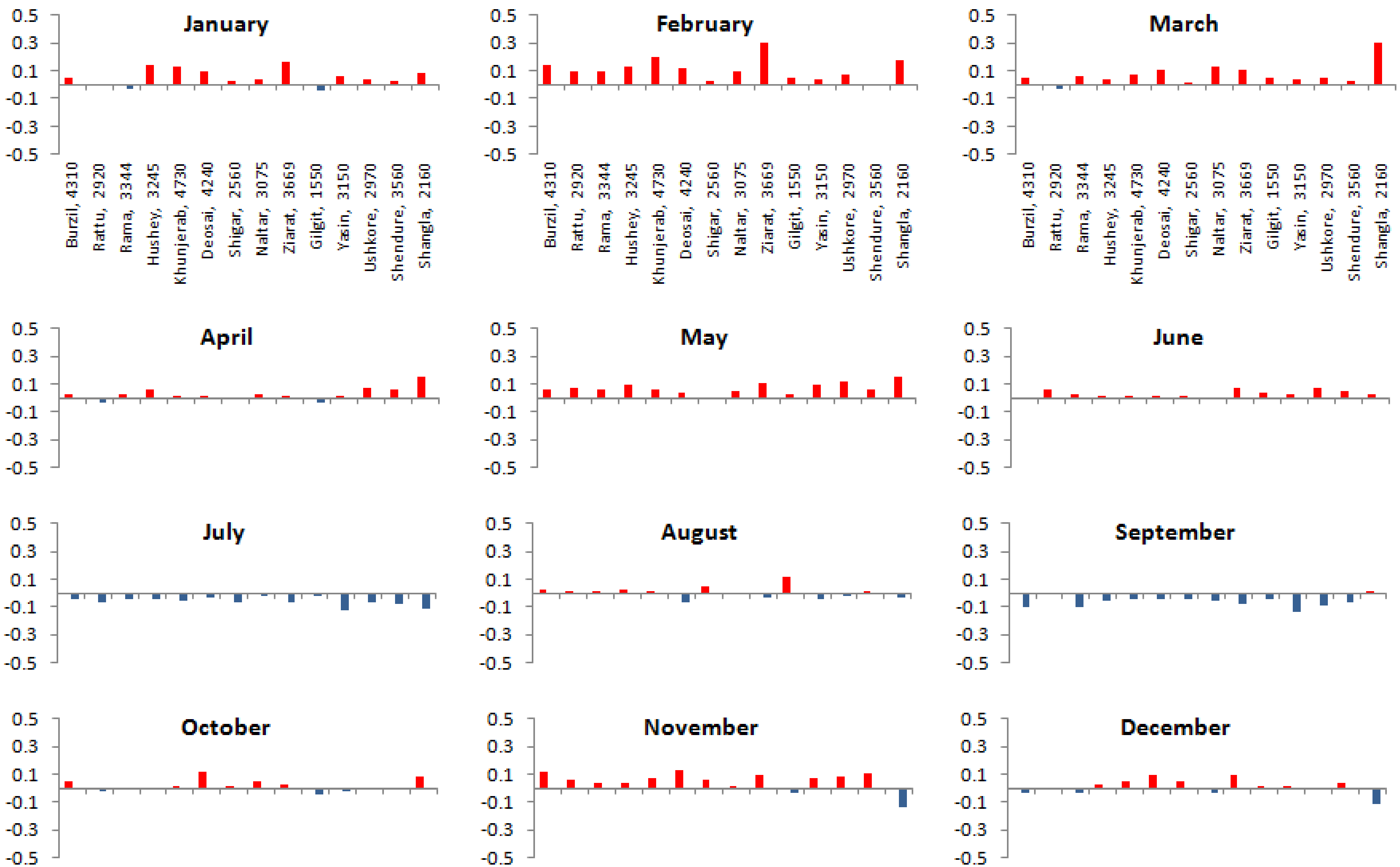

Figure 3-61: Monthly Temperature Trends Between 1995 and 2012 with the X-axis Showing 'Temperature Increase/Decrease per year'

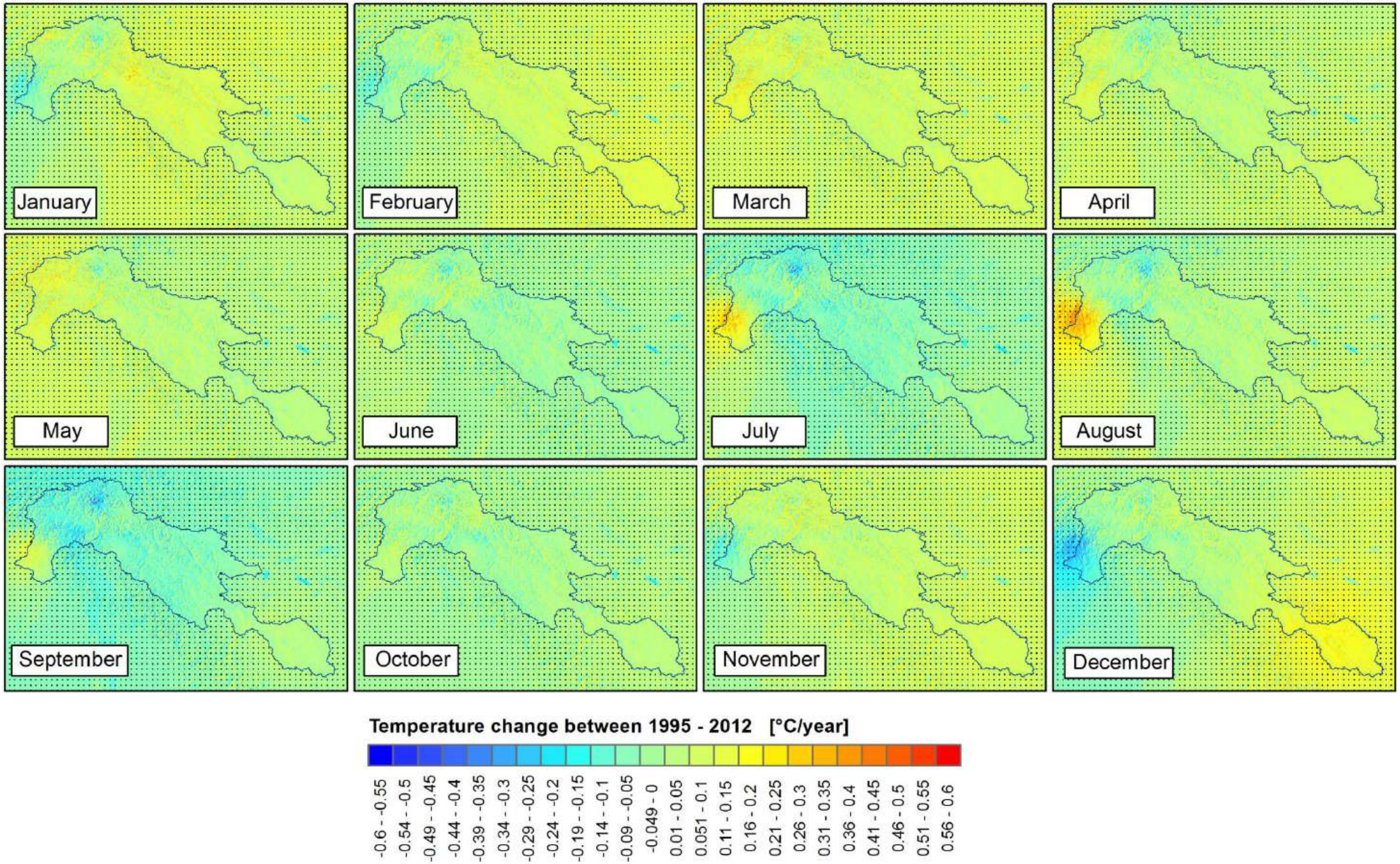

Figure 3-62: Monthly Trends in Mean Temperature between 1995 and 2012

As the spatially distributed trend analysis shows this pattern of seasonal temperature change applies to almost the entire UIB. Only exemptions are the Tibetan plateau showing a remarkable December temperature increase and the lower UIB in the area of Tarbela that is already under strong climatic influence of the down-stream Punjab area. Circular shaped temperature changes around Tarbela – strong summer increases and winter drops - look however somewhat suspicious and may be caused by flawed station data.

3.24.5 Precipitation Seasonal Characteristics and Trends

Precipitation in the UIB originates from two different climatic systems – the South West Indian monsoon and the westerlies – bringing in moisture from different sources, during different times of the year and affecting different areas in the UIB (Anders et al., 2006). The sub-regions defined for monitoring the precipitation change is shown in Figure 3-63. The utmost east and the southern slopes are primarily influenced by the monsoon while precipitation in the north and the west of the basin is controlled by the westerlies. Rainfall in the western basin brought by the westerlies concentrates during winter and early spring. The monsoon, responsible for precipitation in the eastern basin reaches a maximum during the summer months (Figure 3-64).

Different to temperature, precipitation shows a temporally random distribution which makes it poorly suited for trend analyses. Its development between 1901 and 2010 therefore is shown in several diagrams representative for different sub-regions as indicated in Figure 3-65. The corresponding regions which are represented by these diagrams are shown in Figure 3-63. Focus in the diagrams is on temporal variation and trends, absolute precipitation may not be correct as discussed in Section 3.21.1.6. For the long-term precipitation analysis GPCC data were used.

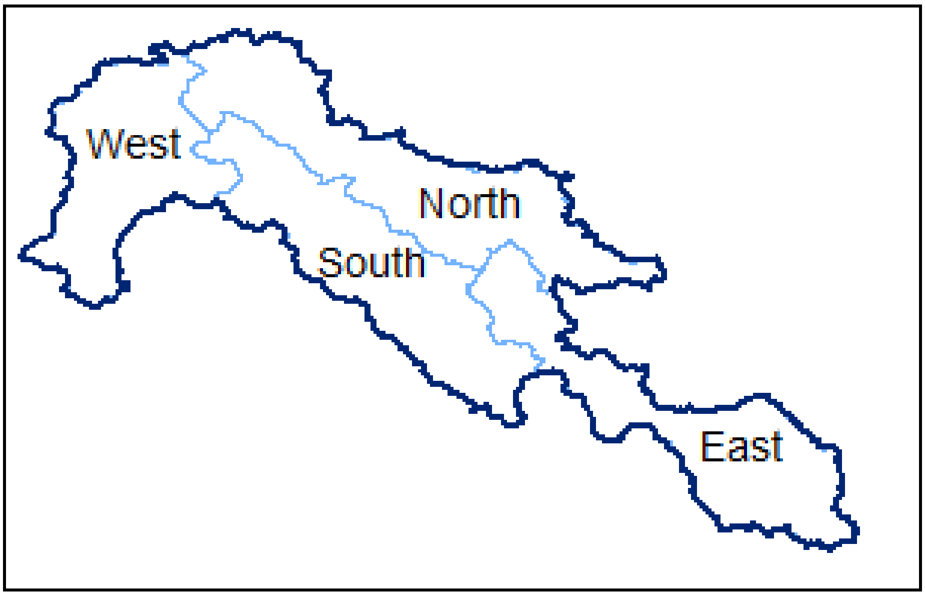

Figure 3-63: Sub-Regions Defined for Monitoring Precipitation Change

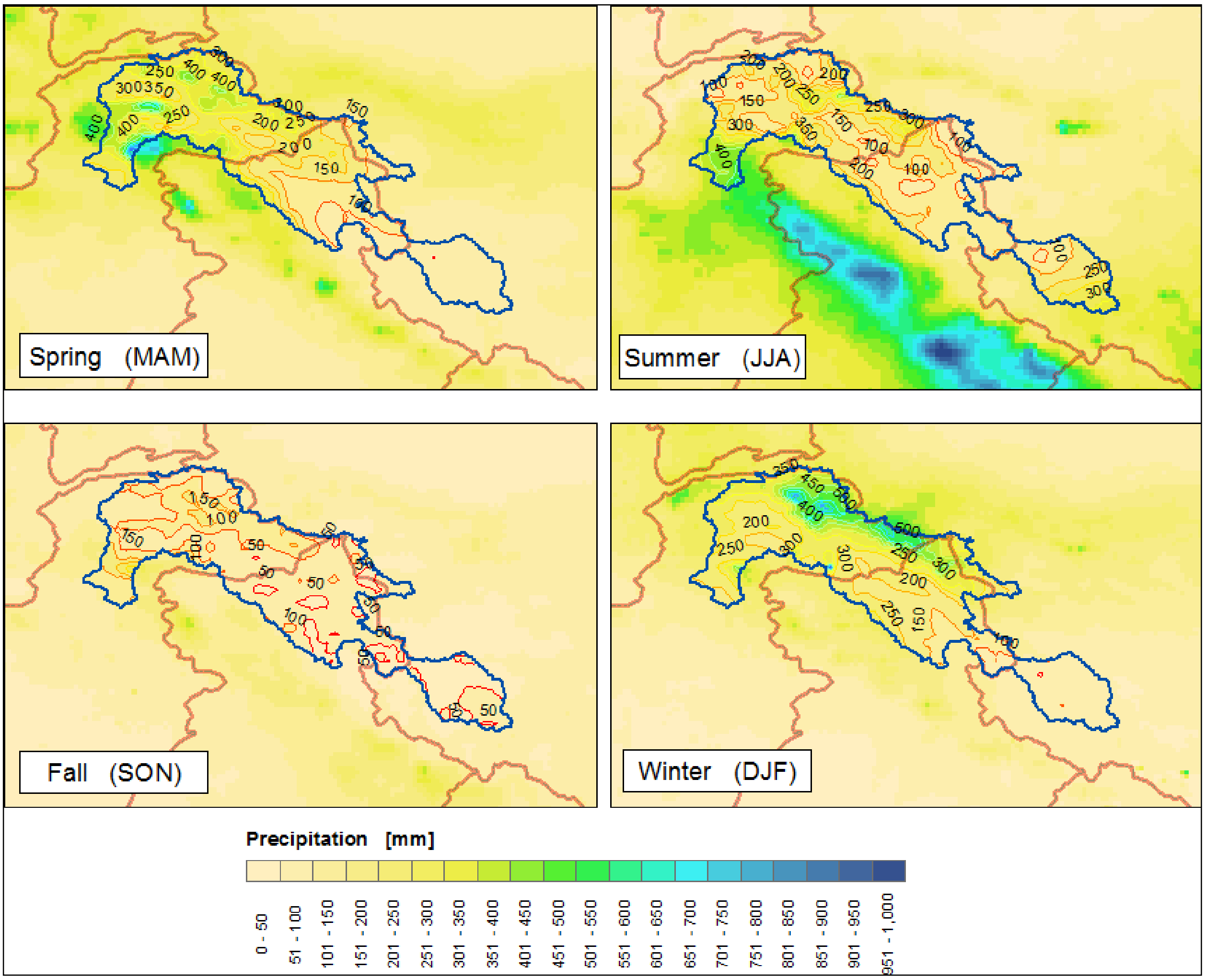

Figure 3-64: Average Seasonal Precipitation in the Upper Indus Basin, Calculated from RFE_Ag Data of Years 2003 to 2013

Among the four sub-regions only the eastern one shows an apparent trend towards lower precipitation starting at around the second half of the last century. In the northern zone a very moderate precipitation increase is visible. While average precipitation amounts remain unchanged in the southern sub-region, precipitation variability starts change onwards the late 50ies. The monthly precipitation development in the sub-regions of UIB is shown in Figure 3-65. The average monthly precipitation calculated from RFE_Ag is shown in Figure 3-66.

Figure 3-65: Monthly Precipitation Development in four UIB Sub-Regions

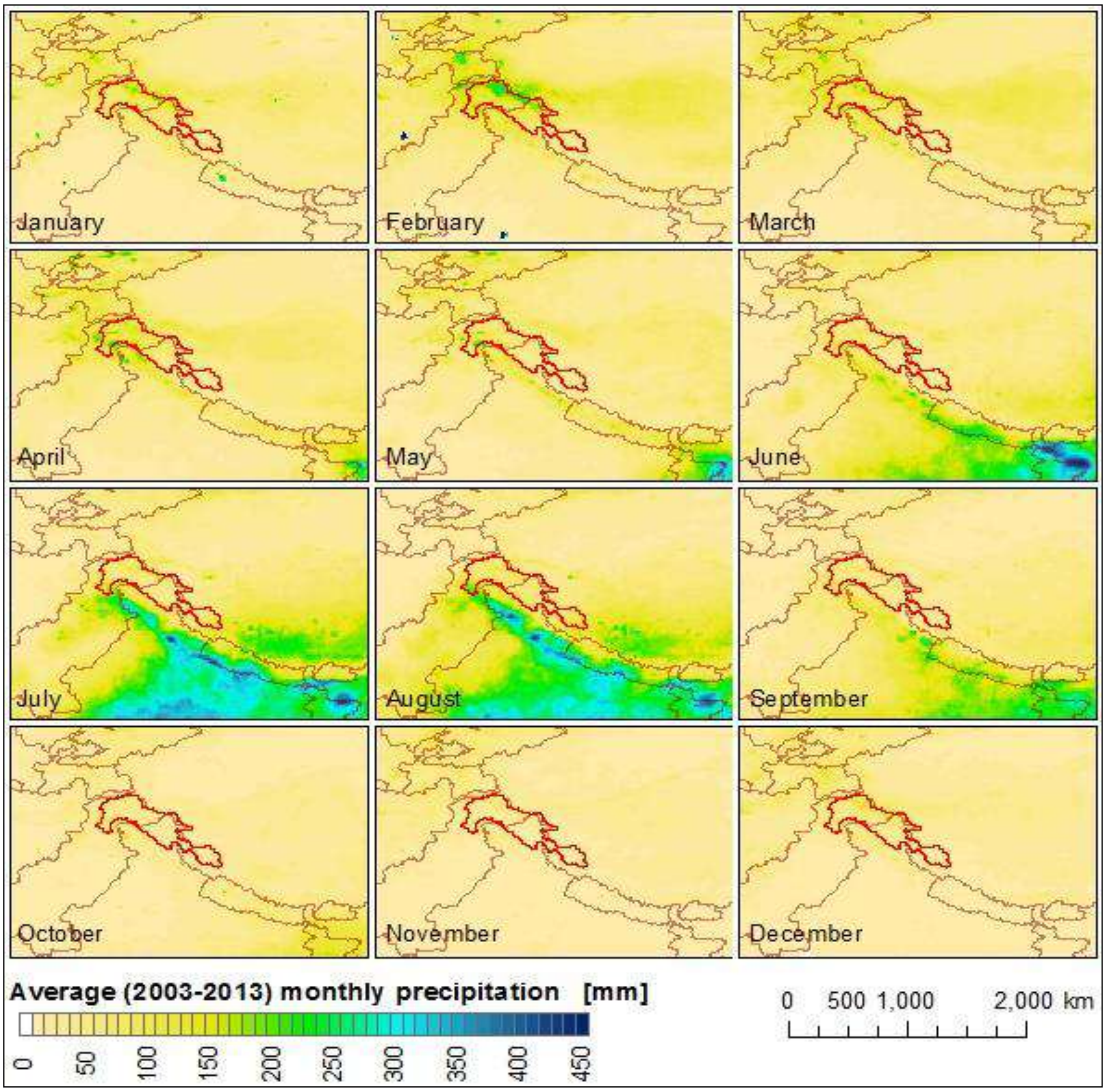

Figure 3-66: Average Monthly Precipitation Calculated from RFE_Ag Data of Years 2003 to 2013

3.24.6 Glacier Distribution in the Upper Indus Basin

Apart from the seasonal snow, it is the glaciers that form a major water reservoir in the UIB. Among scientists there is a general agreement of a worldwide depletion in glacier thickness and their retreat to higher elevations; however for many Himalayan regions no proof exists that may support this assumption. Uncertainties remain, primarily because of a lack of reliable measures and particularly a lack in long-term monitoring programs. To understand the contribution of glaciers to river discharge and project their future role as a water resource and a water reservoir, the spatial glacier coverage needed to be mapped and ongoing trends in glacier movements be monitored. Due to time constraints the monitoring could only focus on a few selected glaciers. Those were used to get an insight into prevalent trends in glacier retreat/growth in the UIB. The results on glacier change also served as a guide line for hydrologic modelling in calibrating glacier melt/accretion. During glacier change mapping the focus was on glaciers located in low topographic elevation, where changes such as glacier retreat should show first.

Glacier data

Existing data on global glacier distribution are limited to those from the GLIMS data archive. A major source for their interpretation (GLIMS) is visually interpreted aerial photographs, giving detailed view on spatial glacier distribution. Though highly accurate in spatial detail, existing GLIMS interpretations do not provide a complete coverage for the UIB as is needed for modelling purposes.

Necessary information on glaciers therefore was interpreted from Landsat8 images of the year 2013. With 30m spatial resolution, the spatial accuracy of Landsat data is certainly less, but from its data a continuous map with glacier coverage could be created that is spatially comparable. Also, at an envisaged spatial modelling resolution of 1000m, the difference in spatial detail is insignificant.

For a full coverage of the UIB, a total of 19 Landsat8 scenes were interpreted (Figure 3-67). Since snow and glaciers display similar spectral characteristics in satellite acquired multispectral images, only scenes acquired during late summer to early fall were processed and interpreted. This assumes that the snow pack, accumulated during the previous winter, has completely melted. Whatever snow cover is left at this time is considered as permanent snow.

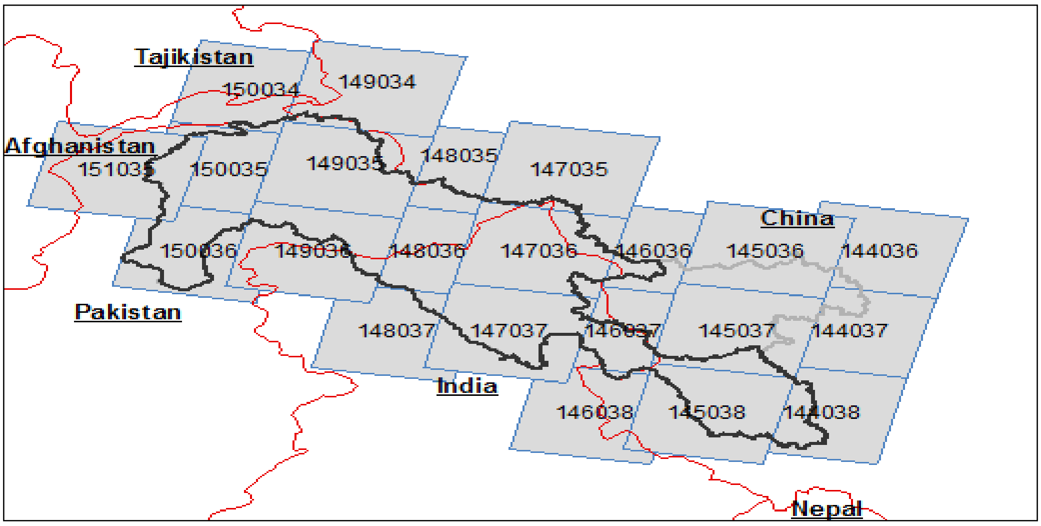

Figure 3-67: Landsat 8 Ft Prints for the Area of the UIB and the Pangong Tso Watershed (outlined in grey).

To avoid misinterpretations due to cloud coverage only data with less than 10% clouds were used. In the few cases where clouds still obscured glaciers, gaps were filled through interpolation from neighbouring areas. Areas affected are exclusively located along the little glacierized south-eastern UIB watershed boundary (scene p148 r036). The processed Landsat scenes are given in Table 3-30.

Table 3-30: Processed Landsat Scenes

No	Path/ Row	Acquis. date	Scene Id	No	Path/ Row	Acquis. date	Scene Id
1	144/36	2013-07-02	LC81440362013215LGN00	12	147/37	2013-06-21	LC81470372013300LGN00
2	144/37	2013-07-02	LC81440372013199LGN00	13	148/35	2013-07-14	LC81480352013211LGN00
3	144/38	2013-07-02	LC81440382013247LGN00	14	148/36	2013-07-14	LC81480362013195LGN00
4	145/36	2013-07-09	LC81450362013270LGN00	15	148/37	2013-07-14	
5	145/37	2013-07-09	LC81450372013270LGN00	16	149/34	2013-06-19	LC81490342013282LGN00
6	145/38	2013-07-09	LC81450382013270LGN00	17	149/35	2013-06-19	LC81490352013282LGN00
7	146/36	2013-06-30	LC81460362013261LGN00	18	149/36	2013-06-19	LC81490362013282LGN00
8	146/37	2013-06-30	LC81460372013261LGN00	19	150/34	2013-06-10	LC81500342013209LGN00
9	146/38	2013-06-30	LC81460382013261LGN00	20	150/35	2013-06-10	LC81500352013209LGN00
10	147/35	2013-06-21	LC81470352013268LGN00	21	150/36	2013-06-10	LC81500362013289LGN00
11	147/36	2013-06-21	LC81470362013268LGN00	22	151/34	2013-06-01	LC81510342013280LGN00

3.24.6.1 Glacier Mapping

For the interpretation of glacierized areas a simple Normalized Difference Ice Index (NDII) was used, with resulting ratios being thresholded to separate glacier covered from non-glacier covered areas. In areas where GLIMS data is available, the resulting glacier distribution compares very well with GLIMS data.

$$NDII = \frac{\#2 - \#7}{\#2 + \#7}$$

From the automated glacier interpretation, glaciers that are covered by debris remained unclassified. This applies to the lower sections of glaciers (glacier tongues), and was completed through visual interpretation. The glacier distribution for UIB is shown in Figure 3-68.

In order to assess glacier depletion under the influence of a changing climate, an approximate glacier thickness needed to be assigned. For reasonable approximations the few published data were consulted ((Huss and Farinotti, 2012; Immerzeel et al.)), though these only give general estimates of ice depths. To produce a spatially distributed map of glacier thickness the equation of LIU and DING (1986) was used and modified to fit glacier thickness as reported in the literature. The result does not accurately reflect actual glacier depth and tends to rather overestimate than underestimate glacier thickness, but represents a sound basis to measure gains and losses in glacier thickness under the influence of climate change (Huss and Farinotti, 2012).

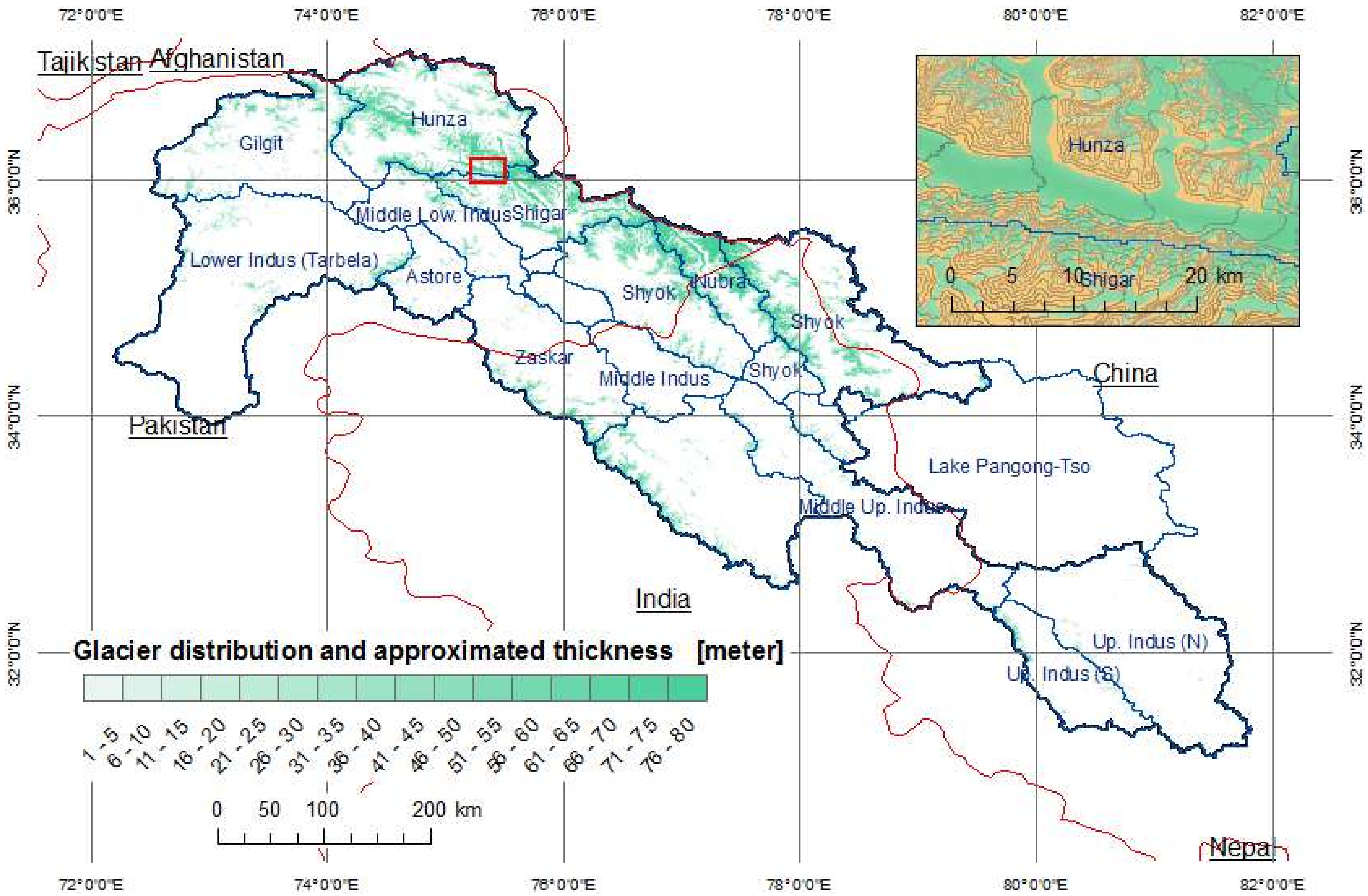

Figure 3-68: Glacier Distribution Interpreted from Landsat Data (2013) and Approximated Ice Thickness. The Inset Box Shows the Detail Acquired at a Spatial Resolution of 30m.

3.24.7 Glacier Analyses, Spatial Distribution and Temporal Changes

Of the entire UIB area, approximately measuring 173,411km^2 (excluding the PangongTso watershed), about 10% or 16,750km^2 are covered by glaciers. The majority of glacierized area (6.8%) is found between elevations of 5,400 and 5,500m (Figure 3-69 right). 20% of all glaciers, comprising an area of 3,349km^2 are found at elevations below 4400m (Figure 3-69 left) (Kuhle, 1986). The lowest elevation covered by any glacier was identified in the western Shigar watershed, with the tip of a glacier tongue reaching as low as 2,600 meters.

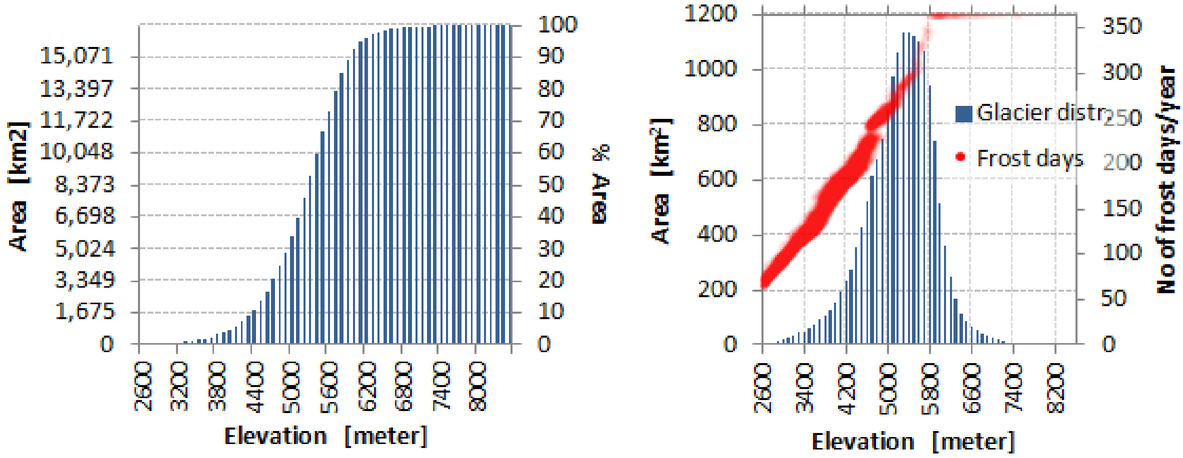

Figure 3-69: Accumulated Glacier Areas (left) and Glacier Area Distribution by Elevation (right) for the UIB. Glaciers are binned into 100m Elevation Intervals.

Permanent frost with temperatures never exceeding 0°C, depending on location, starts at around 5,800m and applies to an area of about 1934km^2. These calculations are based on average mean temperatures from 2003 to 2013 (see section 3.21.1.1).

3.24.8 Monitoring Glacier Growth/Retreat

A comparative evaluation of Landsat data for changes in glacier distribution was intended to better understand recent climate change impacts on glaciers and to prevent possible pitfalls in the modelling of future climate change impacts. As described above, the latest glacier distribution map is derived from Landsat8 data of the year 2013. The earliest period for which a decent spatial coverage of Landsat data is available, also matching the 2013 acquisition date (late summer to fall.), is composed of data from the years 1989 to 1992.

Different to what we would expect from the temperature development, with annual mean temperature showing a steady increase of about 1.5°C since the beginning of the nineties (CRUTEM4 data, Figure 3-60), the extent of the glaciers and particularly its lower stretches the glacier tongues, did not change considerably or not at all (Hewitt, 2011; Kääb et al., 2012), a phenomenon in the literature described as the Karakoram anomaly (Minora et al.). There may be occasional errors in the proper detection of the extent of glaciers due to clouds or the variable extent of snow fields during different years; however according to the Landsat analysis, the past 24 years are marked by a rather stable situation of most glaciers throughout the entire UIB with regard to their spatial distribution and extent. Glacier thickness, of course cannot be monitored this way; though a reduction in glacier thickness is rather likely to have an impact on a glacier's spatial extent as well.

With mean annual temperatures having increased by about 1.5°C since 1995, still most glaciers do not show any impact. The seasonally diverse temperature developments (Figure 3-61 and Figure 3-62) with increasing temperatures during winter months but decreasing during summer, is probably responsible for a more complex pattern of glacier growth and retreat (Matsuo and Heki, 2010). It also needs to be reminded that the majority of climate stations of WAPDA and PMD are located at elevations between 1,200m and 3,300m, only three stations are higher than 4,000m and none higher than 4,730m. This is basically only representative for 20% of glacierized areas (Figure 3-69). Also, a used lapse rate of 6.5°C/1,000m in temperature interpolations may not properly reflect the situation in higher elevation areas.

Figure 3-70 shows the location of change analyses of different low elevation glaciers.

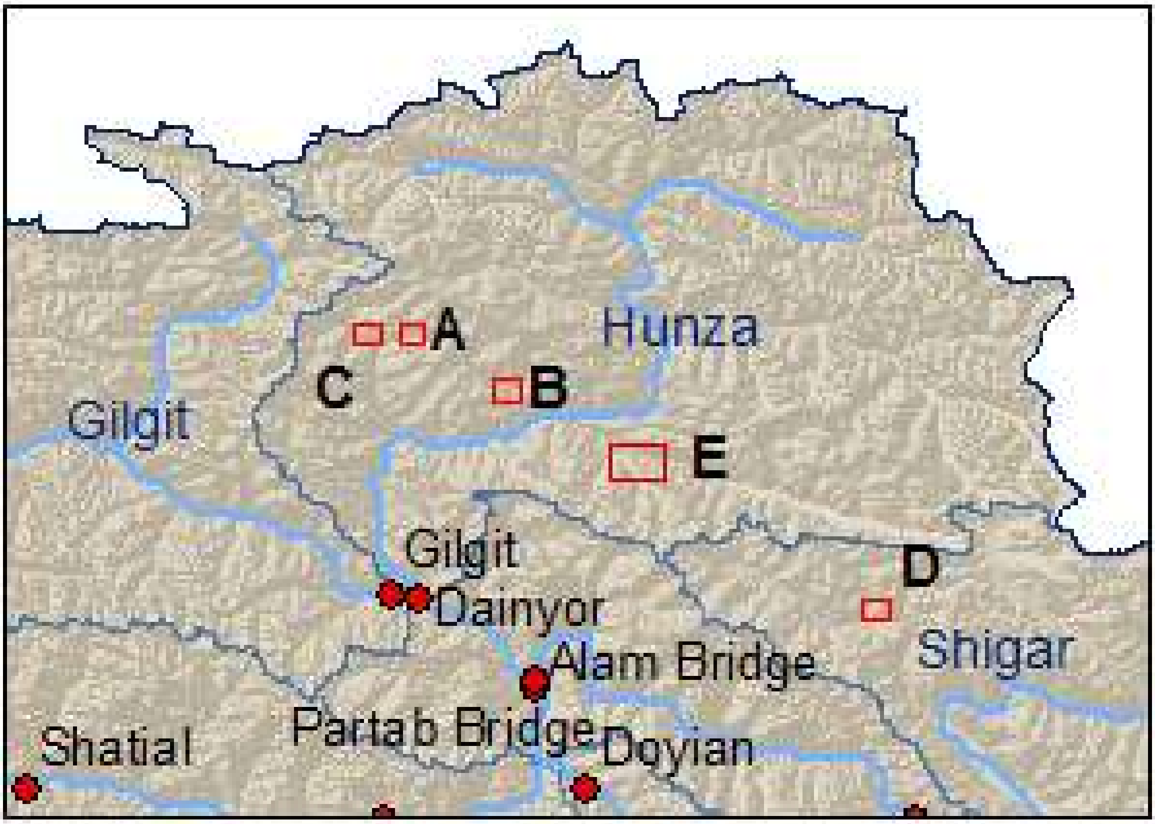

Figure 3-70: Location of Change Analyses of Different Low Elevation Glaciers

Closer, random inspection of selected glaciers suggests that some glacierized areas below 3000m did considerably retreat since 1990, particularly so in the Hunza catchment (Figure 3-71 locations A and B). This however, does not generally apply to all glaciers at elevations between 2,600 and 3,000m as the two examples from Hunza and Shigar watersheds show in Figure 3-72. In contrast, at higher elevations (>3,000m) glaciers appear to be stable, not showing any change (Figure 3-71 bottom) (Cogley; Committee on Himalayan Glaciers, 2012; Gardelle et al.).

Measured rates of retreat range between 90 – 130m/year, where the lower rate applies to a glacier's retreat from 2,800m to 3,000m asl. and the higher rate to a retreat from 2,600 to

3,000 m asl. (Figure 3-71). Other than elevation, geographic location and glacier dynamics, a valley's orientation may also be of influence. The interaction between these parameters and each parameters impact on glacier melt was not investigated. While a receding trend is observed for some glaciers (Prasad et al., 2009; Rasul et al., 2012), the changes are not at all dramatic, since glaciers below 3,000 m asl only amount to <<1% of glacierized areas in the UIB (Figure 3-69). Glaciers under the influence of the westerlies generally show less or are no retreat, different to glaciers in a monsoon controlled climate (Matsuo and Heki, 2010; Scherler et al., 2010; Vaux et al., 2012).

Though not generally applicable to valley glaciers because of other influencing variables (compare Figure 3-72 bottom), receding valley glaciers have been observed at locations where the number of frost days per year is typically around 100 days and less or the number of degree days is 2600 and more.

The 2600 day line may only serve as an orientation, because a range of additional parameters control the advance or the receding of glacier tongues (Hewitt, 2011; Marzeion et al., 2014; Scherler et al., 2010). Among those are:

- Size of the uphill ice field, ice cap or mountain glacier, that feed the valley glacier
- Glacier flow rates, controlled by topography and ice mass
- Precipitation (snow fall in the accumulation area adding to the glaciers' mass)
- Valley orientation (insolation), affecting ablation
- Micro climate affecting ablation
- Kind of debris, its thickness, coverage and materials to name just some of the most relevant factors.

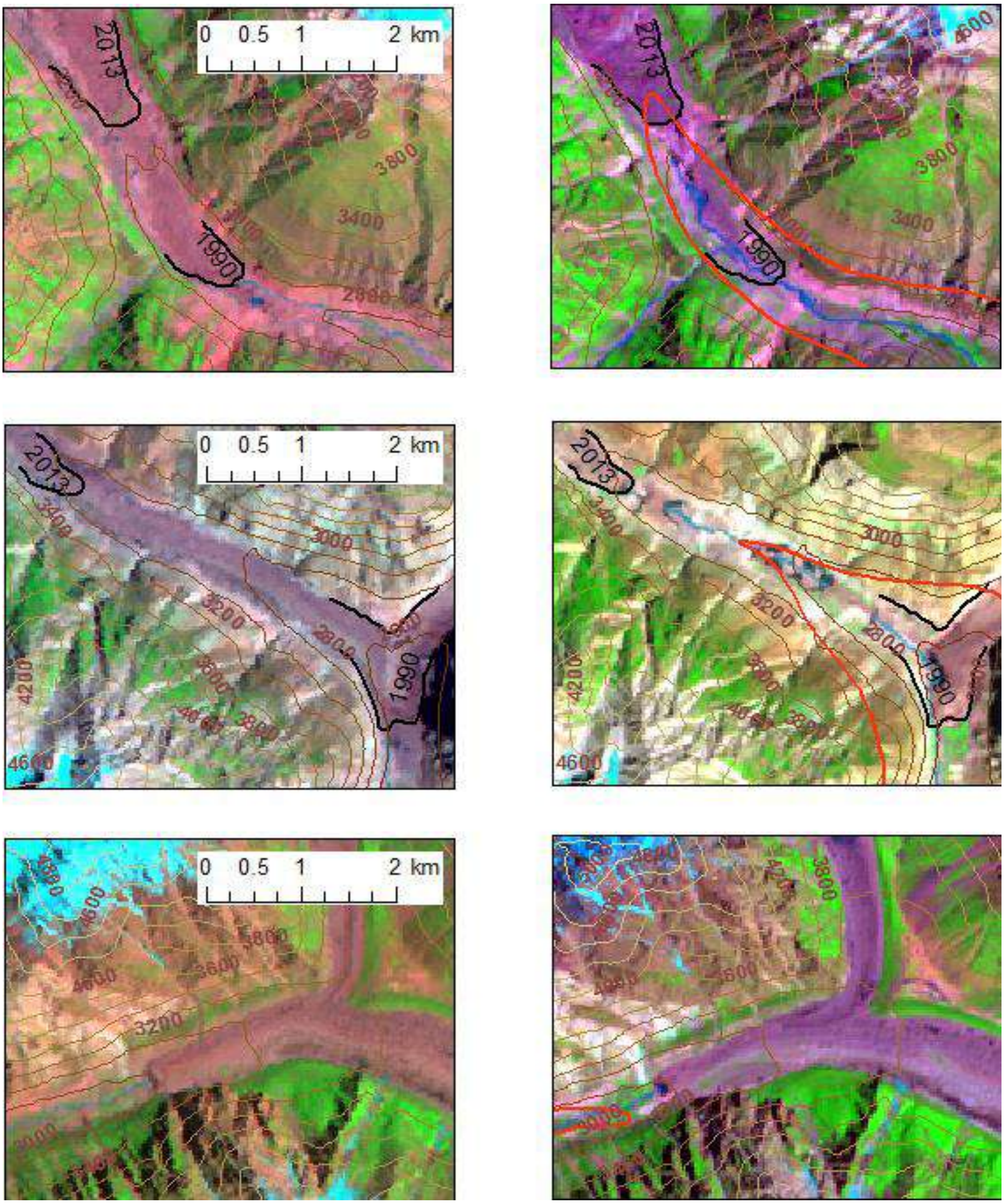

Figure 3-71: Change in Glacier Extent at Various Locations in the Hunza Watershed between Years 1990 (left column) and 2013 (right column).

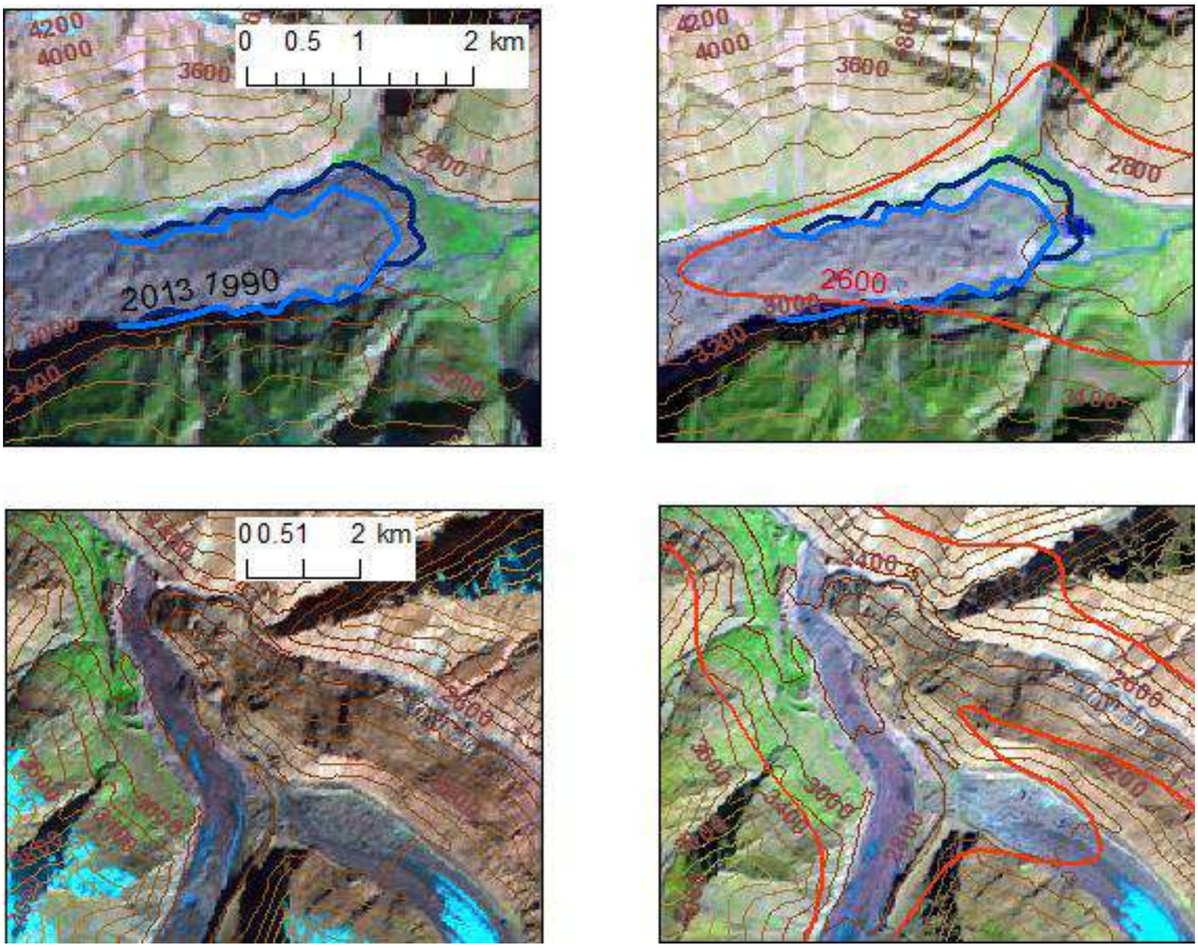

Figure 3-72: Glacier Tongues at Low Elevations in Shigar and Hunza Watersheds

3.24.9 Climate Change Scenarios

For the modelling of future climate change impacts on UIB water resources and discharge, data from different General Circulation Models were tested. As guidance for proper data selection the Consultant tested how well models describe current seasonal temperature variation, how accurate models continue observed seasonal temperature trends and how 'realistic' their projections are in terms of predicted temperature magnitudes.

Among the investigated models the CGCM model from the Canadian Centre for Climate Modelling and Analysis performed best with regard to the above selection criteria. Other models tested included those from the British Hadley Centre (HADGEM1 model), from the Australian CSIRO (CSIROMk3.5 model) and US NCAR's CCSM model (see Annexure-N).

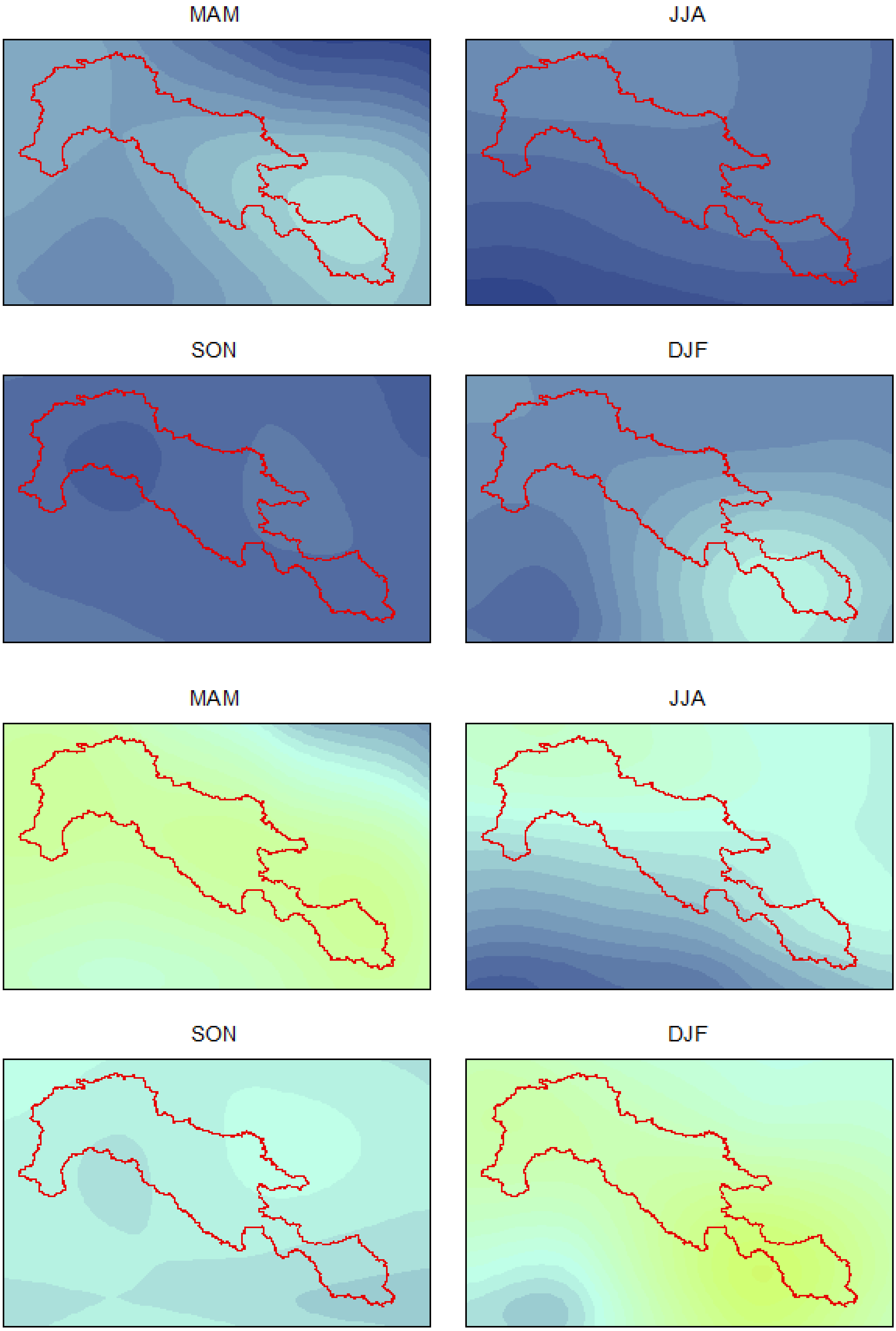
MAM
JJA
SON
DJF
MAM
JJA
SON
DJF

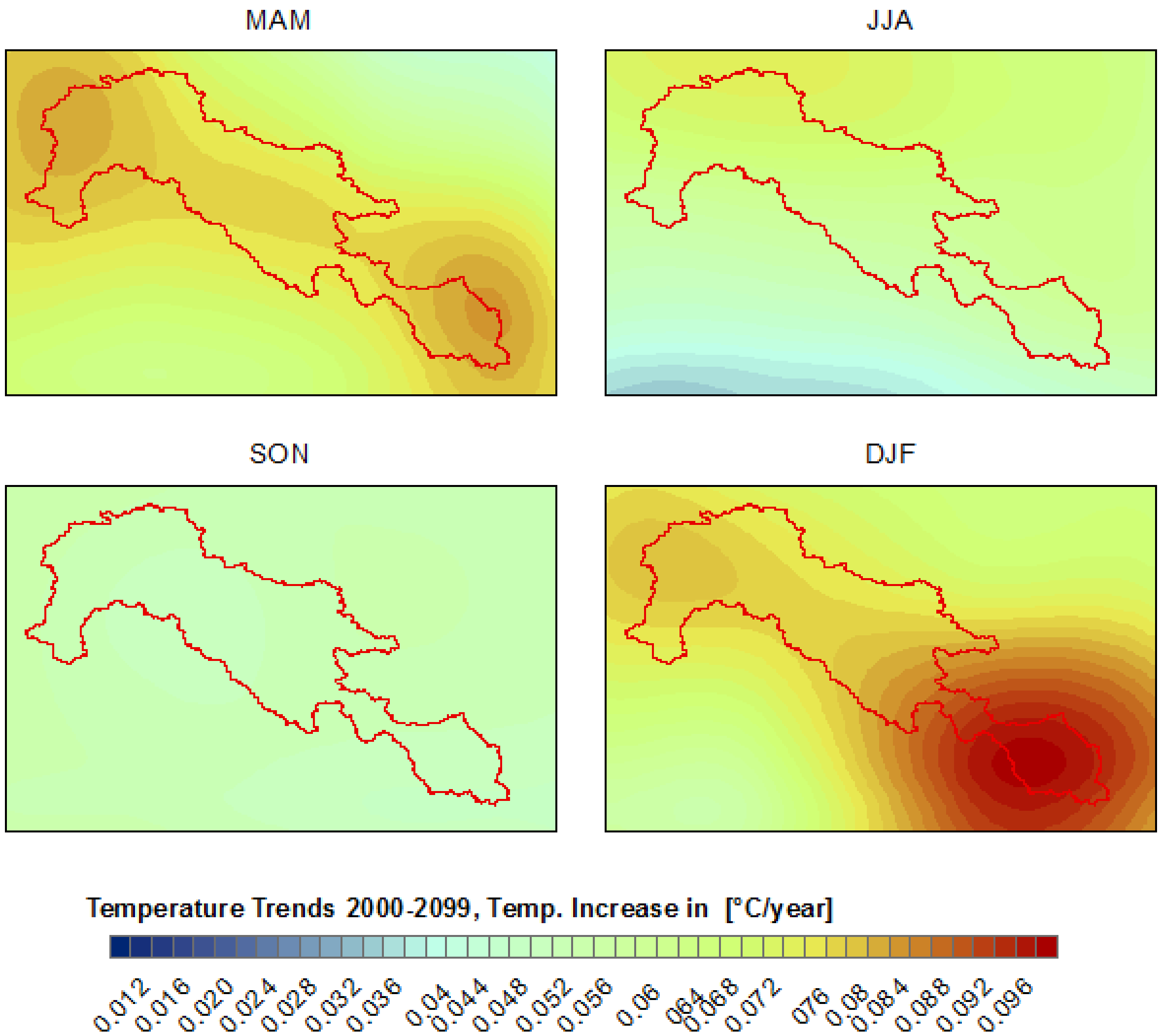

Figure 3-73: Projected Temperature Trends until Year 2099 for a B1, A1b and A2 Scenarios

Typical problems that were found in data from models not considered for this study are a poor reproduction of absolute seasonal temperatures, extraordinary high predicted temperature increases or a seasonal temperature increase that does not reflect the observed pattern of seasonally variable temperature trends (Figure 3-61 and Figure 3-62). As an example the controversial temperature trends as predicted by the CGCM and the CCSM model resp. are shown in the Annexure-N for different scenarios.

The selected CGCM model best reproduces temperatures for the reference period and in its predictions places highest temperature increases in winter and spring reflecting the observed seasonal trends (Figure 3-73).

While reproducing seasonal precipitation distribution reasonably well (Figure 3-74), annual total precipitation was found to be too low in all GCM model outputs (Figure 3-74). Also, inter-annual precipitation variation is far too low compared to observed variations (Figure 3-74). All CGCM change scenarios make similar projections on precipitation development which remains stable over the next 100 years. To consider for unrealistically low, modelled precipitation amounts (CGCM), the consultant only used the relative changes and added those to an observed average precipitation (RFE). This ensures comparability between model outputs from the observed period and outputs for future climate change scenarios.

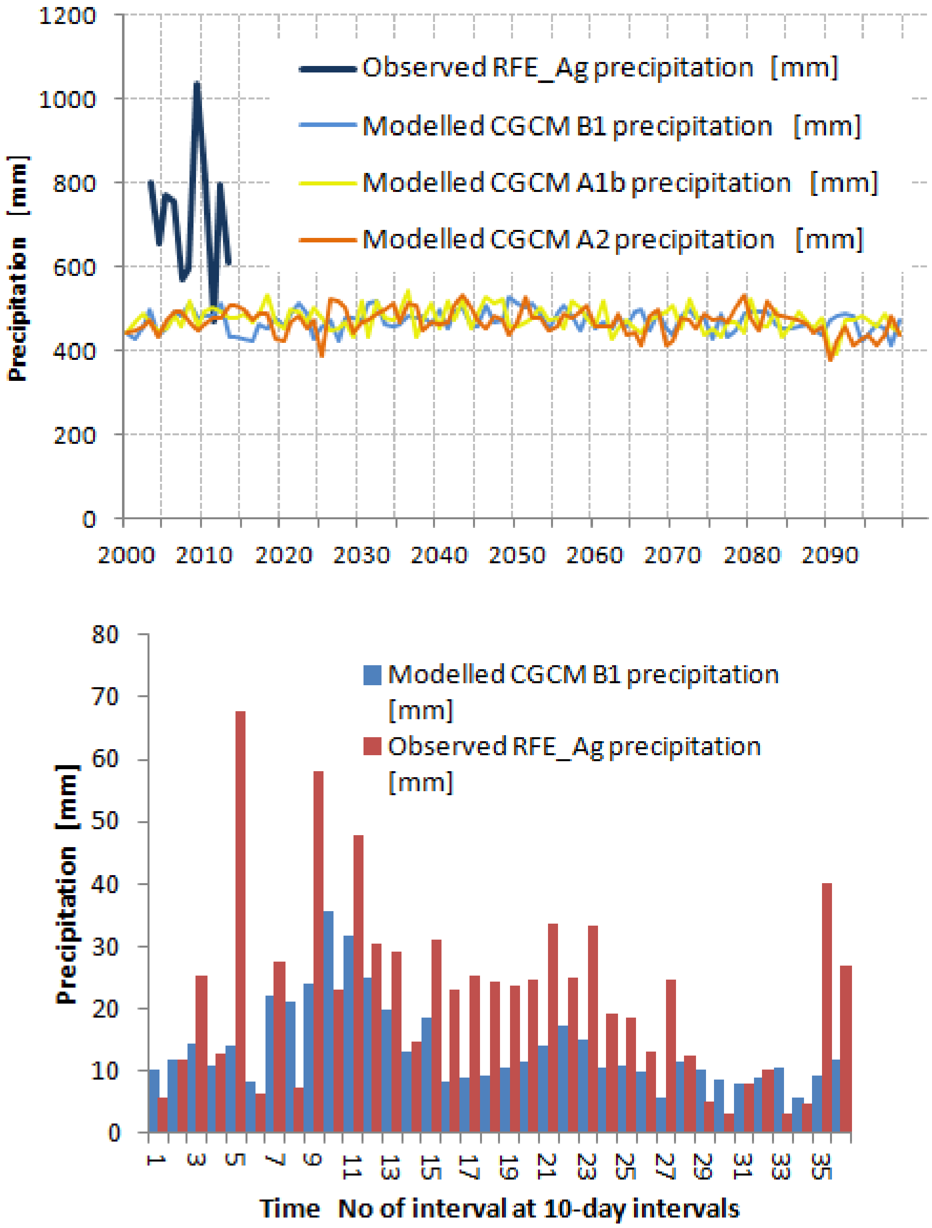

Figure 3-74: Comparison of Observed and CGCM Modelled Precipitation for Annual Total (top) and Seasonal Precipitation (bot.)

As was done for the observed period, future climate change data were processed into 10-day intervals, 1km (temperature) or 12km (precipitation) grids. As the original GCM data come at rather coarse resolution (1.5 – 3.5 degree), data needed to be downscaled to 1km and 12km resolution resp. For temperature the procedure of downscaling follows the same steps as described above in the interpolation between station records. For downscaling GCM precipitation data, the consultant first analyzed precipitation distribution patterns from observed RFE data and applied derived patterns to GCM precipitation data. The process assumes that precipitation distribution patterns do not change in the future.

3.24.10 Hydrologic Modelling

For modelling surface hydrology, the model Hydro-Meteorological Basin Processes (HyMeB) was used, developed at Yale University. HyMeB is designed for the modelling of large basins and, because of its flexibility in required input parameters, is particularly suited for the hydrological modelling of data sparse regions (Geerken et al., 2009). It is a spatially distributed discharge model, allowing the modelling of soil moisture, surface run-off, base flow, snow-and ice melt and river discharge. Minimum input layers include precipitation, temperature and potential evapotranspiration (PET). Other input parameters either spatially variable or as a single scalar are: available water holding capacity, land cover/land use, glacier coverage, surface permeability plus a series of variables such as critical temperature of melting, T_{crit}, proportionally constant for calculating the 'melt rate factor', and several others. Details of the model and some of its most relevant equations are described in the Annexure-M.

The chosen temporal interval for modelling the Upper Indus Basin is 10-day intervals, the spatial resolution was chosen at 1km^2. Parameters prepared at a spatial resolution of 1km^2 are temperature and PET. Glacier coverage was analyzed at 30m and then degraded to 1km^2. Land cover/land use was evaluated at 250m and then degraded to 1km^2. The resolution of the RFE precipitation data remained unchanged at 12 km^2. Some maps/parameters such as FOA's 'Digital Soil Map of the World' are provided as a vector file and were converted for modelling purposes to a 1km^2 resolving grid (Table 3-31).

Table 3-31: Spatially Distributed Input Parameters to the HyMeB Model

Parameter	original	input	Source	Original temporal resolution
Temperature	1km^2	1km^2	Interpolated from station data	Daily
Precipitation	12km^2	12km^2	RFE Afghanistan data	Daily
Radiation	1km^2	1km^2	Calculated	10-day intervals
PET	1km^2	1km^2	Calculated	10-day intervals
Glacier coverage	30m^2	1km^2	Analyzed from Landsat data	n/a
Land cover/land use	250m^2	1km^2	Analyzed from MODIS data	n/a
AWC	Vector	1km^2	Digital soil map of the world	n/a
Permeability	Vector	1km^2	Digital soil map of the world	n/a

PET was calculated after Hargreaves and corrected to Penman PET using a transfer function for alpine regions as described above and in the Annexure-M.

For model calibration, an only short period of 4 years was used. Though for distinct parameters data were available for longer periods, it is only years 2003 to 2006 that were covered by all of the necessary input parameters. While this is not optimal, it still offers a reasonably long period for parameter tuning and model calibration, particularly so, where these data represent a good spread of drier and wetter years.

Model calibration aims at identifying and adjusting individual sub-watershed characteristics, to achieve best matches in modelled and observed river discharge. Individual adjustments were made to various parameters including available water holding capacity, critical temperature of melting, surface- and subsurface flow parameters (Manning coefficients), and to parameters affecting the partitioning of water between surface runoff and infiltration. Due to sparse vegetation growth, vegetation coverage is of minor influence.

3.24.10.1 Surface (Sheet- and Channel-Flow) and Sub-Surface Flow

In the model the partitioning of precipitation between surface flow and sub-surface flow is controlled by soil saturation and to a lesser extent by slope which has merely a modifying influence.

Flow velocity of surface flow is determined from soil specific characteristics, vegetation cover and surface slope. For parametrization the MANNING coefficients are used. For surface flow in open channels, respective semi-empirical Manning coefficients for steady state flow were used, though steady state may not apply in all locations. Manning provides parameters for different channel substrates and for different formations of channel perimeters. Due to unknown details about river bed situations, a single set of coefficients was chosen. Modification of these coefficients showed only insignificant changes in discharge characteristics and justifies this selection. Stronger modifications in discharge characteristics are imposed by modifications to the length of the drainage network. The beginning of open channel flow is defined as a minimum number of pixels that must contribute (flow into) to a pixel and was calculated for all of the UIB using the same threshold. From several calculations a best performing threshold was chosen. Resulting flow velocities for surface flow are shown in Figure 3-75.

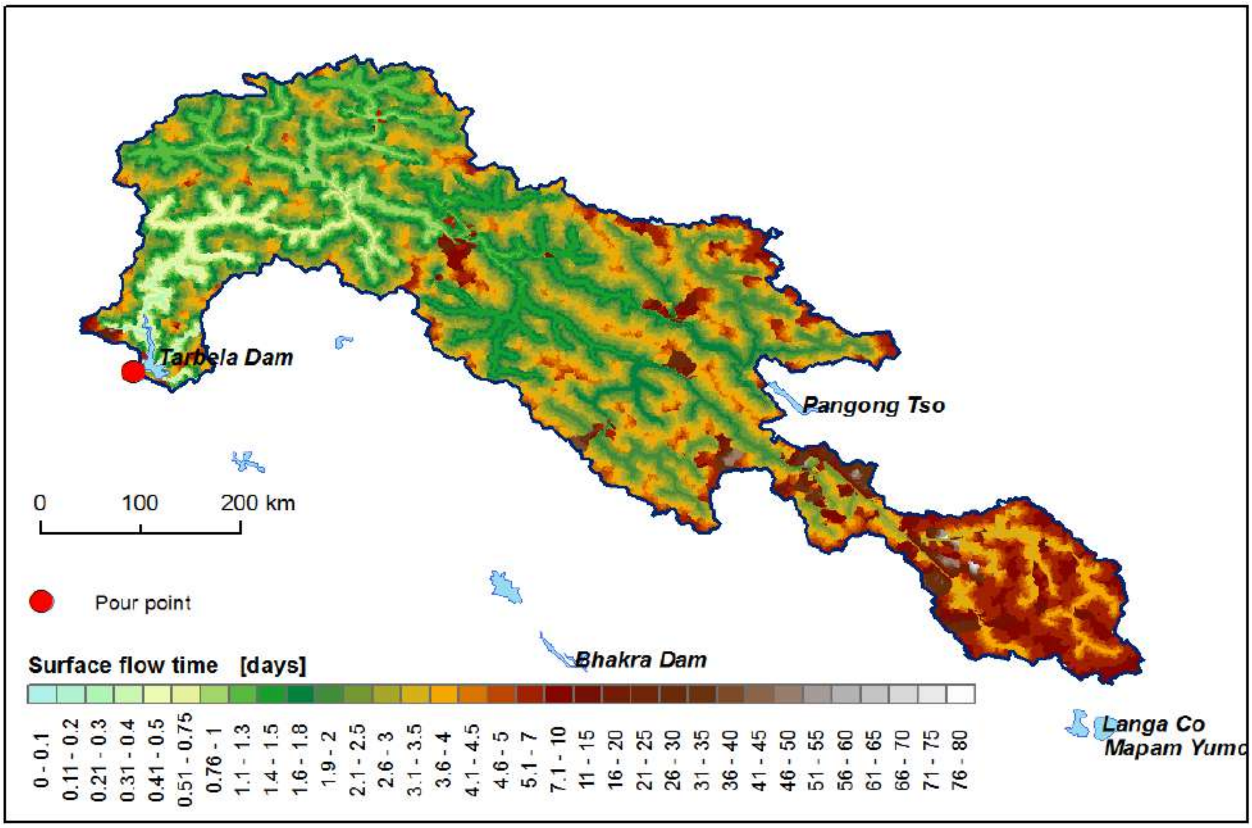

Figure 3-75: Surface Flow Time Calculated as a Function of Topography and Vegetation

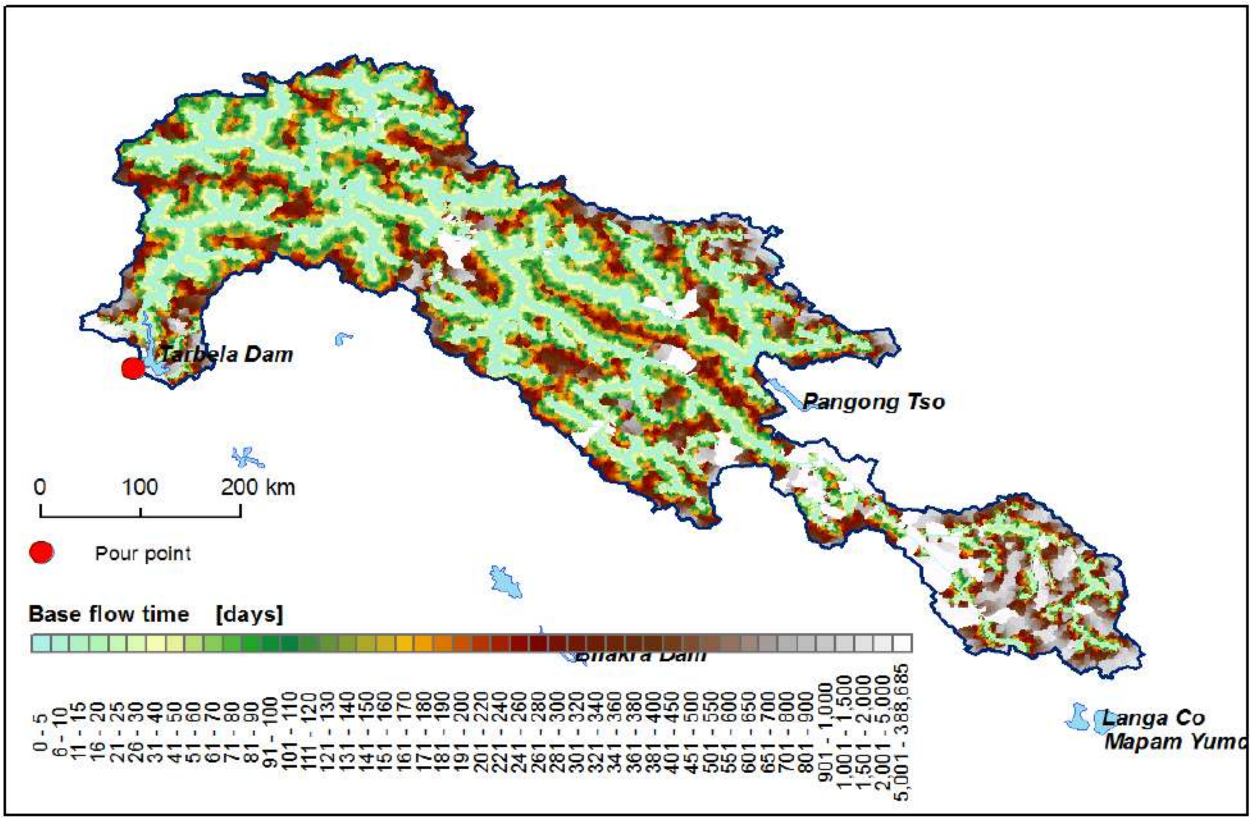

Figure 3-76: Sub-Surface Flow Time Calculated as a Function of Surface Topography and Hydraulic Conductivity of Soils.

Sub-surface flow velocities (Figure 3-76) are calculated in dependence of surface slope and general hydraulic conductivity coefficients (kf value). During model calibration, the kf value was repeatedly modified and adjusted to improve discharge timing and ensure a river flow during dry periods. If sub-surface flow time exceeds two years of travel time to the pour point it is considered to percolate into the underground, and does not reach a drainage channel. This applies to some flat areas in the Upper UIB.

The modelling at 10-day intervals has effects on the proper timing of river flows. Temporal reference for modelled surface run-off – the main contributor to river discharge – is the middle of the decade. Depending on when a maximum in actual run-off is reached (beginning or end of a decade), this may introduce some differences between modelled and observed flood timing due to differing starting points in the creation of the run-off.

3.24.10.2 Impact of Non-Consideration of Glacier Dynamics in the Model

The extent of present glacier coverage was mapped as described in Section 3.21.6.2. While there is high reliability in glaciers spatial distribution, confidence is much lower in approximated glacier thickness, calculated according to the equation of (Liu and Ding)(1986). Calculated glacier thickness tends to be too high creating a water reservoir that stores more water than it has.

Another weakness is the negligence of glacier dynamics that are not considered in regional models due to a lack of detailed glacier information. For these reasons, glacier flow from the accretion area down to the ablation zone is not described.

Uncertainties in glacier tickness and the missing component of glacier flow prevents a sound modelling of changing glacier extent and the prediction of absolute glacier thickness. Instead, temporally changing glacier melting rates and accretion rates resp. will be presented for different climate change scenarios at different times.

Possible scenarios for future spatial glacier extent (mountain glaciers only) are presented in Annexure-O and are based on future temperature situations.

3.24.10.3 Model calibration

For model calibration, five UIB sub-watersheds were identified (Figure 3-77, Figure 3-50 and Table 3-29). Out of the five sub-watersheds, two represent rather large catchment areas, drained through the gauging stations of Kharmong and Kachura respectively. Necessary generalizations in hydro-meteorological parameters across these large catchments may not accurately reflect the local situation in every sub-watershed.

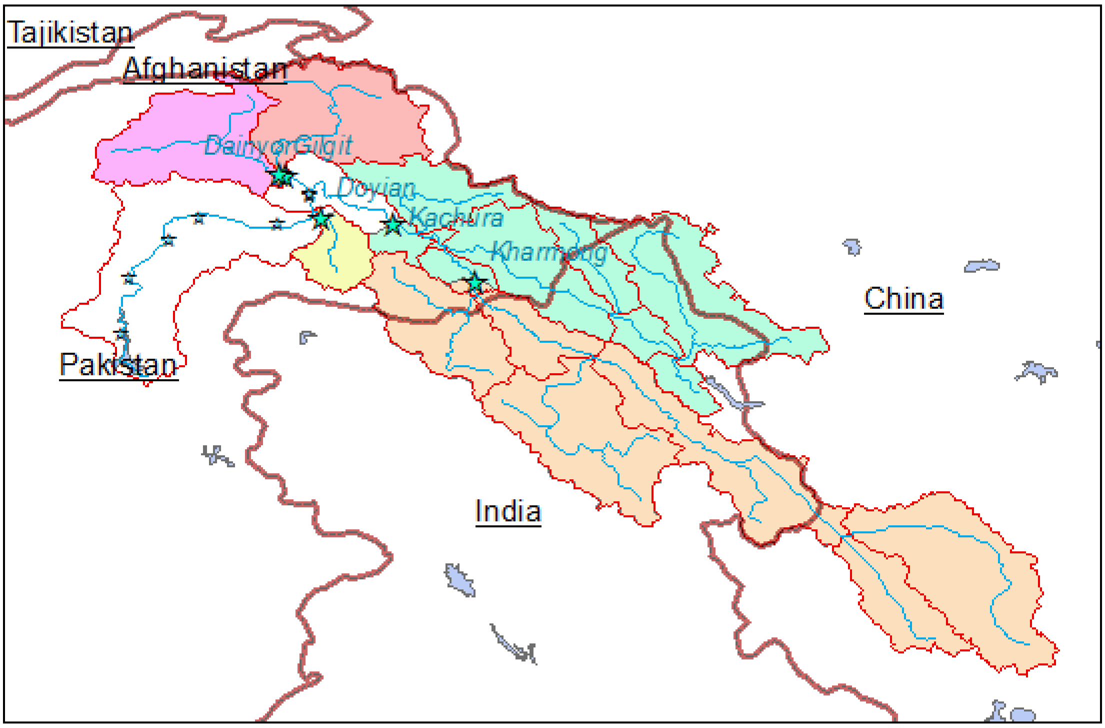

Figure 3-77: Sub-Watersheds Used for Model Calibration

Kharmong sub-watershed
For the Kharmong sub-watershed, the area comprises most different landscapes such as the Tibetan Plateau in the East (Upper UIB watershed) and more typical, alpine landscapes with deep valleys towards the pour point Kharmong (Zanskar and Suru watersheds). Predominantly shallow slopes in the Upper UIB (Tibetan Plateau) delay surface and sub-surface flow, allowing better infiltration.

Kachura sub-watershed

The Kachura sub-watershed which includes Shigar-, Shyok- and Nubra- catchments is topographically, morphologically and climatologically more homogeneous than Kharmong (Ahmad et al., 2012). Rainfall in this catchment is highest in all of the UIB, and with a total of 8440km^2 of glacierized area, it hosts 58% of the glacier covered area in the UIB. Because of the enormous water amount received and stored in the Kachura catchment, better hydro-meteorological description of individual areas would be desirable (Bocchiola et al., 2011). Sparse data coverage and/or inaccessible station records required spatial generalization as well as generalizations across large elevation differences that are likely to conceal actual variability. Chosen model parameters, therefore may not perfectly describe distinct local hydrological situations. Primary orientation in parameter modification was the achievement of a good match between modelled and observed discharge, within reasonable parameter bounds.

Sub-watersheds of the western UIB (Astore, Gilgit, Hunza)

Sub-watersheds, Astore (Doyian station), Gilgit (Gilgit station) and Hunza (Dainyor station) are of smaller extent and at least climatologically more homogenous. They show however considerable spread in elevation and slope, though their inner-quartile range in these parameters is more compact.

Astore sub-watershed (Doyian station)

The modelling of the Astore river discharge at Dainyor station for years 2003 to 2006 produced a significant discrepancy between modelled and observed discharge (Figure 3-78). This is attributed to uncertainties in the precipitation data. Over the modelled years, observed river discharge is between 10 and almost 60% higher than precipitation (RFE_Ag data). Other than the total discharge amount, the timing of discharge peaks triggered by snow melt and rainfall is captured reasonably well.

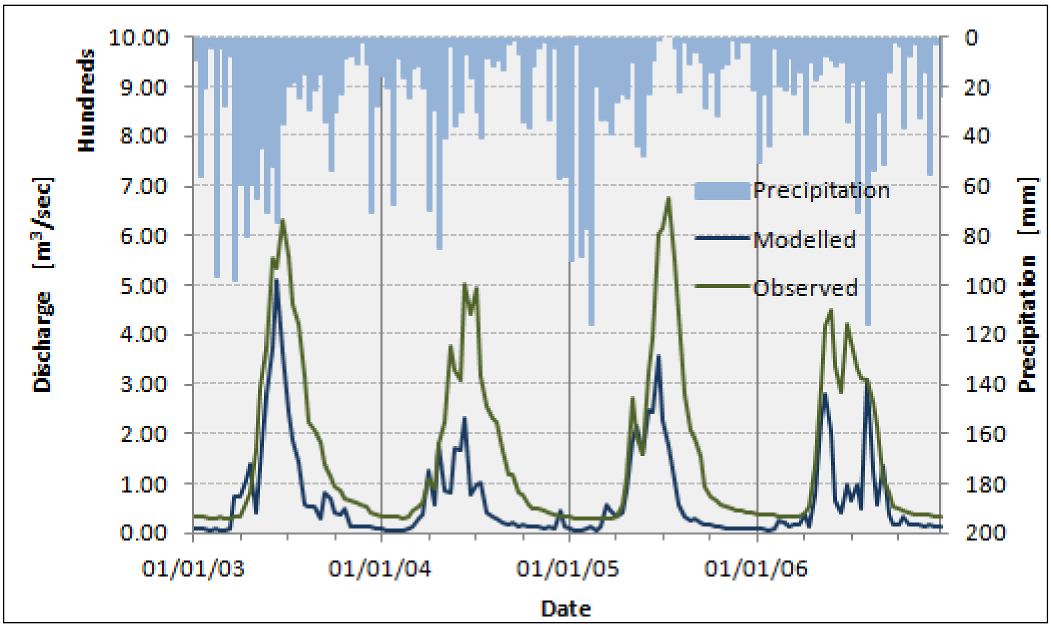

Figure 3-78: Comparison of Observed and Modelled River Discharge at Doyian Station

Gilgit sub-watershed (Gilgit station)

What is described for Astore, similarly applies to the Gilgit sub-watershed: The timing of peaks between observed and modeled discharge matches quite well, deviations are apparent in the discharge amounts or rates (Figure 3-79). Snow cover is depleted too fast, pointing out to insufficient precipitation amounts described in the RFE_Ag data. Observed discharge is between 80 and 130% of RFE_Ag precipitation. Run-off coefficients, the ratio between run-off water and precipitation, depend on a range of different parameters including surface roughness, slope, vegetation cover, soils, climate and several others. Ratios above 0.75 (75%) are more typical for urban environments with large percentages of sealed surfaces. Rainfall coefficients of this magnitude may also occur in barren, rocky landscapes, with steep slopes and shallow soils or ice as encountered in Himalayan watersheds (Hemund et al., 2011). Coefficients of up to 1 (100%) are however more unlikely.

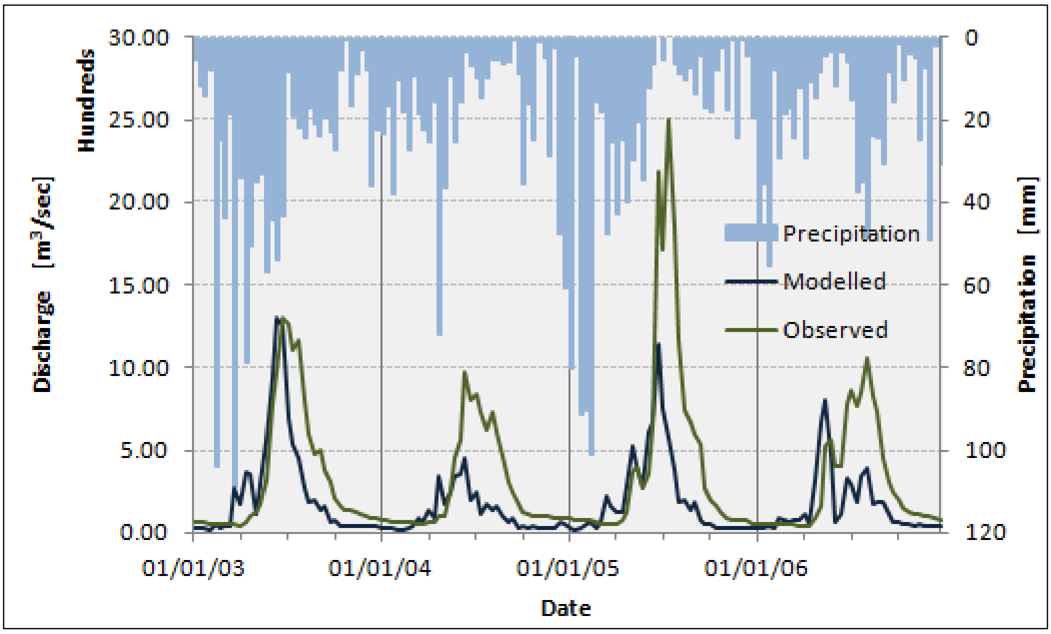

Figure 3-79: Comparison of Observed and Modelled River Discharge at Gilgit Station

Hunza watershed (Dainyor station)

Results for Hunza show a better match between observed and modelled discharge (Figure 3-80). The percentage of total discharge from total incoming precipitation is around 60% (rainfall coefficient 0.6). At least 20 to 30% of precipitate water is lost to evapotranspiration, and the rest contributes to glacier accretion or infiltrates into the deeper underground. Data were only available for years 2003 and 2004.

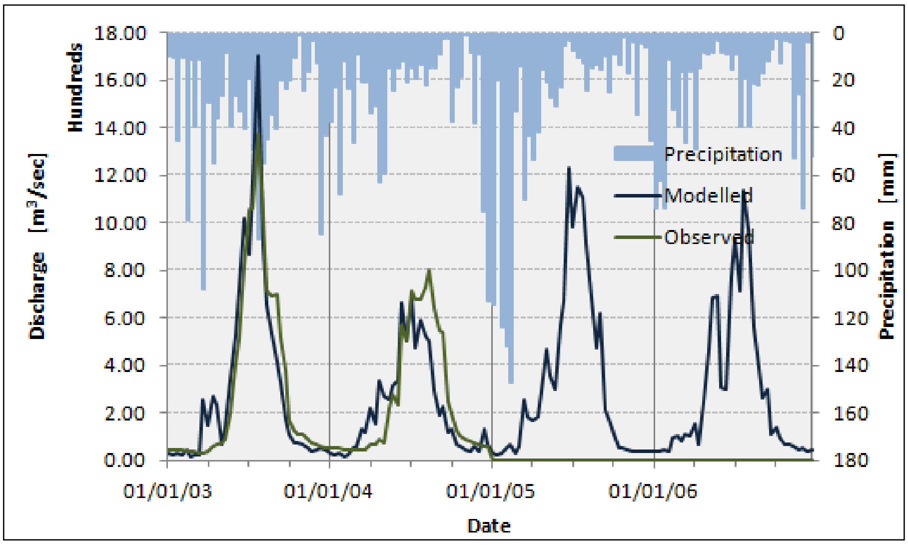

Figure 3-80: Comparison of Observed and Modelled River Discharge at Dainyor Station

Watersheds Shygar, Nubra and Shyok (Kachura station)

As in the case of watersheds of Astore and Gilgit, RFE_Ag precipitation is too low to produce the measured discharge which ranges between 80 and 120% of total precipitation (rainfall coefficient 0.8 to 1.2) (Figure 3-81). Again there is good coincidence in temporal discharge peaks but a mismatch in discharge amounts. As a result, the average modelled discharge is only about 60% of the observed discharge.

Sub-watersheds Suru, Zanskar and Upper UIB (Kharmong station)

Best matches between observed and modelled discharge are achieved for the Kharmong catchment area (Figure 3-82). This is surprising, considering its large E-W extension and the pronounced morphological differences between the Tibetan plateau sub-watersheds of the upper UIB compared to the alpine sub-watersheds of Suru and Zanskar. Precipitation received in the UIB that is mostly under Indian monsoon influence, apparently is better reflected in the RFE_Ag product than those areas under the influence of the Westerlies. Average rainfall coefficient is 0.5 for the entire Kharmong watershed.

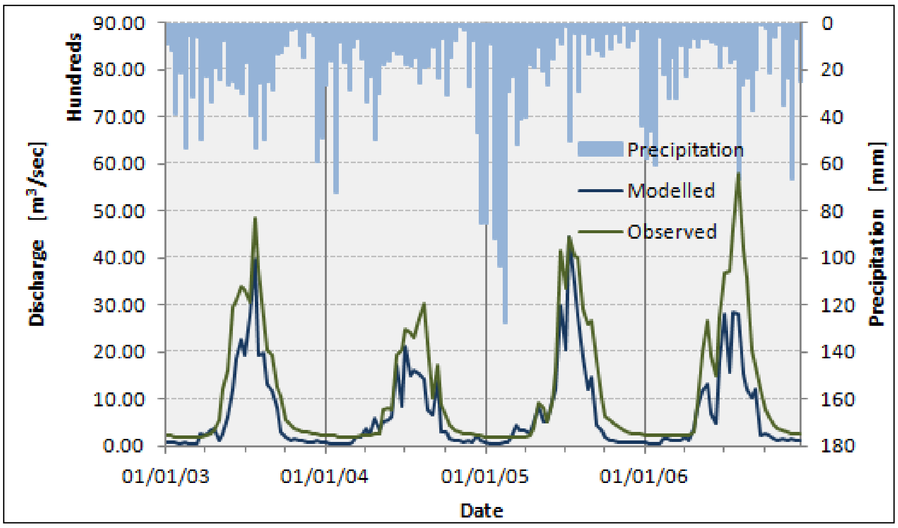

Figure 3-81: Comparison of Observed and Modelled River Discharge at Kachura Station

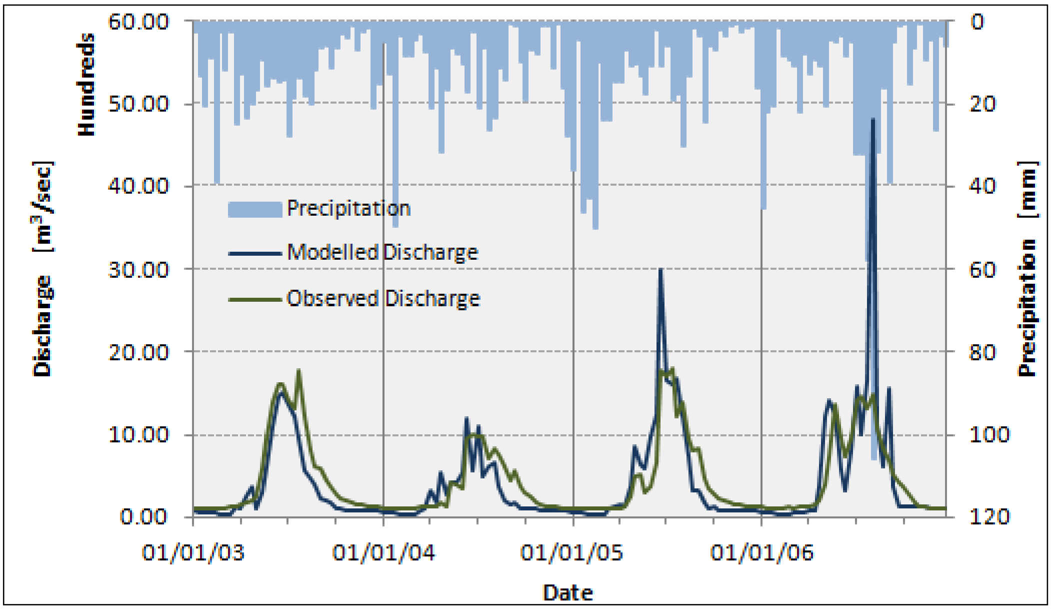

Figure 3-82: Comparison of Observed and Modelled River Discharge at Kharmong Station

3.24.11 Impacts of Precipitation Deficit on Modelling Results

In the long term climate analysis, with the snow pack gone too early, in the model the available energy is now used for the melting of glaciers. The percentage of spatial glacier coverage in watersheds is however much less than typical snow cover and water from glacier melt, therefore cannot fully compensate for the missing snow pack, particularly not in watersheds with little glacier coverage. Accordingly, in model results we see larger discrepancies between modelled and observed river discharge in watersheds with little glacier coverage like Astore and Gilgit but less discharge deviations e.g. in the more densely glacierized Kachura catchment area. For all watersheds, the hydrological modelling results in a more (Astore and Gilgit) or less (Hunza, Kachura, Kharmong) underestimation of river discharge and an overestimation of glacier melt.

To verify whether an increased melting isn't really happening an analysis of temporal changes in glacier extent for selected glaciers was carried out (see section 3.25.7). This analysis could not confirm substantial recessions in glacier extent between 1990 and 2013 as one would expect to see based on modelling results. This confirms the conclusion that rainfall amounts described in RFE_Ag data are too low.

3.24.12 Influence of Modelled Glacier Depth

The approximation of ice thickness using the equation of Liu and Ding (1986) results in glacier depths that is too high. Modelled glacier depths form a basis for modelling, but does not describe in a realistic way the process of glacier retreat In model runs, overestimations of glacier thickness cause a longer than realistic persistence of glaciers, meaning glaciers do not retreat. The modelling of reasonable retreat/growth rates is further compromised by not considering above described glacier dynamics. Projected discharge rates therefore are an upper limit that will never be reached. For the definition of a lower limit, mountain glacier distribution under different temperature situations (meaning for different climate scenarios during different times in this century) using a 'degree line' approach were used as input to the hydrological model (Figure 3-83, for more examples see Annexure-O). Future mountain glacier extension at different times for an A1b scenario using a degree day approach. A 500 degree day (per year) line was identified as a good descriptor for the lower limit for the occurrence of mountain glaciers. This line is valid for most of the UIB with the exemption of those areas that are part of the Tibetan plateau. Here glaciers are typically found at higher altitudes with lower degree day values, ranging around 300 and 400 degree days per year. The offset compared to other areas is owing to a different climate and particularly to low accretion rates controlled by the areas' seasonal precipitation pattern composed of primarily monsoon rainfall but only little winter snow fall.

Based on the degree day line approach, glacierized areas will decrease until 2050 by 36% under a more moderate climate change scenario (B1) but up to 50% under an A1b and A2 scenario. Glacier losses will be higher during the second half of the century with losses of up to 90% (A2). Losses under an A1b scenario are calculated at around 75%, for a B1 scenario around 50%. Shea et al. (2015) report similar glacier losses in the Mount Everest area at the end of this century.

Because the degree line approach does not include a simulation of valley glaciers (entirely missing), such model runs produce too little discharge thus defining the lower limit. Realistic discharge scenarios are located somewhere between the two extremes.

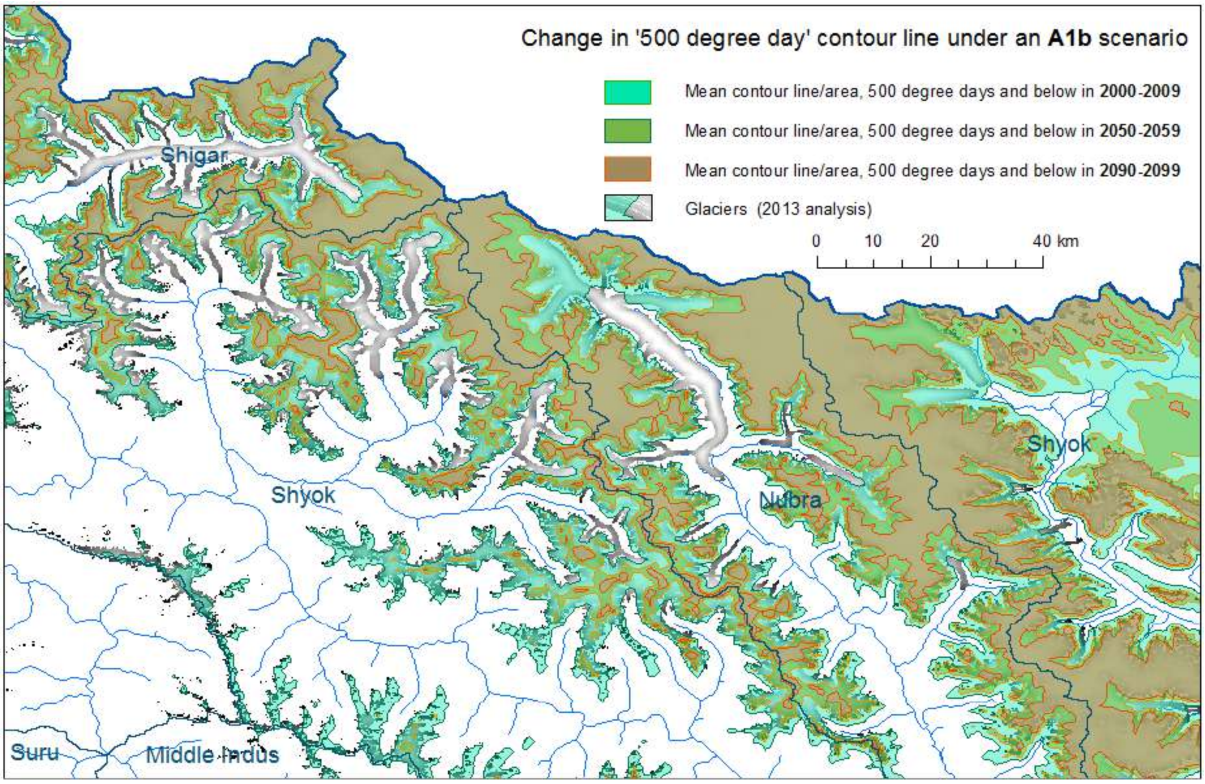

Figure 3-83: Future Mountain Glacier Extension at Different Times for an A1b Scenario using a Degree Day Approach.

3.24.13 Modelling Results

Because of uncertainties in the development of glaciers/glacier tongues and their future situation with regard to extent, ice thickness, glacier dynamics, ablation and accretion, two different scenarios were modelled representing an upper and a lower extreme, with both scenarios being very unlikely to happen: The first scenario assumes stable glacier/glacier tongues extent as we see it today. The second scenario uses the 500 degree day line to simulate the reduction of mountain glaciers as temperatures increase – valley glaciers are neglected, meaning they are removed. While the first scenario overestimates glacier water resources, the second is an underestimation of water resources. The actual, future glacier situation and the run-off/discharge produced from it is found somewhere between these two scenarios. For the second scenario an average situation of mountain glaciers, using the 500 degree day line was calculated for each decade. Figure 3-84 displays the average result calculated from the two scenarios, for the parameter discharge change. Only percent changes are shown (no absolute discharge amounts) because of discussed inaccuracies in precipitation data. Future discharge changes at Tarbela (decadal averages) for a B1, A1b and an A2 climate change scenario. Changes are measured against a 2000-2009 average discharge. Presented discharge is a decadal mean from annual calculations carried out at temporal intervals of 10-days.

The average discharge change (between upper and lower extreme), for all three change scenarios (B1, A1b and A2) shows discharge increases at the beginning of the year, suggesting a shift towards an earlier onset of the snow melt together with an earlier change from snow to rainfall in some elevation zones. Percent increases in discharge rates of up to 2% remain however modest (Kaser et al.,2010) (Figure 3-84).

Figure 3-85 shows the changes in river discharge under different climate change scenarios (B1, A1b and A2). Because of uncertainties in the dynamics of valley glaciers, a lower extreme (only considering mountain glaciers, no valley glaciers) and an upper extreme (valley glaciers remain at current extent) were calculated. The more likely scenario is found between these extremes (black curve). At the beginning of this century, discharge is more likely to follow the upper extreme. A discharge drop as indicated is caused by the removal of glacier tongues that will however remain more or less unchanged during this period.

The earlier onset of melting is at the expense of some discharge reduction, starting at about mid-year. Even increased glacier melt – triggered by higher temperatures – cannot compensate for the missing snow pack that has been melted during early season. The majority of discharge losses that can be seen in the second half of the year must however be attributed to a consistent underestimation of RFE (GCM) rainfall (compare Figure 3-74) during this period of the year.

Another, model-related cause leading to strong discharge reductions as e.g. observed during the 2010-2019 period, is the impact of the removal of glacier tongues in the ‘lower extreme’ scenario. Removal of glacier tongues considerably reduces melt water from glaciers particularly during early decades when glacier tongues are supposed to be still unchanged, less so during later decades when glacier tongues are likely to have retreated. Actual discharge reductions (lower extreme scenario), therefore will be substantially more moderate than calculated. Effects of glacier tongue removal in ‘lower extreme scenarios’ become evident in diagrams shown in Annexure-O. All scenarios show a non-realistic drop in river discharge at the beginning of this century, attributable to reasons explained in the preceding. Accordingly, until the end of the 2020ies discharge trends are better represented by the upper limit (discharge, current glacier extent).

Numeric approximates of changing glacier surface area and discharge change at the UIB pour point are given in Table 3-32 and Table 3-33.

Table 3-32: Approximates of Projected Average Decadal Glacier Losses for Climate Change Scenarios

Decade	Glacierized Area (2013) [km^2]	B1		A1b		A2	
		Glacierized Area [%]	Glacierized Area [km^2]	Glacierized Area^2 [%]	Glacierized Area [km^2]	Glacierized Area [%]	Glacierized Area [km^2]
2000-2009	16746	100	16746	100	16746	100	16746
2010-2019		87	14551	90	15050	93	15546
2020-2029		80	13414	77	12931	75	12580
2030-2039		77	12872	73	12305	72	12042
2040-2049		73	12213	61	10258	62	10318
2050-2059		64	10647	50	8381	63	10466
2060-2069		62	10435	42	7068	32	5428
2070-2079		53	8827	35	5918	22	3753
2080-2089		55	9203	34	5735	16	2723
2090-2099		49	8143	25	4152	7	1152

Percent losses have been modelled using the ‘500 degree day line’. Calculated percentages were then applied to the observed glacier coverage to obtain estimates for absolute glacier losses in km2. The sharp drop in glacierized area 2050 to 2069, (A2) is caused by temperature increase. This results in higher discharge and huge evapotranspiration rates during 2050-59 followed by discharge drops in 2060-69.

Table 3-33 Approximates of Change in Indus River Discharge for Climate Change Scenarios

Decade	Average annual total discharge (1969-2006) [km^3]	B1		A1b		A2	
		Change in discharge [%]	Change in discharge [km^3]	Change in discharge [%]	Change in discharge [km^3]	Change in discharge [%]	Change in discharge [km^3]
	77						
2000-2009		0	77	0	77	0	77
2010-2019		-7	72	-10	69	-2	75
2020-2029		-4	74	-4	74	-2	75
2030-2039		0	77	4	80	2	79
2040-2049		4	80	9	84	4	80
2050-2059		6	82	8	83	11	85
2060-2069		6	81	7	83	5	81
2070-2079		8	83	11	85	10	85
2080-2089		8	83	14	88	13	87
2090-2099		10	84	11	85	5	81

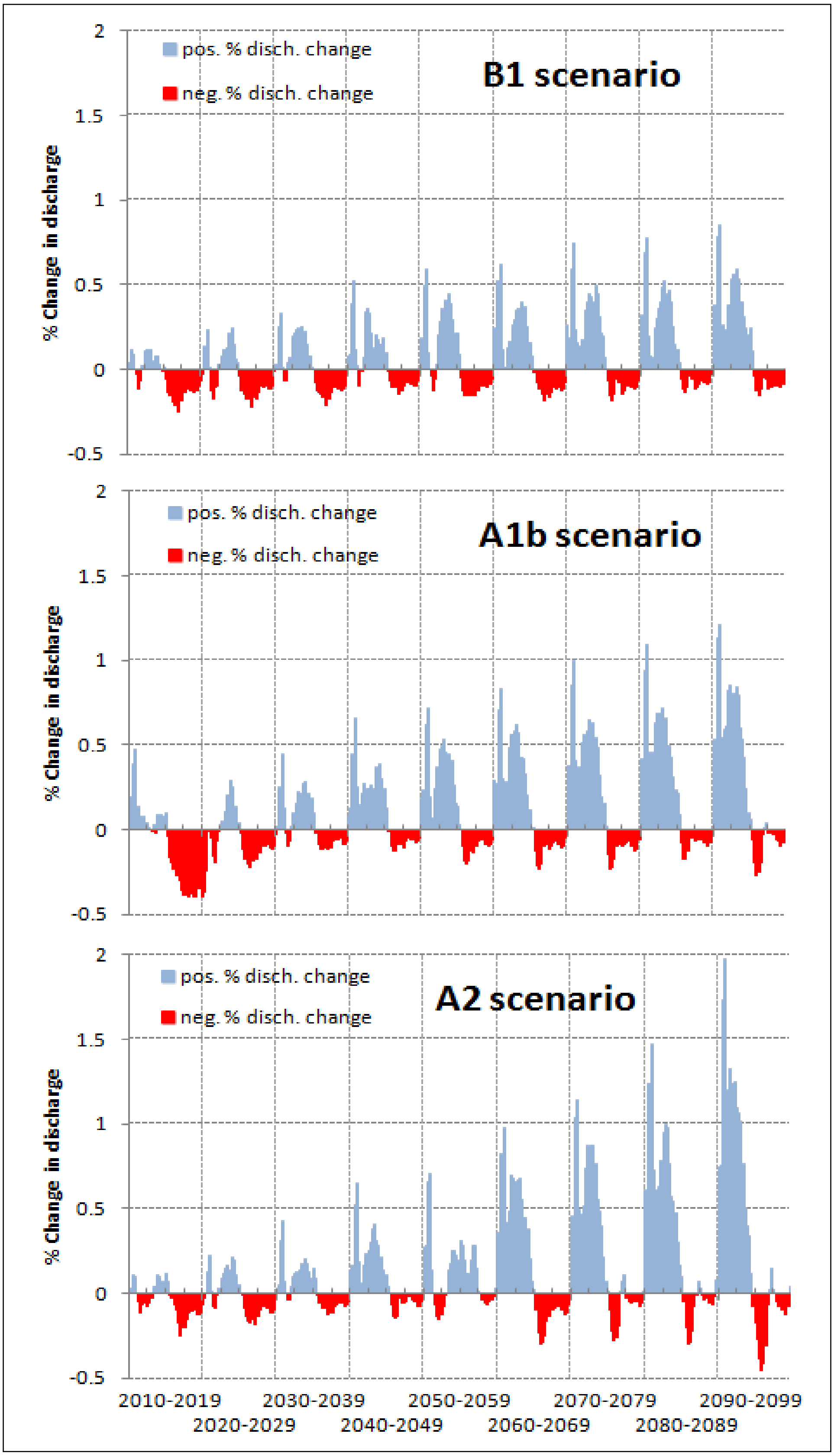

Figure 3-84: Future Discharge Changes at Tarbela (decadal averages) for a B1, A1b and an A2 Climate Change Scenario.

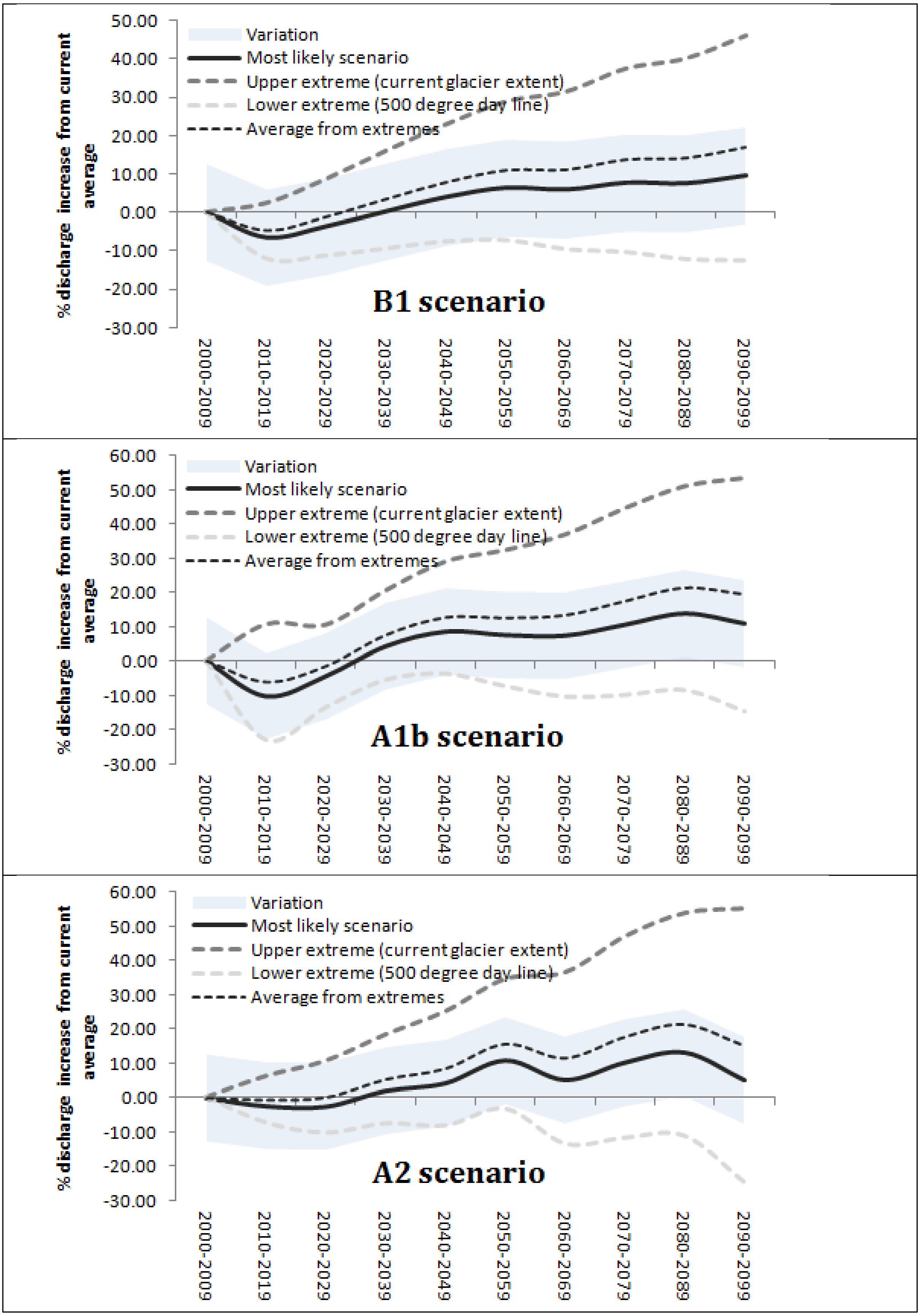

Figure 3-85: Changes in River Discharge under Different Climate Change Scenarios (B1, A1b and A2).

Due to inaccuracies in climate data as described in chapter 3.2 and in chapter 6 only the modelled percent change is given in the table. For the calculation of absolute discharge changes modelled percentages were applied to an observed discharge average (76.96km^3). Discharge drops are an effect of using the degree day line approach for estimating glacier cover (described in the text) and are unlikely to happen in this way. Discharge peaks are reached at around 2050 (A2) and 2080(A1b). Under a B1 scenario the peak falls beyond this century. The negative signs in the table are because of the removal of glacier tongues from the analysis. Which amounts to reduction of about 1/3rd to the actual glacier coverage. With the passage of time the influence of the removal of glacier tongues becomes less and there will be increase of discharge percentage.

3.24.14 Future Situation of ELA

The equilibrium line altitude (ELA) separates the accumulation area of glaciers from the ablation area. Mass balance is zero along this line. The present day ELA, depending on location, is located between 4800m and 4900m. This altitude is derived from model runs. The actual position of the ELA may even be lower, owing to an underestimation of precipitation measurements (explained above).

The equilibrium line will moderately climb to elevations somewhat higher than 4900m asl. until 2050 (A2). Particularly under an A2 scenario, hydrologic model results show a more dramatic shift in the ELA after 2050, reaching a maximum retreat of 5400m until 2099. In both other scenarios (B1 and A1b) the ELA changes much less, retreating to 4900m (B1) and 5100m (A1b) respectively. Figure 3-88 to Figure 3-89 show examples for the shift in ELA from selected decades and scenarios. Areas of ablation are displayed in red, areas of accretion in blue. Changes in ablation and accretion during different times and for different scenarios are shown for the entire currently glacierized area of the UIB. The situation of ablation/accretion and ELA for all of the UIB is shown in Annexure-P.

Modelled water gains and losses across glaciers are measured in millimetres and, using the glacier area, transformed into water volume (km^3). Table 3-34 to Table 3-37 give an impression how temperature increases will affect water gains and losses in different watershed areas. The tables are a summary of changes in ablation and accretion as shown in Annexure-P.

In lower elevation watersheds such as Astore (Table 3-37), even under a B1 scenario the water amount produced over current glacier area will be exceeded by the water amount lost over current glacier area during mid-century (cross-over of lines).

In higher elevation watersheds, this cross over either occurs later or only under the assumption of higher temperature increases such as in A1b or A2 scenarios. These calculations only serve as an orientation, the actual water amounts and the timing of ‘cross-over’ may not be realistic because of the assumptions made on glacier distribution and glacier depth.

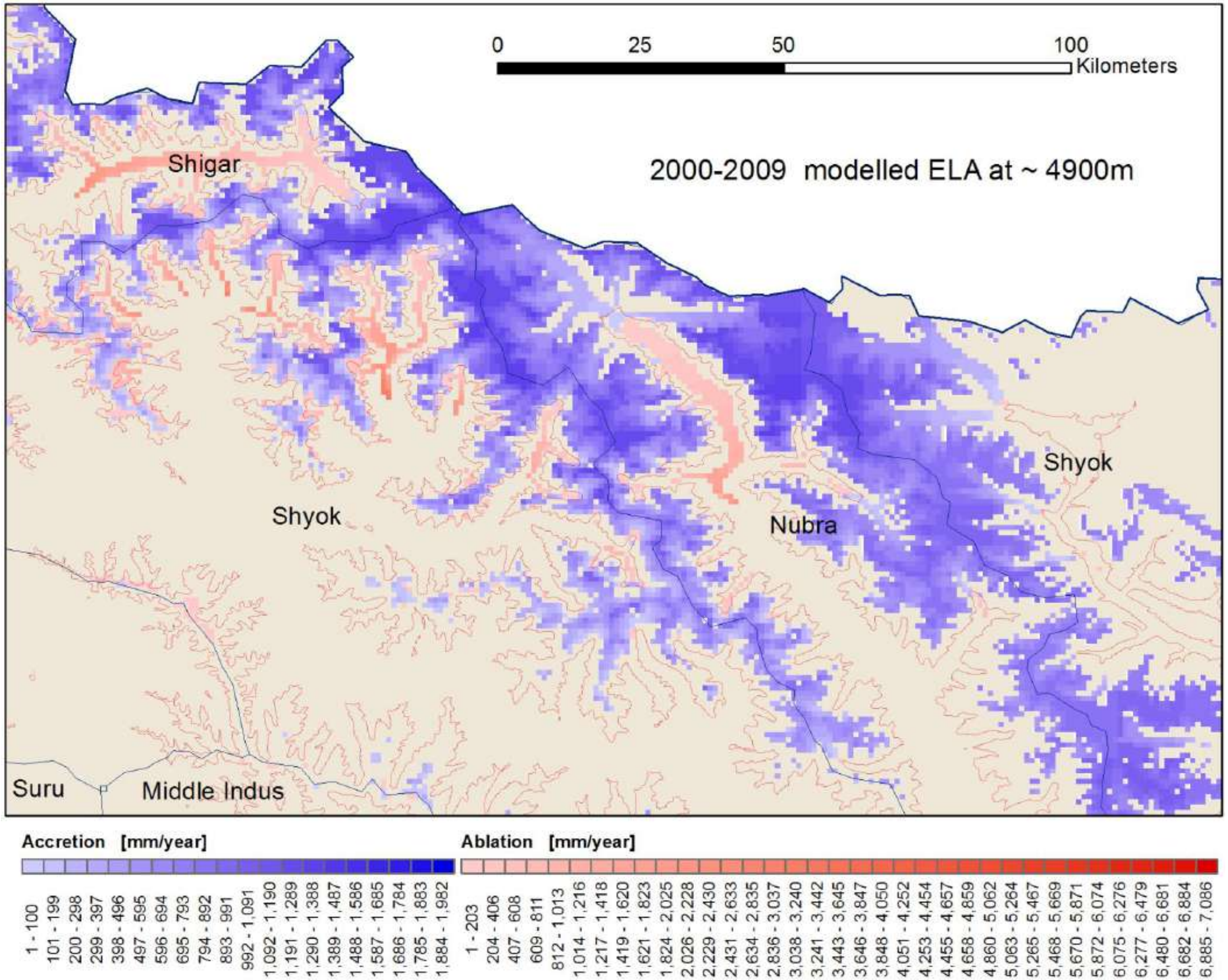

Figure 3-86: The Present Day, Modelled ELA Applicable to Most of the UIB, is Located at Around 4900m

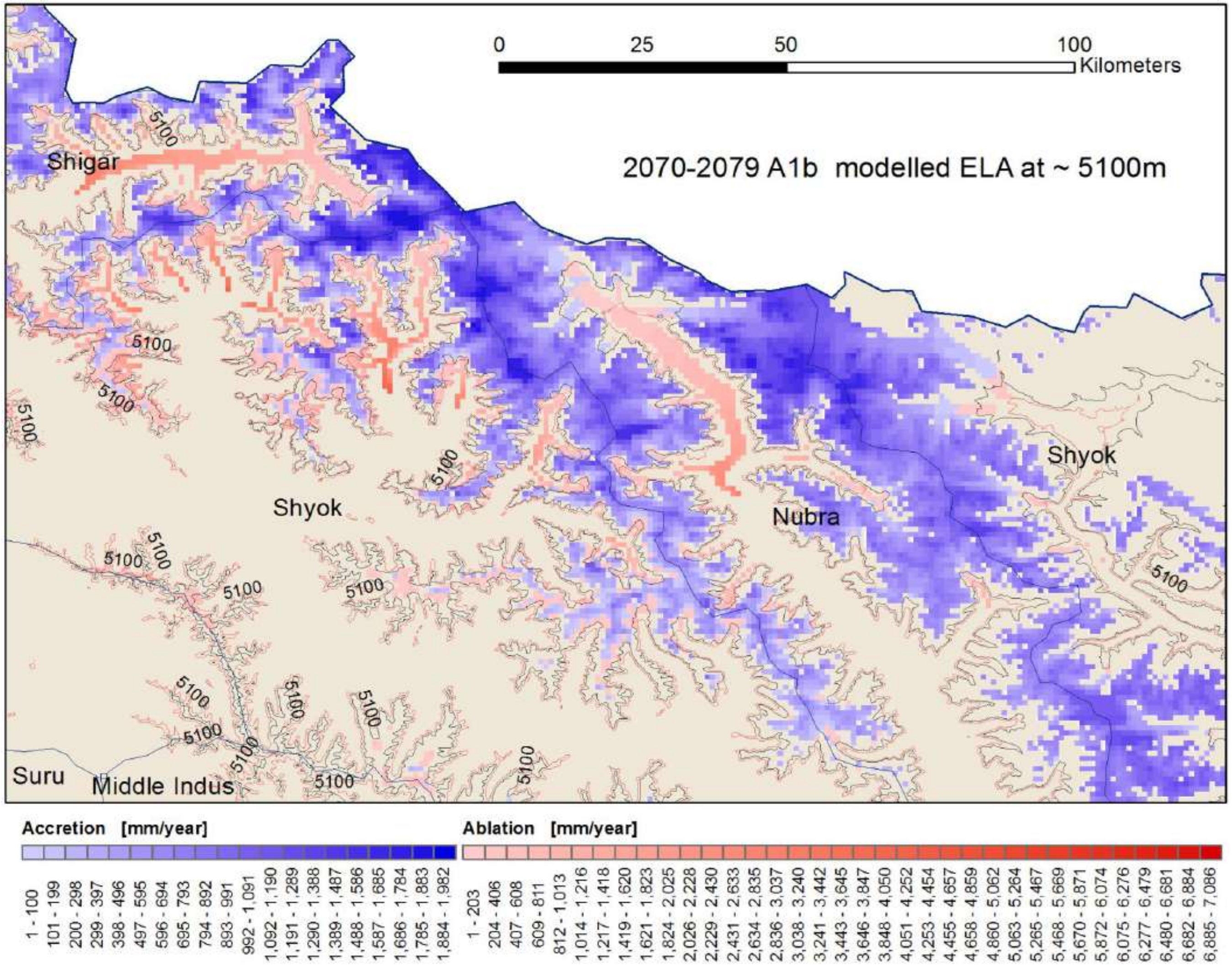

Figure 3-87: Average Position (5100m) of the ELA in the 2070ies under an A1b Scenario.

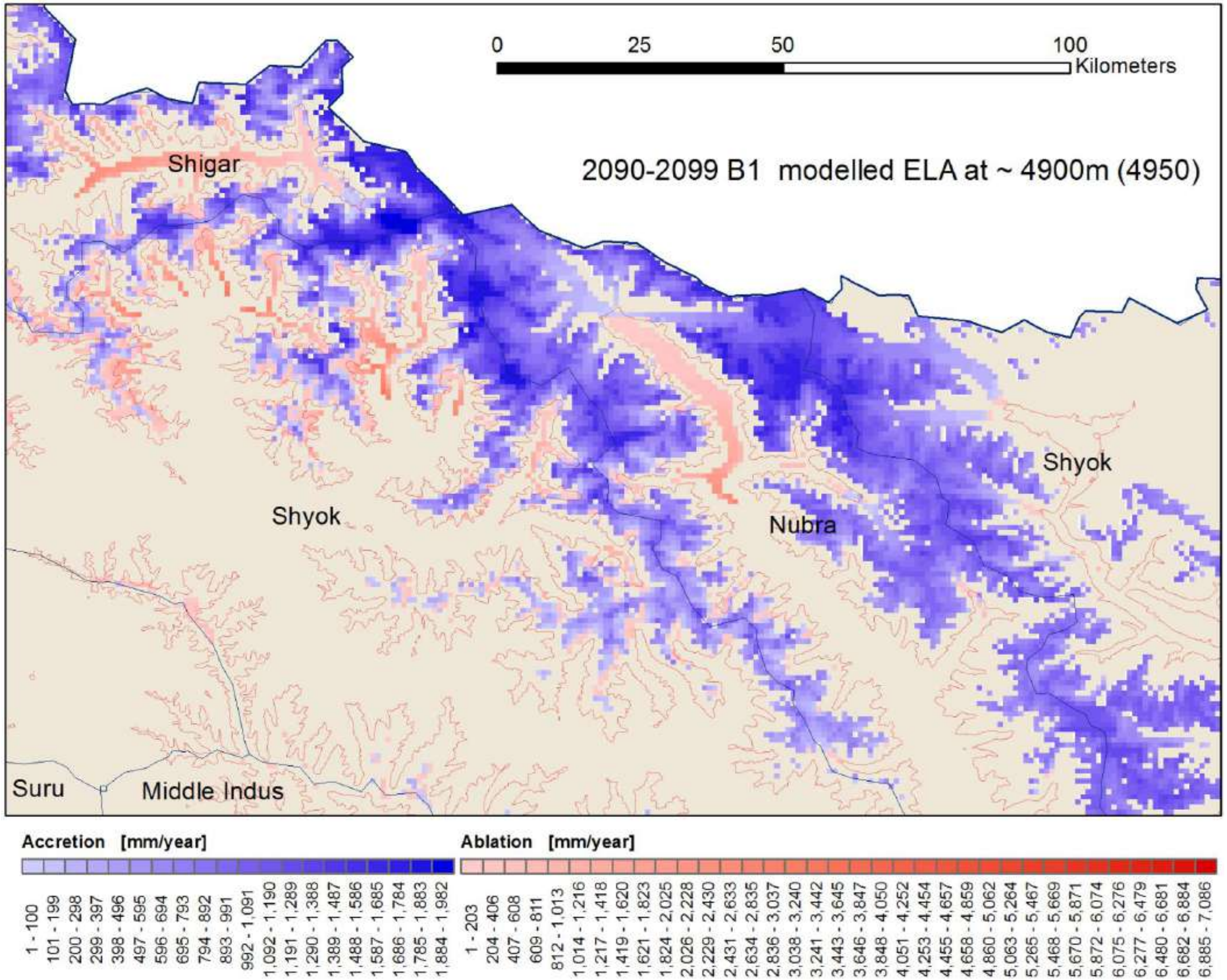

Figure 3-88: For a B1 Scenario an only Minor Shift of the ELA Towards Higher Elevations (4950m) until 2099

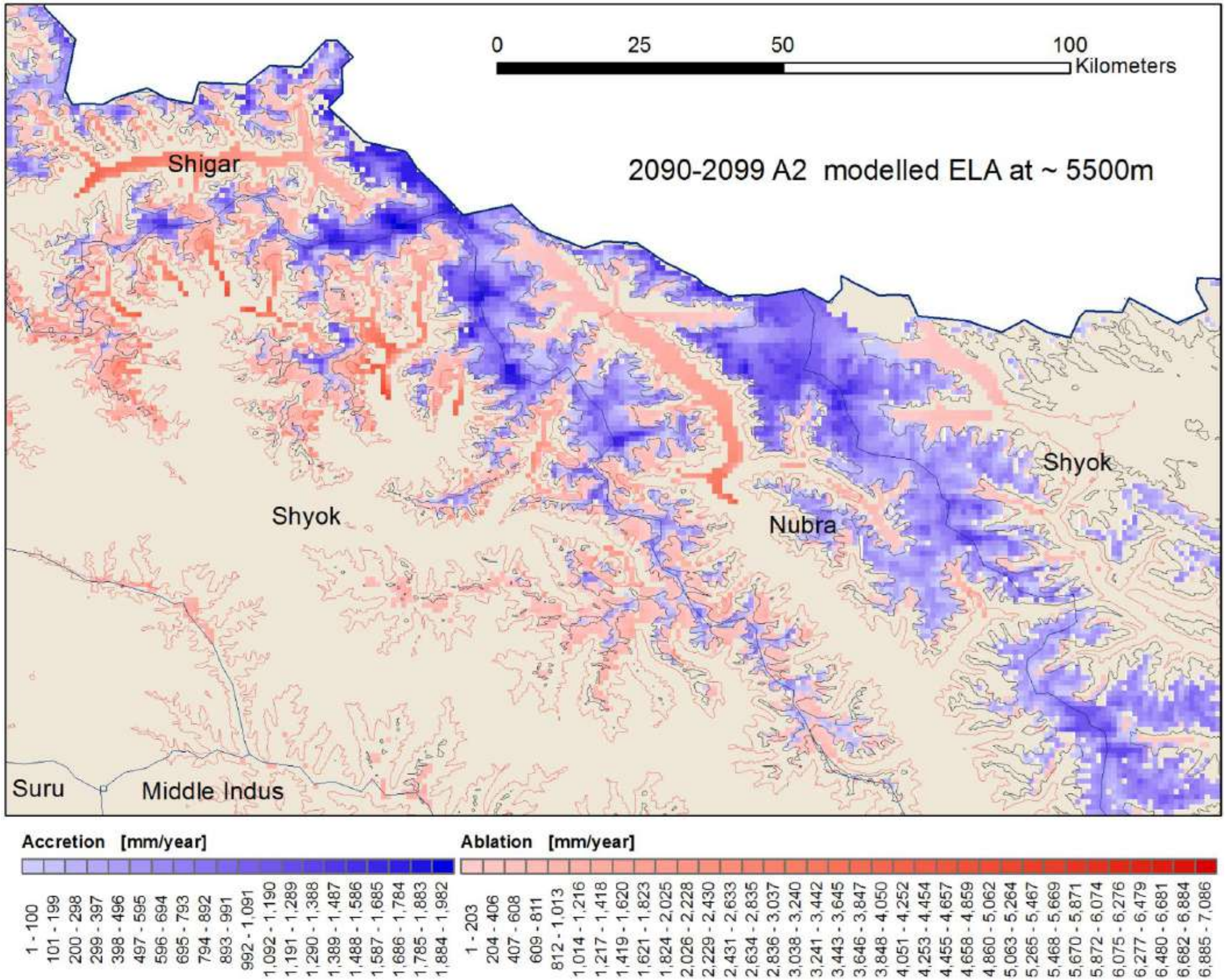

Figure 3-89: Retreat of the ELA until 2099 under an A2 Scenario.

3.24.15 Glacier "Balance" – Accretion and Ablation

Table 3-34: Average Decadal Glacier Water Gains and Losses - Gilgit and Hunza Watersheds.

<table>
<tr><th></th><th>Gilgit</th><th>Hunza</th></tr>
<tr><th>B1 scenario</th><td>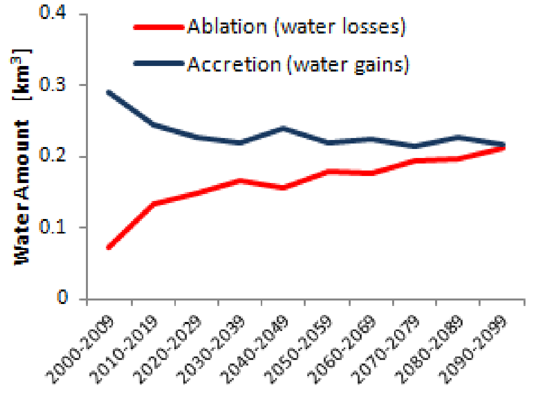
</td><td>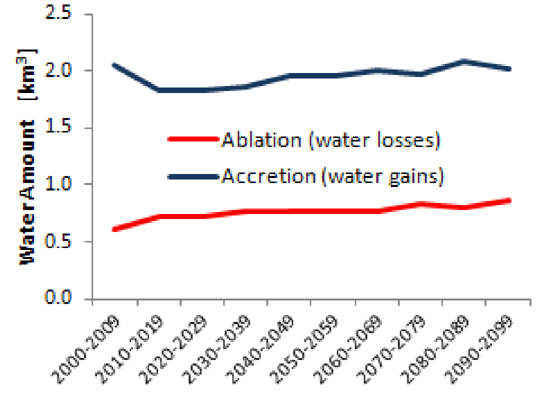
</td></tr>
<tr><th>A1b scenario</th><td>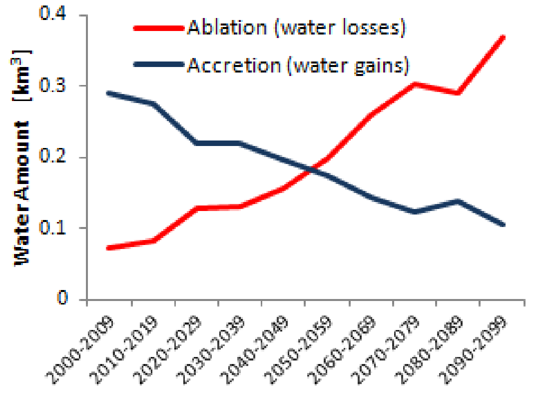
</td><td>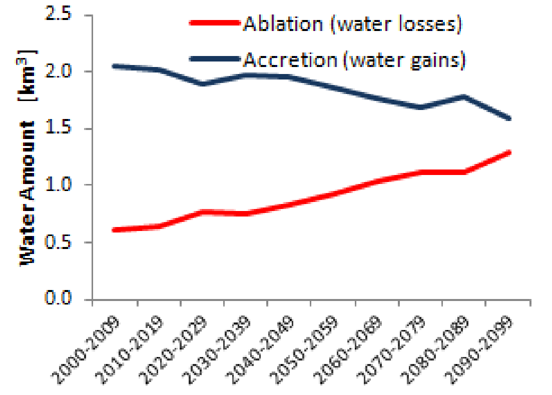
</td></tr>
<tr><th>A2 scenario</th><td>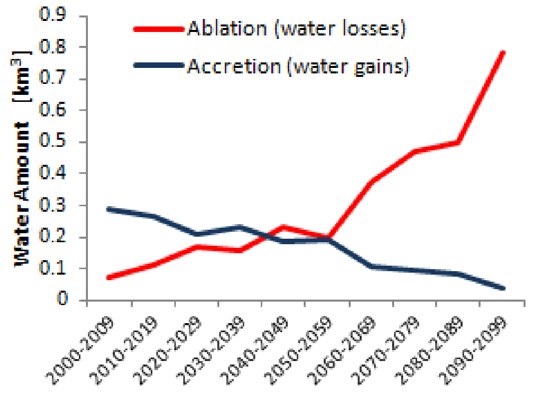
</td><td>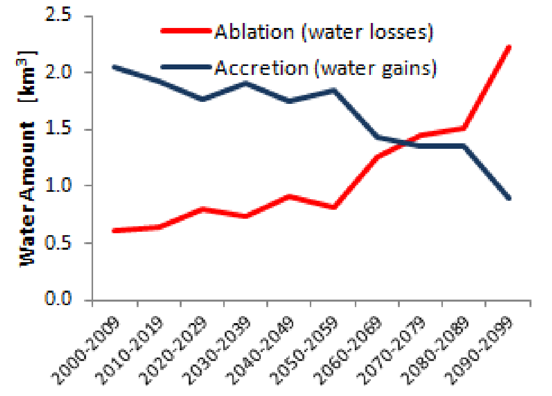
</td></tr>
</table>

Table 3-35: Average Decadal Glacier Water Gains and Losses - Shigar and Shyok-Nubra Watersheds.

<table>
<tr><th></th><th>Shigar</th><th>Shyok-Nubra</th></tr>
<tr><td>B1 scenario</td><td>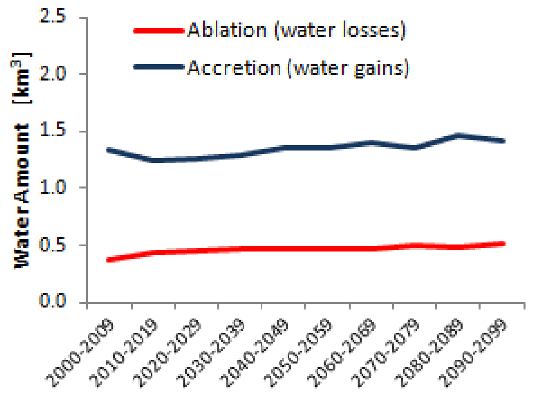
</td><td>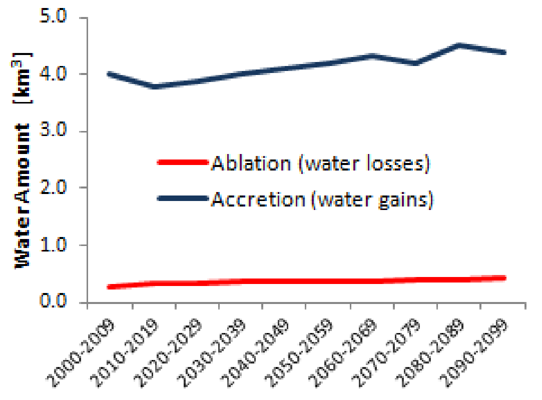
</td></tr>
<tr><td>A1b scenario</td><td>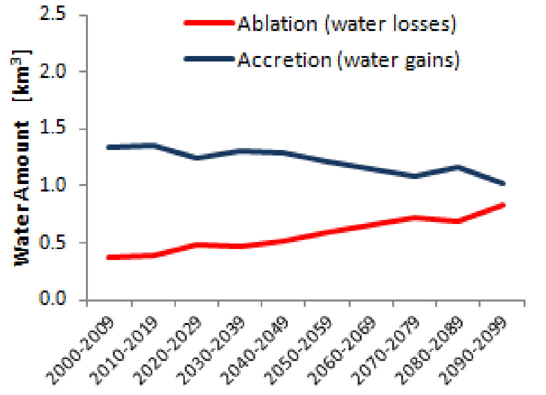
</td><td>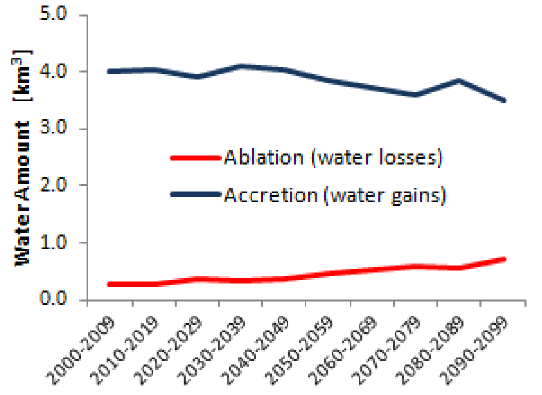
</td></tr>
<tr><td>A2 scenario</td><td>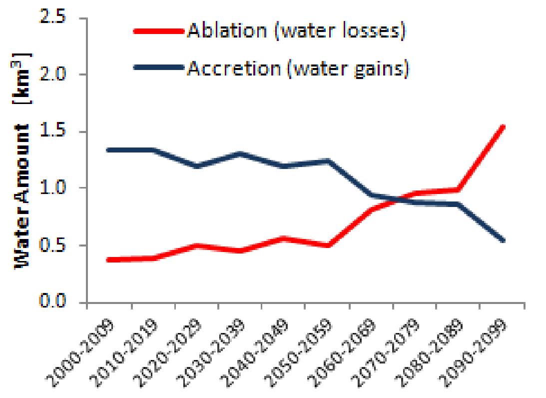
</td><td>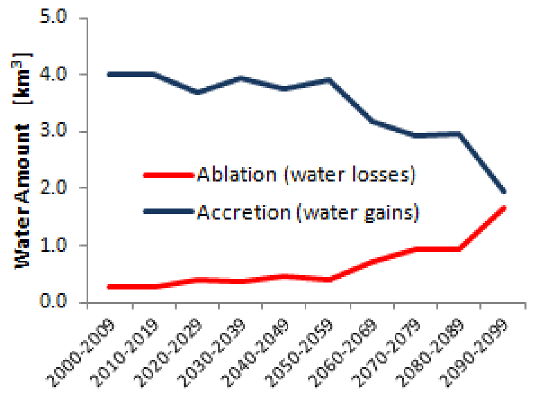
</td></tr>
</table>

Table 3-36: Average Decadal Glacier Water Gains and Losses - Suru and Zanskar Watersheds.

<table>
<tr><th></th><th>Suru</th><th>Zanskar</th></tr>
<tr><td>B1 scenario</td><td>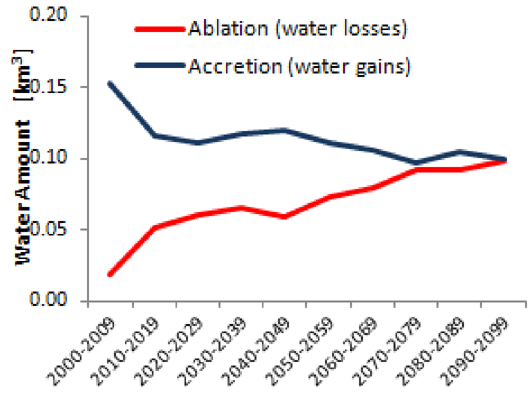
</td><td>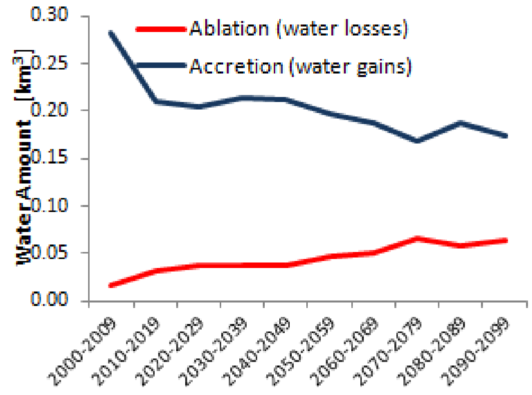
</td></tr>
<tr><td>A1b scenario</td><td>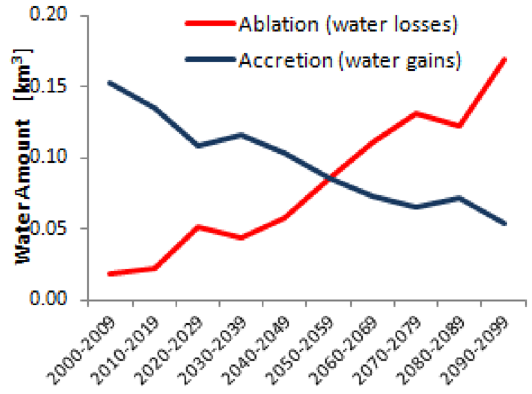
</td><td>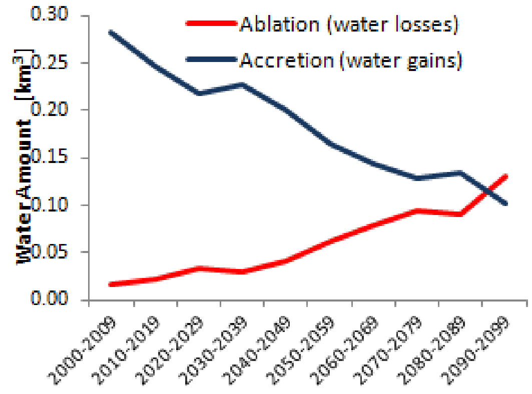
</td></tr>
<tr><td>A2 scenario</td><td>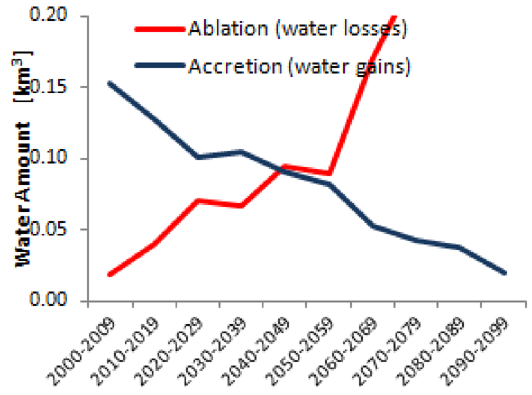
</td><td>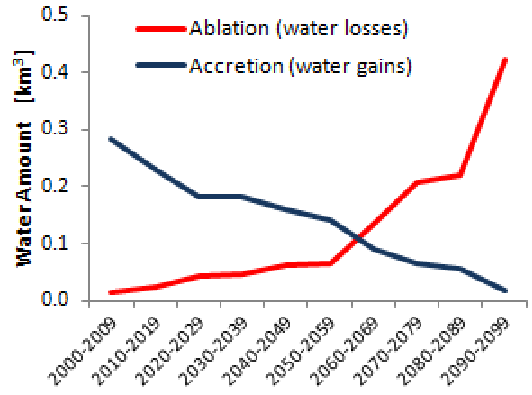
</td></tr>
</table>

Table 3-37: Average Decadal Glacier Water Gains and Losses - Astore Watershed.

	Astore
B1 scenario	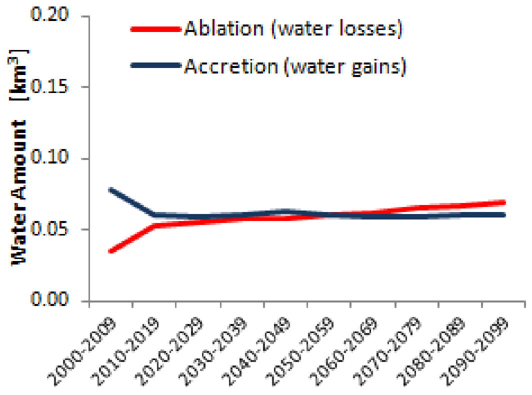
A1b scenario	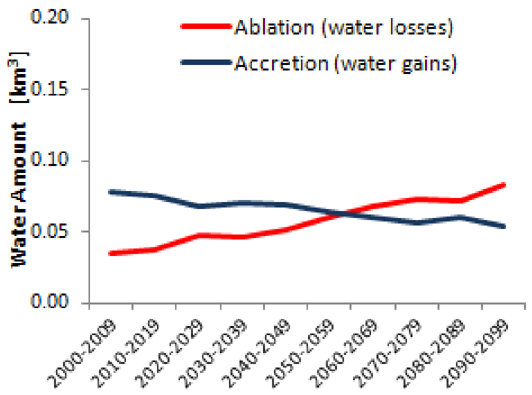
A2 scenario	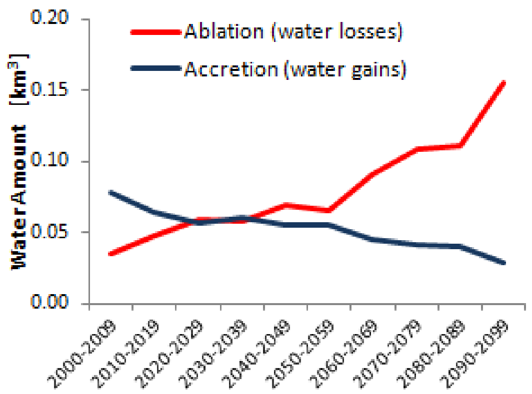

4 REFERENCES

A Productive and Water-Secure Pakistan: The Report of the Water Sector Task Force of the Friends of Democratic Pakistan – 2012.

Ahmad, Z., Hafeez, M. and Ahmad, I., 2012. Hydrology of mountainous areas in the upper Indus Basin, Northern Pakistan with the perspective of climate change. Environmental Monitoring and Assessment, 184: 5255-5274.

Ambast, S.K., Keshari, A.K. and Gosain, A.K., 2002. An operational model for estimating Regional Evapotranspiration through Surface Energy Partitioning (RESEP). International Journal of Remote Sensing, 23(22): 4917-4930.

Anders, A.M. et al., 2006. Spatial patterns of precipitation and topography in the Himalaya. Geological Society of America, Special Paper 398: 39-53.

Bashir, F.; Rasul, G. (2010): Estimation of Water Discharge from Gilgit Basin using Remote Sensing, GIS and Runoff Modeling. Pakistan Journal of Meteorology Vol. 6, Issue 12, 97-113

Bocchiola, D. and Diolaiuti, G., Recent (1980–2009) evidence of climate change in the upper Karakoram, Pakistan. Theoretical and Applied Climatology, 113(3-4).

Bocchiola, D. et al., 2011. Prediction of future hydrological regimes in poorly gauged high altitude basins: the case study of the upper Indus, Pakistan. Hydrol. Earth Syst. Sci., 15(7): 2059-2075.

Caltrans, State of California, Dept. of Transportation, 2003, Storm Water Quality Handbooks, pp229.

Cogley, G., Glaciology: No ice lost in the Karakoram. Nature Geosci, 5(5): 305-306.
Committee on Himalayan Glaciers, H., Climate Change, and Implications for Water Security, 2012. Himalayan glaciers: climate change, water resources, and water security (2012) 143 pp.

DePauw, E., 2014, Agroecological Methods (in prep.), ICARDA, Aleppo (Syria).

Dey, B.; V.K. Sharma; Rango, A. (1989): A Test of Snowmelt-Runoff Model for a Major River Basin in Western Himalayas. Nordic Hydrology, 20, 167-178

Discharge Measurement Structures, Publication No. 20 of International Institute for Land Reclamation and Improvement (ILRI) Delft Hydraulics Laboratory, University of Agriculture, Department of Hydraulics and Irrigation, The Netherlands

Eggleston, E.I. and Riley, J., 1971, J. Hybrid computer simulation of the accumulation and melt processes in a snowpack. Technical Report PRWG65-1, Utah State University, Logan, UT, USA, 1971.

Fowler, H.J. and Archer, D.R., 2006. Conflicting Signals of Climatic Change in the Upper Indus Basin. Journal of Climate, 19(17): 4276-4293.

Gardelle, J., Berthier, E. and Arnaud, Y., Slight mass gain of Karakoram glaciers in the early twenty-first century. Nature Geosci, 5(5): 322-325.

Geerken, R., 2009. An algorithm to classify seasonal variations in vegetation phenologies and their coverage and monitor their inter-annual change. Journal of Photogrammetry and Remote Sensing, 64: 422-431.

Geerken, R.A., Smith, R.B., Masri, Z. and dePauw, E., 2009. Assessment of Water Ressources and Demands of Agriculture in Semiarid Middle East. In: P.S. Thenkabail, J.G.

Lyon, H. Turral and C.M. Biradar (Editors), Remote Sensing of Croplands for Food Security. Series in Remote Sensing Applications. Taylor & Francis, Inc., Boca Raton, pp. 467.

Haq, M. (2008): Snowmelt runoff investigation in river Swat upper basin using snowmelt runoff model, remote sensing and GIS techniques. Enschede, ITC, 2008

Hargreaves, G.H. and Allen, R.G., 2003. History and evaluation of Hargreaves evapotranspiration equation. Journal of Irrigation and Drainage Engineering-Asce, 129(1): 53-63.

Hemund, C., Markart, G., Kohl, B., Dobman, J. and Weingartner, R., 2011. Assessment of surface runoff coefficients in torrential rain – evaluation of the code of practice by Markart et al. (2004) for Swiss catchments. Bundesforschungs- und Ausbildungszentrum für Wald, Naturgefahren und Landschaft, Wien, 2001, BFW-Dokumentation Nr.12, pp 103.

Hewitt, K., 2011. Glacier Change, Concentration, and Elevation Effects in the Karakoram Himalaya, Upper Indus Basin. Mountain Research and Development, 31(3): 188-200.

Huss, M. and Farinotti, D., 2012. Distributed ice thickness and volume of all glaciers around the globe. Journal of Geophysical Research, 117: 1-10.

Immerzeel, W.W. et al., High-resolution monitoring of Himalayan glacier dynamics using unmanned aerial vehicles. Remote Sensing of Environment, 150(0): 93-103.

Immerzeel, W.W., L.P.H. van Beek, M. Konz, A.B. Shrestha, M.F.P. Bierkens (2012): Hydrological response to climate change in a glacierized catchment in the Himalayas. Climatic Change, 110, 721–736

Immerzeel, W.W., P. Droogers, S.M. de Jong, M.F.P. Bierkens (2009): Large-scale monitoring of snow cover and runoff simulation in Himalayan river basins using remote sensing. Remote Sensing of Environment, 113: 40-49

ISO 13550-2002(E): Hydrometric dterminations – Flow measurements in open channels using structures – Use of vertical underflow gates

Kääb, A., Berthier, E., Nuth, C., Gardelle, J. and Arnaud, Y., 2012. Contrasting patterns of early twenty-first-century glacier mass change in the Himalayas. Nature, 488: 495-498.

Kaser, G., Großhauser, M. and Marzeion, B., 2010. Contribution potential of glaciers to water availability in different climate regimes. Proceedings of the National Academy of Sciences, 107(47): 20223-20227.

King, M.D. et al., 2003. EOS data products handbook. NASA Goddard Space Flight Center, Greenbelt, Maryland, pp. 261pp.

Kuhle, M., 1986. The upper limit of glaciation in the Himalayas. GeoJournal, 13(4): 331-346.
Kumar, L., Skidmore, A.K., and Knowles, E., 1997, Modelling topographic variation in solar radiation in a GIS environment. International Journal of Geographical Information Science, Vol.11, No.5, 475-497.

Laws, K.B., Janowiak, J.E. and Huffman, G.J., 2004. Verification of rainfall estimates over Africa using RFE, NASA MPA-RT and CMORPH, 84 AMS Annual Meeting, 18th Conference on Hydrology, Seattle, Wa.

Liu, C. and Ding, L., 1986. The Newely Progress of Glacier Inventory in Tianshan Mountains. Journal of Glaciology and Geocryology, 8(2): 168-169.

Martinec, J. (1975): Snowmelt-Runoff Model for Stream Flow Forecasts. Nordic Hydrology, Vol. 6, No. 3, 145-154

Martinec, J.; Rango, A.; Roberts, R. (2011): Snowmelt Runoff Model User's Manual, WinSRM Version 1.14. Agricultural Experiment Station Special Report 100, New Mexico State University, Las Cruces, NM 88003, U.S.A.

Marzeion, B., Cogley, J.G., Richter, K. and Parkes, D., 2014. Attribution of global glacier mass loss to anthropogenic and natural causes. Science, 345(6199): 919-921.

Matsuo, K. and Heki, K., 2010. Time-variable ice loss in Asian high mountains from satellite gravimetry. Earth Planetary Science Letters, 290: 30-36.

Mejia, J.F., Huntington, J., Hatchett, B., Koracin, D. and Niswonger, R.G., 2012. Linking Global Climate Models to an Integrated Hydrologic Model: Using an Individual Station

Downscaling Approach. Journal of Contemporary Water Research and Education(147): 17-27.
Minora, U. et al., 2001–2010 glacier changes in the Central Karakoram National Park: a contribution to evaluate the magnitude and rate of the "Karakoram anomaly". The Cryosphere Discuss., 7(3): 2891-2941.

Osborn, T.J. and Jones, P.D., 2014. The CRUTEM4 land-surface air temperature data set: construction, previous versions and dissemination via Google Earth. Earth System Science Data, 6: 61-68.

Prasad, A.K., Yang, K.-H.S., El-Askary, H.M. and Kafatos, M., 2009. Melting of major Glaciers in the western Himalayas: evidence of climatic changes from long term MSU derived tropospheric temperature trend (1979–2008). Annales Geophysicae, 27: 4505–4519.

R Core Team (2014): R: A lanGauge and environment for statistical computing. R Foundation for Statistical Computing, Vienna, Austria. http://www.R-project.org/

Rango, A. M., J. (1995) “Re-visiting the degree-day method for snowmelt computation”, Water Resource Bull. Volume 657-669.

Rasul, G., Chaudhry, Q.Z., Mahmood, A., Hyder, K.W. and Dahe, Q., 2012. Glaciers and Glacial Lakes under Changing Climate in Pakistan. Pakistan Journal of Meteorology, 8(15): 1-8.

Rudolf, B., Becker, A., Schneider, U., Meyer-Christoffer, A. and M., Z., 2010. GPCC Status Report December 2010 (On the most recent gridded global data set issued in fall 2010 by the Global Precipitation Climatology Centre (GPCC)).

Sanjay, K. Goswami, J.A.; Saraf A.K. (2010): Snowmelt runoff modelling in a Himalayan basin with the aid of satellite data. International Journal of Remote Sensing, Volume 31 Issue 24

Schaper, J., J. Martinec, K. Seidel (1999): Distributed Mapping of Snow and Glaciers for Improved Runoff Modelling. Hydrological Processes, 13(12-13): 2023-2031

Schaper, J., K. Seidel (2000): Modelling Daily Runoff from Snow and Glacier Melt Using Remote Sensing Data. Proceedings of EARSeL-SIG-Workshop Land Ice and Snow, Dresden, 308-317

Scherler, D., Bookhagen, B. and Strecker, M.R., 2010. Spatially variable response of Himalayan glaciers to climate change affected by debris cover. Nature Geosci, 4(3): 156-159.

Seidel, K., J. Martinec (2003): Advances in remote sensing of snow and ice for modelling the runoff process. In: Benes (ed.): Geoinformation for European-wide integration. Millpress, Rotterdam. 193-200

Shea, J. M., Immerzeel, W.W., Wagnon, P. Vincent, C. and Bajracharya, S., 2015. Modelling glacier change in the Everest region, Nepal Himalaya. The Cryosphere, 9:1105-1128.

Tahir, A.A. et al. (2011): Modeling snowmelt-runoff under climate scenarios in the Hunza River basin, Karakoram Range, Northern Pakistan. J. Hydrol. (2011), doi:10.1016/j.jhydrol.2011.08.035

USACE (1998): Runoff from Snowmelt. US Army Corps of Engineers, Engineer Manual 1110-2-1406, Washington, DC

Vaux, H.J., Jr., et al., 2012. Himalayan Glaciers: Climate Change, Water Resources and Water Security, National Academies Press, Washington.

Wilby, R.L. et al., 1998. Statistical downscaling of general circulation model output: A comparison of methods. Water Resources Research, 34(11): 2995-3008.

WMO (1986): Inter comparison of Models of Snowmelt Runoff. Operation Hydrol, Geneva, Switzerland, WMO